NASA Technical Paper 1538

Simulator Study of Stall/Post-Stall Characteristics of a Fighter Airplane With Relaxed Longitudinal Static Stability

Luat T. Nguyen, Marilyn E. Ogburn, William P. Gilbert,
Kemper S. Kibler, Phillip W. Brown, and Perry L. Deal

DECEMBER 1979

NASA

NASA Technical Paper 1538

Simulator Study of Stall/Post-Stall Characteristics of a Fighter Airplane With Relaxed Longitudinal Static Stability

Luat T. Nguyen, Marilyn E. Ogburn, William P. Gilbert,
Kemper S. Kibler, Phillip W. Brown, and Perry L. Deal
Langley Research Center
Hampton, Virginia

National Aeronautics
and Space Administration

**Scientific and Technical
Information Branch**

1979

TABLE OF CONTENTS

SUMMARY

A real-time piloted simulation has been conducted to evaluate the high-angle-of-attack characteristics of a fighter configuration based on wind-tunnel testing of the F-16, with particular emphasis on the effects of various levels of relaxed longitudinal static stability. The aerodynamic data used in the simulation were based on low-speed wind-tunnel tests of subscale models. The simulation was conducted on the Langley differential maneuvering simulator, and the evaluation involved representative low-speed combat maneuvering.

Results of the investigation showed that the airplane with the basic control system was resistant to the classical yaw departure; however, it was susceptible to pitch departures induced by inertia coupling during rapid, large-amplitude rolls at low airspeed. The airplane also exhibited a deep-stall trim which could be flown into and from which it was difficult to recover. Control-system modifications were developed which greatly decreased the airplane susceptibility to the inertia-coupling departure and which provided a reliable means for recovering from the deep stall.

INTRODUCTION

Rapid advances in aircraft avionic technology in recent years have made possible the application of control configured vehicle (CCV) concepts to fighter aircraft. In particular, considerable attention has been turned to the principle of relaxed static stability (RSS) in which the basic airframe is designed to have low or even negative static pitch stability in certain flight regimes. The performance benefits of this concept are well known (ref. 1); and an airplane currently under development which makes use of RSS is the F-16, which nominally operates at very moderate levels of negative static margin at low subsonic speeds. Advanced designs involving much higher levels of pitch instability are also now being considered for future fighter configurations.

Obviously, CCV designs rely greatly on the control system to provide satisfactory stability and control characteristics. Fundamentally, the control system must provide artificial stability such that the airplane appears to the pilot to have positive static pitch stability throughout the flight envelope. The use of RSS, however, can result in some demanding control problems at high angles of attack which impose severe requirements on the design of the flight control system in order that the desired characteristics of maximum maneuverability and departure/spin resistance are attained. An earlier investigation (ref. 2) identified some of the potential high-angle-of-attack problem areas inherent with the RSS design concept. The present investigation was conducted to evaluate some of these problems and their effects on the stability and control characteristics at high angles of attack of a fighter configuration based on the F-16. The study was conducted on the Langley differential maneuvering simulator (DMS) and used aerodynamic data based on the results of a number of low-speed wind-tunnel tests of subscale models conducted at the NASA Langley and Ames Research Centers. The objectives of the study were (1) to determine the controllability and departure resistance of the subject configuration during 1g and accelerated stalls; (2) to determine the departure susceptibility of the configuration during demanding air-combat maneuvers; (3) to identify high-angle-of-attack problems inherent to the RSS design and assess their impact on maneuverability; and (4) to develop and evaluate control schemes to circumvent or alleviate these shortcomings.

SYMBOLS

All aerodynamic data and flight motions are referenced to the body system of axes shown in figure 1. The units for physical quantities used herein are presented in the International System of Units (SI) and U.S. Customary Units. The measurements and calculations were made in U.S. Customary Units. Conversion factors for the two systems are given in reference 3.

a_n normal acceleration, positive along negative Z body axis, g units ($1g = 9.8\ \text{m/sec}^2$)

a_y lateral acceleration, positive along positive Y body axis, g units

b wing span, m (ft)

C_L lift coefficient, $\dfrac{\text{Aerodynamic lift force}}{\bar{q}S}$

C_l rolling-moment coefficient about X body axis, $\dfrac{\text{Aerodynamic rolling moment}}{\bar{q}Sb}$

$C_{l,t}$ total rolling-moment coefficient

C_m pitching-moment coefficient about Y body axis, $\dfrac{\text{Aerodynamic pitching moment}}{\bar{q}S\bar{c}}$

$C_{m,t}$ total pitching-moment coefficient

C_n yawing-moment coefficient about Z body axis, $\dfrac{\text{Aerodynamic yawing moment}}{\bar{q}Sb}$

$C_{n,t}$ total yawing-moment coefficient

C_X X-axis force coefficient along positive X body axis, $\dfrac{\text{Aerodynamic X-axis force}}{\bar{q}S}$

$C_{X,t}$ total X-axis force coefficient

C_Y — Y-axis force coefficient along positive Y body axis, $\frac{\text{Aerodynamic Y-axis force}}{\bar{q}S}$

$C_{Y,t}$ — total Y-axis force coefficient

C_Z — Z-axis force coefficient along positive Z body axis, $\frac{\text{Aerodynamic Z-axis force}}{\bar{q}S}$

$C_{Z,t}$ — total Z-axis force coefficient

$\bar{c}$ — wing mean aerodynamic chord, m (ft)

F_{lat} — pilot lateral stick force, positive for right roll, N (lb)

F_{long} — pilot longitudinal stick force, positive for aft force, N (lb)

F_{ped} — pilot pedal force, positive for right yaw, N (lb)

G_{ARI} — ARI gain

g — acceleration due to gravity, m/sec^2 (ft/sec^2)

g_{com} — pilot-commanded normal acceleration, g units

H_e — engine angular momentum, kg-m^2/sec (slug-ft^2/sec)

h — altitude, m (ft)

I_X, I_Y, I_Z — moments of inertia about X, Y, and Z body axes, kg-m^2 (slug-ft^2)

I_{XZ} — product of inertia with respect to X and Z body axes, kg-m^2 (slug-ft^2)

M — Mach number

M_{ic} — pitching moment due to inertia coupling, $(I_Z - I_X)pr$, N-m (ft-lb)

m — airplane mass, kg (slugs)

N_{ic} — yawing moment due to inertia coupling, $(I_X - I_Y)pq$, N-m (ft-lb)

P — period, sec

P_1 — engine power command based on throttle position, percent of maximum power

P_2 — engine power command to engine, percent of maximum power

P_3 — engine power, percent of maximum power

p airplane roll rate about X body axis, deg/sec or rad/sec

p_{com} pilot-commanded roll rate, deg/sec

$(p_{com})_{max}$ maximum commandable roll rate, deg/sec

p_{stab} stability-axis roll rate, deg/sec or rad/sec

p_s static pressure, N/m^2 (lb/ft^2)

q airplane pitch rate about Y body axis, deg/sec or rad/sec

$\dot{q}$ airplane pitch acceleration about Y body axis, deg/sec^2 or rad/sec^2

$\dot{q}_a$ component of airplane pitch acceleration due to aerodynamic moments, $\left(\frac{\bar{q}S\bar{c}}{I_Y}\right)C_{m,t}$, deg/sec^2 or rad/sec^2

$\dot{q}_{icl}$ component of airplane pitch acceleration due to inertia coupling, $\left(\frac{I_Z - I_X}{I_Y}\right)pr$, deg/sec^2 or rad/sec^2

$\bar{q}$ free-stream dynamic pressure, N/m^2 (lb/ft^2)

R range, straight-line distance between subject and target airplanes, m (ft)

r yaw rate about Z body axis, deg/sec or rad/sec

r_f filtered yaw-rate signal, deg/sec

r_{stab} stability-axis yaw rate, deg/sec or rad/sec

$\dot{r}$ yaw acceleration about Z body axis, deg/sec^2 or rad/sec^2

$\dot{r}_a$ component of airplane yaw acceleration due to aerodynamic moments, $\left(\frac{\bar{q}Sb}{I_Y}\right)C_{n,t}$, deg/sec^2 or rad/sec^2

$\dot{r}_{icl}$ component of airplane yaw acceleration due to inertia coupling, $\left(\frac{I_X - I_Y}{I_Z}\right)qp$, deg/sec^2 or rad/sec^2

S wing area, m^2 (ft^2)

s Laplace variable, 1/sec

T total instantaneous engine thrust, N (lb)

T_{idle} idle thrust, N (lb)

T_{max} maximum thrust, N (lb)

T_{mil} military thrust, N (lb)

t time, sec

$t_{1/2}$ time to damp to one-half amplitude, sec

u,v,w components of airplane velocity along X, Y, and Z body axes, m/sec (ft/sec)

V airplane resultant velocity, m/sec (ft/sec)

$\dot{w}$ airplane acceleration along Z body axis, m/sec^2 (ft/sec^2)

$\dot{w}_a$ component of $\dot{w}$ due to aerodynamic force, $\left(\frac{\bar{q}S}{m}\right)C_{Z,t}$, m/sec^2 (ft/sec^2)

$\dot{w}_{ac1}$ component of $\dot{w}$ due to pitch rate, qu, m/sec^2 (ft/sec^2)

$\dot{w}_{ac2}$ component of $\dot{w}$ due to kinematic coupling, $-pv$, m/sec^2 (ft/sec^2)

X,Y,Z airplane body axes (see fig. 1)

x_{cg} center-of-gravity location, fraction of $\bar{c}$

$x_{cg,ref}$ reference center-of-gravity location for aerodynamic data

α angle of attack, deg

α_f filtered angle-of-attack signal, deg

α_i indicated angle of attack, deg

β angle of sideslip, deg

δ_a aileron deflection, positive for left roll, deg

$\delta_{a,c}$ aileron deflection commanded by control system, deg

$\delta_{a,max}$ maximum aileron deflection, deg

δ_d differential horizontal-tail deflection, positive for left roll, deg

$\delta_{d,c}$ differential horizontal-tail deflection commanded by control system, deg

δ_h horizontal stabilator deflection, positive for airplane nose-down control, deg

$\delta_{h,c}$ horizontal stabilator deflection commanded by control system, deg

δ_{lef} leading-edge flap deflection, positive for leading edge down, deg

δ_r rudder deflection, positive for left yaw, deg

$\delta_{r,com}$ pilot-commanded rudder deflection, deg

δ_{sb} speed-brake deflection, deg

δ_{tef} trailing-edge flap deflection, positive for trailing edge down, deg

ε tracking error, angle between evaluation airplane X body axis and range vector $\vec{R}$ (angle off), deg

η horizontal stabilator effectiveness factor

λ lateral component of ε, deg

Θ,ϕ,ψ Euler angles, deg

τ_T engine-thrust time constant, sec

Ω aircraft total angular velocity, deg/sec

$$C_{l_p} = \frac{\partial C_l}{\partial \frac{pb}{2V}} \qquad C_{l_r} = \frac{\partial C_l}{\partial \frac{rb}{2V}} \qquad C_{l_\beta} = \frac{\partial C_l}{\partial \beta} \qquad C_{l_{\delta_a}} = \frac{\partial C_l}{\partial \delta_a}$$

$$C_{l_{\delta_r}} = \frac{\partial C_l}{\partial \delta_r} \qquad C_{m_q} = \frac{\partial C_m}{\partial \frac{q\bar{c}}{2V}} \qquad C_{n_p} = \frac{\partial C_n}{\partial \frac{pb}{2V}} \qquad C_{n_r} = \frac{\partial C_n}{\partial \frac{rb}{2V}}$$

$$C_{n_\beta} = \frac{\partial C_n}{\partial \beta} \qquad C_{n_{\beta,dyn}} = C_{n_\beta} - \frac{I_Z}{I_X} C_{l_\beta} \sin \alpha \qquad C_{n_{\delta_a}} = \frac{\partial C_n}{\partial \delta_a} \qquad C_{n_{\delta_r}} = \frac{\partial C_n}{\partial \delta_r}$$

$$C_{X_q} = \frac{\partial C_X}{\partial \frac{q\bar{c}}{2V}} \qquad C_{Z_q} = \frac{\partial C_Z}{\partial \frac{q\bar{c}}{2V}} \qquad C_{Y_p} = \frac{\partial C_Y}{\partial \frac{pb}{2V}} \qquad C_{Y_r} = \frac{\partial C_Y}{\partial \frac{rb}{2V}}$$

Subscripts:

ds deep stall

lef increment of variable produced by full retraction of leading-edge flaps; for example, $\Delta C_{m,lef}$ indicates increment in C_m produced by retraction of leading-edge flaps from 25° to 0°

o	initial value
sb	increment in variable produced by deflection of speed brake
$\delta_{i=j}$	deflection of control surface i to value j; for example, $\Delta C_{l,\delta_{a=20^{o}}}$ indicates increment of C_l produced by deflection of ailerons to $\delta_a = 20^{o}$

Abbreviations:

ACM	air-combat maneuvering
ARI	aileron-rudder interconnect
CAS	command augmentation system
CCV	control configured vehicle
DL	deflection limit, deg
DMS	Langley differential maneuvering simulator
IAS	indicated airspeed, knots
LCDP	lateral control divergence parameter
RL	rate limit, deg/sec
RSS	relaxed static stability
rms	root mean square
SAS	stability augmentation system
SM	static margin

DESCRIPTION OF AIRPLANE

A three-view sketch of the simulated configuration is shown in figure 2, and the mass and geometric characteristics used in the simulation are listed in table I. The airplane control system is described in detail in appendix A. The primary aerodynamic controls include symmetric deflection of the horizontal tail (stabilator) for pitch control, deflection of conventional wing-mounted ailerons and differential deflection of the horizontal stabilators for roll control, and rudder deflection for yaw control.

One special feature of the configuration is the use of a normal-acceleration-command longitudinal control system which provides static stability, normal-acceleration limiting, and angle-of-attack limiting. The airplane is balanced to minimize trim drag, with the effect that it has slightly negative static longitudinal stability at low Mach numbers; the desired static stability is provided artificially by the control system. Other features include (1) wing leading-edge flaps which are automatically deflected as a function of angle of attack and Mach number; (2) a roll-rate command system in the roll axis; (3) an aileron-rudder interconnect and a stability-axis yaw damper in the yaw axis; and (4) a force-sensing (minimum displacement) side-stick controller and force-sensing rudder pedals. The airplane engine characteristics used in the present study are described in appendix B, and the buffet characteristics are described in appendix C.

Most of the simulated flights were made at a center-of-gravity location of $0.35\bar{c}$ although locations as far aft as $0.39\bar{c}$ were also investigated. All results shown in this report are for the $0.35\bar{c}$ center-of-gravity location unless otherwise stated.

DESCRIPTION OF SIMULATOR

The Langley differential maneuvering simulator (DMS) is a fixed-base simulator which has the capability of simultaneously simulating two airplanes as they maneuver with respect to one another and of providing a wide-angle visual display for each pilot. A sketch of the general arrangement of the DMS hardware and control console is shown in figure 3. Two 12.2-m (40-ft) diameter projection spheres each enclose a cockpit, an airplane-image projection system, and a sky-Earth-Sun projection system. A control console located between the spheres is used for interfacing the hardware and the computer, and it displays critical parameters for monitoring hardware operation. Each pilot is provided a projected image of his opponent's airplane, with the relative range and attitude of the target shown by a television system which is controlled by the computer program.

Cockpit and Associated Equipment

A photograph of one of the cockpits and the target visual display is shown in figure 4. A cockpit is provided with an instrument display and a computer-driven gunsight representative of current fighter aircraft equipment. However, this study used a fixed gunsight for tracking. Each cockpit is located to position the pilot's eyes near the center of the sphere so that he has a field of view representative of that obtained in current fighter airplanes. For the present study, a special modification was made to one cockpit to incorporate the side-stick controller as shown in figure 5. The controller was placed in the same general cockpit location as the controller in the F-16 airplane; however, no special armrest was provided (as is the case in the actual airplane) other than the regular seat armrest which provided more of an elbow rest than a support for the forearm. The normal hydraulic control feel system was not employed for this simulation since the side-stick controller and rudder pedals were force sensitive, with no deflection required to activate the controls. Although the cockpits are not provided with attitude motion, each cockpit incorporates a buffet system capable of providing programmable root-mean-square (rms) buffet accelerations as high as 0.5g, with up to three primary structural frequencies simulated.

Visual Display

The visual display in each sphere consists of a target image projected onto a sky-Earth scene. The sky-Earth scene is generated by two point light sources projecting through two hemispherical transparencies, one transparency of blue sky and clouds and the other of terrain features; the scene provides a well-defined horizon band for reference purposes. No provision is made to simulate translational motion with respect to the sky-Earth scene (such as altitude variation); however, spatial attitude motions are simulated. A flashing light located in the cockpit behind the pilot is used as a cue when an altitude of less than 1524 m (5000 ft) is reached. The target-image generation system uses an airplane model mounted in a four-axis gimbal system and a television camera with a zoom lens to provide an image to the target projector within the sphere. For an F-16 size airplane, the system can provide a simulated range from 90 m (300 ft) to 13 700 m (45 000 ft) between airplanes, with a 10-to-1 brightness contrast between the target and the sky-Earth background at minimum range.

Additional special-effects features of the DMS hardware include simulation of blackout at high normal accelerations (see appendix C), the use of an inflatable "anti-g" garment for simulation of normal-acceleration loads, and sound cues to simulate wind, engine, and weapons noise as well as artificial warning systems. Additional details of the DMS facility are given in reference 4.

Computer Program

The DMS is driven by a real-time digital simulation system and a Control Data CYBER 175 computer. The dynamics of the evaluation airplane were calculated by using equations of motion with a fixed-interval (1/32 sec) numerical-integration technique. The equations used nonlinear aerodynamic data as functions of α and/or β in tabular form. These data were derived from results of low-speed ($M = 0.1$ to 0.2) static and dynamic (forced-oscillation) force tests conducted in several wind-tunnel facilities. The data included an angle-of-attack range from -20° to 90° and a sideslip range from -30° to 30°. Effects of Mach number, Reynolds number, or aeroelasticity were not included in the mathematical model. Complete descriptions of the aerodynamic data and the equations of motion are given in appendix B.

EVALUATION PROCEDURES

The results of the investigation were based on pilot comments and time-history records of airplane motions, controls, and tracking for the various maneuvers performed. Most of the evaluations were performed by two NASA research test pilots who were familiar with the air-combat maneuvers used with current fighter airplanes; however, a U.S. Air Force test pilot and a contractor test pilot involved in high-angle-of-attack flight tests of the F-16 airplane also flew the simulator.

The evaluation was conducted in two phases. The first phase involved "open-loop" maneuvers to assess basic stability and control characteristics of the airplane at high angles of attack, and the second phase involved tracking a simulated F-16 as a target airplane through a series of maneuvers representative of those used in air combat in order to examine flying qualities under these conditions. Maneuvers used in the first phase included 1g and accelerated stalls, with various control inputs applied at specific conditions. Table II lists the primary maneuvers used in this phase. In addition to documenting the stability and response to control characteristics of the airplane and familiarizing the pilot with these characteristics, this phase also provided an assessment of the departure and spin susceptibility of the configuration. Results from the first phase of the study were used to design the tracking tasks used in the second phase. Several tasks were chosen for use during the second phase of the study: (1) a steady wind-up turn tracking task, (2) a bank-to-bank maneuvering task, and (3) a complex, vigorous air-combat maneuvering (ACM) task.

Wind-Up Turn Tracking Task

A steady wind-up turn was flown, with the target airplane slowly increasing angle of attack in order to provide a tracking situation in which the pilot could evaluate the fine tracking capability of the evaluation airplane at high angles of attack. Initially, both airplanes were at an altitude of 9144 m (30 000 ft) and $M = 0.6$, with the subject airplane 457.2 m (1500 ft) directly behind the target and at the same heading as the target. Upon initiation of the run, the target established a left-bank attitude which varied between -40° and -100° during the maneuver. Angle of attack was gradually increased up to a maximum of about 3g normal acceleration. The evaluation pilot attempted to track the target as closely as possible while maintaining a range of less than 609.6 m (2000 ft). Time histories of the target motions are shown in figure 6.

Bank-to-Bank Tracking Task

As shown in figure 7, this task involved tracking the target airplane through a series of bank-to-bank maneuvers (or horizontal S's) at high angles of attack. These maneuvers enabled the pilot to evaluate his ability to roll the subject airplane rapidly, to acquire the target, and to stabilize while at high angle of attack.

ACM Tracking Task

The ACM tracking task was developed to be more representative of the complex, nonrepetitive maneuvers which may be encountered during air-to-air combat. The time histories of the target motions are shown in figure 8. In general, the task covered a speed range of 0.25 to 0.6 Mach and required the tracking airplane to perform several large-amplitude rolling maneuvers at low-speed, high-angle-of-attack conditions.

Evaluation of Performance

In evaluating the simulated airplane, numerous runs were made in each of the tasks. Sufficient flights were made to ensure that the pilot's "learning curve" was reasonably well established before drawing any conclusions on evaluation results. Evaluation of performance was based on pilot comments, the ability of the pilot to execute the tasks assigned, and the analysis of time histories of airplane motions and tracking.

DISCUSSION OF STABILITY AND CONTROL CHARACTERISTICS

To provide a foundation for the analysis and interpretation of the simulation results which follow, selected aerodynamic stability and control characteristics of the simulated airplane configuration are presented and discussed in this section.

Longitudinal Characteristics

The aerodynamic data are listed in table III, and the representation of these characteristics in the simulation is discussed in appendix B. The aerodynamic characteristics of the configuration as noted during wind-tunnel flow-visualization tests were such that the outer wing panels stalled near $\alpha = 20^\circ$, but the highly swept wing-body strake continued to produce lift at higher angles of attack, as shown in figure 9. Maximum C_L was obtained near $\alpha = 35^\circ$.

A notable characteristic of the configuration is that it exhibits a modest level of static pitch instability at the nominal center-of-gravity position ($0.35\bar{c}$) at low speeds, as shown in figure 10. Static margin at low angles of attack is approximately -4 percent. To provide satisfactory flying qualities, the longitudinal control system is equipped (see appendix A) with angle-of-attack feedback to provide artificial pitch stability. It is important to note that figure 10 also indicates that the airplane will trim at $\alpha = 66^\circ$ with full nose-up stabilator deflection ($\delta_h = -25^\circ$). To inhibit inadvertent excursions to these extreme angles of attack, the pitch control system incorporates an angle-of-attack/normal-acceleration limiting system which drives the stabilator in an attempt to limit the angle of attack to below 25°. A further discussion of the complete pitch control system is given in appendix A.

Two other important points regarding longitudinal stability should be noted in figure 10. The first is the marked loss in nose-down stabilator effectiveness due to stall of these surfaces for angles of attack greater than 25°. The loss in nose-down control effectiveness is particularly critical because the α limiter system relies on the available nose-down control moment to prevent α from exceeding 25°. The other important characteristic shown in figure 10 is the existence of a stable deep-stall trim point. Note that even with the stabilators deflected for full nose-down control, the airplane exhibits a weak but stable trim point at $\alpha = 60^\circ$.

Another important aerodynamic characteristic exhibited by the simulated airplane is the variation of C_m with β at high angles of attack, an example of which is shown by wind-tunnel data for $\alpha = 25^\circ$ in figure 11. As can be seen, there is very little variation of pitching moment with sideslip for $\delta_h = 0^\circ$. However, the data for nose-down stabilator deflections show a sharp loss in stabilator effectiveness for sideslip magnitudes greater than about 10°.

Thus, if a departure involving large sideslip excursions should occur, the effectiveness of the angle-of-attack limiter system to maintain α at or below 25° will be further degraded by the reduction in available nose-down control moment.

Lateral-Directional Characteristics

Static lateral-directional stability.- The static lateral-directional stability characteristics of the basic airplane with scheduled leading-edge flap deflections are presented in figure 12 in terms of the static directional stability derivative C_{n_β}, the effective dihedral derivative C_{l_β}, and the dynamic directional stability parameter $C_{n_{\beta,dyn}}$ as functions of angle of attack. At each angle of attack, C_{n_β} and C_{l_β} were computed by sloping C_n and C_l between $\beta = \pm 4^{\circ}$. The parameter $C_{n_{\beta,dyn}}$ has been used in past investigations as an indication of the existence of directional divergence (nose slice) at high angles of attack. Negative values of this parameter usually indicate the existence of a divergence. The data of figure 12 indicate that the configuration was statically stable (both directionally and laterally) for angles of attack up to about 28°. Above $\alpha = 30^{\circ}$, C_{n_β} reached large unstable (negative) values, which caused a sharp decrease in the value of $C_{n_{\beta,dyn}}$ at $\alpha = 35^{\circ}$. Nevertheless, it is seen that this parameter remained positive up through $\alpha = 40^{\circ}$, and a directional divergence would therefore not be expected at high angles of attack.

The lateral-directional aerodynamic control characteristics for the configuration at $\beta = 0^{\circ}$ are shown in figure 13 in terms of moment increments caused by full control. The rudder effectiveness was high and essentially constant over the operational range of angle of attack ($\alpha < 25^{\circ}$). Roll-control effectiveness of the ailerons and differential tails was good and well sustained up to the angle-of-attack limit, whereas the adverse yaw produced by these surfaces above $\alpha = 20^{\circ}$ was very small compared with moments produced by the rudder. Only above $\alpha = 40^{\circ}$ do the adverse yawing moments become significant compared with the available rudder moments. These data indicate that the configuration should exhibit good lateral-directional control characteristics up to the angle-of-attack limit ($\alpha = 25^{\circ}$) if proper coordination of roll and yaw controls is used to suppress the roll-control adverse yaw and to minimize sideslip.

The lateral control divergence parameter (LCDP) is often used to appraise roll-control effectiveness at high angles of attack. This parameter is defined as

$$\mathrm{LCDP} = C_{n_\beta} - C_{l_\beta}\left(\frac{C_{n_{\delta_a}}}{C_{l_{\delta_a}}}\right)$$

for ailerons only, or by

$$\text{LCDP} = C_{n_\beta} - C_{l_\beta}\left(\frac{C_{n_{\delta_a}} + G_{ARI}C_{n_{\delta_r}}}{C_{l_{\delta_a}} + G_{ARI}C_{l_{\delta_r}}}\right)$$

where G_{ARI} is the ratio of rudder deflection to aileron deflection for an airplane with an aileron-rudder interconnect (ARI). Positive values of this parameter indicate normal roll response, and negative values indicate reversed response. When reversed response is encountered, a right roll-control input by the pilot will cause the airplane to roll to the left. The variation of LCDP with angle of attack for the subject airplane is presented in figure 14. For the airplane with the basic control system, the parameter becomes negative above $\alpha = 25^\circ$, which indicates reversed response if roll control alone was used in this region. Addition of the ARI provided a large positive increment in LCDP above $\alpha = 15^\circ$ such that the LCDP values remained positive up through $\alpha = 40^\circ$. This result indicates that the augmented airplane should exhibit normal response to roll-command inputs throughout the operational angle-of-attack range.

Dynamic lateral-directional stability.- The classical dynamic lateral-directional stability characteristics of the airplane were calculated on the basis of three degree-of-freedom linearized lateral-directional equations and the aerodynamic data of appendix B. The results of the calculations with the SAS on and off are presented in figure 15 in terms of the damping parameter $1/t_{1/2}$ and the period P of oscillatory modes. Positive values of $1/t_{1/2}$ indicate damped or stable modes of motion. Data are shown for the classical Dutch roll, spiral, and roll modes of motion as a function of angle of attack for 1g trim conditions. The data for the airplane without SAS show that all three modes are stable for values of α up to 30°. The stability of the Dutch roll and roll modes tends to decrease with α, whereas the opposite is true for the spiral mode. Stability characteristics of the airplane with the lateral-directional SAS operative are also shown in figure 15. Figure 15 shows that the roll and yaw SAS significantly enhanced the stability of both the Dutch roll and roll modes in the normal flight envelope ($\alpha \leqq 25^\circ$).

A detailed discussion of the lateral-directional control system is contained in appendix A; the primary features of the roll/yaw SAS are (1) a roll-rate-command augmentation system, (2) a stability-axis yaw damper, (3) an aileron-rudder interconnect, and (4) an automatic spin-prevention system which activates when α exceeds 29°.

DISCUSSION OF HIGH-ANGLE-OF-ATTACK KINEMATIC- AND INERTIA-COUPLING PHENOMENA

As an additional aid in analyzing the simulation results which follow, several kinematic- and inertia-coupling phenomena which significantly influence the high-angle-of-attack characteristics of the F-16 airplane are briefly reviewed in this section.

Figure 16 illustrates the kinematic coupling between angle of attack and sideslip that occurs when an airplane is rolled about its X-axis at high angles of attack. If the airplane is flying at angle of attack with the wings level (fig. 16(a)) and the pilot initiates a pure rolling motion about its X-axis (fig. 16(b)), all the initial angle of attack will have been converted into sideslip after 90° of roll. Because it is undesirable to generate large amounts of sideslip at high angles of attack from a roll-performance, as well as a departure-susceptibility, viewpoint, most current fighters (including the F-16) are designed to roll more nearly about the velocity vector than the body axis. It is obvious that this conical rotational motion (indicated by $\vec{p}_{stab}$) eliminates the coupling between α and β. Resolving $\vec{p}_{stab}$ into the body-axis system shows that this motion involves body-axis yaw rate as well as roll rate and that these rates are related by the expression

$$r = p \tan \alpha$$

If this equality is not satisfied during a roll, then sideslip will be generated due to kinematic coupling, with $\dot{\beta}$ varying as

$$\dot{\beta} \cong p \sin \alpha - r \cos \alpha$$

The control system of the F-16 incorporates an ARI and a stability-axis yaw damper which attempt to make the airplane roll about its velocity vector throughout its normal flight envelope. (See appendix A.)

In the case of rolling with an initial sideslip, it is seen from figure 16(b) that body-axis rolling will result in the initial β being converted into α after 90° of roll, with $\dot{\alpha}$ varying as

$$\dot{\alpha} \cong q - p \cos \alpha \tan \beta$$

The second term in this expression indicates that rolling with adverse sideslip (p and β having the same signs) tends to reduce α, whereas rolling with proverse sideslip (p and β having opposite signs) tends to increase α. This latter effect can be important in CCV configurations requiring an angle-of-attack limit in that substantial increases in α can be generated due to kinematic coupling if the airplane is rolled with proverse β (using excessive rudder, for example).

The second form of coupling that is important to the high-angle-of-attack dynamics of the F-16 configuration is due to inertial effects. Figure 17(a) illustrates the inertial pitching moment that is produced when the airplane is rolled about its velocity vector at high angles of attack. The desirability of this type of roll from a kinematic-coupling viewpoint was previously discussed; unfortunately, the resulting nose-up pitching moment caused by inertia coupling can be a problem for CCV configurations that employ relaxed static pitch stability. As an aid in visualizing this effect, the fuselage-heavy mass distribution of the airplane is represented as a dumbbell, with the mass concentrated at the two ends. If the airplane is flying at some angle of attack and rolls about its velocity vector, the dumbbell will tend to pitch up to align itself perpendicular to the rotation vector $\vec{p}_{stab}$. This nose-up pitching moment due to inertial coupling M_{ic} can be expressed as

$$M_{ic} = (I_Z - I_X)pr$$

Substituting $p = p_{stab} \cos \alpha$ and $r = p_{stab} \sin \alpha$,

$$M_{ic} = (I_Z - I_X)p_{stab}^2 \cos \alpha \sin \alpha = \frac{1}{2}(I_Z - I_X)p_{stab}^2 \sin 2\alpha$$

The preceding expression shows that the pitch inertia-coupling moment resulting from stability-axis rolling is always positive (nose up) for positive α and varies as the square of the stability-axis roll rate p_{stab}.

For CCV configurations with relaxed static stability, the nose-up moment must be opposed by the available nose-down control moment. If this control moment is less than the inertia-coupling moment, the horizontal tail can reach a travel limit, at which time the airplane will lose the stability contribution of the tail and the airplane will pitch up beyond the α limiter boundary, which results in loss of control.

The inertia-coupling moment which results from the combination of roll and pitch rates is illustrated in figure 17(b). The airplane mass distribution is represented by the dumbbell, and the airplane is shown rolling to the right and pitching up. As can be seen, the dumbbell will tend to yaw nose left to align itself perpendicular to the rotation vector $\vec{\Omega}$. The expression for the inertia-coupling moment is given by

$$N_{ic} = (I_X - I_Y)pq$$

Consider the case $q > 0$ (nose-up pitch rate). Because $I_X < I_Y$, the preceding expression shows that the yaw inertia-coupling moment will always be opposite in sign to the roll rate. Recalling that to minimize adverse β generation due to kinematic coupling, r must be equal to $p \tan \alpha$, it is obvious that this form of inertia coupling will inhibit stability-axis rolling that can lead to the buildup of large amounts of adverse β which, in turn, can result in loss of control at high angles of attack.

This section has briefly reviewed kinematic- and inertia-coupling phenomena that, in various degrees, are important to the high α flight dynamics of all modern fighter aircraft. In the section entitled "Departure- and Spin-Resistance Simulation Results," it will be seen how these phenomena interact to significantly influence the characteristics of the subject configuration.

DEPARTURE- AND SPIN-RESISTANCE SIMULATION RESULTS

Basic Control System

The first portion of the simulation investigation consisted of documenting the normal stall-, departure-, and spin-resistance characteristics of the configuration equipped with the basic flight control system described in appendix A. For convenience, this system will be referred to as control system A in this report. Figure 18 shows time histories of a 1g stall to the limit angle of attack ($\alpha = 25^{\circ}$). Rudder doublets were applied at various angles of attack to evaluate lateral-directional stability at these conditions. The data show that the motions were well damped and that the airplane exhibited no tendency toward directional divergence within its normal α envelope, as predicted by the $C_{n_{\beta,dyn}}$ criterion. In addition, application of lateral stick inputs at $\alpha = 25^{\circ}$ resulted in rapid roll response in the commanded direction, as predicted by the LCDP values discussed previously.

Further evaluation of departure/spin resistance was performed by applying cross controls in 1g and accelerated conditions. Figure 19 shows time histories of the motions resulting from cross-control application from 1g trim at $\alpha = 25^{\circ}$. The control traces show that although the pilot was holding full right stick and full left pedal, the roll and yaw controls deflected in a coordinated sense, primarily due to the ARI and the α fade-out of pilot rudder inputs. As a result, the airplane rolled and yawed in the direction of the stick input. Note that the roll and yaw rates were sufficiently high to produce a significant nose-up pitching moment (see $\dot{q}_{icl}$ trace) caused by the inertia-coupling phenomenon previously discussed. This effect caused the airplane to pitch up so that the angle of attack continued to increase beyond 29°. At this point (t = 8.5 sec), the automatic departure-/spin-prevention system activated and applied roll and yaw controls to oppose the yaw rate. As a result, r decreased, which reduced the inertia-coupling moment. Furthermore, the reduction in yaw rate increased the α/β kinematic coupling since the airplane was now rolling more closely about its body axis; the result was a trade-off of angle of attack for sideslip, as evidenced by the rapid growth in adverse β and $\dot{w}_{ac2}$ becoming sharply more negative. The combination of increased kinematic coupling and reduced inertia coupling reversed the growth of angle of attack and caused it to drop back below 29°. Cross controls were held for an additional 9 sec but resulted in no prolonged departure or loss of control. The angle of attack varied between 20° and 36°, and the maximum yaw rate obtained was 48°/sec.

The response to cross controls applied at the limit angle of attack in an accelerated turn is shown in figure 20. As can be seen, the motions were very similar to the 1g case, with inertia coupling causing a "pitch-out" departure in which α increased to about 36°; however, there was no tendency for the departure to develop into a spin. These results indicated that (1) inertia coupling could overpower the α limiter system to cause α to increase far above the 25° limit and (2) the airframe's inherent lateral-directional stability, combined with the effectiveness of the automatic spin-prevention system, minimized the possibility of a departure progressing into a spin entry.

It quickly became obvious that roll-pitch inertial coupling would be a primary cause of departures on this configuration. The reason for its importance is illustrated in figure 21. Shown is the variation with roll rate of the nose-up inertial-coupling moment caused by stability axis rolling; note that the moment varies with p_{stab}^2 so that very significant moments can be produced at high roll rates. Also shown are representations of the available nose-down control moment for a specified α at two values of dynamic pressure, $\bar{q}_1$ and $\bar{q}_2$ ($\bar{q}_1 < \bar{q}_2$). The points of intersection with the coupling-moment curve indicate the highest roll rates (p_1^* and p_2^*) at which there is sufficient control moment to counter the nose-up coupling moment. If p_{stab} should increase and be sustained above these values, then it is very likely that a pitch-out departure will occur. Note that $p_1^* < p_2^*$, which indicates that the susceptibility to this type of departure becomes more acute as dynamic pressure decreases.

The foregoing observations are apparent in figure 22, which shows an attempted 360° roll, starting from a 1g trim condition at $\alpha = 25^\circ$, using full lateral stick input. Note that in addition to maximum roll-control deflections, 30° of coordinating rudder was also obtained due to the ARI. As a result, the roll and yaw rates began to build up rapidly in the direction of stick input. Initially, α dropped to about 20° due to kinematic coupling; however as p and r increased, the inertia-coupling moment (see $\dot{q}_{icl}$ trace) caused a significant nose-up pitch rate to build up and α began to increase. At this point, q coupled with p to create a yaw coupling moment which opposed the yaw rate (see $\dot{r}_{icl}$ trace) and halted its growth ($t \cong 5$ sec); on the other hand, p was still increasing and thus resulted in the kinematic generation of a large amount of adverse β ($t \cong 6$ sec). By this time, α had increased to above 30°, despite the angle-of-attack limiter system applying full nose-down stabilator deflection ($\delta_h = +25^\circ$). Comparison of $\dot{q}_{icl}$ to $\dot{q}_a$ shows that, at this point, the nose-up coupling moment was much greater than the nose-down aerodynamic moment produced by $\delta_h = +25^\circ$; as a result, a pitch-out departure occurred as the airplane completed about 300° of the roll. During this period of loss of control, which lasted about 5.5 sec, α reached a maximum of 41° while β oscillated between ±25°. However, there was no tendency for the yaw rate to diverge into a spin entry (maximum $r \cong 33^\circ$/sec).

An attempted 360° roll from an accelerated turn at the limit α is shown in figure 23. In this case, the pilot banked the airplane to $\phi \cong -60^\circ$ and rapidly applied maximum pitch command, which resulted in about 3.7g as α increased to the limiter value ($\alpha = 25^\circ$). At $V = 170$ knots, the pilot applied and held full right lateral stick input in attempting the roll. The time histories show that the resulting motions are quite similar to those obtained at 1g in that the airplane experienced a pitch-out departure upon completing about 270° of $\Delta\phi$. Again, despite the large excursions in α and β during the loss-of-control period, the yaw rate did not build up and the airplane did not enter a spin.

Because full 360° rolls are not very useful from a tactical viewpoint, assessment was also made of the effects of rolling through smaller bank-angle changes ($\Delta\phi \cong 180^\circ$). Figure 24 shows 70° bank-to-bank reversals using maximum lateral stick inputs starting from 1g trim at $\alpha = 25^\circ$. As expected, the angle-of-attack excursions due to inertia coupling were less than that encountered in the full 360° roll; α never exceeded 32°. Nevertheless, the stabilators were very near saturation ($\delta_h = +25^{\circ}$) during each reversal. Furthermore, large adverse sideslip excursions occurred (reaching -18° at one point), caused by kinematic coupling resulting from the high roll rates combined with insufficient yaw rate $\left(|r| < |p| \tan \alpha\right)$.

These results, along with those obtained in the 360° rolls, strongly indicated that the airplane roll-rate capability at high angles of attack could result in (1) pitch-out departures due to insufficient nose-down pitch control and (2) large adverse sideslip excursions due to insufficient coordinating yaw control. In summary, the airplane equipped with control system A was found to be susceptible to inertia-coupling departures during large-amplitude roll maneuvers. There was no tendency, however, for the departures to progress into spin entries.

Control-System Modifications

Control system B.- It became evident that the most obvious means of alleviating the pitch-out departure problem (other than resizing the airplane control surfaces or further limiting its α envelope) was to limit the airplane roll-rate capability at high angles of attack. Therefore, an alternate flight control system with a lower roll-rate-command limit was investigated. If a pitch-out departure (defined as α exceeding 30°) occurred, the maximum roll rate was reduced. Three center-of-gravity locations were investigated: (1) $0.35\bar{c}$, which is the nominal location and results in a static margin of about a negative 4 percent at low α; (2) $0.41\bar{c}$ which, although outside of the operational center-of-gravity range of the airplane, was chosen to indicate how severely roll performance would have to be compromised in this extreme case; and (3) $0.29\bar{c}$, chosen to indicate the roll performance that the airplane would have if it did not incorporate RSS (positive 2-percent static margin).

The results of the center-of-gravity study are summarized in figure 25. As expected, the $0.29\bar{c}$ (SM = 0.02) configuration did not have an inertia-coupling pitch-out problem, and maximum roll rate was limited only by the available roll control. To avoid coupled departures with the center of gravity at $0.35\bar{c}$ (SM = -0.04), the roll rate above $\alpha = 20^{\circ}$ had to be restricted to values below what the roll control is capable of providing. Comparison to the results obtained at $0.29\bar{c}$ indicates that about a 30-percent penalty in maximum roll rate is incurred at $\alpha = 25^{\circ}$ due to the desire to fly the airplane at a static margin of -0.04. As the center of gravity is moved farther aft of $0.35\bar{c}$, the roll-performance penalty rapidly becomes more severe, as indicated by the data for SM = -0.10. At this level of instability, the roll rate had to be restricted above $\alpha = 13^{\circ}$ such that at $\alpha = 25^{\circ}$, the maximum allowable roll rate was only about 30 percent of what the roll control is capable of providing. Beyond their implications for the subject configuration, these results indicate that future CCV designs incorporating high levels of static pitch instability may face very substantial roll-performance penalties unless they are provided with sufficient nose-down pitch control to prevent inertia-coupling pitch-out departures.

Once an indication of the maximum sustainable roll rates was obtained, a roll-rate limiting scheme was implemented on the subject airplane. As previously discussed, the basic control system includes a high-gain roll-rate-command augmentation system in which the pilot commands a roll rate proportional to lateral stick force, up to a maximum of 308°/sec. (See appendix A.) Obviously, the most straightforward technique for limiting the airplane roll rate is simply to limit the roll rate that the pilot commands. The difficulty lies in determining which parameters to use to evaluate what the roll limit should be at any particular instant. Three roll-rate-scheduling parameters were investigated: angle of attack, dynamic pressure, and symmetric stabilator deflection.

There were two reasons for considering angle of attack as a scheduling parameter: (1) the nose-up inertia-coupling moment varies with $\sin 2\alpha$, and (2) as shown in figure 10, the amount of nose-down control movement available to counter the nose-up coupling moment decreases as angle of attack increases. The same reasoning was used in choosing $\bar{q}$; as illustrated in figure 21, the nose-down control moment decreases with $\bar{q}$, which results in lower rates of roll that can be sustained before a pitch-out departure occurs. Symmetric stabilator deflection was thought to be a proper scheduling parameter in that it directly indicates the pitch control remaining to counter the inertia-coupling moment. The three scheduling schemes were evaluated individually, and it was found that two basic drawbacks are inherent (to varying degrees) with each scheme, as illustrated in table IV.

The use of α and $\bar{q}$ scheduling resulted in the greatest degradation in initial roll response because they do not differentiate between large-amplitude rolling maneuvers ($\Delta\phi \cong 360^{\circ}$) where limiting is needed and smaller amplitude rolls ($\Delta\phi < 120^{\circ}$) which are of sufficiently short duration to preclude pitch-out due to inertia coupling. Scheduling versus stabilator deflection minimizes loss in initial roll response because it operates as a direct function of the remaining restoring control moment. Unfortunately, this scheme also increases the coupling between pitch and roll motions because roll rate is being influenced by the primary pitch control. This increased cross-axes coupling can manifest itself as oscillations about both the roll and pitch axes. It was found that combining all three parameters (α, $\bar{q}$, δ_h) resulted in the most satisfactory compromise in terms of minimizing both initial roll-response degradation and cross-axes coupling.

The control law developed to limit roll rate is shown in figure 26. (The control system incorporating this modification will henceforth be referred to as control system B.) Roll-rate limiting was achieved by reducing maximum commandable roll rate $(p_{com})_{max}$ from the normal value of 308°/sec to as little as 80°/sec, based on instantaneous values of $\bar{q}$, α_i, and $\delta_{h,c}$. The variation with dynamic pressure was $-0.0115^{\circ}/\text{sec}/\text{N/m}^2$ ($-0.55^{\circ}/\text{sec}/\text{lb/ft}^2$) for $\bar{q} < 10\ 500\ \text{N/m}^2$ (219.3 lb/ft²). (The value of 10 500 N/m² corresponds to an indicated airspeed of 250 knots.) This was combined with a reduction of 4°/sec/deg of angle of attack for $\alpha > 15^{\circ}$. Finally, nose-down symmetric stabilator deflections in excess of 5° caused a reduction of commanded roll rate of 4°/sec/deg.

The resulting limit on commanded roll rate is illustrated in figure 27, which shows $(p_{com})_{max}$ versus α for 1g trim flight conditions. With the stabilator deflected for trimmed flight, $(p_{com})_{max}$ is reduced from 280°/sec at $\alpha = 5^{\circ}$ to 170°/sec at $\alpha = 25^{\circ}$; these values would be representative of the $(p_{com})_{max}$ available at the initiation of a roll. Also shown are the values that represent the situation in which full control has been used to counter the inertia-coupling moment with the stabilators deflected full nose down ($\delta_h = +25^{\circ}$). As shown in the figure, this case results in a decrease of 80°/sec in $(p_{com})_{max}$ from the values obtained at trim δ_h such that the maximum commandable roll rate is only about 90°/sec at $\alpha = 25^{\circ}$.

Control system B also incorporated a modification to the pitch axis to assure proper stabilator response during rolling maneuvers. This modification is shown in figure 28 and involved creating an equivalent angle-of-attack signal $\Delta\alpha_p$ based on roll-rate magnitude. The variation of $\Delta\alpha_p$ with $|p|$ is plotted in figure 29; note that a 20°/sec deadband was included so that the system was inactive during low-rate, precision maneuvers when it was not needed. The pseudo angle-of-attack signal was fed to the α limiter, which recognized it as an increase in α and therefore applied nose-down stabilator deflection to oppose it. This system, therefore, assured that the pitch control was deflected in the proper direction to oppose the nose-up coupling moment generated by rapid rolling at high angles of attack.

The effectiveness of control system B in preventing inertia-coupling pitch-out departures is illustrated in figure 30, which shows a 360° roll initiated from 1g trim at $\alpha = 25^{\circ}$ using full lateral stick input. As previously discussed, this maneuver, when performed with the basic control system (control system A), resulted in loss of control. (See fig. 22.) For control system B, figure 30 shows that although the pilot applied maximum lateral stick input, the resulting commanded roll rate was limited to only about 165°/sec (as opposed to 308°/sec for control system A) so that the maximum roll rate achieved was 70°/sec. The resulting nose-up coupling moment was smaller, and there was sufficient aerodynamic nose-down control moment to essentially cancel it, as can be seen by comparing the $\dot{q}_{icl}$ and $\dot{q}_a$ traces. As a result, α never exceeded 26° during the maneuver and the maximum β generated was less than 3°. Thus, in this particular situation at least, roll-rate limiting eliminated the two problems experienced with the basic airplane, that is, α pitch-outs due to excessive roll-pitch coupling and large β excursions due to excessive roll-yaw coupling. Examination of the control traces shows that significantly less than maximum roll-control deflections were used. Even in the initiation of the roll when p is low and coupling is therefore not a problem, only -15° of the available -21.5° of δ_a was obtained. The net result is a slower initial roll response compared with that of the basic airplane (control system A); as discussed previously, this response degradation is due mainly to the use of $\bar{q}$ and α in the limiting scheme. One other point to note on the control time histories is that only about 60 percent of the available rudder is used for coordination through most of the maneuver.

A 360° roll initiated from an accelerated turn at the α limit is shown in figure 31. The results are very similar to the 1g case in that the maneuver was well controlled, with the airplane never approaching an out-of-control condition.

Time histories of the 70° bank-to-bank reversals initiated from 1g trim at $\alpha = 25°$ are shown in figure 32. Again the roll-rate limiting scheme of control system B significantly improved the controllability of the airplane in this maneuver. Angle of attack was maintained below 28° and sideslip excursions below 4°. These results should be contrasted with those obtained with the basic airplane (fig. 24), which encountered momentary departures with α exceeding 32° and β excursions above 15°.

Classical spin-susceptibility testing was conducted by applying cross-controls in 1g and accelerated conditions. An example is shown in figure 33, in which cross controls were applied from an accelerated turn at the limit α. As obtained with the basic control system, the inertia coupling resulting from the generated roll and yaw rates caused α to overshoot above the 25° limit; however, α never exceeded 30°, β was maintained below 11°, and the maximum yaw rate encountered was only about 28°/sec. Recovery was obtained immediately after the controls were neutralized.

The results to this point indicated that the control modifications incorporated in control system B significantly enhanced the departure resistance of the subject airplane in high α maneuvers, during which lateral stick alone or cross controls were used. This improvement resulted primarily from the fact that the pilot was constrained to command less roll- and yaw-control deflections through lateral stick deflections due to the roll-rate limiting scheme employed. However, it was still possible for the pilot to augment rudder deflection by applying pedal inputs in the direction of the lateral stick input. Therefore, an assessment was made to examine how the additional rudder might affect the departure-resistance characteristics of the configuration.

Figure 34 shows time histories of a 360° roll initiated from 1g trim at $\alpha = 25°$ with maximum coordinated stick and pedal inputs. As previously discussed, performance of this maneuver with lateral stick alone resulted in a well-controlled roll, with little fear of encountering a pitch-out departure. (See fig. 30.) However, application of coordinating pedals resulted in quite a different situation, as shown in figure 34. Examination of the control traces indicates that the primary difference in the control inputs was obtaining sustained full (-30°) rudder deflection; the roll-control deflections, on the other hand, were about the same as obtained in the earlier stick-only maneuver. The combination of very large rudder deflections and reduced aileron and differential-tail deflection resulted in overcoordination of roll, to the point that some 8° of proverse β was generated. This large amount of proverse sideslip was detrimental for two reasons: (1) it acted through dihedral effect to augment the roll rate, which in turn coupled with the higher yaw rate caused by the larger δ_r to substantially increase the nose-up inertia-coupling moment (see $\dot{q}_{ic1}$); and (2) it kinematically coupled with the high roll rate to cause an increase in angle of attack ($\dot{\alpha} \cong -p\beta$, see $\dot{w}_{ac2}$). The result was a rapid pitch-out departure despite the application of full nose-down stabilator by the control system; angle of attack reached a maximum of 70°, whereas sideslip oscillated $\pm 30^{\circ}$ during the departure. Use of full coordinated inputs to perform 360° rolls at other 1g and accelerated flight conditions resulted in similar loss of control situations.

In summary, control system B was found to significantly enhance the departure resistance of the subject airplane as long as coordinating pedal inputs were not used during large-amplitude roll maneuvers. Use of large amounts of coordinating pedal in these maneuvers often resulted in severe pitch-out departures. It should be pointed out that there should be no need for the pilot to apply coordinating rudder inputs since this is automatically done for him by the ARI. However, it is felt that during air combat there would be a strong tendency by the pilot to use rudder pedals in an attempt to obtain maximum roll performance, particularly in view of the fact that the roll-rate limiting scheme of control system B resulted in noticeable degradation in the initial roll response of the airplane.

Control system C.- Based on the foregoing results, an attempt was made to correct the two primary deficiencies of the airplane equipped with control system B, that is, (1) susceptibility to pitch-out departures when coordinating pedal inputs are used, and (2) initial roll-response degradation. To accomplish this objective, two modifications to control system B were developed and are shown in figure 35. For convenience, the control system incorporating these additional features will be referred to as control system C. Alleviation of the pitch-out departure problem due to excessive use of coordinating rudder pedals was accomplished by using a scheduled gain in the pilot rudder command path which faded out pilot inputs between roll-rate magnitudes of 20°/sec and 40°/sec. Elimination of pilot rudder inputs at high roll rates $\left(|p| \geqq 40^{\circ}/\text{sec}\right)$ was designed to eliminate any aggravation of the inertia-coupling pitch-out problem. At low roll rates $\left(|p| \leqq 20^{\circ}/\text{sec}\right)$, however, the system allowed the pilot full use of the rudders ($\alpha_i \leqq 20^{\circ}$) and therefore did not detract from his ability to perform smaller amplitude, precision maneuvers such as tracking corrections. The second deficiency of control system B, degraded initial roll response, was corrected by adding a scheduled gain to the roll-rate limiting path such that the limiting did not become fully effective until the roll-rate magnitude exceeded 50°/sec; furthermore, all limiting was eliminated for $|p| \leqq 30^{\circ}$/sec. This scheme, therefore, imposed limiting only at the higher roll rates where it was needed to prevent inertia-coupling departures; at the lower roll rates, however, the pilot was allowed full roll capability so as to obtain maximum initial roll response from the airplane.

The effectiveness of control system C in resolving the critical roll-response problem is illustrated in figure 36, which shows a full lateral stick, 360° roll initiated from 1g flight at $\alpha = 25^{\circ}$. These time histories should be compared with those obtained in the same maneuver with control systems A and B (figs. 22 and 30). Note that with control system C, maximum roll- and yaw-control deflections were obtained during initiation of the roll; in fact, in this phase of the maneuver, the control motions with control system C were very similar to those obtained with the basic control system without roll-rate limiting (control system A). As previously discussed, only about 75 percent of the maximum roll control was available to initiate the maneuver when control system B was used. In examining the response obtained with control system C, it is seen that as the roll rate increased to values where inertia coupling became a factor, roll-rate limiting was imposed and the roll- and yaw-control deflections were reduced to essentially the levels obtained with control system B; a pitch-out departure was avoided.

A quantitative comparison of roll response obtained in this maneuver with all three control systems is shown in table V. The figure of merit that was used was time to bank to 90° and 180°. The data for $\Delta t_{\phi=90^\circ}$ indicate that control system B suffered a 15-percent degradation in response when compared with control system A, whereas there was no degradation with control system C. For 180° of roll, control system C was only 3 percent slower than A, as compared with 13 percent slower for control system B. In summary, control system C was successful in combining the desirable features of control system A (high initial roll response) and control system B (high resistance to inertia-coupling departure) without incurring the deficiencies of either system.

The ability of control system C to prevent pitch-out departures due to excessive pilot coordinating rudder is illustrated in figure 37. Shown are time histories of a 360° roll from 1g trim at $\alpha = 25^\circ$ using full coordinated stick and pedal inputs. It is seen that fade-out of the pilot rudder commands above $|p| = 50^\circ$ caused the resulting airplane motions to be essentially identical to those obtained using lateral stick alone. The maximum angle of attack reached was 25°, and the airplane was not near a departure condition at any point in the maneuver. These results should be contrasted with those obtained with control system B, where a rapid pitch-out departure to $\alpha = 70^\circ$ was encountered (fig. 34).

Further evaluation of departure/spin susceptibility was accomplished by applying maximum cross controls at 1g and accelerated flight conditions. An example is shown in figure 38, in which the controls were applied from 1g trim at $\alpha = 25^\circ$. The time histories show that although full prospin controls were held for 14 sec, α did not exceed 26° and yaw rate was maintained below 35°/sec.

Figure 39 shows cross controls applied from 1g trim at $\alpha = 10^\circ$, followed immediately by rapid full aft stick application. The inertia-coupling moment, combined with the full nose-up pilot command, resulted in α increasing to 28°. Nevertheless, there was sufficient aerodynamic control moment to prevent further α excursions such that although the prospin inputs were held for over 12 sec, angle of attack never exceeded the 25° limit.

A further evaluation of the resistance of control system C to inertia-coupling-induced departures is shown in figure 40. The initial conditions for the maneuver were 1g trim flight at $M = 0.6$ and $h_o = 9144$ m. From this starting point, full lateral stick input was applied, followed immediately by full nose-up pitch command. The large angular rates resulting from these inputs would be expected to maximize inertia-coupling effects. The data show that very high rates, particularly in roll, were generated; however, the limiting features of the control system effectively limited these rates to values that could be handled by the available aerodynamic control moments. As a result, the maximum α excursion was only 27°, despite the fact that the controls were held for approximately 11 sec.

Effect of Aft Center of Gravity

It should be noted that all the maneuvers discussed up to this point were conducted with the airplane center of gravity at its nominal location of $0.35\bar{c}$. As previously discussed, more aft center-of-gravity locations should aggravate the inertia-coupling departure problem because less nose-down aerodynamic control moments would be available. Therefore, a brief investigation was conducted to see what effect more aft center-of-gravity locations might have on the departure-prevention ability of the control system developed for a center of gravity of $0.35\bar{c}$. For this evaluation, center-of-gravity locations of $0.375\bar{c}$ and $0.39\bar{c}$ were evaluated. Figure 41 shows a maximum lateral stick, 360° roll from 1g trim at $\alpha = 25^\circ$ with a center of gravity of $0.375\bar{c}$. The data show that more nose-down stabilator was required to trim at this condition due to the increased static instability caused by the rearward center-of-gravity shift. Comparison of the time histories of this maneuver with those obtained with a center of gravity of $0.35\bar{c}$ (fig. 36) verifies the loss in nose-down aerodynamic pitching moment at $0.375\bar{c}$. This loss is reflected in the δ_h trace which shows that the stabilators were at the full nose-down position through most of the maneuver; nevertheless, angle of attack increased to 27° (as compared with the 25° obtained with a center of gravity of $0.35\bar{c}$). Although a departure did not occur in this case, the fact that the pitch control remained saturated for such an extended period of time and was still unable to hold α below the limit value indicates that control was very marginal in this situation. A more severe coupling maneuver would, therefore, be expected to result in a departure. An example of loss of control is shown in figure 42, which shows the high coupling maneuver previously discussed, in which the pilot applied full roll and pitch inputs from 1g trim flight at $M = 0.6$. As previously discussed, this maneuver performed with the center of gravity at $0.35\bar{c}$ did not result in loss of control. However, figure 42 indicates that with the center of gravity at $0.375\bar{c}$, the available nose-down control was overpowered by the inertia-coupling moment, and a rapid pitch-out to $\alpha = 76^\circ$ ensued. Following the departure, the airplane entered the deep-stall trim condition previously discussed; the deep-stall problem is addressed in more detail in the section entitled "Deep-Stall Simulation Results."

These results indicated that rearward center-of-gravity movement beyond $0.375\bar{c}$ would require further limiting of roll rate in order to obtain an acceptable level of departure resistance. These indications were verified when control system C was flown with the center of gravity at $0.39\bar{c}$. An example is shown in figure 43, which presents time histories of an attempted 360° roll using full lateral stick input starting from 1g trim at $\alpha = 25^\circ$. It is seen that the aerodynamic nose-down control was easily overpowered by the inertia-coupling moment and resulted in a sharp pitch-out departure to $\alpha = 84^\circ$ and entry again into the deep-stall trim condition. Attempts at other roll maneuvers that were accomplished without incident with the center of gravity at $0.35\bar{c}$ resulted in a similar loss of control.

It was found that the airplane equipped with control system C that was flown with the center of gravity at $0.39\bar{c}$ was at least as prone to departures as the basic airplane was at $0.35\bar{c}$. It thus became clear that the roll-rate limit would have to be reduced significantly at a center of gravity of $0.39\bar{c}$ to reestablish a level of departure resistance comparable to that obtained at $0.35\bar{c}$. However, as indicated in figure 25, this level of roll performance may not be adequate from a tactical viewpoint. In summary, control system C was found to provide a high level of departure resistance for the airplane with the center of gravity at its nominal location. Large-amplitude maneuvers at 1g and accelerated flight conditions involving gross application of adverse controls did not result in loss of control. However, rearward center-of-gravity shifts deteriorated departure resistance to the point that it was marginal at $0.375\bar{c}$. Operation at center-of-gravity locations aft of $0.375\bar{c}$ would require further reductions in maximum allowable roll rate.

DEEP-STALL SIMULATION RESULTS

Description of Problem

As discussed in the section entitled "Discussion of Stability and Control Characteristics," the $0.35\bar{c}$ pitching-moment data for the subject configuration exhibit stable deep-stall trim points in the vicinity of $\alpha = 60^{\circ}$, even with the stabilators deflected full nose down. The trim point, however, is comparatively weak, and an investigation therefore was conducted to see if it was possible to fly into a stabilized deep-stall trim point. The departures described in the previous section for aft center-of-gravity locations (figs. 42 and 43) all resulted in the airplane flying into this deep-stall trim condition.

The results of the present study indicated that entry into the deep stall was possible during rolling maneuvers at high angles of attack or from very low airspeed conditions at high angles of attack. One such low airspeed maneuver was to put the airplane into a steep-attitude, decelerating climb, with Θ reaching a maximum of about 70°, with the intention of reaching very low airspeeds at the top of the climb and allowing the airplane to fall through at essentially zero g. The resulting kinematic generation of a large angle-of-attack excursion could not be effectively opposed by the α limiter system due to lack of control effectiveness at low dynamic pressure. An example of such a maneuver is shown in figure 44.

The data of figure 44 show that, at the top of the maneuver, the airspeed and normal acceleration decreased to $M = 0.2$ and 0.1g, respectively. As the airplane fell through, the angle of attack increased to 70°, despite the application of full nose-down pitch control by the α limiter system. After several cycles of oscillation, the airplane stabilized into the deep stall trim point with $\alpha \cong 58^{\circ}$, $\phi \cong 0^{\circ}$, $r \cong 0$, $\Theta \cong 6^{\circ}$, and $a_n \cong 1g$. Note that, at this point, the pilot had absolutely no control over the airplane. In pitch, the α limiter caused the stabilators to remain at the full nose-down position, independent of pilot inputs. In roll and yaw, the automatic spin-prevention system took control away from the pilot, and the system was commanding control deflections to oppose any yaw rate. For a fighter having a fuselage-heavy mass loading, the most effective spin-recovery controls are obtained when the rudders are applied to oppose yaw rate and the ailerons are applied in the direction of the yaw rate. It should be recognized that these systems did successfully prevent any yaw-rate buildup and therefore eliminated the danger of the motions progressing into a spin; nevertheless, this was of little consequence to the pilot since he was locked in the deep-stall condition, with no way of recovering by using his normal controls.

It is important to note that all the maneuvers discussed to this point were conducted with an aerodynamic model which did not include aerodynamic asymmetries; that is, the aerodynamic coefficients C_Y, C_l, and C_n were zero for $\beta = 0^o$ and neutral lateral-directional controls. In the normal angle-of-attack flight envelope of current fighter aircraft, this modeling assumption has been found to be generally valid in that wind-tunnel measured asymmetries are normally insignificantly small. However, experience has shown that, in many configurations, these asymmetries can reach significant magnitudes at post-stall α. Figure 45 shows C_Y, C_l, and C_n asymmetries measured during wind-tunnel tests on the subject configuration. The data confirm that within the normal α flight envelope, these asymmetries are small enough to be ignored. However, they rapidly increase in magnitude for $\alpha > 30^o$. Of particular significance is the fact that the yawing-moment asymmetry reaches its maximum value in the α region of the deep-stall trim point. In order to assess the importance of this characteristic, the deep-stall investigation was conducted with two aerodynamic models, one that included the wind-tunnel measured asymmetries of figure 45 and one that omitted them.

Figure 46 shows time histories of a deep-stall entry with the asymmetries included. Comparison with the results obtained without asymmetries (fig. 44) indicates little difference in the initial phase of the entry. However, once the airplane began to settle into the trim point, figure 44 shows that the nose-left yawing-moment asymmetry caused the yaw rate to build up to about -20^o/sec, despite the application of significant amounts of opposing aileron and rudder deflections by the spin-prevention system. The airplane also assumed a left wing low ($\phi \cong -16^o$) and nose low attitude ($\Theta \cong -23^o$). Note that the nose-up inertia-coupling moment resulting from the nonzero roll and the yaw rates caused the airplane to trim at an angle of attack roughly 4^o higher than that obtained without the asymmetries. Another important indication from these results is that the asymmetries would probably have driven the airplane into a spin without the action of the automatic spin-prevention feature of the control system.

With regard to the ease of experiencing the deep-stall trim, it was found that the first α peak during the entry was critically important in that an overshoot to values of α too much above the trim point resulted in the generation during the downswing of sufficient nose-down pitch rate to drive the airplane nose down over the $C_m > 0$ hump and result in recovery. Generally, the airplane did not consistently drop into the deep-stall trim point if the initial peak in α was greater than 75^o. Control of the initial α excursion was difficult, and the pilots were therefore not able to obtain the deep-stall trim on every attempt.

stick in phase with the airplane motions, with the hope that sufficient angular momentum would be created during a downswing cycle to drive the airplane over the positive C_m hump and back down within the normal α envelope of the airplane.

A recovery attempt using this technique is shown in figure 50. Starting from a stabilized trim at $\alpha \cong 62^\circ$, the pilot activated the pitch rocker system and rapidly applied full aft stick at $t = 71.3$ sec. In response, the stabilators moved from the full nose-down position commanded by the α limiter to full nose up. The resulting nose-up moment caused α to increase to 75°, at which point the pilot reversed his controls and applied full forward stick to obtain $\delta_h = +25^\circ$. This action generated a large nose-down moment, indicated by the $\dot{q}_a$ trace at $t = 74$, and α decreased rapidly. As expected, $\dot{q}_a$ became positive ($t = 75$ sec) for a brief time as α traversed the hump in the C_m curve; however, there was sufficient momentum to cause the airplane to continue to pitch downward until a recovery was obtained at $t = 78$ sec. It should be noted that in this particular case, the pilot very accurately kept his inputs in phase with the motions and therefore obtained a recovery within 1 cycle of the oscillation. However, it was found that in situations where the pilot was somewhat out of phase with the oscillation, recoveries were delayed significantly so that as many as three to four pumping cycles were required for recovery.

Further assessment of the deep-stall and recovery characteristics were obtained by moving the center of gravity aft to $0.375\bar{c}$. Figure 51 shows an entry and recovery attempt using the speed brakes and flaps; aerodynamic asymmetries were not modeled in this case. As can be seen, trim was achieved at $\alpha = 60^\circ$ with $r = 0$, $\phi = -13^\circ$, and $\Theta = 0$. At $t = 67.5$, the speed brakes were deployed and the flaps reconfigured, and a rapid recovery was obtained in 4.5 sec. A quite different result was obtained with asymmetry modeling; an example is shown in figure 52. The data indicate that the airplane trimmed at a mean angle of attack of about 65°, with the asymmetries causing a yaw rate of -16°/sec. At $t = 65$ sec, recovery was attempted using the speed brake and flaps. As can be seen, the resulting nose-down pitching-moment increment caused α to decrease by about 4°; however, it was not sufficient to effect recovery and the airplane established another trim condition with $\alpha \cong 63^\circ$ and $r = -20^\circ$/sec.

Generally, it was found that recovery to normal flight conditions could not be attained with this technique unless the pilot made the speed-brake and flap change early in the entry while there were still large oscillations in the motion and unless the inputs were made during a downswing in α so that they reinforced the downward motion. Obviously this is very difficult to do, and in the majority of cases, recovery was not obtained. The primary reason for the difference in the results obtained with and without asymmetry modeling was the existence of the yaw rate with modeling. Apparently, the additional nose-up inertia-coupling moment caused by the angular rate was sufficient to negate the relatively small amount of nose-down moment generated by the speed-brake and flap changes.

Methods of Recovery

Once it was determined that the airplane could be flown into the deep-stall trim point, techniques were developed to recover from it. As previously discussed, the primary controls could not be used because the pilot had no control over them in this situation. Consequently, other schemes for obtaining the needed nose-down pitching moment were investigated in the wind tunnel, and two potentially useful concepts were identified. The first method involved reconfiguring the flaps by retracting the leading-edge flaps and deploying the trailing-edge flaps ($\delta_{lef} = 0^{\circ}$, $\delta_{tef} = 20^{\circ}$), whereas the second involved speed-brake extension to maximum deflection ($\delta_{sb} = 60^{\circ}$). The locations of these surfaces are shown in figure 2. Note that the speed brakes are located on the upper and lower surfaces of the aft fuselage shelf next to the stabilators, and their deployment therefore would be expected to provide a nose-down moment in the deep-stall region.

Figure 47 compares the resulting pitching moments with those for the normal configuration ($\delta_{lef} = 25^{\circ}$, $\delta_{tef} = 0^{\circ}$, $\delta_{sb} = 0^{\circ}$); note that all data are for the full nose-down stabilator deflection that would be maintained by the α limiter system. The data show that reconfiguring the flaps provides an increment of about -0.018 in C_m in the angle-of-attack range of interest (55° to 60°), whereas speed-brake deployment results in about -0.025. Note that neither scheme clearly eliminates the trim point with the center of gravity at $0.35\bar{c}$, and therefore they would not be expected to be always effective, particularly for center-of-gravity locations aft of $0.35\bar{c}$. However, as shown in figure 47, combining the two schemes results in a pitching-moment-coefficient increment of about -0.05, which eliminates the deep-stall trim point.

Figures 48 and 49 show time histories of recovery attempts using the combination of speed-brake deployment and flap reconfiguration. The results obtained without asymmetry modeling are shown in figure 48. The recovery attempt was initiated at $t = 78$ sec, with the airplane stabilized in the deep-stall trim, and, as can be seen, a rapid, positive recovery was obtained within 4 sec. The results with asymmetry modeling are shown in figure 49. Although a positive recovery was also attained, the recovery was not as rapid, taking some 8 sec to occur. The reason for the slower recovery was the existence of the yaw rate which created an additional nose-up moment due to inertia coupling that had to be overcome by the nose-down recovery moment.

One additional recovery technique that was investigated consisted of reconfiguring the pitch control law to reestablish pilot control over the stabilators in the deep-stall region. The reconfiguration involved deactivating all feedbacks, including the α limiter system, so that the only signal that remained was the pilot stick command. With this system (henceforth to be referred to as the pitch rocker), the deflection of pitch control was directly proportional to pilot inputs. The reason for doing this can be seen by reviewing the pitching-moment data for maximum stabilator deflections shown in figure 10. The data show that at the deep-stall trim point ($\alpha \cong 60^{\circ}$), a large pitching-moment increment results in going from full nose-down to full nose-up control deflection ($\Delta C_m \cong 0.1$). Thus, a possibility exists to use this available control moment to initiate and build up a pitch oscillation by moving the

The effectiveness of the "pitch-rocking" technique in providing recoveries with the center of gravity at $0.375\bar{c}$ is illustrated in figure 53. In this particular case, pitch rocking was initiated early in the entry (t = 52 sec) while the motions were still quite oscillatory; in addition, the pilot did a very good job of phasing his inputs in that the initial aft stick applications were made just as the airplane was beginning a nose-up cycle. As a result, α was driven up to 84° and sufficient momentum was generated in the following downswing to reestablish normal flight. The recovery was obtained within 8 sec after the pilot initiated recovery action. Figure 54 illustrates the results that were obtained when the pilot did not optimally phase his rocking inputs with the airplane motions. In this case, recovery was not obtained until the pilot had completed five rocking cycles, and the time interval between initiation of recovery action and actual attainment of recovery was some 30 sec. These results emphasize the criticality of proper pilot usage of the pitch-rocking technique; nevertheless, this technique was found to be effective in providing deep-stall recovery for all the conditions (center-of-gravity location and asymmetry modeling) investigated in this study.

TRACKING RESULTS

Following completion of the departure, deep-stall, and spin-susceptibility investigation, the tracking evaluation phase of the study was conducted to determine how these characteristics and the control-system changes affected the ability to track a target airplane through maneuvers representative of air combat. The evaluation was conducted at the nominal $0.35\bar{c}$ center-of-gravity location and included an assessment of the three control-system configurations studied in the first phase.

Results of Basic Control System (Control System A)

Time histories of the airplane motions during the wind-up turn tracking task are shown in figure 55; included are the range between the two airplanes R, the total angular tracking error ε, and the lateral component of ε λ. The data indicate that the pilot had little difficulty in tracking the target airplane through the task. Note that the design of the lateral-directional control system allowed him to track using only the stick, and no pedal inputs were required. The airplane motions were well damped and, as expected, none of the inertia-coupling problems previously discussed were encountered in this task due to the absence of any large-amplitude rolling maneuvering.

Figure 56 illustrates the performance of the airplane with the basic control system (control system A) in the bank-to-bank tracking task. As indicated by the pilot-input time histories, this was a much more demanding task than the wind-up turn in that a combination of bank-to-bank reversals followed by rapid pull-ups to high α was required to maintain tracking. The very dynamic nature of the task requiring rapid and accurate control in all three axes simultaneously tended to accentuate any handling-quality deficiencies. Note that the pilot used very large lateral stick inputs to make the reversals, and the inertia-coupling moments resulting from the high roll and yaw rates required large countering nose-down stabilator deflections. Maximum α and β excursions were 30° and 10°, respectively. The ε and λ data show that the pilot had difficulty in maintaining tracking during the reversals; however, once the reversal was completed, he was able to reacquire the target within about 5 to 10 sec. It should be pointed out that the pilot was aware of the potential pitch-out tendency if too much coordinating rudder was used, and he therefore flew the task essentially without pedal inputs. Furthermore, by using only the stick, the amplitude of the bank-angle changes that were required $\left(|\Delta\phi| \leqq 180^{\circ}\right)$ was insufficient to cause a departure due to inertia coupling. As a result, no departures were observed during any of the runs made on this task.

The performance of the basic airplane in the ACM task is illustrated in figure 57. As previously discussed, this task required two rapid, large-amplitude $\left(|\Delta\phi| \cong 180^{\circ}\right)$ rolls at the limit α and low airspeeds and therefore exposed the airplane to potential inertia-coupling departure situations. The data show that in this particular run, a near-departure condition occurred during the first roll maneuver in that full nose-down stabilator was held for over 1 sec to oppose the nose-up coupling moment; maximum α reached 29°. No further near-loss-of-control situations occurred during the remainder of the run. Note that, again, the pilot did not use pedal inputs; this factor certainly accounted, to some extent, for the fact that no pitch-out departures were encountered.

Results of Control Systems B and C

Effects on tracking capability resulting from the control-system modifications incorporated in control systems B and C were assessed by flying the airplane equipped with these systems against the three tracking tasks. The results were compared with those obtained with the basic control system (control system A) to determine whether the roll-rate limiting schemes used to enhance departure resistance had significantly degraded the tactical effectiveness of the airplane.

The results obtained for control systems B and C in the wind-up turn task are essentially identical to those obtained with the basic control system. This was an expected result since this task did not require any rapid, large-amplitude roll maneuvers.

Figure 58 illustrates the performance of the airplane equipped with control system B in the bank-to-bank tracking task. This figure should be compared with figure 56, which shows the basic airplane flying against the same task. Although the pilot generally applied similar amplitude lateral stick inputs in both cases, the resulting roll- and yaw-control deflections were significantly less in control system B due to the rate limiting scheme previously discussed. As a result, the roll and yaw rates were lower, and the reduced inertia-coupling moments are reflected in the decreased use of large nose-down stabilator deflections. Comparison of β traces also shows the reduction in sideslip excursions seen earlier during the departure susceptibility evaluation. The pilots commented that they noticed a definite degradation in initial roll response in going from control system A to control system B. They indicated that this was mildly bothersome since they felt that they had to hold large lateral stick forces longer in order to obtain the same net roll response. One small positive aspect of the slower roll response noted by the pilots was that it reduced the tendency to overcontrol during tracking. This characteristic can be seen by comparing the lateral input traces, which show that the inputs were somewhat less oscillatory with control system B than with A. Overall, the pilots stated that the reduced roll-response characteristic of control system B did not significantly affect their ability to track the target through this task. Comparison of the ε and λ traces tends to confirm this observation.

An example of tracking performance in the bank-to-bank task for the airplane equipped with control system C is shown in figure 59. The time histories show that the pilot accurately tracked the target through all the reversals except the final one. The pilots commented that the initial roll response obtained with this system was noticeably better than that of control system B and was only very slightly slower than that of the basic airplane. Moreover, the improved sideslip control (much smaller sideslip excursions) resulting from the proper limiting of roll rate resulted in much improved bank-angle control; the pilot was able to make the roll reversals rapidly and cleanly with a minimum of oscillations. Comparison of the time histories of lateral stick input in figures 59 and 56 indicates a markedly smoother, less oscillatory trace with control system C than with control system A. Overall, the pilots stated that they could track slightly better and with less workload with control system C than with either A or B.

When the airplane equipped with control systems B and C was flown in the ACM task, the comparative results were essentially the same as those obtained in the bank-to-bank task. Representative runs are shown in figures 60 and 61 for control systems B and C, respectively. Again, the pilots noted the degraded roll response of B but commented that it did not significantly affect their tracking ability. Again, they mildly preferred C over the other two control systems due to the characteristics previously discussed.

In summary, the tracking evaluation phase of the study determined that the roll-rate limiting scheme that was used to prevent pitch-out departures resulted in no significant degradation in tracking capability. On the contrary, the control system using roll-rate limiting but also incorporating features to minimize initial roll-response loss (control system C) was found to provide slightly improved tracking while reducing pilot workload. It should be reemphasized that the evaluation was conducted at the nominal center-of-gravity location of $0.35\bar{c}$. As previously discussed, operation at center-of-gravity locations farther aft, particularly aft of $0.375\bar{c}$, will require further limiting of roll rate to minimize susceptibility to pitch-out departures; the resulting roll-performance degradation would be expected to degrade tracking ability significantly more than previously indicated. With regard to deep-stall trim, it should be pointed out that no deep-stall entries occurred during any of the tracking runs. This was not an unexpected result in view of the fact that no pitch-out departures were encountered, and the tracking tasks did not entail extreme low-speed zero g maneuvers.

INTERPRETATION OF RESULTS

The fidelity of the simulation in representing the actual F-16 airplane was evaluated by comparing simulation results with actual airplane flight test data and by having pilots with F-16 experience fly the simulator. Throughout the present study, close coordination was maintained with the flight testing of the full-scale airplane to ensure correlation between simulation and flight and to expedite development of airplane modifications for testing in flight when problems were encountered. As a result, the major characteristics and results derived from this investigation have also been encountered in flight. Flight test results have confirmed that the airplane can experience pitch departures during rolling maneuvers and/or low-airspeed maneuvers at high angles of attack. Flight results have also shown that the airplane can enter the deep-stall trim condition from the flight conditions described herein. Moreover, the various control-system modifications and deep-stall recovery methods studied in the present simulation have been flight tested and were found to be as effective as the simulation predicted.

It should be recognized, however, that the present study was limited in scope, and these limitations should be kept in mind when applying the results and conclusions of this study. A primary limitation is that the aerodynamic data were measured at low values of Mach number and did not incorporate any compressibility effect; consequently, the results can only be considered valid for Mach numbers less than about 0.6. It should also be kept in mind that only the clean configuration was investigated and that it is likely that certain store configurations (particularly asymmetrical stores) can degrade the departure/spin resistance of the airplane.

SUMMARY OF RESULTS

A piloted simulator investigation has been conducted to evaluate the high-angle-of-attack characteristics of an F-16-based fighter configuration incorporating relaxed longitudinal static stability. The following major results were derived from this study:

1. The airplane with the basic control system was found to be resistant to the classical yaw or nose slice departure; however, it was susceptible to pitch departures caused by having insufficient nose-down control to counter the inertia-coupling moment generated during rapid, large-amplitude roll maneuvers. In addition, the airplane was susceptible to pitch departures when flown to very low airspeeds at high angles of attack.

2. Pitch-out departures produced by inertial coupling were prevented by limiting the maximum roll rates at the lower speeds and higher angle-of-attack flight conditions.

3. A modified control system incorporating roll-rate limiting and other departure-prevention features made the airplane extremely departure resistant without significantly degrading roll performance. However, the airplane could still be flown to angles of attack above the angle-of-attack limit at very low airspeeds.

4. Although the airplane with the nominal center-of-gravity location could be made more departure resistant without sacrificing maneuverability, it appeared that center-of-gravity locations significantly farther aft would require more drastic roll-performance penalties that could compromise tactical effectiveness.

5. The simulated airplane could be flown into a deep-stall trim condition, from which recovery was not possible with the basic control system using the primary pilot controls. The roll-rate limiting control concept developed in this study could not prevent very low airspeed entries into the deep stall.

6. It was not possible to define reasonable control laws (short of limiting minimum airspeed) which could prevent departure and entry into the deep stall at very low airspeeds. Changes to the airframe to increase high-angle-of-attack longitudinal stability and/or control would probably be necessary to eliminate these problems.

7. Reconfiguring the wing leading- and trailing-edge flaps and deploying the speed brakes generated a sufficient nose-down moment increment to recover the airplane from the deep-stall trim point, provided that the rotation rate was very small. However, steady yaw rates as low as 15°/sec could negate the effectiveness of this recovery technique, particularly at the more aft center-of-gravity locations.

8. It was possible for the pilot to oscillate the airplane out of the deep-stall trim point by applying maximum pitch-control inputs in phase with the airplane motions. The effectiveness of this technique was found to be a direct function of proper input timing by the pilot; with correct pilot action, this technique successfully recovered the airplane, even at the aft center-of-gravity locations investigated. Use of this procedure, however, required a modification to the control system to enable reestablishment of pilot control over the stabilators above the limit angle of attack.

Langley Research Center
National Aeronautics and Space Administration
Hampton, VA 23665
September 20, 1979

APPENDIX A

DESCRIPTION OF CONTROL SYSTEM

Longitudinal

A block diagram of the longitudinal control system used in the simulation is presented in figure 62. The implementation was a fly-by-wire, command augmentation system (CAS) whereby the pilot commanded normal acceleration through a minimum deflection, force-sensing side-stick controller. Washed-out pitch rate and filtered normal acceleration were fed back to give the desired response. A forward-loop integration was used in an attempt to make the steady-state acceleration response match the commanded acceleration. The airplane had slightly negative static longitudinal stability at low Mach number; the desired static stability was provided artificially by the control system by means of angle-of-attack feedback.

The longitudinal control system also incorporated an angle-of-attack limiting system which functioned by using an α feedback to modify the pilot-commanded normal acceleration. The angle-of-attack feedback reduced the commanded normal-acceleration limit by 0.322g/deg between $\alpha = 15^{\circ}$ and 20.4° and by 1.322g/deg above $\alpha = 20.4^{\circ}$. This feature resulted in an angle-of-attack limit in 1g flight of approximately 25°. The maximum allowable positive commanded normal acceleration is shown in figure 63. The stabilator actuator was modeled as a first-order lag of 0.0495 sec, with a rate limit of 60°/sec. The surface deflection limit was $\pm 25^{\circ}$.

Leading-edge flap deflection was scheduled with angle of attack and $\bar{q}/p_s$ according to the following relationship:

$$\delta_{lef} = 1.38 \frac{2S + 7.25}{S + 7.25} \alpha - 9.05 \frac{\bar{q}}{p_s} + 1.45$$

The flap actuator was modeled as a first-order lag of 0.136 sec, with a rate limit of 25°/sec. Maximum flap deflection was 25°.

Lateral

The lateral control system is shown by the block diagram given in figure 64. The system incorporated a roll-rate command feature whereby the pilot commanded roll rates up to a maximum 308°/sec through the force-sensing control stick. Above $\alpha = 29^{\circ}$, an automatic departure-/spin-prevention system is activated which uses a yaw-rate feedback to drive the roll-control surfaces to oppose any yaw-rate buildup. In this mode, the roll-rate CAS is disengaged so that the pilot has no control over the airplane laterally.

The roll-control system uses both aileron and differential-tail deflections at a ratio of 4° of δ_a per 1° of δ_d. The surface actuators were modeled as 0.0495-sec first-order lags, with rate limits of 60°/sec for the differential tail and 80°/sec for the ailerons. The surface deflection limits were $\pm 5.38^{\circ}$ and $\pm 21.5^{\circ}$ for the differential tail and ailerons, respectively.

Directional

A block diagram of the directional control system used in the simulation is presented in figure 65. The pilot rudder input was computed directly from pedal force and was limited to $\pm 30^{\circ}$. Furthermore, this command signal was reduced to zero between 20° and 30° angle of attack in an attempt to prevent departures resulting from excessive pilot rudder usage at high angles of attack. Yaw stability augmentation consisted of feedbacks of $r - p\alpha$ ($\approx r_{stab}$) and a_y. The stability-axis yaw damper provided increased lateral-directional damping in addition to reducing sideslip during high α rolling maneuvers. The lateral acceleration feedback had little effect at the low-speed flight conditions of the present investigation. The directional control system also incorporated an aileron-rudder interconnect (ARI) for improved coordination and roll performance. At low speeds, the ARI gain was scheduled as a linear function of angle of attack with a slope of 0.075/deg. As in the roll axis, above $\alpha = 29^{\circ}$, a departure-/spin-prevention mode is activated which drives the rudder at a gain of 0.75 deg/deg/sec to oppose any yaw-rate buildup. The rudder actuator was modeled as a 0.0495-sec first-order lag with a rate limit of 120°/sec. The total rudder travel was limited to $\pm 30^{\circ}$.

APPENDIX B

DESCRIPTION OF EQUATIONS AND DATA EMPLOYED IN SIMULATION

Equations of Motion

The equations used to describe the motions of the airplanes were nonlinear, six-degree-of-freedom, rigid-body equations referenced to a body-fixed axis system shown in figure 1 and are given as follows:

Forces:

$$\dot{u} = rv - qw - g \sin \Theta + \frac{\bar{q}S}{m} C_{X,t} + \frac{T}{m}$$

$$\dot{v} = pw - ru + g \cos \Theta \sin \phi + \frac{\bar{q}S}{m} C_{Y,t}$$

$$\dot{w} = qu - pv + g \cos \Theta \cos \phi + \frac{\bar{q}S}{m} C_{Z,t}$$

Moments:

$$\dot{p} = \frac{I_Y - I_Z}{I_X} qr + \frac{I_{XZ}}{I_X}(\dot{r} + pq) + \frac{\bar{q}Sb}{I_X} C_{l,t}$$

$$\dot{q} = \frac{I_Z - I_X}{I_Y} pr + \frac{I_{XZ}}{I_Y}(r^2 - p^2) + \frac{\bar{q}S\bar{c}}{I_Y} C_{m,t} - H_e r$$

$$\dot{r} = \frac{I_X - I_Y}{I_Z} pq + \frac{I_{XZ}}{I_Z}(\dot{p} - qr) + \frac{\bar{q}Sb}{I_Z} C_{n,t} + H_e q$$

where the total aerodynamic coefficients $C_{X,t}$, $C_{Z,t}$, $C_{m,t}$, $C_{Y,t}$, $C_{n,t}$, and $C_{l,t}$ are defined in the next section. Euler angles were computed by using quaternions to allow continuity of attitude motions. Auxiliary equations included

$$\alpha = \tan^{-1}\left(\frac{w}{u}\right)$$

$$\beta = \sin^{-1}\left(\frac{v}{V}\right)$$

$$V = \sqrt{u^2 + v^2 + w^2}$$

$$a_n = \frac{qu - pv + g \cos \Theta \cos \phi - \dot{w}}{g}$$

$$a_y = \frac{-pw + ru - g \cos \Theta \sin \phi + \dot{v}}{g}$$

Aerodynamic Data

The aerodynamic data used in the simulation were derived from low-speed static and dynamic (force oscillation) wind-tunnel tests conducted with subscale models of the F-16 in wind-tunnel facilities at the NASA Ames and Langley Research Centers. The static aerodynamics were input in tabular form as functions of both angle of attack and sideslip over the ranges $-20^\circ \leqq \alpha \leqq 90^\circ$ and $-30^\circ \leqq \beta \leqq 30^\circ$. The dynamic data were input in tabular form for $\beta = 0^\circ$ over the same α range. Total coefficient equations were used to sum the various aerodynamic contributions to a given force or moment coefficient as follows.

For the X-axis force coefficient:

$$C_{X,t} = C_X(\alpha,\beta,\delta_h) + \Delta C_{X,lef}\left(1 - \frac{\delta_{lef}}{25}\right) + \Delta C_{X,sb}(\alpha)\left(\frac{\delta_{sb}}{60}\right)$$
$$+ \frac{\bar{c}q}{2V}\left[C_{X_q}(\alpha) + \Delta C_{X_{q,lef}}(\alpha)\left(1 - \frac{\delta_{lef}}{25}\right)\right]$$

where

$$\Delta C_{X,lef} = C_{X,lef}(\alpha,\beta) - C_X\left(\alpha,\beta,\delta_h = 0^\circ\right)$$

For the Z-axis force coefficient:

$$C_{Z,t} = C_Z(\alpha,\beta,\delta_h) + \Delta C_{Z,lef}\left(1 - \frac{\delta_{lef}}{25}\right) + \Delta C_{Z,sb}(\alpha)\left(\frac{\delta_{sb}}{60}\right)$$
$$+ \frac{\bar{c}q}{2V}\left[C_{Z_q}(\alpha) + \Delta C_{Z_{q,lef}}(\alpha)\left(1 - \frac{\delta_{lef}}{25}\right)\right]$$

where

$$\Delta C_{Z,lef} = C_{Z,lef}(\alpha,\beta) - C_Z\left(\alpha,\beta,\delta_h = 0^\circ\right)$$

For the pitching-moment coefficient:

$$C_{m,t} = C_m(\alpha,\beta,\delta_h)\eta_{\delta_h}(\delta_h) + C_{Z,t}(x_{cg,ref} - x_{cg}) + \Delta C_{m,lef}\left(1 - \frac{\delta_{lef}}{25}\right)$$
$$+ \Delta C_{m,sb}(\alpha)\left(\frac{\delta_{sb}}{60}\right) + \frac{\bar{c}q}{2V}\left[C_{m_q}(\alpha) + \Delta C_{m_{q,lef}}(\alpha)\left(1 - \frac{\delta_{lef}}{25}\right)\right]$$
$$+ \Delta C_m(\alpha) + \Delta C_{m,ds}(\alpha,\delta_h)$$

where

$$\Delta C_{m,lef} = C_{m,lef}(\alpha,\beta) - C_m\left(\alpha,\beta,\delta_h = 0^\circ\right)$$

For the Y-axis force coefficient:

$$C_{Y,t} = C_Y(\alpha,\beta) + \Delta C_{Y,lef}\left(1 - \frac{\delta_{lef}}{25}\right)$$
$$+ \left[\Delta C_{Y,\delta_{a=20^\circ}} + \Delta C_{Y,\delta_{a=20^\circ},lef}\left(1 - \frac{\delta_{lef}}{25}\right)\right]\left(\frac{\delta_a}{20}\right)$$
$$+ \Delta C_{Y,\delta_{r=30^\circ}}\left(\frac{\delta_r}{30}\right) + \frac{b}{2V}\left\{\left[C_{Y_r}(\alpha) + \Delta C_{Y_{r,lef}}(\alpha)\left(1 - \frac{\delta_{lef}}{25}\right)\right]r\right.$$
$$\left. + \left[C_{Y_p}(\alpha) + \Delta C_{Y_{p,lef}}(\alpha)\left(1 - \frac{\delta_{lef}}{25}\right)\right]p\right\}$$

where

$$\Delta C_{Y,lef} = C_{Y,lef}(\alpha,\beta) - C_Y(\alpha,\beta)$$

$$\Delta C_{Y,\delta_{a=20^\circ}} = C_{Y,\delta_{a=20^\circ}}(\alpha,\beta) - C_Y(\alpha,\beta)$$

$$\Delta C_{Y,\delta_{a=20^\circ},lef} = C_{Y,\delta_{a=20^\circ},lef}(\alpha,\beta) - C_{Y,lef}(\alpha,\beta)$$
$$- \left[C_{Y,\delta_{a=20^\circ}}(\alpha,\beta) - C_Y(\alpha,\beta)\right]$$

$$\Delta C_{Y,\delta_{r=30^\circ}} = C_{Y,\delta_{r=30^\circ}}(\alpha,\beta) - C_Y(\alpha,\beta)$$

For the yawing-moment coefficient:

$$C_{n,t} = C_n(\alpha,\beta,\delta_h) + \Delta C_{n,lef}\left(1 - \frac{\delta_{lef}}{25}\right) - C_{Y,t}\left(x_{cg,ref} - x_{cg}\right)\frac{\bar{c}}{b}$$

$$+ \left[\Delta C_{n,\delta_{a=20^\circ}} + \Delta C_{n,\delta_{a=20^\circ},lef}\left(1 - \frac{\delta_{lef}}{25}\right)\right]\left(\frac{\delta_a}{20}\right)$$

$$+ \Delta C_{n,\delta_{r=30^\circ}}\left(\frac{\delta_r}{30}\right) + \frac{b}{2V}\left\{\left[C_{n_r}(\alpha) + \Delta C_{n_{r,lef}}(\alpha)\left(1 - \frac{\delta_{lef}}{25}\right)\right]r\right.$$

$$\left. + \left[C_{n_p}(\alpha) + \Delta C_{n_{p,lef}}(\alpha)\left(1 - \frac{\delta_{lef}}{25}\right)\right]p\right\} + \Delta C_{n_\beta}(\alpha)\beta$$

where

$$\Delta C_{n,lef} = C_{n,lef}(\alpha,\beta) - C_n\left(\alpha,\beta,\delta_h = 0^\circ\right)$$

$$\Delta C_{n,\delta_{a=20^\circ}} = C_{n,\delta_{a=20^\circ}}(\alpha,\beta) - C_n\left(\alpha,\beta,\delta_h = 0^\circ\right)$$

$$\Delta C_{n,\delta_{a=20^\circ},lef} = C_{n,\delta_{a=20^\circ},lef}(\alpha,\beta) - C_{n,lef}(\alpha,\beta)$$

$$- \left[C_{n,\delta_{a=20^\circ}}(\alpha,\beta) - C_n\left(\alpha,\beta,\delta_h = 0^\circ\right)\right]$$

$$\Delta C_{n,\delta_{r=30^\circ}} = C_{n,\delta_{r=30^\circ}}(\alpha,\beta) - C_n\left(\alpha,\beta,\delta_h = 0^\circ\right)$$

For the rolling-moment coefficient:

$$C_{l,t} = C_l(\alpha,\beta,\delta_h) + \Delta C_{l,lef}\left(1 - \frac{\delta_{lef}}{25}\right)$$

$$+ \left[\Delta C_{l,\delta_{a=20^\circ}} + \Delta C_{l,\delta_{a=20^\circ},lef}\left(1 - \frac{\delta_{lef}}{25}\right)\right]\left(\frac{\delta_a}{20}\right)$$

$$+ \Delta C_{l,\delta_{r=30^\circ}}\left(\frac{\delta_r}{30}\right) + \frac{b}{2V}\left\{\left[C_{l_r}(\alpha) + \Delta C_{l_{r,lef}}(\alpha)\left(1 - \frac{\delta_{lef}}{25}\right)\right]r\right.$$

$$\left. + \left[C_{l_p}(\alpha) + \Delta C_{l_{p,lef}}(\alpha)\left(1 - \frac{\delta_{lef}}{25}\right)\right]p\right\} + \Delta C_{l_\beta}(\alpha)\beta$$

where

$$\Delta C_{l,\mathrm{lef}} = C_{l,\mathrm{lef}}(\alpha,\beta) - C_l(\alpha,\beta,\delta_h = 0^\circ)$$

$$\Delta C_{l,\delta_{a=20^\circ}} = C_{l,\delta_{a=20^\circ}}(\alpha,\beta) - C_l(\alpha,\beta,\delta_h = 0^\circ)$$

$$\Delta C_{l,\delta_{a=20^\circ},\mathrm{lef}} = C_{l,\delta_{a=20^\circ},\mathrm{lef}}(\alpha,\beta) - C_{l,\mathrm{lef}}(\alpha,\beta) - \left[C_{l,\delta_{a=20^\circ}}(\alpha,\beta) - C_l(\alpha,\beta,\delta_h = 0^\circ)\right]$$

$$\Delta C_{l,\delta_{r=30^\circ}} = C_{l,\delta_{r=30^\circ}}(\alpha,\beta) - C_l(\alpha,\beta,\delta_h = 0^\circ)$$

The aerodynamic coefficients contained in the preceding coefficient equations are presented in table III as functions of the indicated independent variables. The aerodynamic moment coefficients are referenced to a center-of-gravity location of $0.35\bar{c}$ and were corrected to the desired flight center-of-gravity position in the coefficient equations.

Engine Simulation

The F-16 is powered by an afterburning turbofan jet engine. The thrust response to throttle inputs was computed by using the mathematical model indicated in figure 66(a). The throttle command gearing is shown in figure 66(b). The response was modeled with a first-order lag which varied as shown in figure 66(c). Presented in table VI are thrust values for idle, military, and maximum thrust levels. Engine gyroscopic effects were simulated by representing the engine angular momentum at a fixed value of 216.9 kg-m^2/sec (160 slug-ft^2/sec).

APPENDIX C

SPECIAL EFFECTS

Buffet Characteristics

Aerodynamic buffeting of the airframe at high angles of attack was simulated by shaking the cockpit with a hydraulic mechanism. The buffet intensity and frequency content were controlled by the computer, with the buffet amplitude varying with angle of attack, as shown in figure 67. Buffet onset occurred near $\alpha = 15^{\circ}$, and the level of buffet increased fairly linearly thereafter with increasing angle of attack. The frequency content was controlled to represent the relative buffet amplitude contributions of the three primary structural modes of the airframe.

Simulation of Blackout

Pilot blackout or "grayout" under sustained high values of normal acceleration was simulated by decreasing the brightness of the projected scene and the cockpit instruments as a function of the cumulative time spent at high load factors. At the same time, dimming of the target image was delayed relative to the scene in order to partially simulate tunnel vision for steady tracking maneuvers. This simulation of blackout provided a cue, in addition to the inflatable anti-g suit, of the extent of operation at high normal acceleration, and it penalized the pilot who flew at unrealistically high values of normal acceleration. The blackout representation assumed that a pilot will experience grayout if exposed to greater than 5g normal acceleration and will tend to recover when returning to below this level. The algorithm used a direct relation between the logarithm of the load factor a_n and the logarithm of the time to blackout; the simulation used 300 sec to blackout at 5g and 10 sec to blackout at 9g, with simulated tunnel vision during the interim period.

REFERENCES

1. Impact of Active Control Technology on Airplane Design. AGARD-CP-157, Oct. 1974.

2. Gilbert, William P.; Nguyen, Luat T.; and Van Gunst, Roger W.: Simulator Study of the Effectiveness of an Automatic Control System Designed to Improve the High-Angle-of-Attack Characteristics of a Fighter Airplane. NASA TN D-8176, 1976.

3. Mechtly, E. A.: The International System of Units - Physical Constants and Conversion Factors (Second Revision). NASA SP-7012, 1973.

4. Ashworth, B. R.; and Kahlbaum, William M., Jr.: Description and Performance of the Langley Differential Maneuvering Simulator. NASA TN D-7304, 1973.

TABLE I.- MASS AND DIMENSIONAL CHARACTERISTICS USED IN SIMULATION

Weight, N (lb)	91 188 (20 500)
Moments of inertia, kg-m^2 (slug-ft^2):	
I_X	12 875 (9496)
I_Y	75 674 (55 814)
I_Z	85 552 (63 100)
I_{XZ}	1331 (982)
Wing dimensions:	
Span, m (ft)	9.144 (30)
Area, m^2 (ft^2)	27.87 (300)
Mean aerodynamic chord, m (ft)	3.45 (11.32)
Reference center-of-gravity location	$0.35\bar{c}$
Surface deflection limits:	
Horizontal tail -	
Symmetric (δ_h), deg	±25
Differential (δ_d), per surface, deg	±5.375
Ailerons (flaperons), deg	±21.5
Rudder, deg	±30
Leading-edge flap, deg	25
Speed brake, deg	60

TABLE II.- DEPARTURE-/SPIN-SUSCEPTIBILITY MANEUVERS

Initial condition	Maneuver	Pilot input
1g trim; $\alpha = 10^{\circ}$; h = 9144 m	360° roll	Maximum lateral stick
1g trim; $\alpha = 10^{\circ}$; h = 9144 m	360° roll	Maximum coordinated lateral stick and pedal
1g trim; $\alpha = 10^{\circ}$; h = 9144 m	Response to cross controls	Maximum opposite stick and pedal, followed by abrupt full aft stick
1g trim; M = 0.6; h = 9144 m	Inertia coupling	Maximum lateral stick, followed by abrupt full aft stick
Maximum g decelerating turn; h = 9144 m	360° roll at 170 knots IAS	Maximum lateral stick
Maximum g decelerating turn; h = 9144 m	360° roll at 170 knots IAS	Maximum coordinated lateral stick and pedal
Maximum g decelerating turn; h = 9144 m	Response to cross controls at 170 knots IAS	Maximum opposite lateral stick and pedal
1g trim; $\alpha = 25^{\circ}$; h = 9144 m	360° roll	Maximum lateral stick
1g trim; $\alpha = 25^{\circ}$; h = 9144 m	360° roll	Maximum coordinated lateral stick and pedal
1g trim; $\alpha = 25^{\circ}$; h = 9144 m	Response to cross controls	Maximum opposite lateral stick and pedal
1g trim; $\alpha = 25^{\circ}$; h = 9144 m	70° bank-to-bank reversals	Maximum lateral stick
Steep-attitude, decelerating climb; h = 9144 m	Deep-stall entry	Stick neutral or full forward

TABLE III.- AERODYNAMIC DATA USED IN SIMULATION

$C_X\left(\alpha,\beta,\delta_h = -25^{\circ}\right)$

BETA	-30.0	-25.0	-20.0	-15.0	-10.0	- 8.0	- 6.0	- 4.0	- 2.0	
	0.0	+ 2.0	+ 4.0	+ 6.0	+ 8.0	+10.0	+15.0	+20.0	+25.0	+30.0
ALPHA										
-20.0	-.18370	-.18530	-.19040	-.18990	-.19490	-.19140	-.18720	-.18600	-.18600	
	-.18680	-.18990	-.19020	-.19000	-.18960	-.18830	-.18330	-.18380	-.17870	-.17710
-15.0	-.17140	-.17650	-.17920	-.18270	-.18160	-.18340	-.18520	-.18530	-.18770	
	-.18750	-.18980	-.18760	-.18680	-.18480	-.18410	-.18520	-.18170	-.17900	-.17390
-10.0	-.15310	-.16270	-.16920	-.17180	-.16950	-.16930	-.17070	-.17350	-.17720	
	-.17870	-.17690	-.17290	-.17110	-.17060	-.16980	-.17210	-.16950	-.16300	-.15340
- 5.0	-.11510	-.12320	-.12760	-.13170	-.13900	-.14150	-.14200	-.14250	-.14370	
	-.14320	-.14250	-.14220	-.14100	-.13970	-.13720	-.12990	-.12580	-.12140	-.11330
0.0	-.09070	-.09850	-.10430	-.10930	-.11200	-.11150	-.11220	-.11240	-.11300	
	-.11320	-.11290	-.11190	-.11100	-.11020	-.10920	-.10650	-.10150	-.09570	-.08790
+ 5.0	-.05140	-.05670	-.06030	-.06400	-.06530	-.06610	-.06680	-.06750	-.06900	
	-.06930	-.06860	-.06800	-.06640	-.06500	-.06490	-.06310	-.05940	-.05580	-.05050
+10.0	-.00790	-.01080	-.00990	-.01010	-.00740	-.00700	-.00780	-.00900	-.01160	
	-.01200	-.01230	-.01060	-.00880	-.00830	-.00800	-.01070	-.01050	-.01140	-.00850
+15.0	.03540	.03580	.03880	.04020	.04770	.05030	.05350	.05530	.05380	
	.05370	.05330	.05360	.05270	.05090	.04850	.04100	.03960	.03660	.03620
+20.0	.07400	.07560	.07460	.07450	.08670	.08880	.09240	.09410	.09480	
	.09510	.09750	.09390	.09130	.08670	.08240	.07020	.07030	.07130	.06970
+25.0	.10920	.11240	.11020	.10670	.11010	.11210	.11260	.11290	.11230	
	.11110	.11220	.11250	.11360	.11150	.10750	.10410	.10760	.10980	.10660
+30.0	.09150	.10100	.09750	.10790	.11880	.13330	.13990	.14220	.14430	
	.14350	.14310	.14070	.13790	.13590	.13230	.12140	.11100	.11450	.10500
+35.0	.10790	.11370	.11980	.12780	.14020	.14250	.14780	.15700	.16230	
	.16630	.16670	.16640	.16370	.15600	.14600	.13360	.12560	.11950	.11370
+40.0	.13060	.14370	.13500	.14410	.15740	.15850	.16010	.16820	.17260	
	.17390	.17110	.16990	.16550	.16110	.15670	.14340	.13430	.14300	.12990
+45.0	.15350	.16030	.16050	.16040	.16370	.16710	.16640	.16390	.16740	
	.16590	.16490	.16500	.16250	.15970	.15730	.15400	.15410	.15390	.14710
+50.0	.14710	.15840	.16460	.16710	.17120	.17120	.16760	.16440	.16560	
	.16930	.17140	.17280	.17490	.17250	.17300	.15370	.14570	.14350	.13620
+55.0	.15540	.16150	.15680	.16610	.17780	.17690	.17650	.17490	.17620	
	.18040	.17430	.16660	.16770	.17240	.17610	.17220	.13470	.14480	.14420
+60.0	.15010	.15990	.16470	.15250	.16640	.16620	.17040	.17100	.17190	
	.17180	.17280	.17300	.17340	.17210	.16880	.14710	.14620	.14860	.14600
+70.0	.15010	.15360	.15690	.14200	.15730	.15950	.17880	.17150	.17380	
	.16950	.17100	.17120	.17300	.17200	.16860	.14740	.15670	.15570	.15450
+80.0	.16850	.16150	.15590	.15200	.15210	.15210	.15350	.15850	.15660	
	.15980	.15730	.15630	.15860	.15580	.15720	.14100	.14100	.14670	.15380
+90.0	.17120	.16510	.16080	.16480	.16760	.16600	.16860	.16670	.16690	
	.16600	.16720	.16620	.16640	.17110	.16770	.15310	.14930	.15490	.16240

TABLE III.- Continued

$$C_X\left(\alpha, \beta, \delta_h = -10^{\circ}\right)$$

BETA	-30.0 0.0	-25.0 + 2.0	-20.0 + 4.0	-15.0 + 6.0	-10.0 + 8.0	- 8.0 +10.0	- 6.0 +15.0	- 4.0 +20.0	- 2.0 +25.0	 +30.0
ALPHA										
-20.0	-.13620	-.13510	-.14190	-.13860	-.13740	-.13300	-.12680	-.12490	-.12220	
	-.12230	-.12460	-.12470	-.12520	-.12570	-.12820	-.12940	-.13270	-.12590	-.12700
-15.0	-.12160	-.12450	-.12350	-.12080	-.11760	-.11760	-.11700	-.11770	-.11840	
	-.11880	-.11850	-.11870	-.11820	-.11780	-.11840	-.12160	-.12430	-.12530	-.12240
-10.0	-.10180	-.10660	-.10680	-.10710	-.10610	-.10680	-.10720	-.10830	-.10940	
	-.11470	-.10950	-.10840	-.10770	-.10630	-.10690	-.10790	-.10760	-.10740	-.10260
- 5.0	-.06550	-.07060	-.07460	-.07710	-.08360	-.08640	-.08760	-.08870	-.08890	
	-.08930	-.08850	-.08750	-.08590	-.08420	-.08120	-.07470	-.07220	-.06820	-.06310
0.0	-.04830	-.05090	-.05320	-.05440	-.05780	-.05890	-.05970	-.06060	-.06130	
	-.06170	-.06110	-.06030	-.05950	-.05770	-.05610	-.05270	-.05150	-.04920	-.04660
+ 5.0	-.01180	-.01060	-.00960	-.01020	-.01420	-.01480	-.01550	-.01610	-.01770	
	-.01720	-.01780	-.01670	-.01560	-.01410	-.01330	-.00930	-.00870	-.01060	-.01270
+10.0	.02680	.03280	.03670	.03990	.04120	.04170	.04080	.04130	.04060	
	.03990	.03990	.04090	.04150	.04140	.04120	.03990	.03670	.03280	.02680
+15.0	.07350	.08000	.08870	.09340	.09830	.10060	.10240	.10340	.10330	
	.10270	.10310	.10270	.10180	.10080	.09830	.09340	.08870	.08000	.07350
+20.0	.12220	.12750	.12580	.12490	.13260	.13470	.13500	.13490	.13250	
	.13220	.13320	.13380	.13430	.13100	.12980	.12210	.12300	.12470	.11940
+25.0	.13740	.14740	.14660	.14540	.14650	.14850	.14850	.14530	.14290	
	.14070	.14180	.14430	.14570	.14420	.14390	.14280	.14400	.14480	.13480
+30.0	.10560	.12610	.12970	.14370	.15000	.16190	.16550	.16600	.16630	
	.16510	.16400	.16430	.16240	.16150	.15930	.15300	.13900	.13540	.11490
+35.0	.10750	.11540	.12990	.13770	.15230	.15810	.17220	.17890	.18010	
	.17950	.17930	.18040	.17820	.17490	.16750	.15290	.14510	.13060	.12270
+40.0	.13350	.14120	.13650	.14560	.15970	.16220	.17250	.17620	.17980	
	.17980	.18100	.17710	.17100	.17020	.16590	.15180	.14270	.14740	.13970
+45.0	.15210	.14860	.15170	.15200	.16080	.16130	.15970	.16710	.16670	
	.16710	.16640	.16530	.16290	.15970	.15690	.14810	.14780	.14470	.14820
+50.0	.13460	.14100	.14220	.14860	.15610	.15700	.15380	.15110	.15150	
	.15440	.15490	.15470	.15600	.15380	.15440	.14690	.14050	.13930	.13290
+55.0	.13750	.13670	.12510	.13360	.14670	.14720	.14750	.14650	.14620	
	.14880	.14330	.13610	.13700	.14050	.14310	.13000	.12150	.13310	.13390
+60.0	.13160	.13600	.13550	.11540	.12850	.12890	.13360	.13510	.13720	
	.13830	.13560	.13200	.13870	.13230	.13100	.11790	.13800	.13850	.13410
+70.0	.11710	.11740	.11850	.11080	.11610	.11870	.13760	.13120	.13530	
	.13280	.13010	.12630	.12700	.12810	.12680	.12150	.12920	.12810	.12780
+80.0	.12010	.11610	.11360	.11240	.11580	.11480	.11490	.11940	.11770	
	.12110	.11950	.11950	.12250	.12040	.11770	.11430	.11550	.11800	.12200
+90.0	.12870	.12410	.12140	.12210	.12650	.12560	.12570	.12360	.12480	
	.12470	.12620	.12560	.12560	.12970	.12570	.12130	.12060	.12330	.12790

TABLE III.- Continued

$C_X(\alpha,\beta,\delta_h = 0^\circ)$

BETA	-30.0 0.0	-25.0 + 2.0	-20.0 + 4.0	-15.0 + 6.0	-10.0 + 8.0	- 8.0 +10.0	- 6.0 +15.0	- 4.0 +20.0	- 2.0 +25.0	+30.0
ALPHA										
-20.0	-.10720	-.10610	-.11290	-.10960	-.10840	-.10400	-.09780	-.09590	-.09320	
	-.09330	-.09560	-.09570	-.09620	-.09670	-.09920	-.10040	-.10370	-.09690	-.09800
-15.0	-.10060	-.10350	-.10250	-.09980	-.09660	-.09660	-.09600	-.09670	-.09740	
	-.09780	-.09750	-.09770	-.09720	-.09680	-.09740	-.10060	-.10330	-.10430	-.10140
-10.0	-.08530	-.09010	-.09030	-.09060	-.08960	-.09030	-.09070	-.09180	-.09290	
	-.09820	-.09300	-.09190	-.09120	-.08980	-.09040	-.09140	-.09110	-.09090	-.08610
- 5.0	-.05460	-.05970	-.06370	-.06620	-.07270	-.07550	-.07670	-.07780	-.07800	
	-.07840	-.07760	-.07660	-.07500	-.07330	-.07030	-.06380	-.06130	-.05730	-.05220
0.0	-.03550	-.03810	-.04040	-.04160	-.04500	-.04610	-.04690	-.04780	-.04850	
	-.04890	-.04830	-.04750	-.04670	-.04490	-.04330	-.03990	-.03870	-.03640	-.03380
+ 5.0	-.00120	0.00000	.00100	.00040	-.00360	-.00420	-.00490	-.00550	-.00710	
	-.00660	-.00720	-.00610	-.00500	-.00350	-.00270	.00130	.00190	0.00000	-.00210
+10.0	.03590	.04910	.04580	.04900	.05030	.05080	.04990	.05090	.04970	
	.04900	.04900	.05000	.05060	.05050	.05030	.04900	.04580	.04190	.03590
+15.0	.07800	.08450	.09320	.09790	.10280	.10510	.10690	.10790	.10780	
	.10720	.10760	.10720	.10630	.10530	.10280	.09790	.09320	.08450	.07800
+20.0	.11830	.12360	.12190	.12100	.12870	.13080	.13110	.13100	.12860	
	.12830	.12930	.12990	.13040	.12710	.12590	.11820	.11910	.12080	.11550
+25.0	.12670	.13670	.13590	.13470	.13580	.13780	.13780	.13460	.13220	
	.13000	.13110	.13360	.13500	.13350	.13320	.13210	.13330	.13410	.12410
+30.0	.09410	.11460	.11820	.13220	.13850	.15040	.15400	.15450	.15480	
	.15360	.15250	.15280	.15090	.15000	.14780	.14150	.12750	.12390	.10340
+35.0	.08850	.09640	.11090	.11870	.13330	.13910	.15320	.15990	.16110	
	.16050	.16030	.16140	.15920	.15590	.14850	.13390	.12610	.11160	.10370
+40.0	.10890	.11660	.11190	.12100	.13510	.13760	.14790	.15160	.15520	
	.15520	.15640	.15250	.14640	.14560	.14130	.12720	.11810	.12280	.11510
+45.0	.12320	.11970	.12280	.12310	.13190	.13240	.13080	.13320	.13780	
	.13820	.13750	.13640	.13400	.13080	.12800	.11920	.11890	.11580	.11930
+50.0	.11350	.11850	.11840	.11710	.12430	.12790	.12790	.12580	.12570	
	.12810	.12580	.12280	.12210	.11860	.11800	.11080	.11210	.11220	.10720
+55.0	.11370	.11950	.11460	.11610	.12090	.12110	.12110	.11950	.11830	
	.12000	.11850	.11530	.11600	.11520	.11350	.10870	.10720	.11210	.10630
+60.0	.10370	.10900	.10940	.10490	.11090	.11230	.11810	.11840	.11700	
	.11470	.11410	.11260	.11290	.11290	.11090	.10490	.10940	.10900	.10370
+70.0	.08570	.08580	.08570	.07960	.08510	.09190	.11500	.10870	.10890	
	.10250	.10220	.10070	.10120	.09940	.09520	.08970	.09580	.09590	.09580
+80.0	.08420	.08070	.07870	.07780	.07910	.07930	.08050	.08460	.08080	
	.08210	.08020	.07990	.08260	.08000	.07090	.07560	.07650	.07850	.08200
+90.0	.08470	.08130	.07980	.08240	.08430	.08430	.08530	.08410	.08580	
	.08640	.08570	.08280	.08170	.08570	.08160	.07970	.07710	.07860	.08200

TABLE III.- Continued

$$C_X\left(\alpha,\beta,\delta_h = 10^{\circ}\right)$$

BETA	-30.0	-25.0	-20.0	-15.0	-10.0	- 8.0	- 6.0	- 4.0	- 2.0	
	0.0	+ 2.0	+ 4.0	+ 6.0	+ 8.0	+10.0	+15.0	+20.0	+25.0	+30.0
ALPHA										
-20.0	-.10230	-.10120	-.10800	-.10470	-.10350	-.09910	-.09290	-.09100	-.08840	
	-.08840	-.09070	-.09080	-.09130	-.09180	-.09430	-.09550	-.09880	-.09200	-.09310
-15.0	-.10380	-.10670	-.10570	-.10300	-.09980	-.09980	-.09920	-.09990	-.10060	
	-.10100	-.10070	-.10090	-.10040	-.10000	-.10060	-.10380	-.10650	-.10750	-.10460
-10.0	-.09630	-.10110	-.10130	-.10160	-.10060	-.10130	-.10170	-.10280	-.10390	
	-.10920	-.10400	-.10290	-.10220	-.10080	-.10140	-.10240	-.10210	-.10190	-.09710
- 5.0	-.06640	-.07150	-.07550	-.07800	-.08450	-.08730	-.08850	-.08960	-.08980	
	-.09020	-.08940	-.08840	-.08680	-.08510	-.08210	-.07560	-.07310	-.06910	-.06400
0.0	-.04720	-.04980	-.05210	-.05330	-.05670	-.05780	-.05860	-.05950	-.06020	
	-.06060	-.06000	-.05920	-.05840	-.05660	-.05500	-.05160	-.05040	-.04810	-.04550
+ 5.0	-.01460	-.01340	-.01240	-.01300	-.01700	-.01760	-.01830	-.01890	-.02050	
	-.02000	-.02060	-.01950	-.01840	-.01690	-.01610	-.01210	-.01150	-.01340	-.01550
+10.0	.01820	.02420	.02810	.03130	.03260	.03310	.03220	.03270	.03200	
	.03130	.03130	.03230	.03290	.03280	.03260	.03130	.02810	.02420	.01820
+15.0	.05370	.06020	.06890	.07360	.07850	.08080	.08260	.08360	.08350	
	.08290	.08330	.08290	.08200	.08100	.07850	.07360	.06890	.06020	.05370
+20.0	.08710	.09240	.09070	.08980	.09750	.09960	.09990	.09980	.09740	
	.09710	.09810	.09870	.09920	.09590	.09470	.08700	.08790	.08960	.08430
+25.0	.09160	.10160	.10080	.09960	.10070	.10270	.10270	.09950	.09710	
	.09490	.09600	.09850	.09990	.09840	.09810	.09700	.09820	.09900	.08900
+30.0	.05090	.07140	.07500	.08900	.09530	.10720	.11080	.11130	.11160	
	.11040	.10930	.10960	.10770	.10680	.10460	.09830	.08430	.08070	.06020
+35.0	.04810	.05600	.07050	.07830	.09290	.09870	.11280	.11950	.12070	
	.12010	.11990	.12100	.11880	.11550	.10810	.09350	.08570	.07120	.06330
+40.0	.06640	.07410	.06940	.07850	.09260	.09510	.10540	.10910	.11270	
	.11270	.11390	.11000	.10390	.10310	.09880	.08470	.07560	.08030	.07260
+45.0	.08460	.08110	.08420	.08450	.09330	.09380	.09220	.09460	.09920	
	.09960	.09890	.09780	.09540	.09220	.08940	.08060	.08030	.07720	.08070
+50.0	.09080	.09850	.10110	.09990	.10630	.10610	.10180	.09960	.10210	
	.10710	.10710	.10640	.10700	.10360	.10320	.09680	.09800	.09540	.08770
+55.0	.08420	.08690	.07900	.08820	.10250	.10100	.09930	.09800	.09910	
	.10300	.09720	.08970	.09140	.09690	.10150	.08720	.07800	.08590	.08320
+60.0	.07490	.08230	.08490	.07940	.08310	.08410	.08960	.09080	.09150	
	.09140	.09080	.08930	.08950	.08890	.08680	.08310	.08860	.08600	.07860
+70.0	.05040	.05000	.05040	.04670	.08130	.08110	.09720	.09500	.10750	
	.11900	.11010	.10010	.09670	.09580	.09310	.05850	.06220	.06180	.06220
+80.0	.04210	.03800	.03550	.03970	.04200	.04170	.04240	.04780	.04730	
	.05190	.04840	.04650	.04890	.04720	.04500	.04270	.03850	.04100	.04510
+90.0	.04330	.04040	.03950	.04670	.04950	.04920	.04990	.04840	.05000	
	.05040	.04950	.04630	.04570	.05100	.04820	.04540	.03820	.03910	.04200

TABLE III.- Continued

$$C_X(\alpha,\beta,\delta_h = 25^{\circ})$$

BETA	-30.0	-25.0	-20.0	-15.0	-10.0	- 8.0	- 6.0	- 4.0	- 2.0	
	0.0	+ 2.0	+ 4.0	+ 6.0	+ 8.0	+10.0	+15.0	+20.0	+25.0	+30.0
ALPHA										
-20.0	-.10680	-.11020	-.11600	-.11760	-.12910	-.12890	-.12440	-.11580	-.11370	
	-.11410	-.11640	-.11920	-.12000	-.12400	-.12430	-.11280	-.11120	-.10540	-.10200
-15.0	-.11220	-.11800	-.12270	-.12920	-.13650	-.13970	-.14060	-.14160	-.14420	
	-.14500	-.14480	-.14280	-.14080	-.14400	-.13970	-.13240	-.12590	-.12120	-.11540
-10.0	-.11020	-.12120	-.13190	-.13590	-.14030	-.14270	-.14540	-.14800	-.15200	
	-.16330	-.15180	-.14820	-.14570	-.14380	-.14190	-.13750	-.13350	-.12280	-.11180
- 5.0	-.09110	-.10270	-.10930	-.11440	-.12440	-.13040	-.13160	-.13200	-.13330	
	-.13370	-.13400	-.13220	-.13090	-.12800	-.12430	-.11430	-.10920	-.10260	-.09100
0.0	-.08110	-.08890	-.09550	-.09960	-.10150	-.10370	-.10560	-.10650	-.10770	
	-.10750	-.10720	-.10610	-.10450	-.10240	-.10030	-.09840	-.09430	-.08770	-.07990
+ 5.0	-.05750	-.05880	-.06310	-.06760	-.06710	-.06940	-.07150	-.07390	-.07750	
	-.07850	-.07870	-.07440	-.07040	-.06880	-.06690	-.06740	-.06240	-.05860	-.05730
+10.0	-.01830	-.01880	-.02110	-.02410	-.02260	-.02540	-.02910	-.03330	-.03700	
	-.03360	-.03450	-.03260	-.02830	-.02470	-.02360	-.02510	-.02210	-.01980	-.01930
+15.0	.01950	.01860	.02040	.01860	.01940	.01810	.01540	.01620	.01980	
	.02120	.01570	.01310	.01360	.01580	.01790	.01710	.01890	.01710	.01800
+20.0	.04940	.06260	.05620	.04770	.03230	.02790	.02890	.02630	.02040	
	.01870	.01730	.02550	.01830	.01650	.01190	.02730	.03580	.04220	.02900
+25.0	.06990	.06950	.06270	.05570	.03660	.03160	.02630	.02070	.01600	
	.01980	.01650	.02180	.02440	.02280	.02140	.04050	.04750	.05430	.05470
+30.0	.02070	.03240	.03230	.02930	.03040	.04040	.04190	.04040	.03850	
	.03810	.03740	.03790	.03890	.04170	.04460	.04250	.04650	.04660	.03490
+35.0	.02110	.02820	.03090	.02630	.03070	.03340	.04370	.04660	.04580	
	.04790	.04950	.04950	.04870	.04670	.04340	.03900	.04360	.04090	.03380
+40.0	.03860	.04620	.03310	.03390	.03650	.04070	.03940	.04110	.04070	
	.04180	.04310	.04260	.03920	.04050	.03810	.03550	.03470	.04780	.04020
+45.0	.04600	.04380	.03410	.03110	.03480	.03730	.03620	.03350	.03380	
	.03630	.03250	.03400	.03420	.03560	.03380	.03010	.03310	.04280	.04500
+50.0	.03940	.04790	.05130	.04470	.05380	.05280	.04830	.04410	.04440	
	.04720	.04880	.04970	.05070	.04870	.04950	.04780	.05250	.04760	.03760
+55.0	.03360	.04110	.03800	.04710	.05430	.05080	.04710	.04450	.04500	
	.04840	.04420	.03830	.04100	.04710	.05220	.04320	.02720	.03470	.03150
+60.0	.01580	.02840	.03610	.03350	.04870	.04430	.04420	.04320	.04510	
	.04600	.04510	.04330	.04350	.04380	.04160	.03630	.03970	.03400	.02460
+70.0	-.01860	-.01210	-.00570	-.00700	.04100	.04510	.06550	.06040	.06550	
	.06410	.06770	.07010	.07020	.06360	.05460	.00330	.00200	-.00050	.00580
+80.0	-.02420	-.02670	-.02770	-.02000	-.02150	-.02240	-.02230	-.01800	-.02020	
	-.01730	-.00460	.02810	.03110	.00530	-.02100	-.02880	-.03120	-.02400	-.01520
+90.0	-.02080	-.02710	-.03150	-.02290	-.01560	-.01650	-.01410	-.01840	-.01730	
	-.01730	-.01680	-.01850	-.01830	-.01300	-.01570	-.02370	-.03230	-.02460	-.01500

TABLE III.- Continued

$C_{X,lef}(\alpha,\beta)$

BETA	-30.0 0.0	-25.0 + 2.0	-20.0 + 4.0	-15.0 + 6.0	-10.0 + 8.0	- 8.0 +10.0	- 6.0 +15.0	- 4.0 +20.0	- 2.0 +25.0	 +30.0
ALPHA										
-20.0	-.02770	-.02850	-.03180	-.02560	-.01840	-.01560	-.01590	-.01620	-.01740	
	-.01810	-.01790	-.01670	-.01680	-.01560	-.01530	-.02250	-.02870	-.02540	-.02460
-15.0	-.03140	-.03100	-.02590	-.01910	-.01610	-.01570	-.01620	-.01730	-.01890	
	-.01930	-.01860	-.01860	-.01700	-.01550	-.01540	-.01840	-.02520	-.03030	-.03070
-10.0	-.02950	-.02980	-.02600	-.02330	-.02090	-.02150	-.02140	-.02240	-.02300	
	-.02240	-.02200	-.02170	-.02130	-.02050	-.01990	-.02230	-.02500	-.02880	-.02850
- 5.0	-.01480	-.01530	-.01630	-.01500	-.01670	-.01730	-.01850	-.01890	-.01930	
	-.01960	-.01920	-.01850	-.01790	-.01780	-.01620	-.01550	-.01680	-.01580	-.01530
0.0	-.01360	-.01490	-.01430	-.01360	-.01680	-.01780	-.01820	-.01880	-.01970	
	-.02020	-.01960	-.01880	-.01800	-.01720	-.01600	-.01440	-.01510	-.01490	-.01440
+ 5.0	-.00290	-.00100	-.00030	-.00050	-.00040	-.00060	-.00170	-.00270	-.00330	
	-.00330	-.00330	-.00240	-.00140	-.00040	.00040	.00130	.00110	-.00020	-.00210
+10.0	.00850	.01040	.01160	.01210	.01310	.01250	.01220	.01190	.01040	
	.00990	.00960	.01060	.01170	.01260	.01270	.01170	.01120	.01000	.00810
+15.0	.01450	.01680	.01960	.02180	.02250	.02310	.02380	.02380	.02310	
	.02240	.02240	.02260	.02270	.02230	.02220	.02150	.01930	.01650	.01420
+20.0	.01650	.01700	.02050	.02260	.02520	.02450	.02360	.02320	.02330	
	.02210	.02320	.02410	.02500	.02670	.02760	.02500	.02290	.02120	.01890
+25.0	.01380	.01720	.01570	.01780	.02260	.02510	.02640	.02740	.02710	
	.02780	.02750	.02710	.02670	.02490	.02520	.02030	.01830	.01980	.01640
+30.0	.00920	.01220	.01290	.01650	.02020	.02530	.02790	.02950	.02960	
	.03010	.03090	.03060	.02780	.02610	.02470	.02000	.01740	.01670	.01370
+35.0	.00990	.01340	.01620	.01490	.02080	.02290	.02730	.02860	.03030	
	.03050	.02860	.03070	.02920	.02590	.02530	.01940	.02070	.01790	.01440
+40.0	.02060	.02020	.02360	.02460	.02890	.02930	.02900	.03200	.03170	
	.03280	.03140	.03050	.02890	.02810	.02620	.02190	.02090	.01750	.01790
+45.0	.02570	.02740	.02660	.02360	.02660	.02830	.02360	.02980	.02680	
	.03090	.03070	.02800	.02380	.02840	.02540	.02240	.02540	.02620	.02450

TABLE III.- Continued

ALPHA	$\Delta C_{X,sb}(\alpha)$
-20.0	-.01010
-15.0	-.01010
-10.0	-.01010
- 5.0	-.01010
0.0	-.01010
+ 5.0	-.03580
+10.0	-.07900
+15.0	-.12270
+20.0	-.18270
+25.0	-.18920
+30.0	-.19880
+35.0	-.20000
+40.0	-.18740
+45.0	-.16730
+50.0	-.14760
+55.0	-.13100
+60.0	-.12790
+70.0	-.13250
+80.0	-.12500
+90.0	-.12500

ALPHA	$C_{X_q}(\alpha)$
-20.0	.95300
-15.0	.95300
-10.0	.95300
- 5.0	1.55000
0.0	1.90000
+ 5.0	2.46000
+10.0	2.92000
+15.0	3.30000
+20.0	2.76000
+25.0	2.05000
+30.0	1.50000
+35.0	1.49000
+40.0	1.83000
+45.0	1.21000
+50.0	1.33000
+55.0	1.61000
+60.0	.91000
+70.0	3.43000
+80.0	.61700
+90.0	.27300

ALPHA	$\Delta C_{X_{q,lef}}(\alpha)$
-20.0	-1.22000
-15.0	-1.22000
-10.0	-1.22000
- 5.0	-1.66000
0.0	-1.62000
+ 5.0	-1.58000
+10.0	-1.96000
+15.0	-2.51000
+20.0	-2.04000
+25.0	-1.64000
+30.0	-.82400
+35.0	-.81700
+40.0	-1.10000
+45.0	-.55000

TABLE III.- Continued

$$C_Z\left(\alpha,\beta,\delta_h = -25^{\circ}\right)$$

BETA	-30.0	-25.0	-20.0	-15.0	-10.0	- 8.0	- 6.0	- 4.0	- 2.0	
	0.0	+ 2.0	+ 4.0	+ 6.0	+ 8.0	+10.0	+15.0	+20.0	+25.0	+30.0
ALPHA										
-20.0	1.19400	1.27200	1.31100	1.35600	1.39600	1.34700	1.33900	1.31400	1.32100	
	1.31500	1.33700	1.33200	1.34000	1.33800	1.29400	1.23500	1.18500	1.14000	1.10000
-15.0	.99600	1.05700	1.09000	1.12100	1.12800	1.12900	1.13100	1.14300	1.15800	
	1.17100	1.17700	1.14200	1.14800	1.13100	1.13700	1.13000	1.10000	1.06000	1.00500
-10.0	.79300	.83200	.84100	.85600	.88700	.88880	.89900	.90900	.91500	
	.92500	.91000	.89200	.88900	.88100	.87500	.83500	.82100	.81500	.78000
- 5.0	.41000	.41000	.42000	.42500	.45100	.46400	.47400	.47200	.47400	
	.46900	.46000	.45400	.44700	.44600	.44000	.42400	.40500	.39400	.40300
0.0	.18000	.15500	.13500	.13000	.14100	.14900	.15400	.15300	.15100	
	.15500	.15400	.15100	.14700	.13800	.12900	.11900	.13700	.12300	.15900
+ 5.0	-.09000	-.13000	-.16000	-.18000	-.18400	-.18600	-.18200	-.18700	-.18700	
	-.18900	-.19300	-.19100	-.19300	-.19500	-.19400	-.18700	-.17100	-.13300	-.09900
+10.0	-.34000	-.40500	-.46000	-.49800	-.51100	-.51800	-.52600	-.53500	-.53400	
	-.53000	-.53200	-.52500	-.52000	-.52100	-.51500	-.49800	-.46500	-.40200	-.34100
+15.0	-.61000	-.66500	-.72000	-.77000	-.80600	-.81800	-.83700	-.84900	-.85100	
	-.85600	-.85400	-.85500	-.85500	-.83600	-.82700	-.80100	-.73800	-.66400	-.60200
+20.0	-.87000	-.95000	-1.01500	-1.08000	-1.12200	-1.13700	-1.14900	-1.15400	-1.15600	
	-1.16900	-1.15100	-1.14800	-1.14600	-1.13500	-1.12900	-1.07700	-.99400	-.94300	-.87300
+25.0	-1.17000	-1.23500	-1.29500	-1.35500	-1.40600	-1.40500	-1.42900	-1.44100	-1.44600	
	-1.44600	-1.45200	-1.44900	-1.45500	-1.44000	-1.41500	-1.35600	-1.28800	-1.21700	-1.16700
+30.0	-1.31500	-1.38000	-1.44500	-1.51500	-1.58100	-1.67100	-1.69700	-1.71400	-1.71900	
	-1.71700	-1.72000	-1.70900	-1.68400	-1.67000	-1.65100	-1.58000	-1.47700	-1.46300	-1.38900
+35.0	-1.52000	-1.57000	-1.63500	-1.71000	-1.78800	-1.81800	-1.83800	-1.88900	-1.91000	
	-1.90900	-1.90900	-1.89300	-1.89100	-1.84600	-1.80000	-1.72100	-1.64000	-1.59000	-1.53100
+40.0	-1.60000	-1.67000	-1.73000	-1.81000	-1.89100	-1.90700	-1.91100	-1.98300	-2.01600	
	-2.03700	-1.93200	-1.99000	-1.96900	-1.83600	-1.91800	-1.83900	-1.75500	-1.67100	-1.63000
+45.0	-1.56000	-1.61500	-1.68500	-1.75000	-1.85400	-1.99100	-2.03300	-1.93900	-2.00300	
	-1.98500	-2.02000	-2.04000	-1.91300	-1.91800	-1.94600	-1.91100	-1.82400	-1.68900	-1.66300
+50.0	-1.30000	-1.48000	-1.60000	-1.72000	-1.88000	-1.92400	-1.91300	-1.86600	-1.87900	
	-1.95900	-1.99200	-2.01700	-2.03000	-1.94200	-2.00200	-1.87000	-1.73800	-1.62300	-1.44700
+55.0	-1.70500	-1.79500	-1.82500	-1.85000	-1.93800	-1.95900	-2.01200	-1.99900	-1.96900	
	-2.01000	-1.96500	-1.84700	-1.89500	-1.92800	-1.96500	-1.75500	-1.69700	-1.70600	-1.61800
+60.0	-1.70000	-1.74000	-1.73000	-1.89500	-1.93300	-1.88000	-1.90700	-1.89800	-1.89200	
	-1.91600	-1.93600	-1.87700	-1.93300	-1.95200	-1.91500	-1.78000	-1.75000	-1.75000	-1.68800
+70.0	-1.69000	-1.74000	-1.73500	-1.83000	-1.81300	-1.86400	-2.00400	-1.95000	-1.92500	
	-1.95700	-1.90500	-1.83300	-1.93200	-1.95200	-1.89300	-1.80000	-1.85300	-1.79900	-1.79100
+80.0	-1.93500	-1.95000	-1.94500	-1.92000	-1.87200	-1.83800	-1.90800	-1.94900	-1.82600	
	-1.81600	-1.83700	-1.75500	-1.84800	-1.85800	-1.77400	-1.81000	-1.86400	-1.88500	-1.83400
+90.0	-1.96000	-1.93500	-1.85000	-1.87000	-1.95300	-2.03600	-2.01300	-1.96800	-1.99000	
	-1.97800	-1.95700	-1.95600	-1.96200	-2.04800	-1.97000	-1.89500	-1.89000	-1.96900	-1.97000

TABLE III.- Continued

$$C_Z\left(\alpha, \beta, \delta_h = -10^{\circ}\right)$$

BETA	-30.0	-25.0	-20.0	-15.0	-10.0	- 8.0	- 6.0	- 4.0	- 2.0	
	0.0	+ 2.0	+ 4.0	+ 6.0	+ 8.0	+10.0	+15.0	+20.0	+25.0	+30.0
ALPHA										
-20.0	1.14900	1.21400	1.26400	1.29400	1.32700	1.28300	1.26600	1.24500	1.23400	
	1.22800	1.25800	1.25700	1.26800	1.26500	1.23600	1.19600	1.15400	1.10900	1.06300
-15.0	.94800	.99500	1.02100	1.04700	1.04300	1.04000	1.03700	1.04200	1.05000	
	1.05900	1.06600	1.04800	1.05100	1.04000	1.05300	1.05100	1.03100	.99900	.95500
-10.0	.75500	.77800	.77700	.78800	.80100	.79900	.80300	.80400	.81200	
	.81500	.81300	.80500	.80400	.80000	.79700	.77600	.76900	.76500	.74700
- 5.0	.32000	.32000	.32700	.33200	.35000	.36500	.37000	.37200	.35700	
	.35600	.35200	.34900	.34300	.33700	.32800	.31700	.30900	.29500	.30600
0.0	.08600	.06100	.04100	.03900	.05200	.05600	.06200	.06200	.06100	
	.06400	.06200	.06100	.05800	.05300	.04700	.03500	.04900	.04400	.07600
+ 5.0	-.19200	-.23200	-.26200	-.27900	-.28000	-.28400	-.28100	-.28700	-.28700	
	-.28700	-.28900	-.29100	-.28900	-.29100	-.29300	-.29200	-.27500	-.24400	-.20500
+10.0	-.45500	-.52200	-.57500	-.61100	-.62400	-.63200	-.64100	-.64700	-.65000	
	-.65000	-.65100	-.64600	-.64200	-.63800	-.63500	-.62200	-.58700	-.52400	-.46300
+15.0	-.71400	-.78400	-.84600	-.89800	-.93300	-.94900	-.96700	-.97600	-.97700	
	-.98000	-.98000	-.97800	-.97700	-.96300	-.95100	-.92300	-.86400	-.79000	-.71700
+20.0	-1.00500	-1.08800	-1.16100	-1.22300	-1.26300	-1.28400	-1.29900	-1.30600	-1.30200	
	-1.30600	-1.29200	-1.28900	-1.28700	-1.27900	-1.26600	-1.22000	-1.14600	-1.09000	-1.00500
+25.0	-1.31300	-1.37800	-1.44500	-1.50900	-1.56000	-1.56600	-1.58300	-1.59000	-1.59500	
	-1.59400	-1.59700	-1.59500	-1.59500	-1.58400	-1.56600	-1.50500	-1.44500	-1.37400	-1.30700
+30.0	-1.41800	-1.49800	-1.57800	-1.66300	-1.74600	-1.82500	-1.84800	-1.86100	-1.86100	
	-1.86300	-1.86300	-1.85600	-1.83600	-1.81600	-1.79500	-1.73500	-1.61300	-1.55700	-1.47000
+35.0	-1.54200	-1.62900	-1.71900	-1.81900	-1.91900	-1.97700	-2.03300	-2.06400	-2.07900	
	-2.09000	-2.08100	-2.07500	-2.06700	-2.03400	-1.98900	-1.89600	-1.80000	-1.69600	-1.61300
+40.0	-1.67100	-1.76800	-1.86200	-1.96700	-2.07400	-2.07700	-2.15100	-2.18400	-2.19900	
	-2.21600	-2.19200	-2.19400	-2.08400	-2.11000	-2.11100	-1.99600	-1.90000	-1.78700	-1.70200
+45.0	-1.61500	-1.57700	-1.77000	-1.96300	-2.13000	-2.21700	-2.18400	-2.21600	-2.30600	
	-2.26300	-2.30400	-2.30400	-2.24200	-2.23500	-2.21000	-2.12100	-1.89100	-1.65400	-1.69600
+50.0	-1.40600	-1.59200	-1.71600	-1.94400	-2.02600	-2.08100	-2.08100	-2.03300	-2.03100	
	-2.09700	-2.11800	-2.13100	-2.14200	-2.06200	-2.12900	-2.04700	-1.81900	-1.69500	-1.50900
+55.0	-1.68800	-1.73800	-1.72100	-1.80900	-2.01400	-2.04800	-2.11200	-2.10000	-2.05800	
	-2.08800	-2.06700	-1.97200	-2.01600	-2.01900	-2.02500	-1.82000	-1.73200	-1.74900	-1.66900
+60.0	-1.72400	-1.79300	-1.80000	-1.75600	-1.94900	-1.92300	-1.97500	-1.99000	-2.00500	
	-2.05100	-2.02100	-1.91400	-1.95600	-1.99800	-1.98500	-1.79200	-1.83600	-1.82900	-1.76000
+70.0	-1.74300	-1.75400	-1.81100	-1.78100	-1.83900	-1.89700	-2.00400	-1.99900	-1.98600	
	-2.02700	-1.94300	-1.83500	-1.92500	-1.99300	-1.92100	-1.86300	-1.89300	-1.83600	-1.82500
+80.0	-1.93500	-1.99300	-1.97900	-1.99100	-1.92800	-1.87700	-1.93100	-1.98100	-1.89200	
	-1.91600	-1.93800	-1.85600	-1.94300	-1.94700	-1.84800	-1.91100	-1.89900	-1.91300	-1.85500
+90.0	-1.99000	-2.00900	-1.95000	-1.97900	-2.00600	-2.08500	-2.01900	-2.00700	-2.01900	
	-1.99800	-1.99000	-2.00400	-2.03600	-2.10200	-2.00300	-1.97600	-1.94700	-2.00600	-1.98700

TABLE III.- Continued

$$C_Z\left(\alpha,\beta,\delta_h = 0^{\circ}\right)$$

BETA	-30.0	-25.0	-20.0	-15.0	-10.0	- 8.0	- 6.0	- 4.0	- 2.0	
	0.0	+ 2.0	+ 4.0	+ 6.0	+ 8.0	+10.0	+15.0	+20.0	+25.0	+30.0
ALPHA										
-20.0	1.09100	1.14000	1.20300	1.21500	1.23900	1.20100	1.17100	1.15700	1.12200	
	1.11600	1.15600	1.16000	1.17500	1.17200	1.16100	1.14500	1.11500	1.07000	1.01500
-15.0	.90500	.93900	.95900	.98000	.96700	.96000	.95400	.95100	.95300	
	.95900	.96600	.96400	.96500	.95900	.97800	.98000	.97000	.94500	.91000
-10.0	.71300	.71800	.70600	.71100	.70500	.69900	.69600	.68700	.69700	
	.69200	.70500	.70800	.71000	.71000	.70900	.71000	.71000	.71000	.71000
- 5.0	.26500	.26500	.27000	.27500	.28800	.30500	.30600	.31100	.28500	
	.28700	.28600	.28500	.28000	.27100	.26000	.25100	.25100	.23400	.24700
0.0	-.00600	-.03000	-.05000	-.05000	-.03600	-.03500	-.02800	-.02700	-.02700	
	-.02500	-.02800	-.02800	-.02900	-.03100	-.03400	-.04800	-.03700	-.03300	-.00600
+ 5.0	-.27500	-.31500	-.34500	-.36000	-.35900	-.36400	-.36200	-.36800	-.36800	
	-.36700	-.36800	-.37200	-.36800	-.37000	-.37300	-.37700	-.36000	-.33500	-.29200
+10.0	-.55000	-.62000	-.67000	-.70500	-.71900	-.72700	-.73700	-.74100	-.74700	
	-.75000	-.75000	-.74600	-.74400	-.73600	-.73500	-.72500	-.68900	-.62600	-.56400
+15.0	-.82500	-.91000	-.98000	-1.03500	-1.06900	-1.08900	-1.10500	-1.11100	-1.11100	
	-1.11200	-1.11200	-1.10800	-1.10600	-1.09800	-1.08300	-1.05300	-.99900	-.92400	-.84000
+20.0	-1.11500	-1.20000	-1.28000	-1.34000	-1.37900	-1.40500	-1.42100	-1.43100	-1.42200	
	-1.41800	-1.40800	-1.40500	-1.40300	-1.39600	-1.38200	-1.33600	-1.27100	-1.21000	-1.11300
+25.0	-1.37500	-1.44000	-1.51000	-1.57500	-1.62600	-1.63500	-1.65000	-1.65500	-1.65900	
	-1.65800	-1.66000	-1.65800	-1.65500	-1.64600	-1.63100	-1.57000	-1.51300	-1.44200	-1.36700
+30.0	-1.52000	-1.61500	-1.71000	-1.81000	-1.91000	-1.97700	-1.99700	-2.00600	-2.00200	
	-2.00800	-2.00600	-2.00100	-1.98100	-1.96100	-1.93900	-1.88800	-1.79900	-1.65100	-1.55000
+35.0	-1.55500	-1.66500	-1.77000	-1.88500	-1.99800	-2.07300	-2.15200	-2.17100	-2.18200	
	-2.20000	-2.18600	-2.18600	-2.17400	-2.14900	-2.10400	-2.00200	-1.89700	-1.76000	-1.66300
+40.0	-1.71500	-1.83000	-1.94500	-2.06500	-2.18800	-2.18300	-2.30100	-2.31000	-2.31400	
	-2.32800	-2.35500	-2.32100	-2.15600	-2.28100	-2.23100	-2.09500	-1.99100	-1.86000	-1.74700
+45.0	-1.62500	-1.57000	-1.78500	-2.00000	-2.17800	-2.27200	-2.21000	-2.26400	-2.35800	
	-2.31100	-2.35300	-2.35000	-2.29900	-2.29000	-2.25500	-2.15700	-2.00200	-1.64800	-1.70200
+50.0	-1.57000	-1.73500	-1.90000	-2.05000	-2.16500	-2.25400	-2.28800	-2.25800	-2.25800	
	-2.32600	-2.31200	-2.29000	-2.27700	-2.18400	-2.23900	-2.10900	-1.98600	-1.84800	-1.64900
+55.0	-1.77500	-1.90000	-1.97000	-2.05500	-2.17600	-2.18400	-2.22300	-2.21100	-2.19600	
	-2.25200	-2.23500	-2.14500	-2.18200	-2.16500	-2.15200	-2.02500	-1.96500	-1.93100	-1.80000
+60.0	-1.90000	-1.93500	-1.96000	-1.99500	-2.12800	-2.11100	-2.17300	-2.18300	-2.18100	
	-2.20800	-2.19000	-2.09400	-2.13100	-2.15000	-2.11400	-1.99000	-1.98600	-1.96200	-1.87600
+70.0	-1.93000	-1.94500	-1.94000	-1.92000	-1.92900	-2.02100	-2.16100	-2.16000	-2.12000	
	-2.13400	-2.08500	-2.01100	-2.10800	-2.12500	-2.06300	-1.97000	-2.01600	-1.94700	-1.92400
+80.0	-2.00000	-2.04500	-2.07500	-2.08000	-2.04500	-1.99400	-2.04800	-2.09200	-1.99200	
	-2.00400	-2.01900	-1.93000	-2.01400	-2.01800	-1.91900	-2.00000	-2.03400	-2.03200	-1.95800
+90.0	-1.96000	-1.95000	-1.90000	-2.01000	-2.06000	-2.15800	-2.11200	-2.11700	-2.14500	
	-2.14000	-2.11300	-2.10700	-2.10100	-2.16900	-2.07300	-2.07400	-2.03800	-2.08800	-2.06000

TABLE III.- Continued

$C_Z(\alpha, \beta, \delta_h = 10^o)$

BETA	-30.0 0.0	-25.0 + 2.0	-20.0 + 4.0	-15.0 + 6.0	-10.0 + 8.0	- 8.0 +10.0	- 6.0 +15.0	- 4.0 +20.0	- 2.0 +25.0	+30.0
ALPHA										
-20.0	1.02100	1.06600	1.11600	1.12600	1.13900	1.10800	1.10300	1.07000	1.04100	
	1.03900	1.07100	1.07600	1.08900	1.08600	1.07800	1.07000	1.04600	1.00700	.95700
-15.0	.81500	.83800	.84600	.86300	.85400	.84800	.84400	.84100	.84600	
	.84900	.85600	.85200	.85300	.84800	.86300	.86300	.85600	.84100	.82000
-10.0	.62200	.61800	.60300	.60900	.60600	.60200	.59900	.59200	.60000	
	.59600	.60500	.60700	.60900	.60900	.60900	.60700	.60700	.61100	.61900
- 5.0	.18100	.17600	.17900	.18400	.19800	.21200	.21300	.21500	.20200	
	.20500	.20200	.19800	.19200	.18300	.18000	.16500	.16300	.15500	.16900
0.0	-.06900	-.10000	-.12500	-.13100	-.12200	-.12000	-.11400	-.11200	-.11500	
	-.11400	-.11700	-.11700	-.12100	-.12300	-.12600	-.13400	-.12200	-.10900	-.07500
+ 5.0	-.33900	-.40000	-.44400	-.47400	-.48000	-.48000	-.48100	-.48600	-.48700	
	-.49000	-.49000	-.50400	-.49600	-.49100	-.49300	-.48300	-.45800	-.41200	-.35400
+10.0	-.58500	-.63000	-.71500	-.76800	-.80600	-.81000	-.82400	-.83300	-.84400	
	-.84900	-.85100	-.84200	-.84600	-.83100	-.82500	-.80100	-.75200	-.67600	-.59500
+15.0	-.84300	-.94700	-1.03100	-1.09700	-1.13300	-1.14700	-1.16700	-1.17500	-1.18200	
	-1.17700	-1.17100	-1.17600	-1.17500	-1.17100	-1.15800	-1.12000	-1.04700	-.95400	-.86400
+20.0	-1.10400	-1.20000	-1.28700	-1.35600	-1.40400	-1.43100	-1.44600	-1.45300	-1.44500	
	-1.44200	-1.43500	-1.43000	-1.43400	-1.42800	-1.41400	-1.35700	-1.28600	-1.21500	-1.11000
+25.0	-1.36200	-1.45800	-1.56000	-1.65500	-1.74100	-1.77100	-1.77100	-1.78200	-1.79400	
	-1.78900	-1.78700	-1.79100	-1.77500	-1.77500	-1.76000	-1.64600	-1.58200	-1.47300	-1.37000
+30.0	-1.52000	-1.63000	-1.74000	-1.85400	-1.96800	-2.03700	-2.07000	-2.08100	-2.08300	
	-2.08200	-2.08000	-2.07000	-2.05400	-2.03900	-2.01600	-1.92900	-1.79000	-1.67300	-1.56300
+35.0	-1.69000	-1.85600	-2.00600	-2.13600	-2.25200	-2.25500	-2.26000	-2.32600	-2.31700	
	-2.30800	-2.35500	-2.34100	-2.30200	-2.25900	-2.21900	-2.08100	-1.93800	-1.76000	-1.67900
+40.0	-1.84900	-1.94900	-2.05400	-2.16900	-2.29000	-2.36100	-2.34300	-2.37500	-2.28400	
	-2.41100	-2.41900	-2.40200	-2.34500	-2.33300	-2.30300	-2.16300	-2.06500	-1.97100	-1.87800
+45.0	-1.59000	-1.48400	-1.74100	-2.00000	-2.19300	-2.27900	-2.18600	-2.26200	-2.39500	
	-2.30600	-2.37300	-2.36900	-2.29500	-2.29300	-2.26200	-2.17500	-1.99300	-1.55500	-1.66100
+50.0	-1.70700	-1.89100	-2.01300	-2.25500	-2.14100	-2.20000	-2.20400	-2.16500	-2.17900	
	-2.26100	-2.28300	-2.28100	-2.29400	-2.18200	-2.21800	-2.17800	-1.93600	-1.81400	-1.63000
+55.0	-1.73500	-1.83800	-1.84400	-1.90400	-2.13300	-2.15900	-2.21700	-2.20900	-2.18400	
	-2.23100	-2.18600	-2.06800	-2.11500	-2.14500	-2.18000	-1.95100	-1.89100	-1.88500	-1.78200
+60.0	-1.79900	-1.88900	-1.91700	-1.94200	-2.09700	-2.06500	-2.11200	-2.12300	-2.14000	
	-2.18500	-2.16400	-2.06500	-2.10700	-2.14200	-2.12100	-1.96600	-1.94100	-1.91300	-1.82300
+70.0	-1.75300	-1.75200	-1.79700	-1.77900	-1.98700	-2.04800	-2.15700	-2.14900	-2.04800	
	-2.26800	-2.17800	-2.06400	-2.14200	-2.16100	-2.10200	-1.89400	-1.91200	-1.86700	-1.86800
+80.0	-2.06700	-2.12300	-2.10700	-2.14500	-2.05300	-1.91100	-1.97400	-2.02400	-1.92600	
	-1.94000	-1.96700	-1.89100	-1.97800	-1.97600	-1.87200	-1.96400	-1.92600	-1.94200	-1.88600
+90.0	-2.00800	-2.02000	-1.95500	-2.07600	-2.02600	-2.11600	-2.06100	-2.05700	-2.07300	
	-2.05700	-2.03400	-2.03300	-2.03000	-2.09500	-1.99600	-2.04600	-1.92500	-1.99000	-1.97800

TABLE III.- Continued

$$C_Z(\alpha, \beta, \delta_h = 25^{\circ})$$

BETA	-30.0	-25.0	-20.0	-15.0	-10.0	- 8.0	- 6.0	- 4.0	- 2.0	
	0.0	+ 2.0	+ 4.0	+ 6.0	+ 8.0	+10.0	+15.0	+20.0	+25.0	+30.0
ALPHA										
-20.0	.72300	.75000	.74400	.74400	.71100	.70900	.69700	.69700	.69600	
	.71000	.70400	.71500	.72000	.72100	.72100	.75000	.75000	.74000	.71000
-15.0	.51200	.49500	.46100	.46500	.47000	.47000	.47100	.46700	.48300	
	.47600	.48100	.47200	.47500	.47300	.47300	.46500	.47000	.49000	.51500
-10.0	.24900	.21200	.18600	.19500	.20300	.20500	.20200	.20300	.20700	
	.20500	.20000	.19400	.19800	.19800	.20100	.18500	.19000	.21000	.25000
- 5.0	.10000	.09000	.09000	.09500	.11100	.12200	.12200	.12200	.12100	
	.12500	.12100	.11400	.10700	.09700	.10100	.08100	.07700	.07700	.09300
0.0	-.15000	-.19000	-.22000	-.23500	-.23200	-.22400	-.22400	-.22100	-.22700	
	-.22800	-.23100	-.23200	-.23900	-.24100	-.24400	-.24400	-.23200	-.20700	-.16400
+ 5.0	-.38500	-.46000	-.51500	-.55500	-.56600	-.56300	-.56600	-.57100	-.57200	
	-.57800	-.57800	-.59900	-.58800	-.57700	-.57900	-.55900	-.52800	-.46700	-.39800
+10.0	-.62000	-.69000	-.76000	-.83000	-.89200	-.89100	-.91000	-.92400	-.93900	
	-.94600	-.94900	-.93600	-.94500	-.92400	-.91300	-.87600	-.81300	-.72400	-.62600
+15.0	-.86500	-.99000	-1.09000	-1.17000	-1.20800	-1.21500	-1.23900	-1.25000	-1.26900	
	-1.25300	-1.24000	-1.25500	-1.25500	-1.25700	-1.24500	-1.19800	-1.10300	-.99000	-.89100
+20.0	-1.05500	-1.19500	-1.32000	-1.43000	-1.51900	-1.55000	-1.56400	-1.55800	-1.55500	
	-1.55400	-1.56300	-1.54900	-1.57700	-1.57800	-1.56300	-1.45300	-1.35800	-1.24100	-1.09700
+25.0	-1.36000	-1.46000	-1.57000	-1.67000	-1.76300	-1.79700	-1.79400	-1.80600	-1.82000	
	-1.81400	-1.81100	-1.81600	-1.79800	-1.80000	-1.78500	-1.66100	-1.59500	-1.47900	-1.37100
+30.0	-1.52000	-1.63500	-1.75000	-1.87000	-1.98900	-2.05800	-2.09500	-2.10700	-2.11200	
	-2.10800	-2.10600	-2.09400	-2.07900	-2.06600	-2.04300	-1.94300	-1.80400	-1.68100	-1.56800
+35.0	-1.61500	-1.75000	-1.87500	-1.99500	-2.11100	-2.15400	-2.20000	-2.24000	-2.24200	
	-2.24800	-2.26100	-2.25500	-2.23100	-2.19800	-2.15500	-2.03700	-1.91500	-1.76000	-1.67000
+40.0	-1.77500	-1.87500	-1.98000	-2.09500	-2.21600	-2.28700	-2.26900	-2.30100	-2.21000	
	-2.33700	-2.34500	-2.32800	-2.27100	-2.25900	-2.22900	-2.08900	-1.99100	-1.89700	-1.80400
+45.0	-1.74000	-1.84500	-1.92500	-2.00000	-2.13000	-2.25100	-2.28600	-2.27000	-2.23900	
	-2.32700	-2.28900	-2.28800	-2.31200	-2.28200	-2.23200	-2.09900	-2.03000	-1.94500	-1.83400
+50.0	-1.57000	-1.74000	-1.90000	-2.05000	-2.15600	-2.21600	-2.20300	-2.15800	-2.17500	
	-2.26100	-2.26600	-2.26200	-2.25500	-2.15300	-2.20100	-2.11000	-1.98400	-1.84100	-1.63700
+55.0	-1.70000	-1.81000	-1.88000	-1.95000	-2.04300	-2.17000	-2.18400	-2.11100	-2.20400	
	-2.23100	-2.20300	-2.10200	-2.13500	-2.17300	-2.10700	-1.95000	-1.89200	-1.87700	-1.76500
+60.0	-1.79500	-1.89500	-1.96000	-2.02000	-2.11300	-2.09400	-2.12400	-2.12400	-2.13400	
	-2.17400	-2.17700	-2.10300	-2.15300	-2.17600	-2.14400	-2.00000	-1.96000	-1.93000	-1.83800
+70.0	-1.78000	-1.78500	-1.79000	-1.81000	-1.87300	-1.94300	-2.05900	-2.27400	-2.00000	
	-2.25900	-2.21100	-1.88500	-2.22100	-2.21200	-2.12500	-1.97000	-1.90700	-1.88200	-1.87400
+80.0	-1.95000	-1.98000	-1.98000	-1.96000	-1.91100	-1.88100	-1.95500	-2.00500	-1.89400	
	-1.89900	-2.00900	-2.01400	-2.10100	-2.01400	-1.82500	-1.84000	-1.89900	-1.92200	-1.87300
+90.0	-1.92500	-1.92000	-1.87000	-1.88500	-1.96900	-2.07100	-2.02900	-2.03900	-2.07000	
	-2.06900	-2.02600	-2.00500	-2.00000	-2.08500	-2.00700	-1.93500	-1.94800	-1.98900	-1.95100

TABLE III.- Continued

$C_{Z,lef}(\alpha,\beta)$

ALPHA \ BETA	-30.0 / 0.0	-25.0 / + 2.0	-20.0 / + 4.0	-15.0 / + 6.0	-10.0 / + 8.0	- 8.0 / +10.0	- 6.0 / +15.0	- 4.0 / +20.0	- 2.0 / +25.0	+30.0
-20.0	1.18300	1.24600	1.27900	1.29000	1.36900	1.36400	1.29700	1.27700	1.27600	
	1.25600	1.28100	1.28000	1.31200	1.31500	1.30600	1.22700	1.21600	1.18300	1.12000
-15.0	.96000	1.01800	1.05500	1.09300	1.05800	1.03900	1.03100	1.01900	1.02500	
	1.03500	1.03300	1.04200	1.04300	1.05600	1.05600	1.09100	1.05300	1.01600	.95800
-10.0	.70900	.71000	.70200	.70400	.70100	.71000	.73000	.72900	.72900	
	.72500	.72900	.72800	.72800	.72300	.71100	.71400	.71200	.72000	.71900
- 5.0	.22200	.21600	.23100	.22700	.24000	.24300	.24400	.24900	.24900	
	.24800	.24800	.24200	.23900	.23500	.22900	.21600	.22000	.20500	.21100
0.0	-.06600	-.08400	-.09000	-.10500	-.10400	-.09900	-.10700	-.09900	-.09900	
	-.10000	-.10100	-.10400	-.10400	-.10400	-.10600	-.10700	-.09200	-.08600	-.06800
+ 5.0	-.31700	-.34700	-.39000	-.41400	-.42000	-.41700	-.41700	-.42100	-.42400	
	-.42800	-.42100	-.42800	-.42200	-.42300	-.42500	-.41900	-.39500	-.35200	-.32200
+10.0	-.56900	-.61900	-.67900	-.70300	-.72800	-.76500	-.77200	-.77400	-.77200	
	-.77400	-.77000	-.76700	-.76100	-.75400	-.75600	-.73100	-.70700	-.64500	-.59700
+15.0	-.85300	-.92900	-1.01800	-1.07000	-1.09800	-1.11600	-1.11440	-1.15100	-1.14200	
	-1.13900	-1.13500	-1.11800	-1.11200	-1.10700	-1.09900	-1.07100	-1.01900	-.93000	-.85400
+20.0	-1.10600	-1.16800	-1.22800	-1.31400	-1.34800	-1.35900	-1.36200	-1.35200	-1.35700	
	-1.35500	-1.37100	-1.37600	-1.37000	-1.37900	-1.39900	-1.36500	-1.27900	-1.21900	-1.15700
+25.0	-1.31400	-1.40700	-1.46500	-1.50600	-1.56400	-1.59800	-1.62800	-1.64700	-1.64600	
	-1.65000	-1.64200	-1.64100	-1.61800	-1.59900	-1.58500	-1.52700	-1.48600	-1.42800	-1.33500
+30.0	-1.49600	-1.51000	-1.58900	-1.69200	-1.77500	-1.81400	-1.84600	-1.87500	-1.87900	
	-1.88300	-1.89100	-1.87600	-1.84300	-1.83800	-1.81100	-1.72800	-1.62500	-1.54600	-1.53200
+35.0	-1.59400	-1.69400	-1.80700	-1.87500	-1.95700	-1.97600	-2.03200	-2.06000	-2.07000	
	-2.07700	-2.03800	-2.03900	-2.02800	-2.00500	-1.98600	-1.90400	-1.83600	-1.71300	-1.62300
+40.0	-1.68300	-1.75500	-1.91200	-1.99900	-2.11100	-2.14900	-2.14700	-2.20400	-2.20700	
	-2.20400	-2.20500	-2.19500	-2.19300	-2.17400	-2.13300	-2.02100	-1.93400	-1.77700	-1.70500
+45.0	-1.66400	-1.78300	-1.85900	-1.96200	-2.03000	-2.12900	-1.91700	-2.14300	-2.05000	
	-2.20800	-2.20100	-2.18200	-2.07700	-2.20900	-2.12600	-2.05800	-1.95500	-1.87900	-1.76000

TABLE III.- Continued

ALPHA	$\Delta C_{Z,sb}(\alpha)$
-20.0	-.38580
-15.0	-.38580
-10.0	-.38580
- 5.0	-.38580
0.0	-.38580
+ 5.0	-.26850
+10.0	-.30210
+15.0	-.42480
+20.0	-.20940
+25.0	-.09690
+30.0	.04380
+35.0	.09470
+40.0	.00140
+45.0	-.00970
+50.0	-.01530
+55.0	-.05200
+60.0	-.00100
+70.0	-.02020
+80.0	-.03690
+90.0	-.03690

ALPHA	$C_{Z_q}(\alpha)$
-20.0	-23.90000
-15.0	-23.90000
-10.0	-23.90000
- 5.0	-29.50000
0.0	-29.50000
+ 5.0	-30.50000
+10.0	-31.30000
+15.0	-30.10000
+20.0	-27.70000
+25.0	-28.20000
+30.0	-29.00000
+35.0	-29.80000
+40.0	-38.30000
+45.0	-35.30000
+50.0	-32.30000
+55.0	-27.30000
+60.0	-25.20000
+70.0	-27.30000
+80.0	-9.35000
+90.0	-2.16000

ALPHA	$\Delta C_{Z_{q,lef}}(\alpha)$
-20.0	15.10000
-15.0	15.10000
-10.0	15.10000
- 5.0	3.70000
0.0	.60000
+ 5.0	-1.30000
+10.0	.30000
+15.0	-3.80000
+20.0	-4.60000
+25.0	-.20000
+30.0	-2.70000
+35.0	-3.50000
+40.0	-1.30000
+45.0	-.65000

TABLE III.- Continued

$C_m(\alpha, \beta, \delta_h = -25^{\circ})$

ALPHA \ BETA	-30.0	-25.0	-20.0	-15.0	-10.0	- 8.0	- 6.0	- 4.0	- 2.0	0.0	+ 2.0	+ 4.0	+ 6.0	+ 8.0	+10.0	+15.0	+20.0	+25.0	+30.0
-20.0	.20590	.19370	.19180	.18500	.16920	.16930	.17700	.17460	.17420	.17500	.17210	.17580	.18010	.18260	.19120	.20700	.21400	.21600	.22700
-15.0	.16980	.16500	.17330	.17230	.15330	.16180	.16390	.16070	.15970	.15840	.15890	.16150	.15730	.15340	.14640	.16500	.16700	.15800	.16300
-10.0	.14260	.15790	.18070	.16410	.15330	.15860	.15950	.16290	.16150	.15900	.15660	.15340	.15230	.14890	.14930	.15800	.17500	.15300	.13800
- 5.0	.16200	.17700	.15300	.14500	.13800	.13650	.13290	.12690	.12420	.12160	.11830	.12120	.12360	.12670	.13030	.13730	.14440	.16790	.15380
0.0	.15300	.15400	.14800	.14500	.14450	.14380	.14300	.14110	.14120	.14090	.14100	.14090	.14030	.14090	.14140	.14480	.14530	.15230	.15130
+ 5.0	.14700	.15300	.15600	.15700	.15860	.15950	.15850	.15770	.15800	.15800	.15910	.15840	.15760	.15720	.15730	.15680	.15570	.15400	.14720
+10.0	.15000	.16200	.16500	.17000	.17460	.17580	.17680	.17780	.18330	.18450	.18400	.18240	.18110	.17970	.17840	.17500	.17010	.16630	.15470
+15.0	.16700	.17600	.19100	.19600	.20000	.20120	.20410	.20620	.20690	.20870	.20700	.20660	.20550	.20220	.20000	.19580	.19010	.17550	.16680
+20.0	.15100	.17000	.19000	.20200	.20730	.20980	.21220	.21290	.21370	.21520	.21330	.21180	.21090	.20820	.20610	.19910	.18780	.16180	.14790
+25.0	.12000	.14700	.17500	.19400	.20430	.20280	.20280	.19910	.19810	.19780	.19690	.19570	.19580	.19480	.19530	.18770	.16870	.14060	.11300
+30.0	.10800	.06700	.09800	.15000	.17040	.19300	.19850	.20090	.20220	.20220	.20210	.20070	.19720	.19470	.19010	.16960	.11860	.08890	.12700
+35.0	.08200	.04700	.06800	.08100	.11740	.12330	.15220	.17130	.17890	.18140	.18150	.17990	.17900	.17030	.14590	.11240	.09620	.07570	.11320
+40.0	.11300	.05000	.06000	.08700	.11310	.12790	.13410	.14330	.14830	.14780	.12910	.13120	.12450	.10250	.10280	.07450	.04950	.04060	.10240
+45.0	.09300	.06600	.06500	.05300	.07340	.09140	.09680	.08480	.09350	.09220	.09400	.08380	.06100	.04910	.04200	.02080	.03430	.03380	.06000
+50.0	-.01500	-.01100	-.02500	.01500	.06630	.06440	.04980	.04070	.05210	.07450	.06700	.04530	.03730	.03200	.03970	-.01140	-.05140	-.03710	-.04080
+55.0	.01900	.01700	-.08600	-.00400	.07940	.04940	.01740	.05300	.02920	.07130	.04040	.00070	-.00240	.01650	.02810	-.05620	-.13730	-.03430	-.03350
+60.0	-.03600	-.02300	-.07500	-.06000	-.06270	-.07050	-.05560	-.05340	-.05490	-.05400	-.06180	-.06740	-.08280	-.08490	-.10040	-.09760	-.11170	-.05990	-.07140
+70.0	-.30700	-.30800	-.28500	-.30500	-.27690	-.26480	-.18280	-.21150	-.20320	-.22440	-.22640	-.21950	-.20540	-.22030	-.21910	-.24790	-.22760	-.25180	-.25030
+80.0	-.36500	-.39800	-.40300	-.38700	-.34110	-.33440	-.34250	-.34550	-.32540	-.33890	-.35220	-.31870	-.32620	-.32830	-.32850	-.37630	-.39230	-.38570	-.35320
+90.0	-.52600	-.52700	-.51500	-.50400	-.49000	-.51570	-.48010	-.49700	-.48310	-.47230	-.48300	-.48180	-.49110	-.50740	-.48630	-.50010	-.51240	-.52270	-.52190

TABLE III.- Continued

$$C_m(\alpha, \beta, \delta_h = -10^{\circ})$$

BETA	-30.0	-25.0	-20.0	-15.0	-10.0	- 8.0	- 6.0	- 4.0	- 2.0	
	0.0	+ 2.0	+ 4.0	+ 6.0	+ 8.0	+10.0	+15.0	+20.0	+25.0	+30.0
ALPHA										
-20.0	.14690	.12720	.12100	.10750	.07980	.07560	.08000	.08270	.08530	
	.08640	.07820	.08110	.08210	.08470	.09650	.12400	.13760	.14390	.16310
-15.0	.10870	.09560	.09470	.08850	.05810	.05490	.05050	.04270	.03780	
	.03280	.03530	.04260	.04810	.04990	.05240	.08230	.08910	.08980	.10020
-10.0	.07840	.07430	.08520	.06190	.03900	.03440	.02900	.02490	.01770	
	.00410	.01690	.02270	.02800	.03110	.03570	.05850	.08200	.07070	.07520
- 5.0	.05700	.06200	.04400	.03200	.01700	.01600	.01200	.00800	.01000	
	.00760	.00700	.00800	.01000	.01100	.01200	.02700	.03900	.05800	.05200
0.0	.05200	.05400	.04300	.03900	.04200	.04100	.04200	.04300	.04300	
	.04300	.04200	.04300	.03700	.03800	.03780	.04300	.04500	.05700	.05000
+ 5.0	.05200	.04200	.05000	.05300	.05400	.05300	.05400	.05300	.05200	
	.05010	.05200	.05100	.05100	.05100	.05100	.05100	.04900	.04300	.05200
+10.0	.02800	.03500	.04000	.04000	.04700	.04800	.05000	.05000	.05100	
	.05530	.05200	.05300	.05200	.05200	.05100	.04300	.04200	.03800	.03000
+15.0	.04300	.04000	.05300	.06000	.06300	.06300	.06700	.06900	.07200	
	.07060	.07100	.07000	.07000	.06800	.06300	.05900	.05300	.04000	.04200
+20.0	.02700	.02500	.04000	.05000	.05700	.05600	.05800	.06000	.06500	
	.06740	.06900	.06600	.06200	.05500	.05200	.04600	.03600	.02000	.02200
+25.0	.01000	.00800	.02300	.03800	.04700	.04800	.04800	.04600	.04800	
	.04920	.04600	.04700	.04400	.04300	.04300	.03400	.01900	.00200	.00500
+30.0	.01500	-.03500	-.01700	.00300	.02000	.04000	.04700	.04900	.05100	
	.05280	.04800	.04800	.04500	.04000	.03300	.01600	-.00500	-.02400	.02800
+35.0	.01600	-.02700	-.03400	-.02400	-.00600	.00400	.01600	.02400	.03100	
	.02780	.02800	.02500	.01200	.01300	.00300	-.02100	-.02600	-.02000	.02300
+40.0	.06800	.01900	-.01600	-.01300	-.00800	-.00700	-.00600	-.00500	-.00600	
	-.00940	-.02200	-.02200	-.04400	-.03800	-.04100	-.04700	-.05000	-.01300	.03300
+45.0	.02500	-.02100	-.02700	-.05400	-.05000	-.03900	-.05300	-.05400	-.03900	
	-.04110	-.04700	-.05800	-.07200	-.07500	-.08100	-.08500	-.05600	-.05100	-.00600
+50.0	-.01110	0.00000	-.00700	-.01050	.00730	-.00850	-.03710	-.05190	-.03790	
	-.01290	-.02210	-.04550	-.05420	-.05940	-.05150	-.06930	-.06580	-.05880	-.06990
+55.0	.00020	.00430	-.09360	-.04250	.03590	.01340	-.01100	-.01690	-.01130	
	.02020	-.01310	-.05530	-.06020	-.04240	-.03190	-.11040	-.16140	-.06350	-.06760
+60.0	-.08790	-.03150	-.03840	-.17570	-.09620	-.10500	-.09120	-.08570	-.07940	
	-.07080	-.08870	-.10450	-.12470	-.12640	-.14140	-.22090	-.08360	-.07670	-.13310
+70.0	-.34290	-.35790	-.34300	-.35640	-.35200	-.33630	-.26910	-.30050	-.29240	
	-.31370	-.31130	-.30010	-.28680	-.30760	-.31240	-.31680	-.30340	-.31820	-.30330
+80.0	-.42940	-.47150	-.48770	-.48330	-.43150	-.42350	-.42380	-.43210	-.41100	
	-.42360	-.44450	-.41850	-.42680	-.42310	-.41750	-.46930	-.47370	-.45750	-.41540
+90.0	-.62080	-.61730	-.60280	-.59590	-.55320	-.58810	-.56170	-.58590	-.57730	
	-.57180	-.57280	-.56180	-.56800	-.58780	-.57020	-.57890	-.58580	-.60030	-.60380

TABLE III.- Continued

$$C_m(\alpha, \beta, \delta_h = 0^{\circ})$$

BETA / ALPHA	-30.0 / 0.0	-25.0 / + 2.0	-20.0 / + 4.0	-15.0 / + 6.0	-10.0 / + 8.0	- 8.0 / +10.0	- 6.0 / +15.0	- 4.0 / +20.0	- 2.0 / +25.0	+30.0
-20.0	.09780	.07190	.06210	.04300	.00540	-.00230	-.00060	.00620	.01140	
	.01270	.00010	.00230	.00060	.00330	.01770	.05500	.07400	.08400	.11000
-15.0	.05600	.03570	.02640	.01630	-.02400	-.03720	-.04720	-.05900	-.06740	
	-.07550	-.07120	-.06000	-.04600	-.03930	-.02870	.01100	.02200	.03100	.04600
-10.0	.03420	.01670	.01940	-.00890	-.04100	-.05100	-.06080	-.07000	-.08130	
	-.10250	-.07930	-.06730	-.05760	-.05000	-.04240	-.01000	.01800	.01400	.03200
- 5.0	-.02400	-.02400	-.03900	-.05500	-.07580	-.07730	-.08020	-.08020	-.07740	
	-.07440	-.07740	-.07820	-.07840	-.07820	-.07700	-.05720	-.04000	-.02510	-.02600
0.0	-.05500	-.04600	-.05900	-.06400	-.06600	-.06600	-.06390	-.06150	-.06050	
	-.05980	-.06000	-.06060	-.06080	-.06170	-.06210	-.06060	-.05870	-.04840	-.05170
+ 5.0	-.04600	-.06400	-.05500	-.05200	-.05140	-.05070	-.05090	-.05010	-.04990	
	-.04980	-.05000	-.05180	-.05260	-.05320	-.05370	-.05450	-.05640	-.06190	-.06510
+10.0	-.06700	-.06200	-.05600	-.05300	-.04950	-.04840	-.04670	-.04570	-.04440	
	-.04370	-.04480	-.04580	-.04800	-.04900	-.04980	-.05340	-.05550	-.06190	-.06580
+15.0	-.06700	-.07700	-.06800	-.05900	-.05360	-.05140	-.04890	-.04560	-.04190	
	-.04070	-.04100	-.04220	-.04320	-.04470	-.04840	-.05360	-.06090	-.07150	-.06130
+20.0	-.05700	-.07100	-.06200	-.05200	-.04780	-.05180	-.04980	-.04630	-.03840	
	-.03420	-.03290	-.03660	-.04260	-.05320	-.05550	-.06200	-.07050	-.08000	-.06600
+25.0	-.06400	-.08800	-.07700	-.06700	-.05480	-.05390	-.05300	-.05200	-.04990	
	-.05070	-.05010	-.05060	-.05260	-.05390	-.05600	-.06490	-.07610	-.08880	-.06330
+30.0	-.04500	-.10500	-.09200	-.09200	-.07820	-.06080	-.05290	-.05000	-.04710	
	-.04590	-.05100	-.05200	-.05420	-.06120	-.06800	-.08470	-.08490	-.09710	-.03640
+35.0	-.02200	-.07200	-.09200	-.08800	-.07380	-.06390	-.05940	-.05720	-.05670	
	-.06050	-.06050	-.06250	-.07290	-.07470	-.08040	-.09300	-.09740	-.07750	-.02790
+40.0	.04500	.00500	-.05200	-.06100	-.06620	-.07290	-.07390	-.07890	-.08200	
	-.08350	-.09170	-.09710	-.12520	-.10710	-.11160	-.10570	-.09790	-.04020	.00220
+45.0	-.00100	-.05200	-.06000	-.09200	-.09270	-.08610	-.10560	-.09660	-.08620	
	-.09230	-.09750	-.10800	-.11680	-.12090	-.12430	-.12340	-.08970	-.08200	-.02940
+50.0	-.00900	-.01300	-.01700	-.03500	-.07800	-.07130	-.07740	-.08900	-.09130	
	-.08260	-.08980	-.11120	-.12010	-.12770	-.12220	-.12200	-.08520	-.06480	-.06240
+55.0	-.05100	-.01800	-.06500	-.05300	-.04770	-.05200	-.05830	-.06630	-.08300	
	-.07380	-.08510	-.10530	-.10500	-.09880	-.10000	-.10760	-.11520	-.05890	-.10470
+60.0	-.18300	-.14800	-.17300	-.17200	-.15120	-.14280	-.11180	-.10940	-.12660	
	-.14140	-.14360	-.14370	-.15210	-.14590	-.15300	-.17090	-.17410	-.14750	-.18410
+70.0	-.38300	-.39800	-.38200	-.38700	-.38690	-.36370	-.27060	-.29670	-.29440	
	-.32160	-.32520	-.31990	-.31230	-.33850	-.34870	-.34860	-.34450	-.35930	-.34440
+80.0	-.48300	-.51800	-.52800	-.50600	-.48500	-.47850	-.48040	-.48690	-.46050	
	-.46780	-.48830	-.46200	-.47440	-.47920	-.48210	-.50220	-.52420	-.51450	-.47880
+90.0	-.63300	-.63000	-.61600	-.61600	-.60670	-.63660	-.60530	-.62810	-.62170	
	-.61840	-.61630	-.60220	-.60730	-.62810	-.61150	-.62090	-.62100	-.63510	-.63810

TABLE III.- Continued

$$C_m\left(\alpha, \beta, \delta_h = 10^\circ\right)$$

BETA	-30.0	-25.0	-20.0	-15.0	-10.0	- 8.0	- 6.0	- 4.0	- 2.0	
	0.0	+ 2.0	+ 4.0	+ 6.0	+ 8.0	+10.0	+15.0	+20.0	+25.0	+30.0
ALPHA										
-20.0	.02000	-.00360	-.01070	-.03340	-.07780	-.09440	-.09260	-.08550	-.08150	
	-.08350	-.09550	-.09300	-.09430	-.08810	-.07430	-.02650	-.00400	.00340	.02680
-15.0	-.01530	-.03850	-.05250	-.07430	-.12330	-.13760	-.14660	-.15510	-.16630	
	-.17190	-.16830	-.15680	-.14370	-.13710	-.12950	-.07980	-.05890	-.04450	-.02410
-10.0	-.05490	-.07920	-.09320	-.12260	-.15210	-.16090	-.16880	-.17740	-.18800	
	-.21530	-.18390	-.17380	-.16480	-.15940	-.15250	-.12250	-.09310	-.12760	-.05480
- 5.0	-.11200	-.12400	-.15200	-.16800	-.18300	-.18800	-.19100	-.19200	-.18900	
	-.18880	-.19000	-.19300	-.19300	-.19100	-.18300	-.16800	-.15200	-.12500	-.11200
0.0	-.11700	-.12700	-.15200	-.15900	-.16000	-.16000	-.15900	-.15700	-.16200	
	-.16100	-.16200	-.16300	-.16700	-.16200	-.16200	-.16200	-.15300	-.12600	-.11700
+ 5.0	-.10500	-.13300	-.14400	-.15500	-.15500	-.15500	-.15500	-.15500	-.15800	
	-.16060	-.16100	-.16200	-.15700	-.15700	-.15600	-.15600	-.14500	-.13300	-.11800
+10.0	-.09700	-.11200	-.12200	-.13500	-.14200	-.14200	-.15100	-.15300	-.15700	
	-.15480	-.15500	-.15200	-.15300	-.14500	-.14600	-.14000	-.12600	-.11700	-.10400
+15.0	-.09700	-.11800	-.13300	-.15100	-.15200	-.15000	-.15500	-.15500	-.15200	
	-.14520	-.14800	-.15500	-.15500	-.15700	-.15200	-.15100	-.13400	-.11800	-.09600
+20.0	-.06200	-.08300	-.09700	-.10600	-.13400	-.14200	-.13800	-.13400	-.13000	
	-.12640	-.12600	-.12600	-.15100	-.16100	-.16600	-.13700	-.12600	-.11500	-.09400
+25.0	-.07500	-.10300	-.11300	-.10800	-.13700	-.14400	-.15300	-.15400	-.15400	
	-.15300	-.15500	-.15000	-.15000	-.16000	-.16400	-.13300	-.13800	-.12900	-.09900
+30.0	-.08800	-.16800	-.16500	-.17200	-.17100	-.15500	-.15000	-.14700	-.14400	
	-.14400	-.14500	-.14600	-.15300	-.15700	-.15600	-.15900	-.15200	-.15500	-.07500
+35.0	-.10500	-.16110	-.18620	-.20950	-.19510	-.17600	-.15140	-.14440	-.14270	
	-.14110	-.14500	-.15130	-.15650	-.16270	-.17050	-.18360	-.16110	-.13630	-.08150
+40.0	-.04380	-.10790	-.12810	-.14850	-.14050	-.12720	-.13010	-.13670	-.15550	
	-.14500	-.15430	-.15950	-.15270	-.16440	-.16820	-.17910	-.15530	-.13620	-.07440
+45.0	-.14480	-.09310	-.13190	-.17930	-.15180	-.12640	-.10530	-.15750	-.18070	
	-.14110	-.16350	-.16550	-.16350	-.18150	-.18720	-.22060	-.16440	-.13200	-.19350
+50.0	-.15300	-.13300	-.12800	-.14700	-.10770	-.10300	-.11110	-.11540	-.11610	
	-.10080	-.10600	-.12540	-.12730	-.12280	-.10520	-.14420	-.12530	-.12860	-.14980
+55.0	-.07600	-.06300	-.15200	-.05700	-.00750	-.04600	-.08650	-.06140	-.09760	
	-.06790	-.09220	-.12530	-.12210	-.09720	-.07970	-.13010	-.22550	-.13580	-.14810
+60.0	-.17100	-.12000	-.13500	-.14000	-.15880	-.16340	-.14550	-.14440	-.15120	
	-.15560	-.16530	-.17190	-.18660	-.18590	-.19850	-.18080	-.17580	-.16210	-.21160
+70.0	-.40010	-.40440	-.37890	-.40500	-.34190	-.33640	-.26100	-.27140	-.22010	
	-.19830	-.23630	-.26550	-.26950	-.28440	-.28330	-.37340	-.34730	-.37280	-.36850
+80.0	-.50820	-.53380	-.53330	-.52530	-.48770	-.48480	-.49020	-.49700	-.46770	
	-.47210	-.49290	-.46690	-.47760	-.47870	-.47790	-.51550	-.52350	-.52400	-.49840
+90.0	-.63680	-.63260	-.61740	-.62170	-.59090	-.62140	-.59060	-.61460	-.60990	
	-.60830	-.60800	-.59580	-.59790	-.61090	-.58650	-.61730	-.61300	-.62820	-.63240

TABLE III.- Continued

$$C_m\left(\alpha,\beta,\delta_h = 25^{\circ}\right)$$

BETA	-30.0	-25.0	-20.0	-15.0	-10.0	- 8.0	- 6.0	- 4.0	- 2.0	
	0.0	+ 2.0	+ 4.0	+ 6.0	+ 8.0	+10.0	+15.0	+20.0	+25.0	+30.0
ALPHA										
-20.0	-.08180	-.10230	-.10600	-.13340	-.18660	-.21490	-.21280	-.20550	-.20300	
	-.20930	-.22040	-.21760	-.21850	-.20770	-.19460	-.13300	-.10600	-.10200	-.08200
-15.0	-.11600	-.14320	-.16460	-.20200	-.26350	-.27920	-.28680	-.29060	-.30590	
	-.30790	-.30520	-.29330	-.28160	-.27500	-.27170	-.20800	-.17300	-.15100	-.12300
-10.0	-.15270	-.18450	-.21680	-.24800	-.27400	-.28160	-.28740	-.29520	-.30250	
	-.33910	-.29880	-.29070	-.28250	-.27940	-.27340	-.24600	-.21500	-.18300	-.15000
- 5.0	-.17700	-.20000	-.23700	-.25200	-.26300	-.26980	-.27340	-.27370	-.27380	
	-.27410	-.27610	-.27820	-.27850	-.27560	-.26320	-.25270	-.23700	-.20020	-.17720
0.0	-.17400	-.19700	-.23400	-.24700	-.24870	-.24860	-.24930	-.24890	-.25390	
	-.25270	-.25240	-.25240	-.25320	-.25170	-.24910	-.24910	-.23590	-.19830	-.17480
+ 5.0	-.16400	-.19200	-.21900	-.24300	-.24290	-.24250	-.24410	-.24760	-.25400	
	-.25620	-.25890	-.25810	-.24820	-.24280	-.24270	-.24340	-.21990	-.19390	-.16120
+10.0	-.12800	-.16200	-.18800	-.21600	-.22970	-.22890	-.23910	-.25190	-.26260	
	-.25540	-.25990	-.25300	-.25010	-.23670	-.23300	-.22200	-.19380	-.16640	-.13380
+15.0	-.11600	-.14800	-.18100	-.21500	-.21860	-.21740	-.22720	-.22830	-.22580	
	-.21570	-.21840	-.22970	-.23050	-.23100	-.21900	-.21750	-.18380	-.15020	-.11950
+20.0	-.06800	-.09300	-.12400	-.15400	-.22030	-.23110	-.22720	-.22050	-.22050	
	-.21650	-.21820	-.21380	-.25890	-.27050	-.27510	-.21110	-.18110	-.14820	-.12270
+25.0	-.07500	-.10900	-.13200	-.13300	-.18820	-.21230	-.22640	-.23040	-.23370	
	-.23250	-.23220	-.22690	-.22430	-.23820	-.24650	-.18280	-.18480	-.15950	-.12500
+30.0	-.09700	-.18600	-.18600	-.19800	-.19890	-.18280	-.17980	-.17620	-.17510	
	-.17400	-.17320	-.17820	-.18550	-.18750	-.18520	-.18240	-.17320	-.14780	-.08140
+35.0	-.10400	-.16000	-.18500	-.20800	-.19360	-.17460	-.15030	-.14330	-.14160	
	-.14010	-.14400	-.15020	-.15550	-.16160	-.16940	-.18250	-.16030	-.13560	-.08080
+40.0	-.02500	-.08400	-.11200	-.13000	-.12480	-.11570	-.11820	-.12450	-.14000	
	-.13200	-.14110	-.14630	-.15320	-.15230	-.15620	-.16360	-.14320	-.11590	-.05820
+45.0	-.05700	-.06800	-.08800	-.12600	-.11570	-.10180	-.10550	-.12030	-.12300	
	-.11130	-.12320	-.13040	-.13500	-.14450	-.14880	-.16180	-.11880	-.10030	-.09330
+50.0	-.10800	-.09300	-.09300	-.08700	-.07450	-.08940	-.11980	-.13880	-.13660	
	-.12340	-.12540	-.14160	-.14630	-.15080	-.14210	-.15500	-.15850	-.15880	-.17710
+55.0	-.12500	-.11500	-.20700	-.10300	-.05880	-.08310	-.10950	-.07910	-.11890	
	-.09290	-.11860	-.15330	-.15230	-.13040	-.11580	-.15800	-.26120	-.17020	-.18120
+60.0	-.14300	-.08200	-.08500	-.09100	-.12510	-.14920	-.15070	-.15700	-.15890	
	-.15840	-.16890	-.17730	-.19470	-.19820	-.21500	-.18080	-.17370	-.17190	-.23330
+70.0	-.42200	-.43800	-.42500	-.43300	-.33900	-.32310	-.23730	-.25470	-.22770	
	-.23030	-.35050	-.19310	-.18800	-.23710	-.27010	-.36350	-.35630	-.36970	-.35340
+80.0	-.45000	-.50000	-.52400	-.51400	-.46330	-.46480	-.47460	-.48620	-.46210	
	-.47160	-.44740	-.39160	-.40820	-.42990	-.45930	-.51130	-.52020	-.49610	-.44600
+90.0	-.56000	-.59200	-.51300	-.59300	-.56740	-.60300	-.57740	-.60210	-.59380	
	-.58860	-.58390	-.56730	-.57000	-.58850	-.56960	-.59610	-.61580	-.59510	-.56340

TABLE III.- Continued

$C_{m,lef}(\alpha,\beta)$

BETA	-30.0	-25.0	-20.0	-15.0	-10.0	- 8.0	- 6.0	- 4.0	- 2.0	
	0.0	+ 2.0	+ 4.0	+ 6.0	+ 8.0	+10.0	+15.0	+20.0	+25.0	+30.0
ALPHA										
-20.0	.09220	.05590	.05250	-.03380	-.05180	-.06050	-.05740	-.05540	-.05500	
	-.05030	-.05210	-.04830	-.04590	-.04040	-.03730	-.01930	.06700	.07040	.10670
-15.0	.03720	.00620	-.00670	-.02170	-.07020	-.08600	-.10010	-.10000	-.10020	
	-.10120	-.09740	-.09390	-.08390	-.08370	-.07590	-.02740	-.01240	.00050	.03150
-10.0	.02510	.00060	.00140	-.02290	-.05360	-.06340	-.06540	-.06560	-.06520	
	-.06470	-.06530	-.06590	-.06540	-.06310	-.05700	-.02630	-.00200	-.00280	.02170
- 5.0	-.00060	-.01930	-.02340	-.03210	-.03860	-.03890	-.03850	-.03860	-.03880	
	-.03870	-.03890	-.03870	-.03880	-.03920	-.03860	-.03210	-.02340	-.01930	-.00060
0.0	-.02730	-.02460	-.02300	-.02310	-.02590	-.02550	-.02860	-.02710	-.02710	
	-.02670	-.02660	-.02720	-.02800	-.02670	-.02700	-.02420	-.02410	-.02570	-.02840
+ 5.0	-.03190	-.02720	-.02040	-.01700	-.01520	-.01480	-.01450	-.01380	-.01270	
	-.01280	-.01330	-.01410	-.01490	-.01570	-.01640	-.01820	-.02160	-.02870	-.03310
+10.0	-.04460	-.03680	-.02660	-.01660	-.01270	-.01130	-.00920	-.00570	-.00330	
	-.00160	-.00170	-.00250	-.00380	-.00490	-.00850	-.01240	-.02240	-.03260	-.04040
+15.0	-.06820	-.05870	-.04250	-.01970	0.00000	.00260	.00780	.01580	.02430	
	.03230	.03280	.02900	.01890	.01200	.00610	-.01360	-.03640	-.05260	-.06210
+20.0	-.09470	-.08510	-.06420	-.05360	-.03080	-.02930	-.02750	-.02340	-.01880	
	-.01610	-.01410	-.01360	-.01540	-.01800	-.02730	-.05010	-.06070	-.08160	-.09120
+25.0	-.10900	-.12350	-.09380	-.07770	-.06740	-.06480	-.16070	-.05580	-.05260	
	-.04550	-.04710	-.04790	-.05300	-.05630	-.06100	-.07130	-.08740	-.11710	-.10260
+30.0	-.01350	-.08570	-.09070	-.10130	-.08750	-.09830	-.09510	-.09130	-.09020	
	-.08710	-.08650	-.08960	-.09620	-.09970	-.10600	-.11980	-.10920	-.10420	-.03200
+35.0	.02020	-.05100	-.08910	-.10860	-.10180	-.10140	-.11050	-.11170	-.11270	
	-.11510	-.11670	-.12300	-.13010	-.13870	-.14020	-.14700	-.12750	-.08940	-.01420
+40.0	-.01160	-.06390	-.09710	-.11560	-.11700	-.11420	-.11820	-.11600	-.11780	
	-.12060	-.12800	-.13470	-.14360	-.15120	-.15160	-.15020	-.13170	-.09850	-.04620
+45.0	-.00230	-.01640	-.04170	-.09870	-.09850	-.09750	-.12780	-.10420	-.11560	
	-.09790	-.11220	-.12250	-.14440	-.13400	-.14610	-.14630	-.08930	-.06400	-.04990

TABLE III.- Continued

ALPHA	$\Delta C_{m,sb}(\alpha)$
-20.0	-.00340
-15.0	-.00340
-10.0	-.00340
- 5.0	-.00340
0.0	-.00340
+ 5.0	.02890
+10.0	.02150
+15.0	.01220
+20.0	.02410
+25.0	.02630
+30.0	-.01630
+35.0	-.04280
+40.0	-.07040
+45.0	-.08440
+50.0	-.07890
+55.0	-.06030
+60.0	-.04500
+70.0	-.05780
+80.0	-.01070
+90.0	-.01070

ALPHA	$\Delta C_m(\alpha)$
-20.0	.019
-15.0	.019
-10.0	.019
- 5.0	.019
0.0	.019
+ 5.0	.019
+10.0	.02
+15.0	.04
+20.0	.04
+25.0	.05
+30.0	.06
+35.0	.06
+40.0	.06
+45.0	.06
+50.0	.06
+55.0	.06
+60.0	.06
+70.0	.06
+80.0	.06
+90.0	.06

δ_h	$\eta_{\delta_h}(\delta_h)$
-25.0	1.00
-10.0	1.00
0.0	1.00
+10.0	1.00
+25.0	.95

TABLE III.- Continued

ALPHA	$C_{m_q}(\alpha)$
-20.0	-6.84000
-15.0	-6.84000
-10.0	-6.84000
- 5.0	-3.42000
0.0	-5.48000
+ 5.0	-5.45000
+10.0	-6.02000
+15.0	-6.70000
+20.0	-5.69000
+25.0	-6.00000
+30.0	-6.20000
+35.0	-6.40000
+40.0	-6.60000
+45.0	-6.00000
+50.0	-5.50000
+55.0	-5.00000
+60.0	-4.50000
+70.0	-3.50000
+80.0	-5.60000
+90.0	-4.04000

ALPHA	$\Delta C_{m_{q,lef}}(\alpha)$
-20.0	-.36700
-15.0	-.36700
-10.0	-.36700
- 5.0	2.88000
0.0	.25000
+ 5.0	.27000
+10.0	-.21000
+15.0	.36000
+20.0	-1.26000
+25.0	-2.51000
+30.0	-1.66000
+35.0	-1.72000
+40.0	-1.20000
+45.0	-.60000

TABLE III.- Continued

$\Delta C_{m,ds}(\alpha, \delta_h)$

δ_h / ALPHA	-25.0	-10	0	10	15	20	25
-20.0	0.00000	0.00000	0.00000	0.00000	0.00000	0.00000	0.00000
-15.0	0.00000	0.00000	0.00000	0.00000	0.00000	0.00000	0.00000
-10.0	0.00000	0.00000	0.00000	0.00000	0.00000	0.00000	0.00000
- 5.0	0.00000	0.00000	0.00000	0.00000	0.00000	0.00000	0.00000
0.0	0.00000	0.00000	0.00000	0.00000	0.00000	0.00000	0.00000
+ 5.0	0.00000	0.00000	0.00000	0.00000	0.00000	0.00000	0.00000
+10.0	0.00000	0.00000	0.00000	0.00000	0.00000	0.00000	0.00000
+15.0	0.00000	0.00000	0.00000	0.00000	0.00000	0.00000	0.00000
+20.0	0.00000	0.00000	0.00000	0.00000	0.00000	0.00000	0.00000
+25.0	0.00000	0.00000	0.00000	0.00000	0.00000	0.00000	0.00000
+30.0	0.00000	0.00000	0.00000	0.00000	0.00000	0.00000	0.00000
+35.0	0.00000	0.00000	0.00000	0.00000	-.01130	-.01320	0.00000
+40.0	0.00000	.01000	.01000	.02000	.00410	.02970	.02540
+45.0	.04800	.05700	.06400	.07000	.07060	.05060	.04070
+50.0	.03900	.05400	.10500	.07500	.07920	.07470	.08220
+55.0	0.00000	.02500	.07500	.04000	.04160	.05000	.05830
+60.0	.08400	.08000	.10600	.10000	.08860	.07760	.07850
+70.0	.09900	.07500	.13200	.02000	.02875	.03610	.04680
+80.0	.02000	.01000	.05000	0.00000	.02180	-.02510	-.02100
+90.0	0.00000	.01000	.04000	0.00000	-.03445	-.03780	-.03780

TABLE III.- Continued

$C_Y(\alpha,\beta)$

BETA	-30.0	-25.0	-20.0	-15.0	-10.0	- 8.0	- 6.0	- 4.0	- 2.0	
	0.0	+ 2.0	+ 4.0	+ 6.0	+ 8.0	+10.0	+15.0	+20.0	+25.0	+30.0
ALPHA										
-20.0	.36770	.30700	.24600	.18440	.10620	.08500	.06770	.03800	.01860	
	0.00000	-.02320	-.04670	-.07470	-.10780	-.14210	-.22210	-.28610	-.34610	-.40810
-15.0	.40190	.32200	.26510	.19640	.13320	.10390	.07530	.04420	.01750	
	0.00000	-.01880	-.04020	-.06810	-.10040	-.13170	-.19300	-.25400	-.31900	-.39800
-10.0	.43670	.38230	.31850	.24620	.15130	.11560	.07600	.04340	.01610	
	0.00000	-.01240	-.04300	-.07920	-.11710	-.15420	-.24820	-.32120	-.38420	-.43820
- 5.0	.55380	.47780	.37580	.28180	.18330	.14490	.10550	.06620	.03250	
	0.00000	-.04200	-.07630	-.11770	-.15750	-.20720	-.30410	-.40010	-.50130	-.57940
0.0	.62180	.52580	.42080	.30880	.20140	.15530	.11380	.07260	.03710	
	0.00000	-.03940	-.07640	-.11910	-.16740	-.21340	-.31980	-.43150	-.53690	-.64000
+ 5.0	.65440	.55140	.42940	.31240	.20280	.16070	.11330	.07670	.03310	
	0.00000	-.03830	-.08190	-.12330	-.17050	-.21730	-.32570	-.44300	-.55060	-.65140
+10.0	.62550	.51850	.42250	.30650	.20160	.15970	.11310	.07480	.03450	
	0.00000	-.03830	-.07860	-.12040	-.16680	-.21710	-.32040	-.43470	-.53130	-.63710
+15.0	.58850	.46650	.37550	.28750	.18370	.14730	.10690	.06520	.02980	
	0.00000	-.03830	-.07700	-.12000	-.16420	-.20560	-.30910	-.39660	-.48680	-.61000
+20.0	.57830	.46330	.33830	.25630	.18140	.15040	.11160	.07030	.03320	
	0.00000	-.02480	-.05580	-.09840	-.13660	-.17290	-.24790	-.32800	-.45420	-.56980
+25.0	.50050	.41950	.30050	.22950	.16430	.14090	.10290	.06540	.03430	
	0.00000	-.03350	-.06770	-.10280	-.13690	-.16920	-.23370	-.30440	-.42410	-.50300
+30.0	.37510	.31610	.22910	.14110	.09270	.10570	.09110	.06300	.02970	
	0.00000	-.03060	-.06470	-.09060	-.11590	-.13530	-.18410	-.27430	-.36000	-.41890
+35.0	.32920	.29520	.21120	.14720	.08570	.05810	.06510	.05630	.02640	
	0.00000	-.02140	-.05130	-.08060	-.09710	-.10220	-.16320	-.22820	-.31410	-.34880
+40.0	.44700	.38850	.30250	.21350	.07480	.05310	.03030	.03600	.01230	
	0.00000	-.03200	-.04840	-.06640	-.09580	-.10750	-.15390	-.15750	-.18070	-.22420
+45.0	.16340	.08940	.04440	.08940	.07820	.06120	.04580	.03980	.02790	
	0.00000	-.08680	-.10480	-.13650	-.15410	-.18300	-.19400	-.15060	-.19510	-.26620
+50.0	.13660	.10360	.09160	.15560	.08660	.07850	.05550	.03990	.03020	
	0.00000	-.01780	-.07910	-.10600	-.11770	-.15080	-.22010	-.15650	-.16790	-.20080
+55.0	.17350	.13550	.17950	.17250	.11040	.09260	.06630	.04600	.04240	
	0.00000	-.00870	-.07180	-.10650	-.12250	-.14680	-.20900	-.21530	-.17090	-.21070
+60.0	.22330	.17130	.20830	.18830	.12300	.10510	.07880	.05460	.04740	
	0.00000	-.00480	-.05710	-.08400	-.10470	-.12420	-.18850	-.20770	-.17190	-.20990
+70.0	.26090	.22790	.17390	.14690	.10740	.09410	.07650	.05640	.03710	
	0.00000	-.01130	-.03000	-.04770	-.07150	-.08590	-.12660	-.15340	-.20780	-.24210
+80.0	.30550	.25950	.21650	.16350	.10960	.08710	.07530	.04980	.02120	
	0.00000	-.02030	-.03610	-.06550	-.08040	-.10270	-.15540	-.20750	-.24950	-.29540
+90.0	.30780	.24980	.19980	.15680	.10890	.08430	.06580	.04460	.02030	
	0.00000	-.02630	-.04180	-.06110	-.08360	-.10680	-.15470	-.19860	-.24740	-.30470

TABLE III.- Continued

$C_{Y,lef}(\alpha,\beta)$

BETA	-30.0 0.0	-25.0 + 2.0	-20.0 + 4.0	-15.0 + 6.0	-10.0 + 8.0	- 8.0 +10.0	- 6.0 +15.0	- 4.0 +20.0	- 2.0 +25.0	+30.0
ALPHA										
-20.0	.36920	.29910	.24170	.16920	.10780	.08740	.08370	.05720	.02600	
	0.00000	-.02580	-.05920	-.08630	-.12090	-.15040	-.21060	-.28360	-.33960	-.41060
-15.0	.43680	.37970	.32490	.26360	.18260	.14560	.10680	.07010	.03360	
	0.00000	-.03370	-.07020	-.11000	-.15000	-.19020	-.27120	-.33320	-.38820	-.44520
-10.0	.50000	.44410	.36710	.28960	.18710	.14750	.10960	.07570	.03770	
	0.00000	-.03390	-.07080	-.11080	-.15130	-.19490	-.29780	-.37580	-.45280	-.50780
- 5.0	.56830	.49130	.39130	.29430	.19260	.14900	.11250	.07230	.03690	
	0.00000	-.03630	-.07650	-.11690	-.16440	-.21320	-.31480	-.41180	-.51300	-.58890
0.0	.62930	.53130	.41730	.30530	.20240	.15820	.11160	.07290	.03740	
	0.00000	-.03740	-.07760	-.12230	-.17120	-.21580	-.31960	-.43080	-.54430	-.64260
+ 5.0	.63970	.53670	.42670	.30970	.20420	.16300	.11740	.07750	.03940	
	0.00000	-.03520	-.07850	-.11890	-.16890	-.21500	-.32180	-.43640	-.54480	-.64960
+10.0	.61320	.51920	.43020	.31420	.20800	.16310	.11870	.07840	.03700	
	0.00000	-.03780	-.07740	-.12280	-.16640	-.21530	-.31960	-.43530	-.52370	-.61770
+15.0	.54160	.48760	.41260	.30660	.20230	.15760	.11680	.07180	.03770	
	0.00000	-.03680	-.07840	-.11940	-.16360	-.20960	-.31430	-.42230	-.49470	-.54990
+20.0	.47500	.37500	.29500	.23000	.15760	.12540	.09190	.05900	.02820	
	0.00000	-.03130	-.06700	-.10230	-.13740	-.17100	-.24520	-.30890	-.38690	-.48800
+25.0	.48780	.37080	.25080	.15780	.11760	.11740	.08930	.05850	.02860	
	0.00000	-.03010	-.05660	-.09250	-.11260	-.13210	-.17140	-.26470	-.38500	-.50250
+30.0	.34360	.32260	.22860	.13960	.08250	.08010	.07570	.05490	.02870	
	0.00000	-.02890	-.05270	-.07240	-.09390	-.11360	-.16940	-.25890	-.35110	-.37420
+35.0	.24370	.22670	.17570	.13070	.07760	.06020	.05350	.04070	.01810	
	0.00000	-.02140	-.05370	-.08080	-.10090	-.12260	-.17660	-.22080	-.27140	-.29010
+40.0	.19760	.17760	.15660	.12860	.09060	.07370	.05930	.05050	.01880	
	0.00000	-.02860	-.05160	-.07370	-.09380	-.11320	-.15030	-.17910	-.19960	-.21950
+45.0	.17410	.12510	.12010	.13210	.11100	.08540	.05500	.03390	.01830	
	0.00000	-.05440	-.09290	-.13120	-.15810	-.17660	-.19770	-.18590	-.19000	-.23850

TABLE III.- Continued

$C_{Y,\delta_{a=20^{\circ}}}(\alpha,\beta)$

BETA	-30.0	-25.0	-20.0	-15.0	-10.0	- 8.0	- 6.0	- 4.0	- 2.0	
	0.0	+ 2.0	+ 4.0	+ 6.0	+ 8.0	+10.0	+15.0	+20.0	+25.0	+30.0
ALPHA										
-20.0	.37470	.31130	.28550	.21840	.13760	.11090	.09190	.06260	.04090	
	.01900	-.00630	-.02450	-.05030	-.07850	-.10400	-.18510	-.25310	-.27910	-.34310
-15.0	.39720	.32930	.28070	.21100	.14680	.12070	.09140	.06380	.03830	
	.01570	-.00350	-.02420	-.05010	-.08490	-.11660	-.18100	-.25100	-.29900	-.36900
-10.0	.42520	.36790	.31450	.23560	.16790	.12870	.09390	.06180	.03150	
	.01600	-.00010	-.03070	-.06360	-.09970	-.13520	-.20180	-.28020	-.33620	-.39120
- 5.0	.60080	.51480	.41580	.31480	.20500	.16560	.12760	.08800	.05090	
	.01520	-.01620	-.05400	-.08890	-.13200	-.17380	-.28430	-.38590	-.48430	-.56690
0.0	.66280	.56680	.45280	.33380	.21680	.18370	.14280	.10010	.06110	
	.02350	-.01280	-.04900	-.09190	-.13120	-.17830	-.29620	-.41520	-.52880	-.62560
+ 5.0	.70240	.60940	.48940	.35840	.22460	.18940	.14860	.10640	.06650	
	.02880	-.00870	-.04230	-.08800	-.13060	-.17560	-.29770	-.42810	-.54790	-.63960
+10.0	.67150	.58550	.47150	.35350	.22930	.19340	.14920	.10930	.06600	
	.02840	-.00930	-.04720	-.08850	-.13180	-.18320	-.29890	-.42770	-.54010	-.62670
+15.0	.64650	.53550	.43950	.32850	.21890	.17860	.13750	.09780	.05780	
	.02220	-.01380	-.05040	-.09510	-.13470	-.18140	-.29140	-.40320	-.49770	-.60210
+20.0	.58730	.49730	.40130	.31330	.20830	.16730	.13190	.09030	.04800	
	.01810	-.00470	-.03570	-.07360	-.11200	-.15140	-.25630	-.34330	-.43830	-.52620
+25.0	.49950	.41850	.32150	.24950	.17050	.14960	.11620	.08420	.04700	
	.01410	-.01680	-.04890	-.08340	-.11900	-.15750	-.23630	-.30790	-.40620	-.48740
+30.0	.37890	.32020	.22950	.14810	.09860	.11190	.10100	.07490	.04310	
	.01430	-.01460	-.04450	-.07630	-.10240	-.12540	-.17490	-.25630	-.34730	-.40570
+35.0	.32860	.27120	.19660	.13500	.07090	.05090	.06260	.05770	.03160	
	.00670	-.01540	-.04070	-.06790	-.08680	-.10760	-.17170	-.23330	-.30790	-.36530
+40.0	.18120	.16700	.11940	.09230	.05350	.03530	.02690	.03120	.01490	
	.00050	-.01910	-.04260	-.06150	-.09180	-.10740	-.14830	-.17120	-.21840	-.23380
+45.0	.10540	.07750	.05950	.04560	.03460	.00390	.00150	-.01170	-.01980	
	-.02500	-.06680	-.13260	-.15570	-.17450	-.19430	-.20570	-.18140	-.21600	-.28530
+50.0	.09470	.07170	.06680	.06680	.03400	.03210	.01330	-.01100	-.02570	
	-.04120	-.05970	-.10520	-.13220	-.12790	-.18260	-.21610	-.21420	-.21750	-.24340
+55.0	.12640	.10260	.13460	.11860	.05460	.03590	.02490	-.01360	-.02700	
	-.05440	-.05890	-.10260	-.13400	-.14190	-.17840	-.24090	-.25570	-.22240	-.24540
+60.0	.16550	.14440	.15740	.13050	.07340	.04240	.03290	-.00800	-.02240	
	-.04970	-.05530	-.08660	-.11170	-.12910	-.15270	-.21230	-.24230	-.22330	-.24450
+70.0	.25610	.22500	.16880	.11690	.08200	.05360	.03580	.00650	-.01320	
	-.02080	-.05120	-.06010	-.06940	-.09070	-.11360	-.14560	-.19300	-.24910	-.27940
+80.0	.29460	.25000	.20100	.13970	.09410	.07530	.05000	.04110	.01010	
	-.00810	-.04390	-.06170	-.07830	-.09850	-.12210	-.16730	-.22530	-.27660	-.32060
+90.0	.28330	.22900	.17880	.14980	.09860	.07650	.05650	.03390	.00990	
	-.00600	-.03320	-.04880	-.07820	-.10010	-.12160	-.17470	-.21650	-.25840	-.31850

TABLE III.- Continued

$C_{Y,\delta_{a=20^{o}},lef}(\alpha,\beta)$

ALPHA \ BETA	-30.0	-25.0	-20.0	-15.0	-10.0	- 8.0	- 6.0	- 4.0	- 2.0	0.0	+ 2.0	+ 4.0	+ 6.0	+ 8.0	+10.0	+15.0	+20.0	+25.0	+30.0
-20.0	.37440	.30910	.26610	.17220	.11740	.10990	.09350	.06420	.03820	.01310	-.01830	-.04500	-.07610	-.10550	-.13640	-.19060	-.28460	-.32760	-.39260
-15.0	.42250	.35830	.31680	.25100	.18900	.15570	.11970	.08490	.05070	.01560	-.01820	-.05270	-.08870	-.12950	-.16720	-.22820	-.29520	-.33620	-.40020
-10.0	.47730	.40650	.35060	.27360	.19810	.16270	.12300	.08900	.05580	.02170	-.01490	-.05030	-.08570	-.12180	-.16210	-.23980	-.31380	-.37180	-.44080
- 5.0	.63130	.54630	.44030	.33130	.21020	.17680	.13720	.09330	.05780	.01950	-.01390	-.05450	-.09080	-.13330	-.17930	-.29780	-.40710	-.51280	-.59650
0.0	.66630	.57530	.45430	.33730	.21310	.17790	.13990	.09600	.05680	.02120	-.01760	-.05490	-.09610	-.13440	-.17990	-.30460	-.42300	-.54340	-.63410
+ 5.0	.67070	.58370	.46370	.33970	.22090	.18480	.14480	.10390	.05860	.02370	-.01570	-.05220	-.09330	-.13770	-.18570	-.30440	-.42810	-.54670	-.63350
+10.0	.65220	.56920	.46520	.34320	.22620	.19000	.14530	.10270	.06340	.02360	-.01590	-.05100	-.09690	-.13900	-.18900	-.30640	-.42500	-.53210	-.61360
+15.0	.59760	.54460	.46460	.33760	.22230	.18560	.14130	.10260	.05810	.02270	-.01470	-.05070	-.09220	-.13620	-.18060	-.29500	-.42210	-.50090	-.55270
+20.0	.49100	.41400	.34300	.27500	.18370	.15420	.11800	.08060	.04960	.01920	-.01260	-.04590	-.08060	-.11200	-.15150	-.24200	-.31060	-.38110	-.45850
+25.0	.50280	.37380	.28280	.19180	.13540	.13140	.10430	.07840	.04460	.01180	-.01530	-.04230	-.06930	-.09530	-.11660	-.17150	-.26060	-.35230	-.48220
+30.0	.34660	.32960	.23860	.14660	.08650	.08770	.07960	.06040	.03850	.01140	-.01270	-.04490	-.06550	-.08540	-.09910	-.15800	-.24830	-.33940	-.35550
+35.0	.29870	.25570	.16470	.11670	.06010	.05750	.05560	.04560	.02470	.01120	-.01930	-.04310	-.07780	-.09260	-.12150	-.17780	-.22360	-.26110	-.30460
+40.0	.20260	.15760	.14460	.12060	.07180	.05410	.05090	.02410	.01040	-.01010	-.03080	-.05840	-.07250	-.09380	-.11580	-.16280	-.18620	-.19790	-.24320
+45.0	.11610	.06610	.08310	.07910	.05970	.03530	.01590	-.01190	-.02510	-.04700	-.09150	-.14660	-.15880	-.18200	-.21270	-.23150	-.23540	-.21720	-.26870

TABLE III.- Continued

$C_{Y,\delta_{r=30^{o}}}(\alpha,\beta)$

BETA	-30.0	-25.0	-20.0	-15.0	-10.0	- 8.0	- 6.0	- 4.0	- 2.0	
	0.0	+ 2.0	+ 4.0	+ 6.0	+ 8.0	+10.0	+15.0	+20.0	+25.0	+30.0
ALPHA										
-20.0	.41050	.34190	.28860	.23230	.18150	.17360	.16690	.13550	.11730	
	.08540	.06810	.04470	.02290	-.01090	-.05560	-.10610	-.16210	-.21410	-.28210
-15.0	.43870	.36840	.31340	.24710	.20720	.19710	.17320	.14050	.11440	
	.09000	.07320	.05220	.02710	-.01070	-.04760	-.08700	-.14200	-.19700	-.26700
-10.0	.47710	.41960	.37280	.30130	.22580	.20340	.17180	.13500	.10430	
	.08690	.07170	.04780	.01280	-.02910	-.07130	-.14820	-.21920	-.26620	-.32320
- 5.0	.60480	.53880	.47380	.36280	.25990	.22590	.18890	.15160	.11800	
	.08150	.05100	.01460	-.02670	-.07150	-.11900	-.22250	-.33390	-.40120	-.46920
0.0	.63880	.56980	.49980	.38380	.27360	.24450	.20170	.16100	.12400	
	.08590	.05300	.01850	-.02590	-.07500	-.12710	-.23690	-.35260	-.42120	-.49120
+ 5.0	.66740	.60640	.52340	.40340	.28800	.25740	.21120	.16900	.12640	
	.09230	.05740	.01750	-.02440	-.07410	-.12580	-.24070	-.35940	-.43160	-.50260
+10.0	.70150	.60150	.52950	.41350	.29630	.24620	.20340	.16290	.12070	
	.08510	.05110	.01610	-.03350	-.08000	-.13190	-.23880	-.35640	-.42850	-.52950
+15.0	.66950	.55550	.47550	.36150	.25840	.23530	.19840	.15820	.11810	
	.08340	.04770	.01210	-.03480	-.07850	-.12510	-.22950	-.34110	-.42150	-.53650
+20.0	.67030	.55830	.45330	.36430	.25240	.23160	.20940	.16080	.13340	
	.09360	.06260	.03520	-.00260	-.03850	-.07600	-.18590	-.27580	-.38570	-.49470
+25.0	.58150	.49150	.40350	.31850	.22990	.22390	.20400	.17530	.13640	
	.09940	.06610	.03470	-.00450	-.04050	-.07820	-.16680	-.25360	-.35050	-.44750
+30.0	.41410	.35410	.27810	.20610	.13230	.15690	.17370	.15990	.13580	
	.10710	.07090	.04190	.01150	-.02470	-.06190	-.13470	-.20780	-.28590	-.34590
+35.0	.36320	.34420	.28220	.22020	.13210	.11600	.12190	.13400	.11210	
	.08850	.07310	.04710	.01800	-.01150	-.03950	-.12780	-.19040	-.26180	-.28080
+40.0	.23650	.24650	.20350	.17550	.12140	.08870	.09090	.08210	.07810	
	.07490	.04680	.03040	-.00050	-.02420	-.05930	-.11220	-.14150	-.18660	-.17790
+45.0	.21340	.14340	.11340	.12740	.09650	.08490	.07980	.08550	.06690	
	.03870	-.04120	-.07130	-.09540	-.12750	-.14470	-.17350	-.15910	-.18970	-.25830
+50.0	.16060	.11560	.11160	.12860	.09460	.09290	.08030	.05110	.04760	
	.02510	-.01200	-.04410	-.08360	-.11460	-.13700	-.17260	-.15330	-.15530	-.20040
+55.0	.18950	.14950	.19050	.17550	.12350	.09990	.07690	.04070	.03660	
	.01220	-.00790	-.06390	-.09200	-.12520	-.14480	-.19720	-.21290	-.16980	-.20950
+60.0	.21830	.18330	.21730	.18830	.13750	.10670	.08460	.04420	.03110	
	.00660	-.00410	-.05510	-.07620	-.07220	-.12820	-.17900	-.20920	-.17370	-.20950
+70.0	.26890	.22890	.19890	.17290	.11630	.09680	.08500	.05430	.02720	
	.00610	-.01010	-.02560	-.04080	-.06090	-.08720	-.14420	-.17020	-.20180	-.24160
+80.0	.29150	.24450	.20450	.15150	.10750	.08670	.06960	.05430	.02930	
	.01750	-.00690	-.02760	-.05700	-.07470	-.10270	-.14840	-.20130	-.24570	-.29240
+90.0	.29880	.23980	.18980	.15680	.10420	.07720	.06160	.04700	.02400	
	.00520	-.01240	-.03350	-.06460	-.08410	-.10160	-.15390	-.18730	-.23740	-.30090

TABLE III.- Continued

ALPHA	$C_{Y_r}(\alpha)$
-20.0	1.44000
-15.0	1.44000
-10.0	1.44000
- 5.0	1.05000
0.0	.98100
+ 5.0	.93900
+10.0	.99900
+15.0	.98100
+20.0	.81900
+25.0	.48300
+30.0	.59000
+35.0	1.21000
+40.0	-.49300
+45.0	-1.04000
+50.0	-1.21000
+55.0	-1.58000
+60.0	-1.37000
+70.0	-.02590
+80.0	-.12700
+90.0	.19300

ALPHA	$\Delta C_{Y_{r,lef}}(\alpha)$
-20.0	-.55800
-15.0	-.55800
-10.0	-.55800
- 5.0	-.19800
0.0	-.10700
+ 5.0	.02700
+10.0	-.08500
+15.0	-.04600
+20.0	.33100
+25.0	.21500
+30.0	.43000
+35.0	-.06000
+40.0	-.37400
+45.0	-.18700

ALPHA	$C_{Y_p}(\alpha)$
-20.0	.03330
-15.0	.03330
-10.0	.03330
- 5.0	-.17700
0.0	.00550
+ 5.0	.06790
+10.0	.31000
+15.0	.23400
+20.0	.34400
+25.0	.36200
+30.0	.61100
+35.0	.52900
+40.0	.29800
+45.0	-2.27000
+50.0	.97100
+55.0	1.02000
+60.0	2.90000
+70.0	.45100
+80.0	-.29400
+90.0	-.26100

ALPHA	$\Delta C_{Y_{p,lef}}(\alpha)$
-20.0	-.14100
-15.0	-.14100
-10.0	-.14100
- 5.0	.06900
0.0	-.19700
+ 5.0	.06010
+10.0	-.12100
+15.0	-.05200
+20.0	.07500
+25.0	.10600
+30.0	-.07700
+35.0	-.64200
+40.0	-.25500
+45.0	-.12800

TABLE III.- Continued

$$C_n\left(\alpha,\beta,\delta_h = -25^{\circ}\right)$$

BETA	-30.0	-25.0	-20.0	-15.0	-10.0	- 8.0	- 6.0	- 4.0	- 2.0	
	0.0	+ 2.0	+ 4.0	+ 6.0	+ 8.0	+10.0	+15.0	+20.0	+25.0	+30.0
ALPHA										
-20.0	-.06330	-.06670	-.05650	-.04180	-.01750	-.00930	-.00060	.00470	.00340	
	0.00000	-.00480	-.01060	-.00740	-.00150	.00520	.02970	.04430	.05450	.05100
-15.0	-.06210	-.05790	-.04540	-.02850	-.01810	-.01330	-.00670	-.00100	.00100	
	0.00000	.00040	.00280	.00710	.01510	.02000	.03030	.04730	.06020	.06410
-10.0	-.06780	-.05880	-.04930	-.03930	-.02420	-.01670	-.00980	-.00220	.00220	
	0.00000	.00470	.00960	.01630	.02450	.03200	.04730	.05720	.06660	.07540
- 5.0	-.08500	-.07610	-.06390	-.04780	-.03540	-.02630	-.01840	-.01140	-.00550	
	0.00000	.00540	.01120	.01890	.02900	.03920	.05160	.06800	.08000	.08860
0.0	-.09950	-.08690	-.07950	-.05280	-.03750	-.02800	-.01930	-.01180	-.00530	
	0.00000	.00550	.01220	.02080	.03020	.03930	.05470	.07060	.08910	.10340
+ 5.0	-.10440	-.08240	-.06910	-.05210	-.03520	-.02800	-.01930	-.01210	-.00500	
	0.00000	.00560	.01320	.02100	.03010	.03830	.05530	.07210	.08580	.10750
+10.0	-.09810	-.07590	-.06310	-.04780	-.03580	-.02830	-.02010	-.01250	-.00540	
	0.00000	.00540	.01310	.02250	.03090	.03910	.05120	.06680	.07980	.10180
+15.0	-.09760	-.06180	-.04750	-.04470	-.03390	-.02670	-.01900	-.01140	-.00450	
	0.00000	.00550	.01290	.02230	.03040	.03720	.04800	.05090	.06470	.09090
+20.0	-.06770	-.05060	-.02900	-.02760	-.02590	-.02160	-.01510	-.00880	-.00400	
	0.00000	-.00220	.00210	.00990	.01610	.02100	.02260	.02410	.04600	.06270
+25.0	-.04880	-.03510	-.01630	-.01280	-.01550	-.01150	-.00720	-.00370	-.00160	
	0.00000	.00130	.00470	.00850	.01320	.01570	.01320	.01620	.03470	.04870
+30.0	-.01020	.01550	.02870	.02560	.02940	.00670	.00400	.00460	.00380	
	0.00000	-.00420	-.00500	-.00690	-.00900	-.01150	-.02140	-.02180	.00550	.04170
+35.0	-.00280	.03140	.05720	.07120	.05450	.05370	.04130	.02540	.01450	
	0.00000	-.01040	-.01620	-.02230	-.03120	-.05060	-.06700	-.05360	-.02760	.00690
+40.0	-.00370	.01670	.07700	.08030	.05730	.04330	.02920	.01840	.00680	
	0.00000	-.00480	-.01150	-.02330	-.03320	-.04920	-.07620	-.07270	-.01250	.00790
+45.0	-.01200	.00270	.03970	.05770	.03990	.03040	.02000	.01470	.00620	
	0.00000	-.01450	-.03560	-.04420	-.05800	-.06980	-.09000	-.07040	-.03360	-.01910
+50.0	-.03730	-.02740	-.00960	.02160	.03190	.02960	.02980	.01570	.01040	
	0.00000	-.00820	-.02550	-.04410	-.06190	-.07880	-.06930	-.03840	-.02170	-.01200
+55.0	-.04490	-.03240	.01020	-.00770	-.01610	-.00900	-.00570	-.00650	.00400	
	0.00000	-.00190	-.01520	-.02750	-.03150	-.03050	-.03860	-.05640	-.01370	-.00170
+60.0	-.00550	.00680	.03740	.01190	.02340	.01270	-.00160	-.01200	-.00290	
	0.00000	.00520	.00570	-.01010	-.02150	-.02210	-.02630	-.03580	-.00550	.00660
+70.0	.02320	.02800	.02030	.01270	.00070	-.00310	-.00700	-.01370	-.01680	
	0.00000	.00280	.01330	.01380	.00830	.00180	-.01000	-.01730	-.02510	-.02070
+80.0	.02360	.02370	.01610	.01160	.00990	.01100	.01080	.00870	.00590	
	0.00000	-.00130	.00350	-.00540	-.00690	-.00540	-.00750	-.01170	-.01920	-.01910
+90.0	.03190	.01990	.01080	.00180	.00790	.00620	.00390	.00290	.00180	
	0.00000	-.00640	-.00510	-.00980	-.00970	-.01010	-.00380	-.00720	-.01590	-.02770

TABLE III.- Continued

$C_n(\alpha, \beta, \delta_h = 0^{o})$

ALPHA \ BETA	-30.0	-25.0	-20.0	-15.0	-10.0	- 8.0	- 6.0	- 4.0	- 2.0	0.0	+ 2.0	+ 4.0	+ 6.0	+ 8.0	+10.0	+15.0	+20.0	+25.0	+30.0
-20.0	-.05510	-.05880	-.04960	-.04060	-.02190	-.01450	-.00750	-.00120	.00020	0.00000	-.00090	.00120	.00590	.00990	.01410	.03330	.04250	.05160	.04770
-15.0	-.05610	-.05270	-.04560	-.03330	-.02480	-.01790	-.01270	-.00570	-.00180	0.00000	.00250	.00580	.01110	.01800	.02380	.03300	.04500	.05210	.05530
-10.0	-.06660	-.06370	-.05450	-.04680	-.02970	-.02330	-.01450	-.00790	-.00310	0.00000	.00280	.00750	.01500	.02210	.03020	.04740	.05520	.06460	.06740
- 5.0	-.09020	-.08120	-.06640	-.05230	-.03660	-.02770	-.01940	-.01170	-.00550	0.00000	.00630	.01270	.02140	.02970	.03980	.05530	.06930	.08430	.09330
0.0	-.10580	-.09160	-.07490	-.05780	-.04130	-.03170	-.02260	-.01380	-.00660	0.00000	.00610	.01350	.02250	.03240	.04140	.05790	.07460	.09140	.10550
+ 5.0	-.10740	-.09160	-.07540	-.05870	-.04150	-.03290	-.02270	-.01450	-.00640	0.00000	.00610	.01480	.02310	.03350	.04210	.05940	.07620	.09140	.10790
+10.0	-.09810	-.07980	-.07180	-.05680	-.04160	-.03260	-.02320	-.01460	-.00620	0.00000	.00630	.01470	.02400	.03320	.04270	.05790	.07270	.08090	.09950
+15.0	-.08120	-.05920	-.05370	-.05130	-.03750	-.03010	-.02120	-.01210	-.00520	0.00000	.00630	.01410	.02430	.03340	.04040	.05410	.05660	.06220	.08400
+20.0	-.06840	-.04910	-.02900	-.03210	-.03080	-.02620	-.01790	-.01020	-.00420	0.00000	.00180	.00680	.01520	.02330	.02960	.03090	.02790	.04790	.06740
+25.0	-.05280	-.04110	-.02230	-.02290	-.02400	-.01880	-.01290	-.00720	-.00290	0.00000	.00330	.00880	.01470	.02160	.02580	.02510	.02420	.04290	.05470
+30.0	-.03000	.00020	.01150	.01640	.00910	-.00370	-.00240	.00090	.00250	0.00000	-.00290	-.00230	-.00130	-.00030	-.00190	-.00970	-.00420	.00690	.03700
+35.0	-.00980	.01680	.03920	.05140	.03960	.03400	.01630	.01030	.00690	0.00000	-.00970	-.01470	-.01570	-.01890	-.02950	-.04150	-.02910	-.00680	.01940
+40.0	-.00250	.00540	.06830	.07440	.05060	.03510	.02070	.01310	.00520	0.00000	-.00710	-.01360	-.02160	-.03290	-.04400	-.06770	-.06220	.00120	.02020
+45.0	-.01110	.00100	.02940	.06120	.04510	.03690	.02930	.02010	.01160	0.00000	-.02370	-.03750	-.04600	-.05650	-.06940	-.08470	-.05300	-.02460	-.01260
+50.0	-.02560	-.01360	.00580	.02870	.02540	.02310	.02330	.01050	.00780	0.00000	-.00630	-.02170	-.03550	-.04560	-.05480	-.05740	-.03460	-.01610	-.00460
+55.0	-.03020	-.02280	.01300	.01400	.00400	.00270	-.00230	-.00700	.00430	0.00000	.00280	-.00580	-.01720	-.02390	-.02580	-.03610	-.03550	.00140	.00730
+60.0	-.01880	-.00750	.02110	.00800	-.00610	-.01000	-.01740	-.02190	-.00790	0.00000	.00750	.01030	.00430	-.00130	-.00190	-.01560	-.02840	.00040	.01100
+70.0	.02960	.03160	.02100	.00920	.00030	-.00620	-.01280	-.01930	-.01870	0.00000	.00390	.01510	.01630	.01160	.00590	-.00230	-.01410	-.02460	-.02280
+80.0	.02640	.03510	.02540	.01800	.01330	.01260	.01070	.00790	.00550	0.00000	-.00010	.00600	-.00330	-.00690	-.00750	-.01300	-.01980	-.02420	-.02090
+90.0	.02740	.01280	.01180	.00590	.00510	.00440	.00310	.00270	.00170	0.00000	-.00180	-.00230	-.00310	-.00480	-.00480	-.00540	-.01110	-.01210	-.01630

TABLE III.- Continued

$$C_n\left(\alpha,\beta,\delta_h = 25^{o}\right)$$

BETA	-30.0	-25.0	-20.0	-15.0	-10.0	- 8.0	- 6.0	- 4.0	- 2.0	
	0.0	+ 2.0	+ 4.0	+ 6.0	+ 8.0	+10.0	+15.0	+20.0	+25.0	+30.0
ALPHA										
-20.0	-.04880	-.05150	-.04420	-.04280	-.02150	-.01360	-.00460	-.00180	.00010	
	0.00000	-.00050	-.00030	.00480	.00840	.01430	.03560	.03690	.04410	.04250
-15.0	-.04990	-.04630	-.04020	-.03240	-.02010	-.01540	-.00950	-.00290	-.00130	
	0.00000	.00050	.00310	.00930	.01450	.01950	.03190	.03980	.04590	.04920
-10.0	-.05740	-.05340	-.04770	-.04240	-.02770	-.02080	-.01340	-.00730	-.00250	
	0.00000	.00180	.00750	.01400	.02220	.02770	.04210	.04760	.05340	.05720
- 5.0	-.07580	-.07140	-.06170	-.05070	-.03680	-.02900	-.02080	-.01280	-.00610	
	0.00000	.00640	.01390	.02220	.03040	.03990	.05360	.06450	.07420	.07870
0.0	-.09190	-.08180	-.06940	-.05600	-.04020	-.03110	-.02230	-.01410	-.00650	
	0.00000	.00690	.01470	.02300	.03190	.04080	.05650	.06960	.08240	.09240
+ 5.0	-.08600	-.07490	-.06590	-.05310	-.04060	-.03220	-.02230	-.01270	-.00470	
	0.00000	.00420	.01240	.02210	.03230	.04150	.05670	.06940	.07860	.08920
+10.0	-.08210	-.07230	-.06530	-.05340	-.04030	-.03280	-.02330	-.01350	-.00610	
	0.00000	.00490	.01260	.02180	.03100	.04000	.05310	.06490	.07180	.08140
+15.0	-.06710	-.05160	-.04860	-.04960	-.03570	-.02890	-.01950	-.01070	-.00480	
	0.00000	.00380	.01080	.02080	.03060	.03810	.05100	.04990	.05320	.06840
+20.0	-.03980	-.03550	-.02370	-.02840	-.03110	-.02700	-.01830	-.00910	-.00350	
	0.00000	.00280	.00520	.01780	.02680	.03320	.03050	.02590	.03740	.04170
+25.0	-.02730	-.02100	-.01320	-.01480	-.02190	-.01960	-.01590	-.00890	-.00330	
	0.00000	.00430	.01030	.01790	.02640	.03110	.02390	.02240	.03020	.03620
+30.0	-.01160	.01420	.02730	.02420	.01110	-.00660	-.00630	-.00200	.00090	
	0.00000	-.00100	-.00060	.00180	.00390	.00180	-.01110	-.01460	-.00120	.02440
+35.0	.00180	.02820	.04990	.05500	.04300	.03820	.01930	.00990	.00690	
	0.00000	-.00860	-.01260	-.01540	-.01810	-.02880	-.04560	-.04020	-.01850	.00710
+40.0	.00030	-.01930	.06980	.07880	.05340	.03720	.02520	.01690	.00730	
	0.00000	-.00840	-.01470	-.02480	-.03620	-.04800	-.07330	-.06410	-.00520	.00510
+45.0	-.01490	-.00070	.02260	.05690	.04550	.03630	.02880	.01880	.00890	
	0.00000	-.02520	-.04030	-.05110	-.06210	-.07120	-.08040	-.04800	-.02470	-.02070
+50.0	-.02190	-.01740	-.00770	.01710	.03100	.03070	.03280	.01890	.01200	
	0.00000	-.00580	-.02510	-.04080	-.05430	-.06640	-.05300	-.02920	-.01870	-.01510
+55.0	-.05180	-.04350	-.00530	-.03070	-.02310	-.01080	-.00220	-.00160	.00650	
	0.00000	-.00260	-.00850	-.02230	-.02570	-.02440	-.01710	-.04240	-.00420	.00310
+60.0	-.02700	-.02070	.00420	-.01370	-.01370	-.01380	-.01730	-.02030	-.00710	
	0.00000	.00930	.01380	.00670	-.00280	-.00730	-.00720	-.02540	-.00080	.00560
+70.0	.01580	.02700	.02520	.01170	-.00100	-.00390	-.00680	-.01320	-.01590	
	0.00000	-.00390	.01100	.00880	.00840	.00690	-.00590	-.01910	-.02090	-.01040
+80.0	.01060	.01820	.01820	.01170	.00810	.00960	.00990	.00810	.00560	
	0.00000	-.00100	.00420	-.00430	.00160	-.00350	-.01120	-.01350	-.01350	-.00580
+90.0	.01180	.01010	.01170	.00360	.00600	.00530	.00410	.00350	.00210	
	0.00000	-.00020	.00080	.00080	-.00080	-.00080	.00140	-.00680	-.00540	-.00720

TABLE III.- Continued

$C_{n,lef}(\alpha,\beta)$

ALPHA \ BETA	-30.0	0.0	-25.0	+ 2.0	-20.0	+ 4.0	-15.0	+ 6.0	-10.0	+ 8.0	- 8.0	+10.0	- 6.0	+15.0	- 4.0	+20.0	- 2.0	+25.0	+30.0
-20.0	-.05410	0.00000	-.05630	.00370	-.04610	.00760	-.04950	.01210	-.02960	.01860	-.02080	.02310	-.01730	.04280	-.01000	.03930	-.00430	.04940	.04680
-15.0	-.06780	0.00000	-.07280	.00570	-.06580	.01250	-.05390	.02060	-.03580	.02880	-.02820	.03640	-.02040	.05390	-.01260	.06580	-.00580	.07300	.06830
-10.0	-.07800	0.00000	-.07730	.00690	-.06290	.01410	-.05550	.02240	-.03700	.03010	-.02890	.03870	-.02180	.05720	-.01420	.06450	-.00680	.07150	.07940
- 5.0	-.08810	0.00000	-.08510	.00670	-.07530	.01440	-.05560	.02340	-.04020	.03280	-.03080	.04300	-.02540	.05860	-.01410	.07850	-.00670	.08720	.09130
0.0	-.10600	0.00000	-.09290	.00660	-.07540	.01430	-.05930	.02340	-.04200	.03400	-.03190	.04290	-.02220	.05950	-.01350	.07590	-.00620	.09380	.10660
+ 5.0	-.10510	0.00000	-.08770	.00620	-.07280	.01490	-.05730	.02290	-.04100	.03360	-.03240	.04230	-.02250	.05890	-.01400	.07470	-.00610	.08770	.10690
+10.0	-.09260	0.00000	-.07970	.00640	-.07310	.01500	-.05800	.02430	-.04240	.03300	-.03270	.04250	-.02350	.05790	-.01540	.07300	-.00640	.07960	.09250
+15.0	-.06320	0.00000	-.06700	.00550	-.06530	.01430	-.05490	.02320	-.04140	.03250	-.03160	.04170	-.02230	.05330	-.01350	.06560	-.00590	.06730	.06350
+20.0	-.03590	0.00000	-.01910	.00300	-.01730	.00870	-.02300	.01590	-.02160	.02270	-.01740	.02790	-.00760	.02920	-.00580	.02370	-.00150	.02530	.04210
+25.0	-.03420	0.00000	-.02080	.00080	-.00170	.00380	.00630	.00690	-.00590	.00780	-.00940	.00340	-.00610	-.00880	-.00290	-.00080	-.00120	.01830	.03170
+30.0	-.02650	0.00000	-.00470	-.00320	.01280	-.00770	.02490	-.01170	.01980	-.02010	.01140	-.02760	.00550	-.03320	.00570	-.02090	.00300	-.00340	.01880
+35.0	.01380	0.00000	.03910	-.00900	.05330	-.01340	.05530	-.01900	.04340	-.02630	.03970	-.03280	.02630	-.04440	.02060	-.04270	.01190	-.02790	-.00210
+40.0	.03020	0.00000	.03570	-.00600	.06750	-.01360	.06450	-.01550	.04450	-.02660	.03300	-.03300	.02140	-.05320	.01560	-.05610	.00650	-.02400	.00140
+45.0	.00030	0.00000	-.00380	-.01700	.02140	-.03690	.04000	-.04640	.03260	-.05330	.02610	-.06110	.01990	-.06810	.01300	-.04950	.00470	-.02450	-.02800

TABLE III.- Continued

$C_{n,\delta_{a=20^{\circ}}}(\alpha,\beta)$

ALPHA \ BETA	-30.0 / 0.0	-25.0 / +2.0	-20.0 / +4.0	-15.0 / +6.0	-10.0 / +8.0	-8.0 / +10.0	-6.0 / +15.0	-4.0 / +20.0	-2.0 / +25.0	+30.0
-20.0	-.06390	-.06280	-.06160	-.05500	-.03590	-.02670	-.01880	-.01190	-.00930	
	-.00890	-.00810	-.00710	-.00430	-.00040	.00200	.02110	.02770	.02890	.03000
-15.0	-.06190	-.05540	-.04900	-.03840	-.03360	-.02790	-.02320	-.01740	-.01370	
	-.00980	-.00660	-.00420	.00020	.00880	.01340	.01820	.02880	.03520	.04170
-10.0	-.06790	-.05990	-.05440	-.04650	-.03960	-.03220	-.02540	-.01930	-.01390	
	-.00910	-.00550	-.00070	.00470	.01200	.01860	.02550	.03340	.03890	.04690
- 5.0	-.10800	-.09940	-.08380	-.06770	-.04600	-.03980	-.03210	-.02480	-.01760	
	-.01110	-.00540	.00080	.00740	.01590	.02460	.04630	.06240	.07800	.08660
0.0	-.12340	-.10940	-.09150	-.07210	-.04980	-.04480	-.03770	-.02770	-.01930	
	-.01200	-.00560	.00150	.00920	.01750	.02680	.04910	.06850	.08640	.10040
+ 5.0	-.12450	-.11000	-.09390	-.07300	-.04960	-.04400	-.03600	-.02650	-.01760	
	-.01050	-.00370	.00240	.01090	.01940	.02850	.05190	.07280	.08890	.10340
+10.0	-.11180	-.10200	-.08940	-.06900	-.04860	-.04400	-.03490	-.02670	-.01710	
	-.00900	-.00200	.00470	.01320	.02200	.03180	.05220	.07260	.08520	.09500
+15.0	-.09670	-.08070	-.07370	-.06280	-.04720	-.04160	-.03790	-.02340	-.01360	
	-.00660	-.00030	.00690	.01580	.02310	.03280	.04840	.05930	.06630	.08230
+20.0	-.06700	-.05610	-.05050	-.04720	-.03580	-.02690	-.01980	-.01110	-.00290	
	.00010	.00150	.00520	.01210	.02040	.02730	.03870	.04200	.04760	.05850
+25.0	-.03530	-.03160	-.02010	-.02430	-.01750	-.01300	-.00790	-.00370	.00120	
	.00450	.00720	.01060	.01590	.02170	.02770	.03450	.03030	.04180	.04550
+30.0	-.01870	.00910	.02300	.01960	.01320	.00260	.00210	.00560	.00820	
	.00650	.00390	.00220	.00300	.00550	.00450	-.00190	-.00530	.00860	.03640
+35.0	.00700	.03570	.05480	.06580	.04680	.03830	.02190	.01780	.01380	
	.00990	.00110	-.00520	-.00820	-.00980	-.01740	-.03640	-.02540	-.00630	.02240
+40.0	.00560	.03220	.08310	.08810	.05630	.03950	.02710	.01870	.01270	
	.00440	-.00090	-.00600	-.01310	-.02240	-.03280	-.06460	-.05780	-.00870	.01790
+45.0	.00460	.01410	.04040	.06420	.05130	.04160	.03190	.02520	.01640	
	.00970	-.00620	-.02830	-.03860	-.04750	-.05830	-.07120	-.04740	-.02110	-.01160
+50.0	-.01090	-.00430	.01570	.03850	.03860	.03570	.02820	.02290	.01960	
	.01300	.00710	-.01400	-.02110	-.01980	-.04520	-.04510	-.02230	-.00230	.00430
+55.0	-.01000	-.01240	.02560	.03030	.02370	.02330	.01660	.01320	.01930	
	.01670	.01750	.00250	-.00420	-.00600	-.01830	-.02490	-.02020	.01780	.01540
+60.0	.00470	-.00080	.02810	.02570	.01650	.01690	.01150	.00920	.02070	
	.01820	.02360	.01950	.01580	.01120	.00390	-.00530	-.00770	.02120	.01570
+70.0	.04700	.04260	.03080	.03010	.02530	.01860	.01600	.02060	.01900	
	.01540	.02450	.02160	.02830	.02180	.01560	.01080	.01010	-.00170	-.00610
+80.0	.04100	.04140	.03680	.03140	.02510	.02480	.02330	.01840	.01560	
	.01380	.01540	.01330	.01010	.00750	.00810	.00180	-.00360	-.00820	-.00780
+90.0	.03200	.02870	.02370	.01650	.01650	.01530	.01510	.01550	.01380	
	.01250	.01130	.01100	.01010	.01010	.01170	.01170	.00450	-.00050	-.00380

TABLE III.- Continued

$C_{n,\delta_{a=20^{\circ}},lef}(\alpha,\beta)$

BETA ALPHA	-30.0 0.0	-25.0 + 2.0	-20.0 + 4.0	-15.0 + 6.0	-10.0 + 8.0	- 8.0 +10.0	- 6.0 +15.0	- 4.0 +20.0	- 2.0 +25.0	 +30.0
-20.0	-.06830	-.06150	-.05560	-.05190	-.03930	-.03140	-.02640	-.01990	-.01400	
	-.00960	-.00540	-.00290	.00190	.00740	.01240	.02510	.02930	.03540	.04210
-15.0	-.07330	-.07020	-.06630	-.05510	-.04370	-.03720	-.03010	-.02330	-.01700	
	-.01080	-.00460	.00170	.00820	.01590	.02300	.03430	.04550	.04970	.05280
-10.0	-.07750	-.06830	-.06100	-.05270	-.04340	-.03850	-.03010	-.02400	-.01750	
	-.01080	-.00400	.00270	.00890	.01610	.02360	.03270	.04070	.04790	.05750
- 5.0	-.11490	-.10670	-.08980	-.07160	-.04820	-.04290	-.03590	-.02670	-.01880	
	-.01130	-.00500	.00240	.00930	.01860	.02780	.05110	.06890	.08560	.09320
0.0	-.12250	-.11060	-.09090	-.07220	-.04820	-.04280	-.03590	-.02560	-.01700	
	-.00990	-.00270	.00420	.01210	.01970	.02920	.05330	.07200	.09150	.10340
+ 5.0	-.11620	-.10300	-.08730	-.06770	-.04650	-.04060	-.03280	-.02400	-.01450	
	-.00770	-.00080	.00550	.01340	.02220	.03160	.05390	.07290	.08880	.10240
+10.0	-.10240	-.09440	-.08270	-.06580	-.04500	-.04010	-.03070	-.02240	-.01370	
	-.00560	.00150	.00790	.01640	.02510	.03450	.05500	.07190	.08380	.09170
+15.0	-.07990	-.08160	-.07890	-.06080	-.04330	-.03780	-.02860	-.02010	-.01040	
	-.00370	.00240	.00800	.01590	.02490	.03410	.05130	.06970	.07210	.06830
+20.0	-.03640	-.02850	-.03040	-.03550	-.02730	-.02330	-.01670	-.01060	-.00560	
	-.00260	.00040	.00450	.00950	.01640	.02290	.03120	.02600	.02420	.03230
+25.0	-.03700	-.01630	-.00250	.00280	-.00870	-.01050	-.00710	-.00490	-.00190	
	-.00060	.00040	.00240	.00410	.00550	.00150	-.00980	-.00500	.00890	.03070
+30.0	-.01690	.00370	.02100	.03030	.02110	.01330	.00960	.01000	.00810	
	.00430	-.00050	-.00440	-.00780	-.01550	-.02400	-.03180	-.02420	-.00660	.01390
+35.0	.02130	.05430	.06020	.06590	.05150	.04390	.03110	.02360	.01780	
	.00680	.00020	-.00470	-.00960	-.01950	-.02750	-.04190	-.03610	-.02980	.00290
+40.0	.01890	.04630	.08030	.07860	.05190	.03920	.02870	.02090	.01270	
	.00620	-.00170	-.00790	-.01050	-.01610	-.02210	-.04860	-.04970	-.01550	.01160
+45.0	.00550	.00450	.02240	.04320	.04190	.03550	.02740	.02020	.01410	
	.00690	-.01050	-.03210	-.03750	-.04680	-.05360	-.05490	-.03440	-.01640	-.01740

TABLE III.- Continued

$C_{n,\delta_{r=30^{o}}}(\alpha,\beta)$

BETA	-30.0	-25.0	-20.0	-15.0	-10.0	- 8.0	- 6.0	- 4.0	- 2.0	
	0.0	+ 2.0	+ 4.0	+ 6.0	+ 8.0	+10.0	+15.0	+20.0	+25.0	+30.0
ALPHA										
-20.0	-.07870	-.08150	-.07410	-.06560	-.06200	-.06270	-.06160	-.05510	-.05200	
	-.04810	-.04940	-.04860	-.04650	-.03960	-.03100	-.02700	-.01910	-.01130	-.01430
-15.0	-.07580	-.07450	-.07080	-.06100	-.06230	-.06580	-.06490	-.05800	-.05220	
	-.04840	-.04650	-.04370	-.03950	-.02980	-.02020	-.02160	-.01170	-.00820	-.00690
-10.0	-.08500	-.08330	-.08280	-.07490	-.06700	-.06850	-.06570	-.05900	-.05200	
	-.04760	-.04470	-.04070	-.03380	-.02380	-.01250	-.00460	.00330	.00430	.00560
- 5.0	-.14220	-.12700	-.11700	-.09320	-.07740	-.07450	-.06710	-.05990	-.05220	
	-.04490	-.04010	-.03370	-.02580	-.01470	-.00450	.01520	.03520	.04980	.05980
0.0	-.15760	-.13810	-.11810	-.09810	-.07910	-.07830	-.06930	-.06100	-.05270	
	-.04510	-.03890	-.03230	-.02300	-.01160	0.00000	.01900	.03890	.05840	.07840
+ 5.0	-.15910	-.14060	-.12160	-.10260	-.08190	-.07930	-.06960	-.06100	-.05200	
	-.04500	-.03880	-.03110	-.02200	-.01000	.00090	.02150	.04050	.05940	.07940
+10.0	-.15200	-.13500	-.11700	-.09900	-.08160	-.07790	-.06900	-.06000	-.05130	
	-.04410	-.03820	-.03090	-.02000	-.00830	.00310	.02070	.03810	.05500	.07250
+15.0	-.13060	-.10910	-.10260	-.09060	-.07520	-.07590	-.06940	-.06050	-.05170	
	-.04460	-.03860	-.03200	-.02010	-.00880	.00190	.01730	.02890	.03490	.05690
+20.0	-.12710	-.10710	-.08660	-.08360	-.06770	-.06850	-.06760	-.06280	-.05430	
	-.04750	-.04310	-.04040	-.03210	-.02300	-.00470	.00120	.00430	.02490	.04470
+25.0	-.10410	-.09250	-.07380	-.06830	-.05420	-.06000	-.06200	-.05890	-.05270	
	-.04830	-.04510	-.04110	-.03330	-.02540	-.01790	-.00420	.00130	.01970	.03170
+30.0	-.05980	-.02950	-.01830	-.00980	-.00490	-.02810	-.04220	-.04750	-.04740	
	-.04940	-.05100	-.05140	-.05040	-.04370	-.03670	-.03250	-.02420	-.01300	.01800
+35.0	-.04670	-.02010	.00610	.01860	.01590	.01230	-.00850	-.02430	-.03630	
	-.04490	-.05270	-.05710	-.06070	-.05830	-.05850	-.06110	-.04510	-.02280	.01040
+40.0	-.02890	-.01110	.03860	.04840	.03210	.01450	.00130	-.01030	-.02430	
	-.03280	-.04050	-.04490	-.04960	-.05700	-.06590	-.08240	-.07260	-.02270	-.00530
+45.0	-.02430	-.01290	.02130	.04470	.03250	.02480	.01400	.00470	-.00530	
	-.01620	-.04100	-.05450	-.06170	-.06970	-.07840	-.09120	-.06720	-.03320	-.02220
+50.0	-.03950	-.02470	-.00630	.01770	.01960	.01490	.00820	.00220	.00030	
	-.00810	-.01660	-.03000	-.04380	-.05580	-.06550	-.06320	-.03940	-.02020	-.00580
+55.0	-.03640	-.03050	.00880	.00670	.00060	-.00180	-.00750	-.00750	.00040	
	-.00400	-.00120	-.00890	-.02030	-.02890	-.03180	-.03830	-.04010	-.00110	.00510
+60.0	-.01620	-.01270	.01810	.00260	-.00840	-.01210	-.01950	-.01930	-.00820	
	-.00120	.00660	.00960	.00460	-.00330	-.00480	-.01630	-.03170	-.00120	.00260
+70.0	.02670	.02970	.01770	.00690	-.00160	-.00810	-.01560	-.02030	-.01520	
	-.00150	.00150	.01430	.01570	.00940	.00490	-.00350	-.01480	-.02630	-.02360
+80.0	.02230	.02610	.02150	.01670	.01090	.00840	.00500	.00160	-.00020	
	-.00610	-.00550	-.00890	-.00960	-.01050	-.01140	-.01720	-.02250	-.02680	-.02330
+90.0	.00890	.00770	.00680	.00140	-.00360	-.00440	-.00570	-.00100	-.00090	
	-.00240	-.00420	-.00470	-.00540	-.00580	-.00570	-.01090	-.01570	-.01700	-.01810

TABLE III.- Continued

ALPHA	$C_{n_r}(\alpha)$
-20.0	-.51700
-15.0	-.51700
-10.0	-.51700
- 5.0	-.46100
0.0	-.41400
+ 5.0	-.39700
+10.0	-.37300
+15.0	-.45500
+20.0	-.55000
+25.0	-.58200
+30.0	-.59500
+35.0	-.63700
+40.0	-1.02000
+45.0	-.84000
+50.0	-.54100
+55.0	-.35000
+60.0	-.35000
+70.0	-.07000
+80.0	-.15000
+90.0	-.15000

ALPHA	$\Delta C_{n_\beta}(\alpha)$
-20.0	.0
-15.0	.0
-10.0	.0
- 5.0	.0
0.0	.0
+ 5.0	.0
+10.0	.0
+15.0	.0
+20.0	.0
+25.0	-.0008
+30.0	.001
+35.0	.0
+40.0	.0
+45.0	.0
+50.0	.0
+55.0	.0
+60.0	.0
+70.0	.0
+80.0	.0
+90.0	.0

ALPHA	$\Delta C_{n_{\delta_a}}(\alpha)$
-20.0	.0
-15.0	.0
-10.0	.0
- 5.0	.0
0.0	.0001
+ 5.0	.00008
+10.0	.00016
+15.0	.00010
+20.0	.0
+25.0	.0
+30.0	.0
+35.0	.0
+40.0	.0
+45.0	.0
+50.0	.0
+55.0	.0
+60.0	.0
+70.0	.0
+80.0	.0
+90.0	.0

TABLE III.- Continued

ALPHA	$\Delta C_{n_{r,lef}}(\alpha)$
-20.0	.13700
-15.0	.13700
-10.0	.13700
- 5.0	.09800
0.0	.03700
+ 5.0	.01600
+10.0	.00700
+15.0	.01400
+20.0	-.10300
+25.0	-.09800
+30.0	-.31000
+35.0	-.43700
+40.0	.16700
+45.0	.08400

ALPHA	$C_{n_p}(\alpha)$
-20.0	-.00060
-15.0	-.00060
-10.0	-.00060
- 5.0	.04240
0.0	-.00750
+ 5.0	-.02140
+10.0	-.03200
+15.0	-.03200
+20.0	.05000
+25.0	.15000
+30.0	.13000
+35.0	.15800
+40.0	.24000
+45.0	.15000
+50.0	0.00000
+55.0	-.20000
+60.0	-.30000
+70.0	.15000
+80.0	0.00000
+90.0	0.00000

ALPHA	$\Delta C_{n_{p,lef}}$
-20.0	.06150
-15.0	.06150
-10.0	.06150
- 5.0	.00910
0.0	.06100
+ 5.0	.01290
+10.0	.04390
+15.0	.05120
+20.0	-.02940
+25.0	.00170
+30.0	.05840
+35.0	.21100
+40.0	.39200
+45.0	.19600

TABLE III.- Continued

$C_l(\alpha, \beta, \delta_h = -25^o)$

ALPHA \ BETA	-30.0	-25.0	-20.0	-15.0	-10.0	- 8.0	- 6.0	- 4.0	- 2.0	0.0	+ 2.0	+ 4.0	+ 6.0	+ 8.0	+10.0	+15.0	+20.0	+25.0	+30.0
-20.0	-.00600	.00650	.01330	.02170	.02680	.02380	.02190	.01790	.01210	0.00000	-.00960	-.01670	-.02100	-.02390	-.02450	-.01960	-.01070	-.00390	-.01180
-15.0	-.00480	.00590	.01780	.02420	.01870	.01570	.01300	.01060	.00610	0.00000	-.00590	-.01010	-.01460	-.01620	-.01890	-.02450	-.01790	-.00600	-.00480
-10.0	-.00330	.00950	.01730	.01840	.01280	.01000	.00880	.00560	.00270	0.00000	-.00470	-.00770	-.01180	-.01360	-.01580	-.02200	-.01400	-.00600	.00690
- 5.0	.02980	.02450	.02330	.02110	.01780	.01440	.01130	.00720	.00300	0.00000	-.00390	-.00810	-.01230	-.01490	-.01880	-.02210	-.02410	-.02530	-.02090
0.0	.02760	.02850	.02620	.02250	.01890	.01510	.01120	.00750	.00350	0.00000	-.00350	-.00750	-.01140	-.01510	-.01870	-.02230	-.02600	-.02830	-.02740
+ 5.0	.03900	.03370	.03290	.02820	.02400	.01950	.01420	.00960	.00490	0.00000	-.00470	-.00940	-.01380	-.01880	-.02300	-.02920	-.03390	-.03490	-.03980
+10.0	.05620	.05580	.05400	.04550	.03460	.02850	.02180	.01470	.00670	0.00000	-.00680	-.01430	-.02190	-.02820	-.03430	-.04470	-.05310	-.05460	-.05500
+15.0	.07370	.06700	.06290	.05680	.04390	.03610	.02720	.01850	.00910	0.00000	-.00870	-.01830	-.02860	-.03670	-.04330	-.05680	-.06260	-.06720	-.07360
+20.0	.07610	.07080	.06540	.05510	.04540	.03770	.02840	.01850	.00930	0.00000	-.01010	-.01800	-.02930	-.03690	-.04480	-.05420	-.06420	-.06940	-.07430
+25.0	.09100	.07130	.06270	.05130	.03970	.03310	.02610	.01750	.00880	0.00000	-.00890	-.01740	-.02630	-.03470	-.04110	-.05250	-.06370	-.07240	-.07970
+30.0	.07430	.04290	.01010	.01100	.00250	.01520	.01800	.01260	.00910	0.00000	-.00660	-.01240	-.01600	-.01940	-.02250	-.03080	-.03500	-.06280	-.09430
+35.0	.07040	.05300	.04530	.01840	.00670	-.00200	-.00170	.00280	-.00110	0.00000	.00180	.00090	-.00030	.00300	.01000	-.00170	-.02810	-.03580	-.05330
+40.0	.06650	.06050	.03530	.01320	.00770	.00920	.01560	.00960	.00480	0.00000	-.00770	-.01170	-.01230	-.01500	-.01300	-.01800	-.04030	-.06560	-.07160
+45.0	.07880	.05630	.03440	.02340	.01500	.01400	.00910	.00890	.00370	0.00000	-.00520	-.00820	-.01240	-.01350	-.01780	-.02740	-.03700	-.05790	-.08040
+50.0	.06050	.05680	.04690	.03400	.01690	.01460	.01290	.00890	.00550	0.00000	-.00220	-.00650	-.00900	-.01700	-.02000	-.03710	-.05000	-.05990	-.06360
+55.0	.04530	.03230	.02570	.01400	-.00030	.00240	.00420	.00250	.00250	0.00000	-.00640	-.01300	-.01760	-.02800	-.01730	-.03160	-.04330	-.04990	-.06290
+60.0	.06100	.04130	.03360	.02300	.01370	.01220	.01060	.00640	.00480	0.00000	-.00260	-.00490	-.00950	-.01320	-.01410	-.02340	-.03400	-.04170	-.06140
+70.0	.07130	.06030	.05010	.01910	.02210	.01900	.01240	.00970	.00570	0.00000	-.00660	-.01020	-.01430	-.01530	-.01720	-.02920	-.04660	-.05680	-.06780
+80.0	.06140	.05070	.04050	.03090	.02020	.01670	.01670	.00780	.00670	0.00000	-.00390	-.00750	-.01240	-.01560	-.01900	-.02970	-.03930	-.04950	-.06020
+90.0	.06010	.04600	.03630	.02530	.02130	.01830	.01470	.00910	.00560	0.00000	-.00060	-.00120	-.00860	-.01520	-.01910	-.02310	-.03410	-.04380	-.05790

TABLE III.- Continued

$C_l(\alpha,\beta,\delta_h = 0^o)$

BETA	-30.0	-25.0	-20.0	-15.0	-10.0	- 8.0	- 6.0	- 4.0	- 2.0	
	0.0	+ 2.0	+ 4.0	+ 6.0	+ 8.0	+10.0	+15.0	+20.0	+25.0	+30.0
ALPHA										
-20.0	-.01530	-.00280	.00910	.01880	.02340	.01730	.01060	.00900	.00410	
	0.00000	-.00310	-.00640	-.00840	-.01280	-.01710	-.01200	-.00220	.00970	.02250
-15.0	-.01320	-.00280	.00770	.01453	.01040	.00840	.00600	.00390	.00250	
	0.00000	-.00290	-.00500	-.00800	-.00860	-.01160	-.01600	-.00900	.00150	.01190
-10.0	-.01020	-.00130	.00940	.01340	.01070	.01020	.00810	.00600	.00110	
	0.00000	-.00040	-.00480	-.00710	-.00910	-.01020	-.01350	-.00940	.00130	.01080
- 5.0	.00870	.01530	.01860	.01940	.01830	.01560	.01250	.00880	.00430	
	0.00000	-.00380	-.00870	-.01260	-.01580	-.01860	-.01990	-.01890	-.01570	-.00950
0.0	.01570	.01900	.01990	.02070	.01850	.01530	.01100	.00710	.00330	
	0.00000	-.00300	-.00670	-.01070	-.01470	-.01820	-.02040	-.01960	-.01870	-.01540
+ 5.0	.03180	.03070	.02960	.02720	.02190	.01800	.01320	.00890	.00430	
	0.00000	-.00370	-.00810	-.01260	-.01730	-.02090	-.02630	-.02880	-.02990	-.03100
+10.0	.05100	.05100	.04960	.04220	.03280	.02710	.02070	.01390	.00560	
	0.00000	-.00650	-.01370	-.02070	-.02660	-.03220	-.04180	-.04860	-.05010	-.05010
+15.0	.07320	.06790	.06380	.05740	.04330	.03570	.02740	.01870	.00900	
	0.00000	-.00880	-.01880	-.02840	-.03690	-.04300	-.05670	-.06240	-.06630	-.07140
+20.0	.08950	.08150	.06920	.05790	.04530	.03540	.02700	.01710	.00760	
	0.00000	-.00850	-.01770	-.02710	-.03650	-.04400	-.05690	-.06820	-.08040	-.08840
+25.0	.08840	.07850	.06650	.05360	.04000	.03260	.02540	.01810	.00810	
	0.00000	-.00820	-.01650	-.02580	-.03300	-.04030	-.05380	-.06690	-.07880	-.08820
+30.0	.08200	.05050	.02340	.01430	.00640	.01890	.01960	.01330	.00710	
	0.00000	-.00570	-.01180	-.01650	-.02050	-.02480	-.03270	-.04180	-.06870	-.10030
+35.0	.07900	.06100	.03900	.00950	.00370	.00290	.01500	.01430	.00970	
	0.00000	.00160	.00030	-.00180	-.00170	.00110	-.00340	-.03260	-.05470	-.07260
+40.0	.07210	.05730	.03020	.00870	.00500	.01040	.01740	.01240	.00620	
	0.00000	-.00750	-.01080	-.01310	-.01450	-.01480	-.01850	-.03990	-.06710	-.08150
+45.0	.07440	.05760	.03310	.02480	.01700	.01790	.01630	.01910	.01150	
	0.00000	-.00420	-.01080	-.01480	-.01560	-.02060	-.02850	-.03640	-.06080	-.07780
+50.0	.05340	.04110	.02620	.02380	.01470	.01440	.01300	.00910	.00560	
	0.00000	-.00510	-.01230	-.01520	-.02120	-.02220	-.03130	-.03370	-.04860	-.06090
+55.0	.05870	.04220	.03200	.02610	.01760	.01510	.01170	.00650	.00450	
	0.00000	-.00400	-.00810	-.01330	-.01870	-.02010	-.02860	-.03460	-.04480	-.06130
+60.0	.06500	.04810	.03870	.03010	.02290	.01920	.01550	.00940	.00630	
	0.00000	-.00290	-.00550	-.01110	-.01630	-.01880	-.02600	-.03460	-.04400	-.06090
+70.0	.06630	.05380	.04220	.03070	.02450	.02200	.01600	.01280	.00730	
	0.00000	-.00500	-.00690	-.01200	-.01650	-.02200	-.02820	-.03970	-.05130	-.06380
+80.0	.06830	.05540	.04300	.03250	.02080	.01490	.01260	.00360	.00450	
	0.00000	-.00450	-.00860	-.01340	-.01590	-.01860	-.03030	-.04080	-.05320	-.06610
+90.0	.07010	.05340	.04100	.02930	.02050	.01880	.01630	.01100	.00660	
	0.00000	0.00000	-.00010	-.00670	-.01240	-.01540	-.02420	-.03590	-.04830	-.06500

TABLE III.- Continued

$C_l(\alpha,\beta,\delta_h = 25^{\circ})$

ALPHA \ BETA	-30.0	-25.0	-20.0	-15.0	-10.0	- 8.0	- 6.0	- 4.0	- 2.0	0.0	+ 2.0	+ 4.0	+ 6.0	+ 8.0	+10.0	+15.0	+20.0	+25.0	+30.0
-20.0	-.01380	-.00090	.01060	.02270	.02480	.01450	.01120	.00500	.00310	0.00000	-.00330	-.00810	-.00770	-.01600	-.01860	-.01670	-.00440	.00740	-.02560
-15.0	-.00610	.00330	.01400	.02090	.01570	.01050	.00660	.00600	.00270	0.00000	-.00240	-.00490	-.00750	-.00900	-.01340	-.01930	-.01230	-.00170	.00810
-10.0	0.00000	.00740	.01310	.01510	.01390	.01080	.00880	.00340	.00080	0.00000	-.00060	-.00510	-.00760	-.00960	-.01300	-.01400	-.01230	-.00650	.00080
- 5.0	.01710	.01960	.01860	.02040	.01810	.01420	.01110	.00810	.00390	0.00000	-.00350	-.00710	-.01090	-.01410	-.01750	-.02030	-.01840	-.01940	-.01740
0.0	.02670	.02610	.02450	.02150	.01880	.01470	.01050	.00580	.00260	0.00000	-.00290	-.00650	-.01080	-.01520	-.01880	-.02150	-.02470	-.02630	-.02690
+ 5.0	.04270	.03760	.03550	.02850	.02200	.01800	.01380	.00990	.00650	0.00000	-.00610	-.01110	-.01430	-.01860	-.02280	-.02930	-.03580	-.03780	-.04250
+10.0	.06220	.05960	.05510	.04540	.03310	.02660	.02080	.01460	.00740	0.00000	-.00670	-.01580	-.02210	-.02710	-.03320	-.04410	-.05340	-.05730	-.05970
+15.0	.07760	.06960	.06230	.05440	.04350	.03720	.03030	.02130	.01120	0.00000	-.01100	-.02190	-.03030	-.03790	-.04540	-.05600	-.06370	-.07080	-.07830
+20.0	.08300	.07940	.06940	.05580	.04270	.03320	.02430	.01720	.00790	0.00000	-.01020	-.02020	-.02150	-.02940	-.03940	-.05200	-.06530	-.07530	-.07840
+25.0	.08920	.07600	.06350	.05240	.03060	.02140	.01740	.01360	.00610	0.00000	-.00770	-.01420	-.02020	-.02210	-.02770	-.04930	-.06050	-.07320	-.08640
+30.0	.07910	.04520	.01940	.00410	-.00460	.01120	.01090	.00610	.00310	0.00000	-.00380	-.00720	-.01070	-.01280	-.01560	-.02410	-.03910	-.06490	-.09890
+35.0	.07510	.05630	.03480	.00710	-.00300	-.00770	-.00020	.00850	.00160	0.00000	-.00040	-.00060	.00050	.00290	.00860	-.00130	-.02910	-.05030	-.06910
+40.0	.06730	.05830	.02970	.00500	-.00020	.00310	.01060	.00530	.00550	0.00000	-.00540	-.00770	-.00990	-.00580	-.00680	-.01200	-.03670	-.06540	-.07410
+45.0	.07780	.06250	.04110	.03260	.01870	.01630	.01410	.01650	.01150	0.00000	-.00210	-.00790	-.01050	-.01340	-.01490	-.02880	-.03750	-.05880	-.07380
+50.0	.06190	.05190	.03930	.03260	.01920	.01770	.01510	.01030	.00620	0.00000	-.00470	-.01150	-.01510	-.02300	-.02580	-.03920	-.04590	-.05850	-.06850
+55.0	.04760	.03360	.02580	.01490	.00160	.00450	.00660	.00460	.00350	0.00000	-.00780	-.01570	-.02150	-.02440	-.02320	-.03650	-.04740	-.05520	-.06920
+60.0	.06110	.04280	.03210	.02630	.02190	.01650	.01610	.01020	.00710	0.00000	-.00420	-.00810	-.01420	-.01900	-.02110	-.02550	-.03130	-.04200	-.06030
+70.0	.06540	.05020	.03580	.02240	.01850	.01750	.01300	.01120	.00640	0.00000	-.00640	-.00970	-.01460	-.01810	-.02090	-.02900	-.04240	-.05680	-.07200
+80.0	.06380	.05060	.03800	.02870	.01790	.01380	.01340	.00500	.00520	0.00000	-.00280	-.00520	-.01010	-.01470	-.01940	-.03020	-.03950	-.05210	-.06530
+90.0	.06070	.04860	.04070	.03050	.02110	.01800	.01650	.01160	.00700	0.00000	-.00080	-.00170	-.01980	-.01300	-.01500	-.02440	-.03460	-.04250	-.05460

TABLE III.- Continued

$C_{l,lef}(\alpha,\beta)$

BETA	-30.0	-25.0	-20.0	-15.0	-10.0	- 8.0	- 6.0	- 4.0	- 2.0	
	0.0	+ 2.0	+ 4.0	+ 6.0	+ 8.0	+10.0	+15.0	+20.0	+25.0	+30.0
ALPHA										
-20.0	-.02050	-.01700	-.00760	.00470	.01500	.01340	.00080	.00130	.00270	
	0.00000	-.00120	-.00310	-.00540	-.00510	-.00540	.00360	.01590	.02560	.02970
-15.0	-.00600	-.00420	-.00070	.00330	.00060	-.00020	.00220	.00390	.00190	
	0.00000	-.00150	-.00300	-.00390	-.00280	-.00030	-.00240	.00230	.00520	.00720
-10.0	-.00810	-.00610	-.00010	.00180	.00340	.00220	.00160	.00060	0.00000	
	0.00000	-.00030	-.00080	-.00110	-.00200	-.00260	-.00070	.00070	.00710	.00930
- 5.0	.01060	.01020	.01040	.01030	.00930	.00730	.00520	.00300	.00120	
	0.00000	-.00100	-.00270	-.00440	-.00650	-.00870	-.01000	-.01030	-.01020	-.01060
0.0	.02380	.02320	.02240	.02040	.01680	.01340	.00980	.00600	.00290	
	0.00000	-.00270	-.00580	-.00940	-.01340	-.01640	-.02000	-.02200	-.02280	-.02340
+ 5.0	.03900	.03610	.03530	.03150	.02480	.02020	.01490	.01000	.00490	
	0.00000	-.00490	-.01000	-.01490	-.02060	-.02500	-.03170	-.03550	-.03630	-.03920
+10.0	.04850	.04630	.04300	.03470	.02630	.02130	.01550	.01000	.00460	
	0.00000	-.00480	-.01150	-.01750	-.02270	-.02780	-.03600	-.04430	-.04760	-.04980
+15.0	.04620	.04620	.04500	.04200	.02970	.02410	.01720	.01130	.00520	
	0.00000	-.00560	-.01230	-.01870	-.02480	-.03040	-.03690	-.03990	-.04110	-.04110
+20.0	.04800	.03350	.02900	.02090	.01580	.01410	.00950	.00580	.00050	
	0.00000	-.00600	-.01170	-.01750	-.01830	-.02030	-.02500	-.03350	-.03780	-.05210
+25.0	.07310	.05730	.03710	.02210	.02330	.02030	.01750	.01200	.00610	
	0.00000	-.00580	-.01280	-.01830	-.01860	-.02600	-.02480	-.03980	-.06100	-.07580
+30.0	.07520	.06320	.04280	.02350	.01060	.01330	.01380	.00940	.00750	
	0.00000	-.00630	-.00950	-.01100	-.01010	-.01510	-.02800	-.04730	-.06770	-.07970
+35.0	.05280	.04790	.04220	.01900	.00780	.00690	.01170	.00700	.00220	
	0.00000	.00140	-.00570	-.00760	-.00770	-.00910	-.02030	-.04350	-.04920	-.05410
+40.0	.05550	.04350	.03390	.01730	.00940	.01560	.01930	.01100	.01100	
	0.00000	-.00740	-.01260	-.01940	-.02130	-.02530	-.03320	-.04980	-.05940	-.07140
+45.0	.05000	.04930	.03510	.03060	.01790	.01580	.01280	.00770	.00190	
	0.00000	-.01180	-.01240	-.01500	-.01730	-.02140	-.03410	-.03860	-.05280	-.05350

TABLE III.- Continued

$C_{l,\delta_{a=20^{\circ}}}(\alpha,\beta)$

BETA	-30.0 0.0	-25.0 + 2.0	-20.0 + 4.0	-15.0 + 6.0	-10.0 + 8.0	- 8.0 +10.0	- 6.0 +15.0	- 4.0 +20.0	- 2.0 +25.0	+30.0
ALPHA										
-20.0	-.05140	-.03400	-.01990	-.01280	-.00380	-.00740	-.01400	-.01310	-.01850	
	-.02260	-.02570	-.02860	-.03460	-.03670	-.04070	-.03170	-.02460	-.01050	.00690
-15.0	-.04920	-.03620	-.02310	-.01480	-.01960	-.02270	-.02620	-.02640	-.03000	
	-.03270	-.03360	-.03570	-.03820	-.03650	-.04020	-.04500	-.03670	-.02360	-.01060
-10.0	-.04550	-.03420	-.02750	-.02480	-.02530	-.02620	-.02700	-.02950	-.03400	
	-.03280	-.03300	-.03520	-.03740	-.04040	-.04360	-.04410	-.04140	-.03470	-.02340
- 5.0	-.03430	-.03020	-.02570	-.02290	-.02410	-.02690	-.03000	-.03330	-.03670	
	-.04010	-.04390	-.04790	-.05100	-.05400	-.05540	-.05660	-.05380	-.04930	-.04520
0.0	-.04030	-.03710	-.03260	-.03010	-.03220	-.03410	-.03720	-.04130	-.04500	
	-.04810	-.05090	-.05350	-.05690	-.05940	-.06230	-.06440	-.06190	-.05740	-.05420
+ 5.0	-.02450	-.02500	-.02350	-.02460	-.02910	-.03280	-.03720	-.04190	-.04660	
	-.05110	-.05480	-.05800	-.06120	-.06470	-.06790	-.07240	-.07350	-.07200	-.07250
+10.0	-.00290	-.00240	-.00250	-.00890	-.01830	-.02330	-.02990	-.03640	-.04350	
	-.04990	-.05550	-.06060	-.06630	-.07150	-.07690	-.08630	-.09270	-.09280	-.09230
+15.0	.01590	.01460	.01220	.00640	-.00670	-.01340	-.02130	-.03120	-.04000	
	-.04910	-.05750	-.06550	-.07280	-.07790	-.08540	-.09850	-.10430	-.10670	-.10800
+20.0	.00720	.00430	.00360	.00610	.00240	-.00550	-.01390	-.02300	-.03240	
	-.04180	-.05170	-.06080	-.06910	-.07860	-.08650	-.09020	-.08770	-.08840	-.09130
+25.0	.02980	.02600	.02390	.01590	.00480	-.00230	-.01030	-.02000	-.02850	
	-.03720	-.04520	-.05340	-.06150	-.06840	-.07610	-.08720	-.09520	-.09730	-.10110
+30.0	.04020	.00790	-.01510	-.00760	-.01980	-.01070	-.01240	-.01950	-.02460	
	-.03080	-.03640	-.04310	-.04580	-.04950	-.05030	-.06250	-.05500	-.07800	-.11030
+35.0	.04110	.02280	.01220	-.01440	-.01210	-.01440	-.00700	-.01130	-.01730	
	-.02560	-.02520	-.02710	-.02590	-.02410	-.02220	-.01990	-.04650	-.05710	-.07540
+40.0	.04480	.02820	.00700	-.01540	-.01250	-.00320	.00150	-.00280	-.00880	
	-.01660	-.02470	-.02810	-.03180	-.03170	-.03100	-.02810	-.05050	-.07170	-.08830
+45.0	.05730	.04120	.01750	.01040	.00290	.00130	-.00060	-.00160	-.00240	
	-.01220	-.01760	-.02040	-.02490	-.02420	-.03170	-.03920	-.04630	-.07000	-.08610
+50.0	.04080	.02970	.02030	.01870	.00650	.00540	.00390	0.00000	-.00240	
	-.00760	-.01360	-.02250	-.02560	-.03090	-.03040	-.04260	-.04420	-.05360	-.06470
+55.0	.04720	.02960	.02440	.01850	.00880	.00590	.00180	-.00210	-.00430	
	-.00950	-.01380	-.01990	-.02320	-.02780	-.02910	-.03880	-.04470	-.04990	-.06750
+60.0	.05170	.03500	.02940	.02090	.01160	.00730	.00220	-.00160	-.00430	
	-.00920	-.01280	-.01660	-.02080	-.02500	-.02690	-.03620	-.04470	-.05030	-.06700
+70.0	.04180	.04090	.02990	.01970	.00830	.00830	-.00220	-.00470	-.00540	
	-.00750	-.01330	-.01430	-.01940	-.02370	-.02570	-.03710	-.04730	-.05830	-.06720
+80.0	.05980	.04650	.03690	.02750	.01430	.01090	.00730	.00300	.00090	
	-.00410	-.00870	-.01540	-.01580	-.02030	-.02430	-.03750	-.04690	-.05650	-.06980
+90.0	.07160	.05320	.04100	.03270	.01920	.01530	.01150	.00860	.00470	
	.00220	-.00250	-.00520	-.00900	-.01230	-.01600	-.02950	-.03780	-.05000	-.06840

TABLE III.- Continued

$C_{l,\delta_{a=20^{\circ}},lef}(\alpha,\beta)$

BETA	-30.0	-25.0	-20.0	-15.0	-10.0	- 8.0	- 6.0	- 4.0	- 2.0	
	0.0	+ 2.0	+ 4.0	+ 6.0	+ 8.0	+10.0	+15.0	+20.0	+25.0	+30.0
ALPHA										
-20.0	-.05360	-.04020	-.03090	-.02040	-.01470	-.02280	-.02440	-.02280	-.02270	
	-.02330	-.02310	-.02560	-.02880	-.03030	-.03180	-.02590	-.01510	-.00520	.00870
-15.0	-.04670	-.04550	-.04450	-.04240	-.03780	-.03560	-.03330	-.02880	-.02890	
	-.03120	-.03290	-.03330	-.03440	-.03530	-.03620	-.03180	-.02890	-.02770	-.02580
-10.0	-.04920	-.04810	-.04120	-.04140	-.03870	-.03660	-.03800	-.03850	-.03960	
	-.04040	-.04080	-.04110	-.04170	-.04440	-.04510	-.04320	-.04300	-.03520	-.03410
- 5.0	-.04130	-.04410	-.04220	-.04010	-.04400	-.04520	-.04630	-.04870	-.05020	
	-.05180	-.05270	-.05310	-.05440	-.05600	-.05720	-.06080	-.05850	-.05730	-.05970
0.0	-.02930	-.02900	-.03050	-.03110	-.03520	-.03850	-.04080	-.04480	-.04840	
	-.05100	-.05390	-.05660	-.05970	-.06210	-.06490	-.06940	-.06970	-.07050	-.07020
+ 5.0	-.01630	-.01860	-.01720	-.02020	-.02690	-.03140	-.03620	-.04120	-.04720	
	-.05250	-.05720	-.06160	-.06590	-.07030	-.07480	-.08170	-.08380	-.08390	-.08560
+10.0	.00360	.00050	-.00380	-.02100	-.01910	-.02330	-.02890	-.03410	-.04010	
	-.04440	-.04910	-.05410	-.05880	-.06370	-.06860	-.07710	-.08420	-.08840	-.09130
+15.0	-.00580	-.00570	-.00520	-.00780	-.01450	-.01840	-.02540	-.03100	-.03670	
	-.04360	-.04780	-.05150	-.05730	-.06320	-.06880	-.07500	-.07840	-.07760	-.07720
+20.0	.00880	-.00200	-.00150	-.00310	-.01330	-.01430	-.01680	-.02160	-.02580	
	-.02970	-.03500	-.04130	-.04370	-.04730	-.04830	-.05840	-.05950	-.05890	-.07020
+25.0	.03110	.02470	.00810	-.00990	-.00180	-.00030	-.00830	-.01410	-.01930	
	-.02580	-.03030	-.03660	-.04140	-.04380	-.04610	-.03830	-.04820	-.06540	-.08170
+30.0	.03960	.03180	.01650	.00320	-.00640	-.00230	-.00950	-.01320	-.01960	
	-.02220	-.03170	-.03560	-.03600	-.03380	-.03410	-.04420	-.05730	-.07260	-.08010
+35.0	.02910	.02480	.02270	.00100	-.00620	-.00940	-.00480	-.01070	-.01790	
	-.02040	-.02420	-.02590	-.02980	-.02970	-.02950	-.03700	-.05850	-.06060	-.06480
+40.0	.03730	.02820	.01540	.00240	-.00300	.00580	.00250	.00270	.00080	
	-.01430	-.01600	-.02730	-.03510	-.04100	-.04140	-.04680	-.05970	-.07280	-.08170
+45.0	.04480	.03990	.02990	.02120	.00770	.00460	.00380	.00070	-.00490	
	-.01100	-.01470	-.02190	-.02230	-.02830	-.02840	-.04290	-.05110	-.06110	-.06500

TABLE III.- Continued

$C_{l,\delta_{r=30^{\circ}}}(\alpha,\beta)$

ALPHA \ BETA	-30.0	-25.0	-20.0	-15.0	-10.0	- 8.0	- 6.0	- 4.0	- 2.0	0.0	+ 2.0	+ 4.0	+ 6.0	+ 8.0	+10.0	+15.0	+20.0	+25.0	+30.0
-20.0	-.01150	.00420	.01630	.02760	.03500	.03490	.03210	.03010	.02360	.02010	.01440	.01390	.01270	.00850	-.00100	.00640	.01760	.02960	.04500
-15.0	-.00780	.00480	.01760	.02330	.02420	.02470	.02550	.02270	.01970	.01760	.01520	.01330	.01050	.00930	.00500	.00600	.01340	.02590	.04240
-10.0	-.00570	.00550	.01690	.02090	.02370	.02520	.02650	.02430	.02020	.01840	.01690	.01280	.01100	.00950	.00440	.00730	.01120	.02270	.03400
- 5.0	.02610	.03170	.03430	.03310	.03110	.03120	.02900	.02530	.02050	.01540	.01120	.00730	.00320	-.00090	-.00460	-.00670	-.00780	-.00490	.00070
0.0	.02920	.03290	.03390	.03300	.02940	.02990	.02620	.02210	.01820	.01460	.01120	.00790	.00360	-.00090	-.00530	-.00860	-.00920	-.00790	-.00430
+ 5.0	.04160	.04360	.04360	.04000	.03360	.03200	.02770	.02360	.01890	.01440	.01030	.00620	.00140	-.00390	-.00810	-.01460	-.01770	-.01770	-.01990
+10.0	.06400	.06400	.06260	.05520	.04420	.04010	.03430	.02800	.02090	.01370	.00730	.00060	-.00690	-.01360	-.01990	-.03070	-.03810	-.03950	-.03950
+15.0	.08210	.07710	.07310	.06540	.05190	.04820	.04110	.03290	.02280	.01350	.00470	-.00440	-.01420	-.02380	-.03190	-.04530	-.05290	-.05690	-.06190
+20.0	.10880	.09280	.08080	.07080	.05300	.04740	.04120	.03130	.02250	.01370	.00560	-.00320	-.01220	-.02330	-.03260	-.05030	-.06000	-.07210	-.08010
+25.0	.09320	.08380	.07180	.06110	.04490	.04270	.03690	.03090	.02300	.01470	.00510	-.00300	-.01160	-.02100	-.03000	-.04640	-.05690	-.06880	-.07820
+30.0	.08180	.05030	.02340	.01680	.00450	.02400	.02690	.02440	.02130	.01260	.00800	.00100	-.00540	-.00940	-.01670	-.02930	-.03600	-.06270	-.09410
+35.0	.07420	.06520	.04320	.01350	.00840	.00650	.02010	.02230	.01780	.01140	.01090	.01020	.00920	.00870	.00690	.00170	-.02770	-.04980	-.05880
+40.0	.06130	.06060	.03890	.01170	.00760	.01210	.01720	.01690	.01580	.00590	.00230	-.00240	-.00440	-.00590	-.00810	-.01140	-.03970	-.06120	-.06190
+45.0	.08190	.06290	.03990	.03130	.02230	.01940	.02230	.02300	.01330	.00070	.00110	-.00620	-.00970	-.01150	-.01800	-.02690	-.03550	-.05840	-.07770
+50.0	.05290	.04390	.02950	.02430	.01570	.01550	.01490	.01170	.00800	.00260	-.00420	-.00810	-.01440	-.01500	-.02020	-.02860	-.03390	-.04860	-.05770
+55.0	.05850	.04350	.03300	.02650	.01660	.01480	.01250	.00860	.00690	.00190	-.00340	-.00640	-.01330	-.01560	-.01890	-.02760	-.03420	-.04490	-.05950
+60.0	.06270	.04750	.03770	.02970	.02090	.01840	.01570	.01040	.00750	.00150	-.00280	-.00510	-.01130	-.01450	-.01750	-.02630	-.03480	-.04430	-.05970
+70.0	.06690	.05630	.04530	.03430	.02420	.02190	.01750	.01250	.00520	.00080	-.00100	-.00640	-.01120	-.01520	-.01960	-.02950	-.04070	-.05160	-.06230
+80.0	.06620	.05520	.04320	.03230	.02010	.01650	.00980	.01000	.00450	-.00230	-.00630	-.00830	-.01260	-.01800	-.01910	-.03100	-.04190	-.05400	-.06520
+90.0	.06700	.05420	.04000	.02790	.01840	.01660	.01120	.00990	.00790	.00180	-.00200	-.00410	-.00640	-.01220	-.01460	-.02370	-.03580	-.05030	-.06280

TABLE III.- Continued

ALPHA	$C_{l_r}(\alpha)$
-20.0	-.15500
-15.0	-.15500
-10.0	-.15500
- 5.0	-.20100
0.0	-.00240
+ 5.0	.08800
+10.0	.20500
+15.0	.22000
+20.0	.31900
+25.0	.43700
+30.0	.68000
+35.0	.10000
+40.0	.44700
+45.0	-.33000
+50.0	-.06800
+55.0	.11800
+60.0	.08020
+70.0	.05290
+80.0	.08680
+90.0	-.01830

ALPHA	$\Delta C_{l_\beta}(\alpha)$
-20.0	.0
-15.0	.0
-10.0	.0
- 5.0	.0
0.0	.0
+ 5.0	.0
+10.0	.0
+15.0	.0007
+20.0	.0005
+25.0	.0003
+30.0	.0
+35.0	.0
+40.0	.0
+45.0	.0
+50.0	.0
+55.0	.0
+60.0	.0
+70.0	.0
+80.0	.0
+90.0	.0

ALPHA	$\Delta C_{l_{r,lef}}(\alpha)$
-20.0	.02900
-15.0	.02900
-10.0	.02900
- 5.0	.17500
0.0	.06650
+ 5.0	.03600
+10.0	.00700
+15.0	.06600
+20.0	.20100
+25.0	.00600
+30.0	-.06800
+35.0	-.53700
+40.0	-.78700
+45.0	-.39400

TABLE III.- Concluded

ALPHA	$C_{l_p}(\alpha)$
-20.0	-.36600
-15.0	-.36600
-10.0	-.36600
- 5.0	-.37700
0.0	-.34500
+ 5.0	-.43400
+10.0	-.40800
+15.0	-.38800
+20.0	-.32900
+25.0	-.29400
+30.0	-.23000
+35.0	-.21000
+40.0	-.12000
+45.0	-.10000
+50.0	-.10000
+55.0	-.12000
+60.0	-.14000
+70.0	-.10000
+80.0	-.15000
+90.0	-.20000

ALPHA	$\Delta C_{l_{p,lef}}(\alpha)$
-20.0	.00600
-15.0	.00600
-10.0	.00600
- 5.0	.01800
0.0	-.10000
+ 5.0	.02000
+10.0	.05800
+15.0	.08700
+20.0	.02700
+25.0	-.05600
+30.0	-.08200
+35.0	.36200
+40.0	.19400
+45.0	.09700

TABLE IV.- LEVELS OF ROLL-RESPONSE DEGRADATION

AND CROSS-AXES COUPLING FOR VARIOUS

ROLL-RATE LIMITING TECHNIQUES

Scheduling parameter	Initial roll-response degradation	Cross-axes coupling
$\bar{q}$	High	Low
α	Moderate	Moderate
δ_h	Low	High

TABLE V.- COMPARISON OF ROLL RESPONSE TO

FULL LATERAL STICK INPUT

Control system	$\delta_{a,max}$, deg	$\Delta t_{\phi=90^\circ}$	$\Delta t_{\phi=180^\circ}$
A	-21.5	2.6	3.8
B	-16.1	3	4.3
C	-21.5	2.6	3.9

TABLE VI.- THRUST VALUES USED IN SIMULATION

(a) SI Units

m	Thrust values at an altitude, m, of -					
	0	3 048	6 096	9 144	12 192	15 240
	T_{idle}					
0.2	2 824	1 890	3 069	4 492	5 916	7 562
.4	267	111	1 535	3 358	5 026	6 783
.6	-4 537	-3 158	-1 334	1 557	4 048	6 049
.8	-12 010	-8 451	-5 782	-1 099	2 669	4 893
1.0	-16 013	-6 227	-2 647	-1 521	-890	3 114
	T_{mil}					
0.2	56 401	40 699	28 080	17 970	10 987	6 227
.4	56 089	41 420	29 401	19 082	11 565	6 939
.6	56 223	43 764	31 536	20 728	12 632	7 384
.8	55 111	45 263	34 472	23 663	14 456	8 585
1.0	51 953	43 804	35 806	27 133	16 902	10 275
	T_{max}					
0.2	95 276	69 834	49 929	32 573	19 727	11 565
.4	100 970	74 993	54 488	36 269	22 240	12 610
.6	107 820	84 112	61 204	41 300	25 354	14 300
.8	115 959	93 742	71 057	49 440	30 513	17 570
1.0	128 485	103 723	81 398	59 977	38 440	22 494

(b) U.S. Customary Units

m	Thrust values at an altitude, ft, of -					
	0	10 000	20 000	30 000	40 000	50 000
	T_{idle}					
0.2	635	425	690	1 010	1 330	1 700
.4	60	25	345	755	1 130	1 525
.6	-1 020	-710	-300	350	910	1 360
.8	-2 700	-1 900	-1 300	-247	600	1 100
1.0	-3 600	-1 400	-595	-342	-200	700
	T_{mil}					
0.2	12 680	9 150	6 313	4 040	2 470	1 400
.4	12 610	9 312	6 610	4 290	2 600	1 560
.6	12 640	9 839	7 090	4 660	2 840	1 660
.8	12 390	10 176	7 750	5 320	3 250	1 930
1.0	11 680	9 848	8 050	6 100	3 800	2 310
	T_{max}					
0.2	21 420	15 700	11 225	7 323	4 435	2 600
.4	22 700	16 860	12 250	8 154	5 000	2 835
.6	24 240	18 910	13 760	9 285	5 700	3 215
.8	26 070	21 075	15 975	11 115	6 860	3 950
1.0	28 886	23 319	18 300	13 484	8 642	5 057

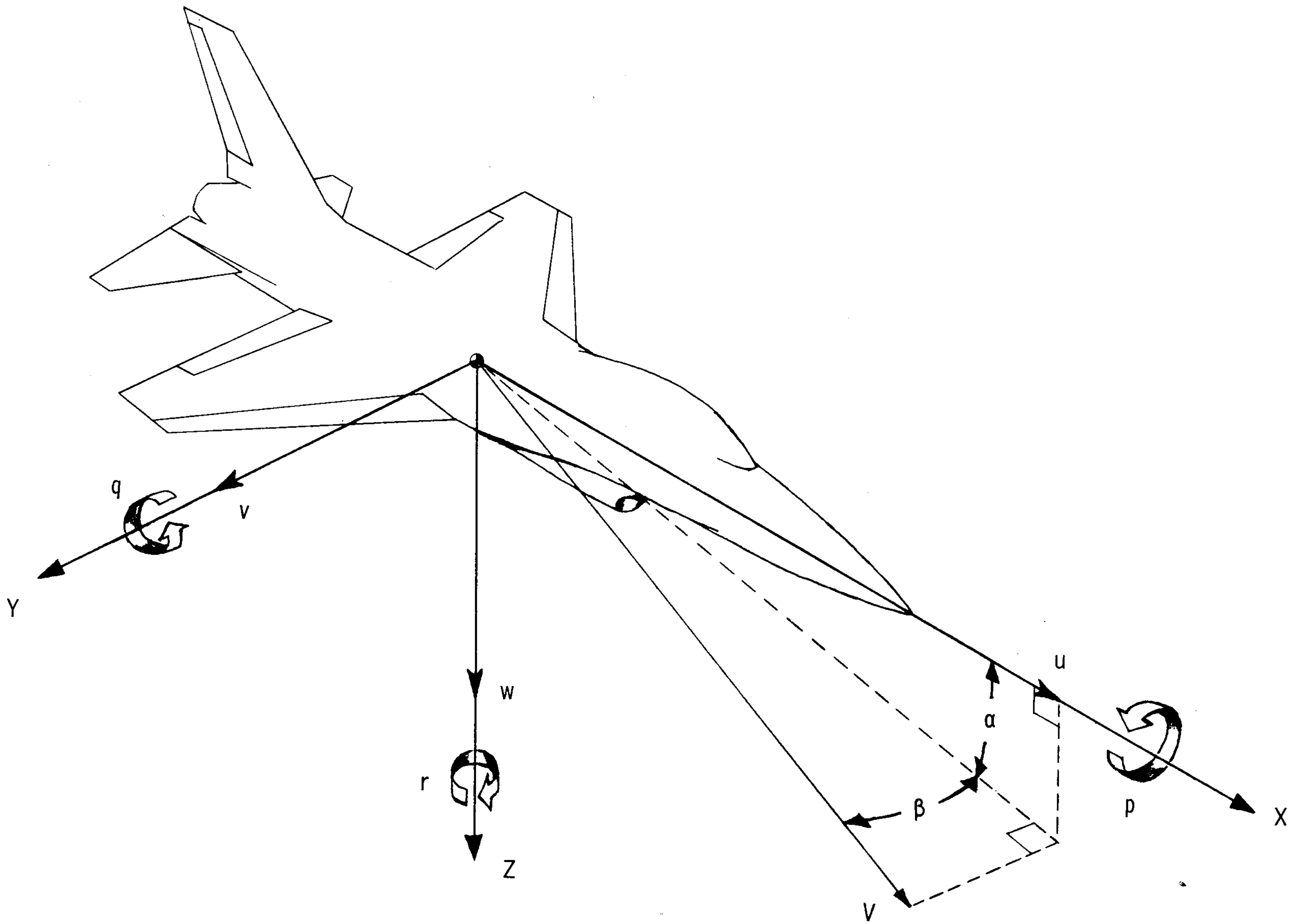

Figure 1.- Body system of axes.

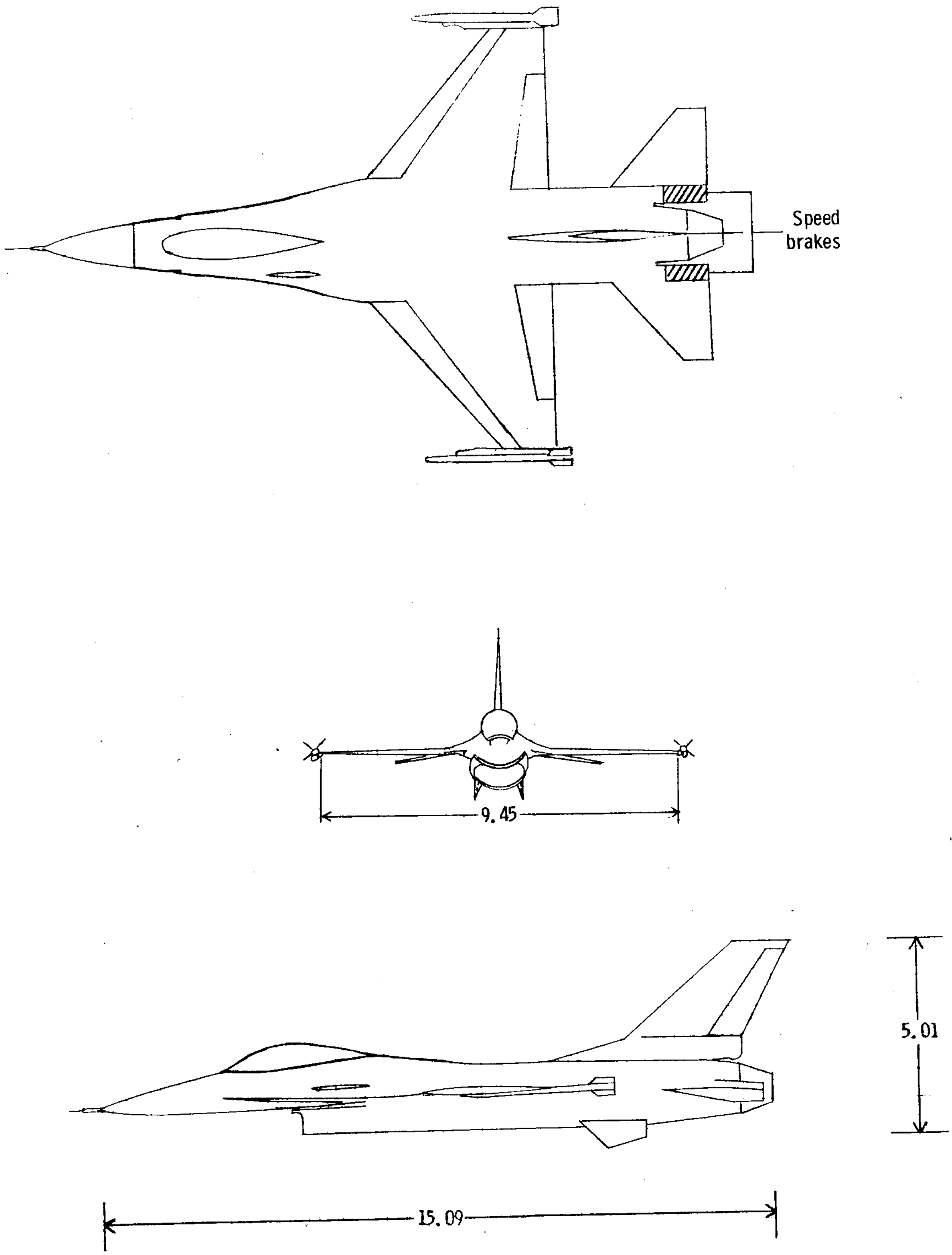

Figure 2.- Three-view sketch of airplane configuration.
All dimensions given in meters.

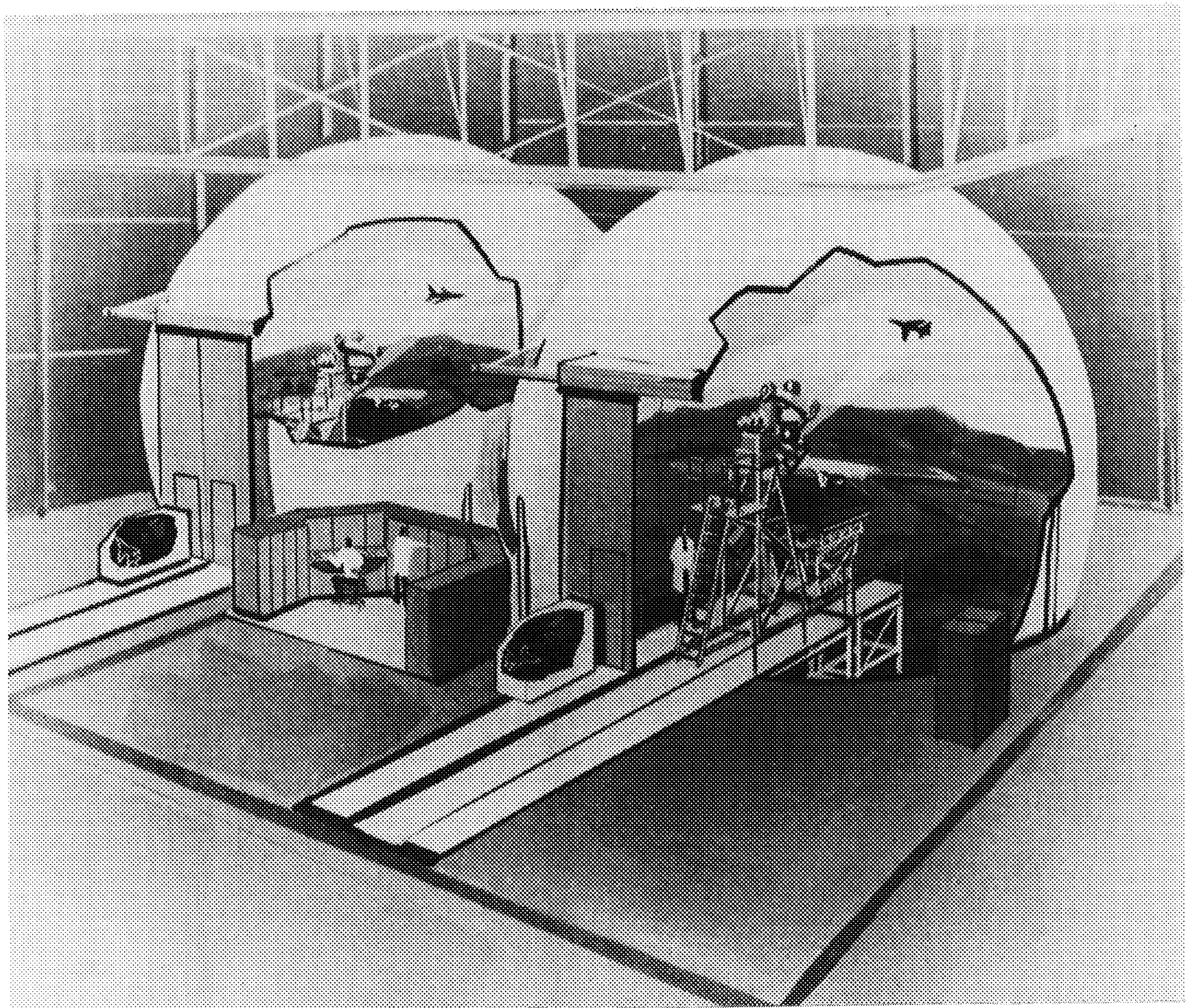

L-71-8700

Figure 3.- General arrangement of Langley differential maneuvering simulator (DMS) facility.

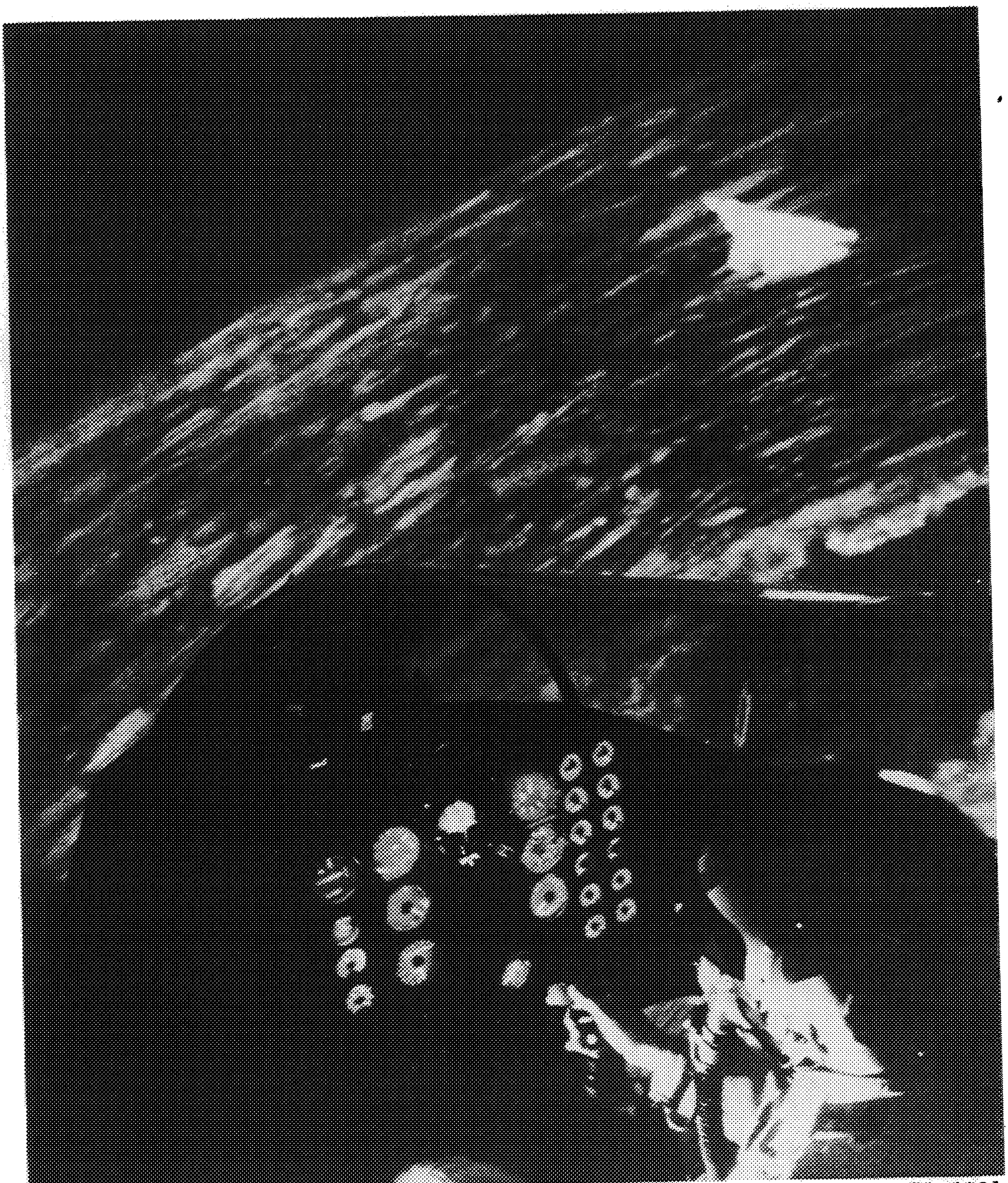

L-73-6831

Figure 4.- View of cockpit and visual display within one sphere of DMS.

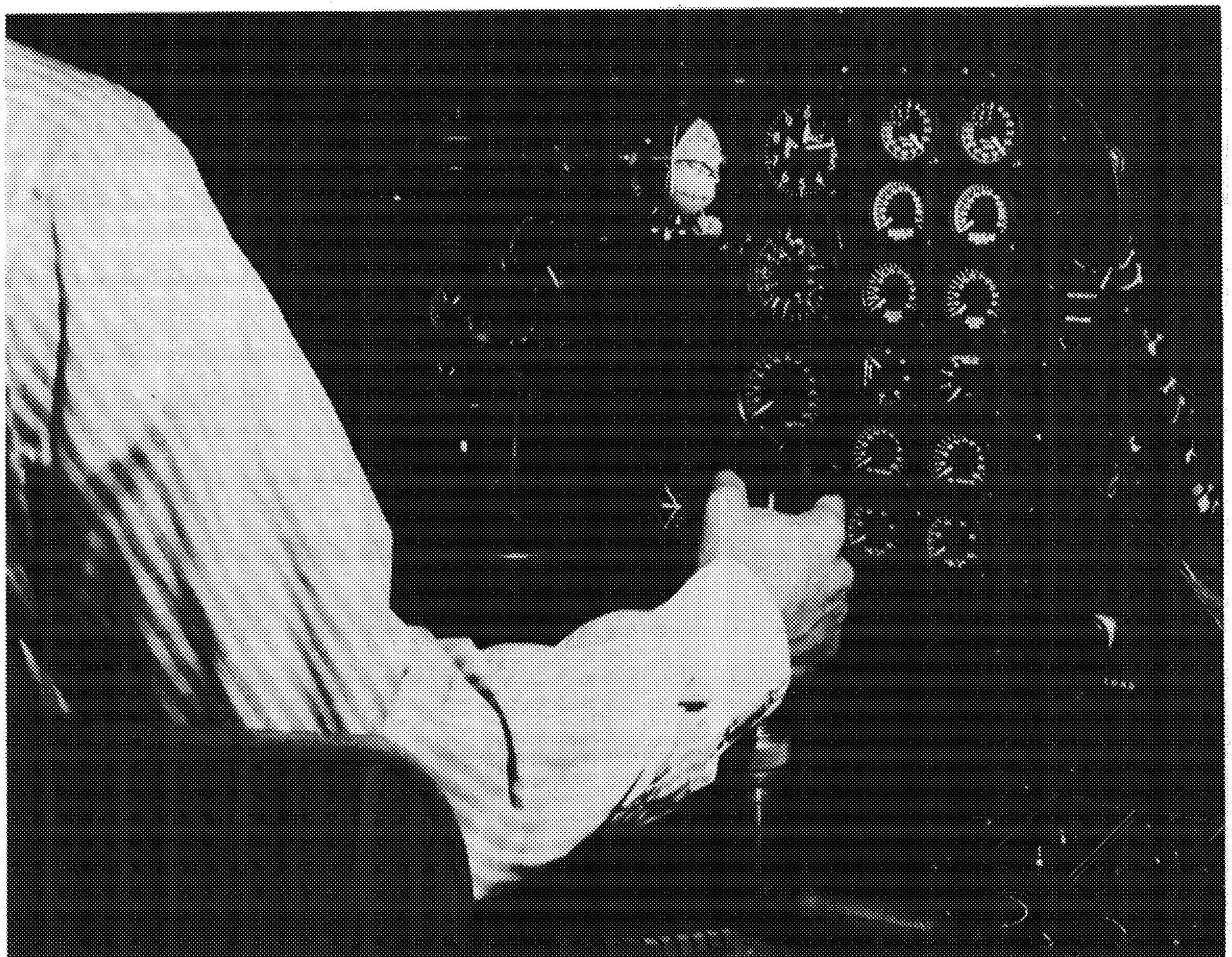

L-73-8778

Figure 5.- View of side-stick installation in simulator cockpit.

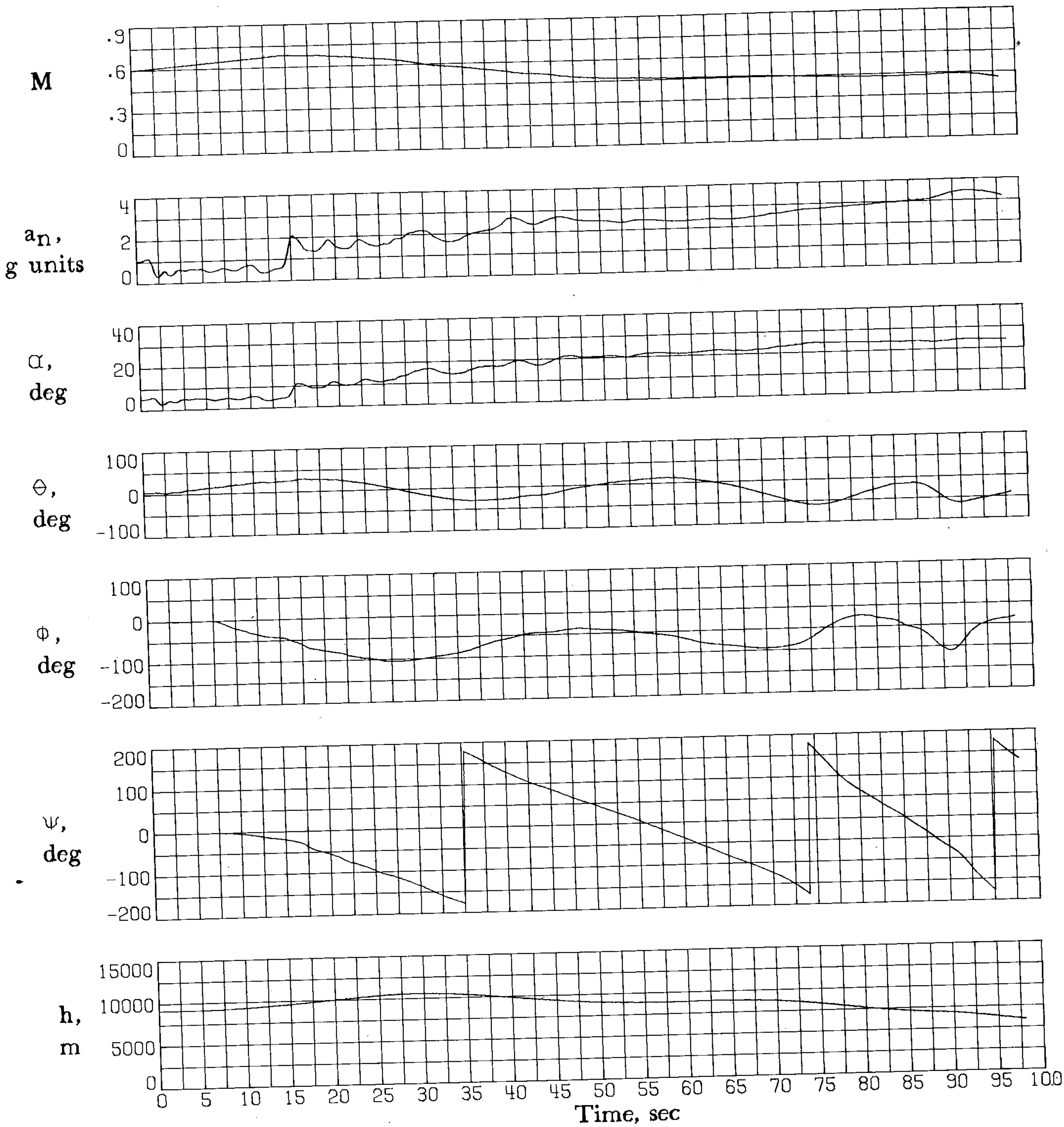

Figure 6.- Time histories of target motions in wind-up turn task.

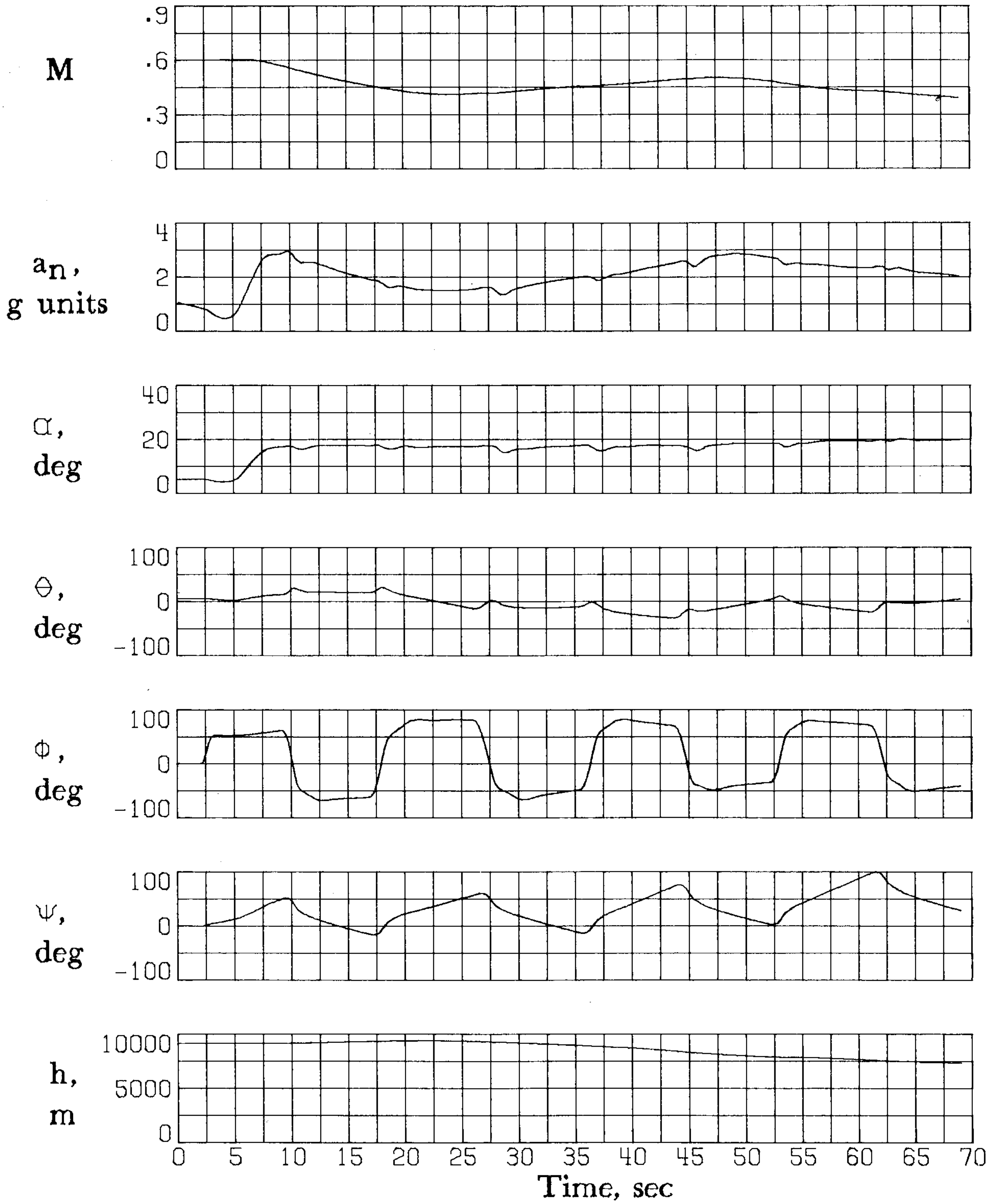

Figure 7.- Time histories of target motions in bank-to-bank task.

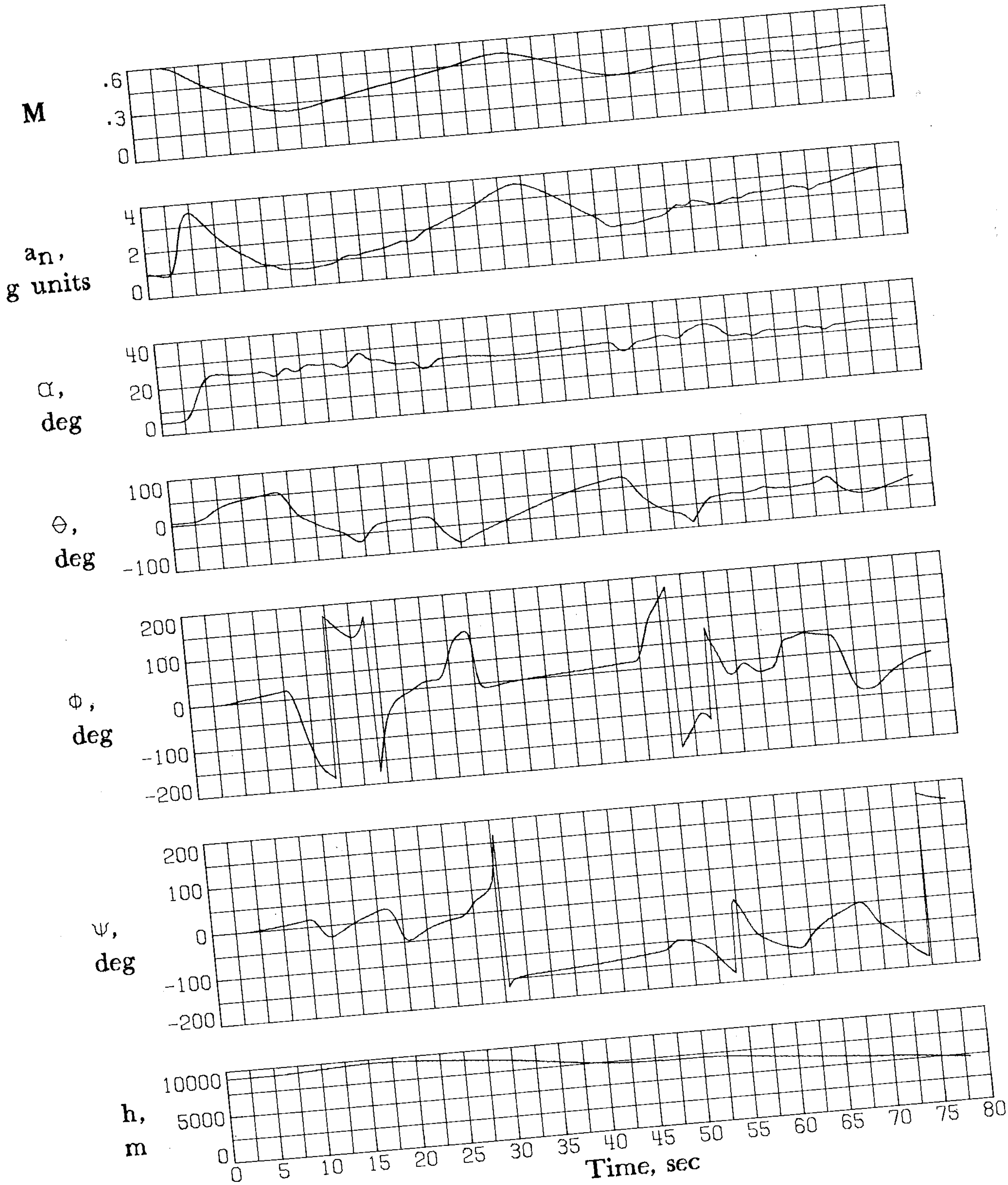

Figure 8.- Time histories of target motions in ACM task.

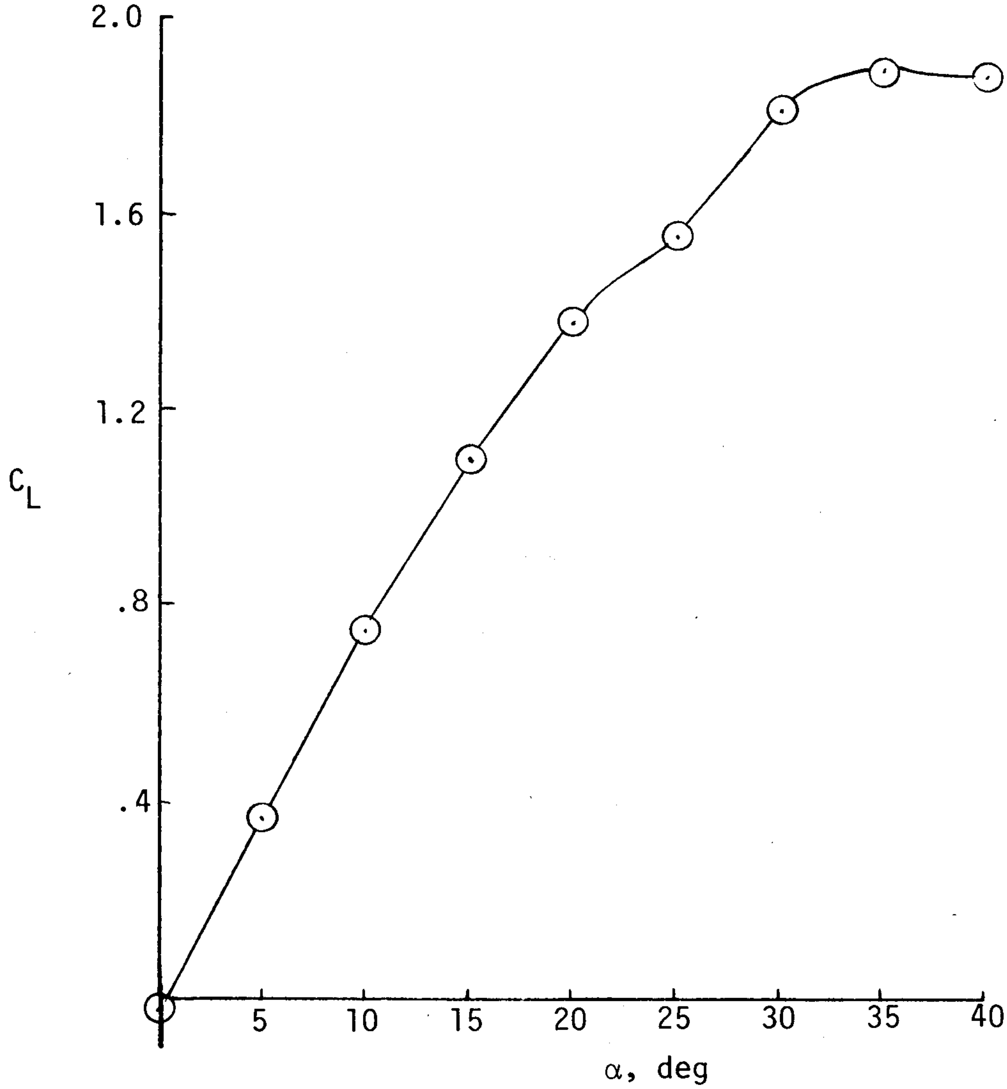

Figure 9.- Untrimmed lift characteristics of simulated configuration. $\beta = 0^{\circ}$.

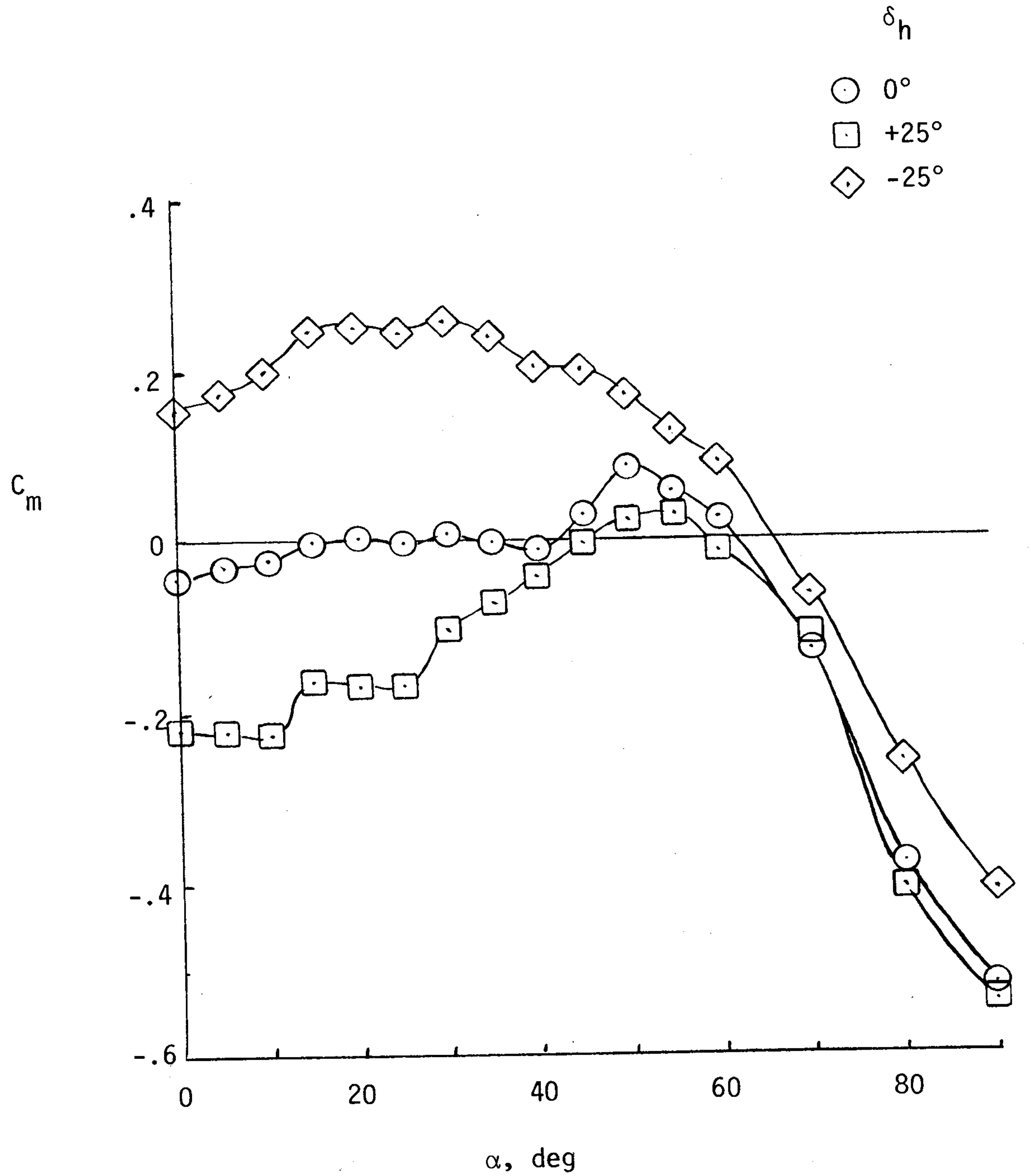

Figure 10.- Variation of pitching moment with α for various stabilator deflections. Center of gravity at $0.35\bar{c}$.

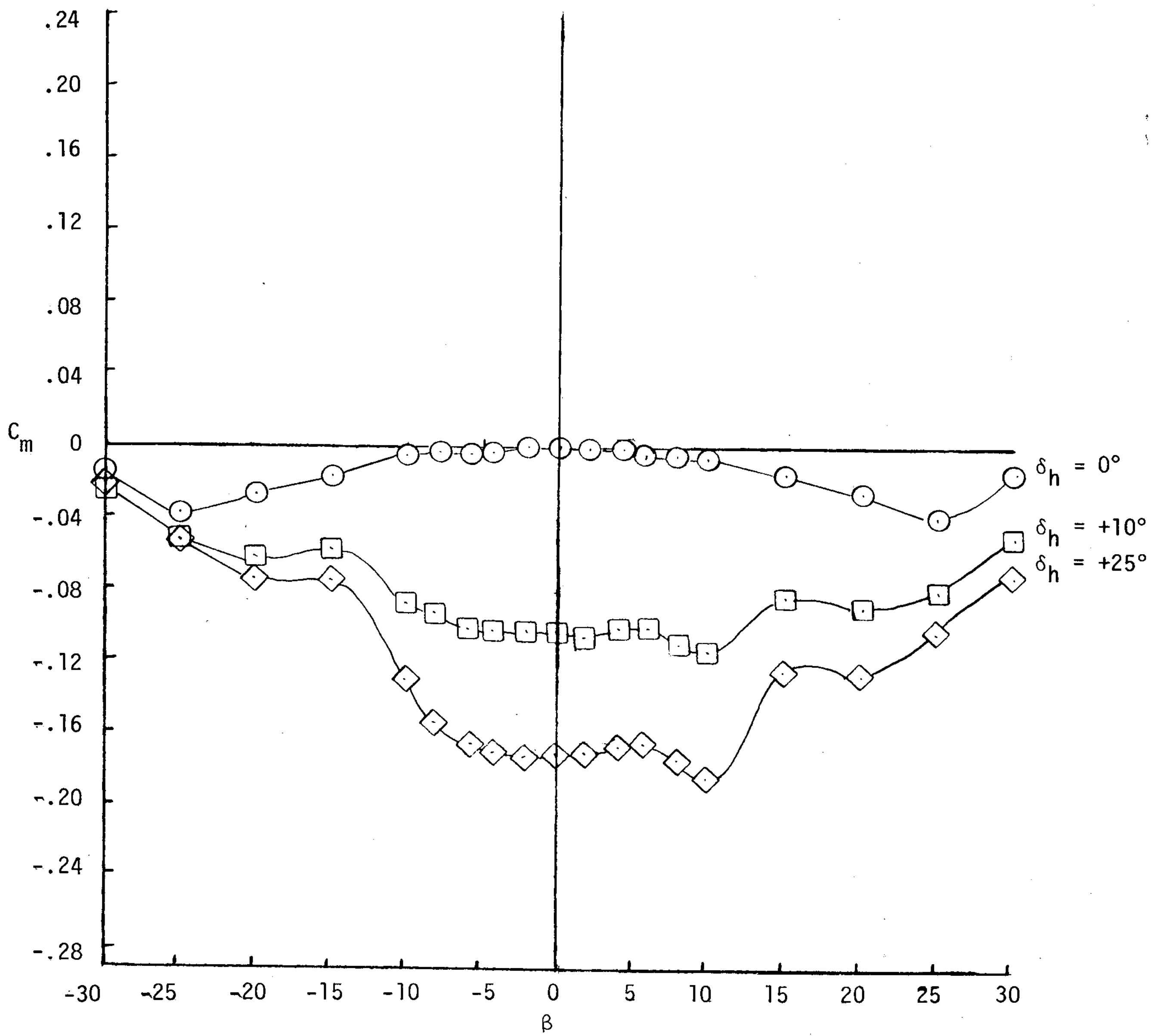

Figure 11.- Variation of pitching moment with sideslip for various stabilator deflections. $\alpha = 25^{\circ}$.

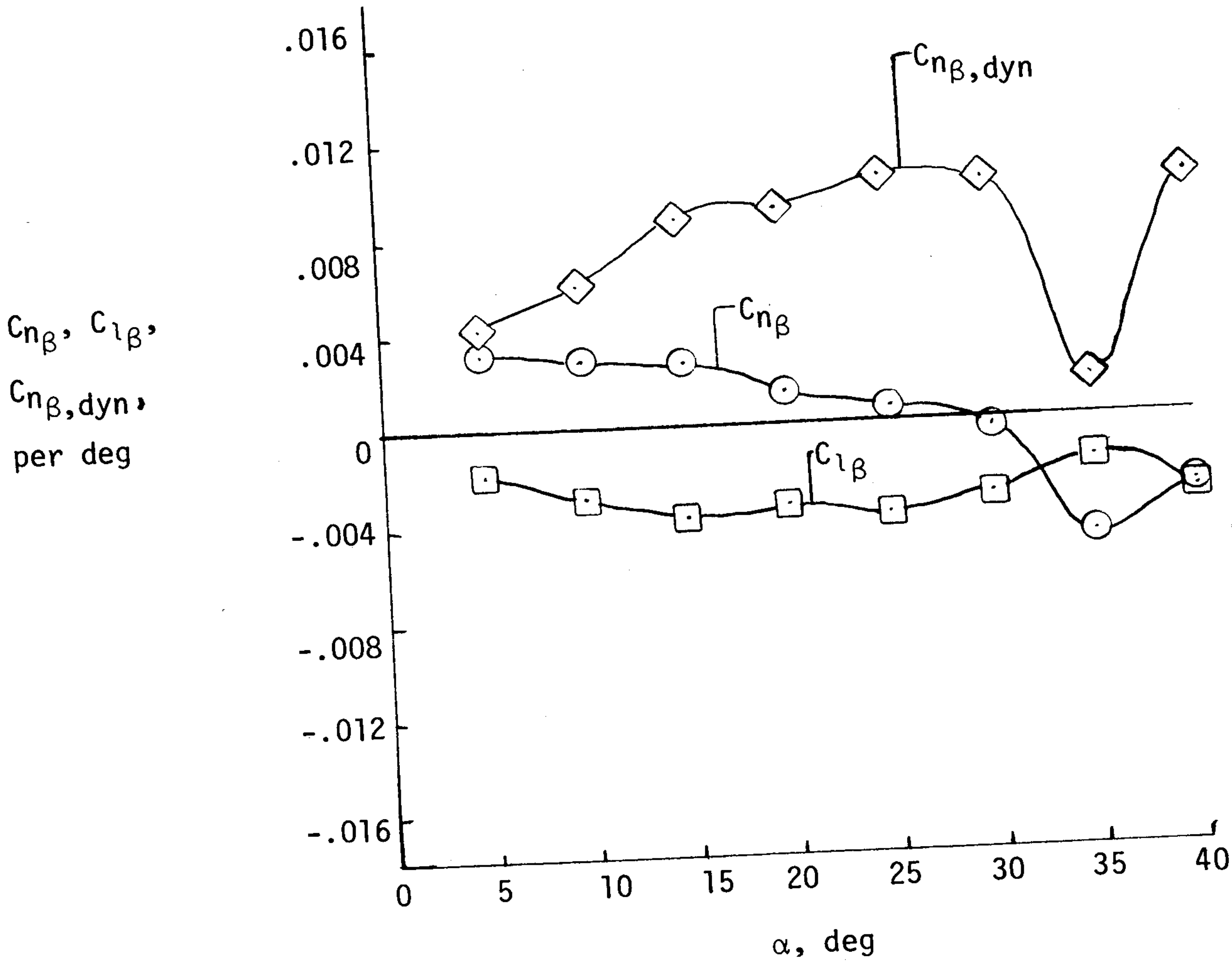

Figure 12.- Variation of lateral-directional stability characteristics of basic configuration with angle of attack for scheduled leading-edge flap deflections. $\delta_h = 0^o$.

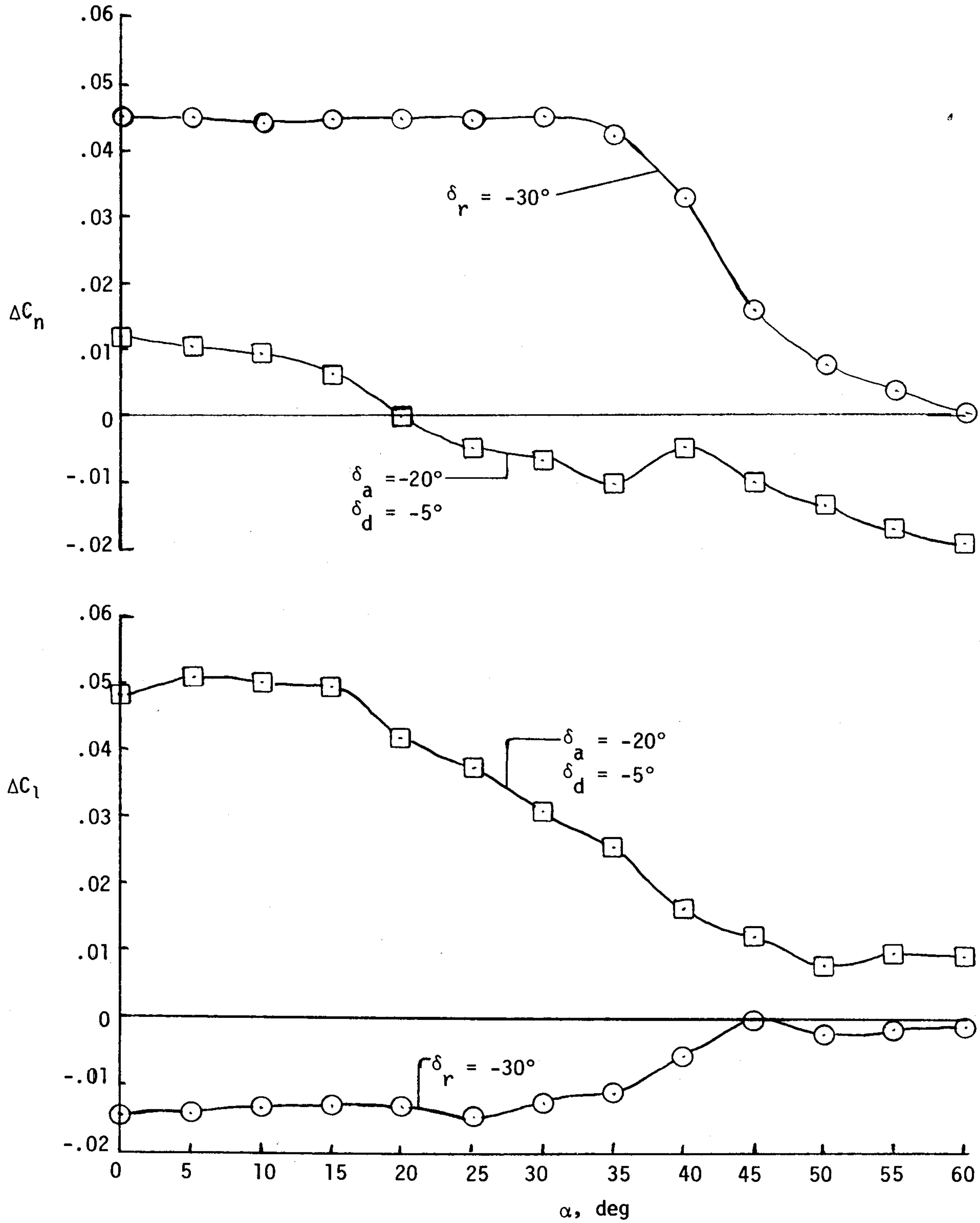

Figure 13.- Variation of lateral-directional control derivatives with angle of attack. $\beta = 0^{\circ}$.

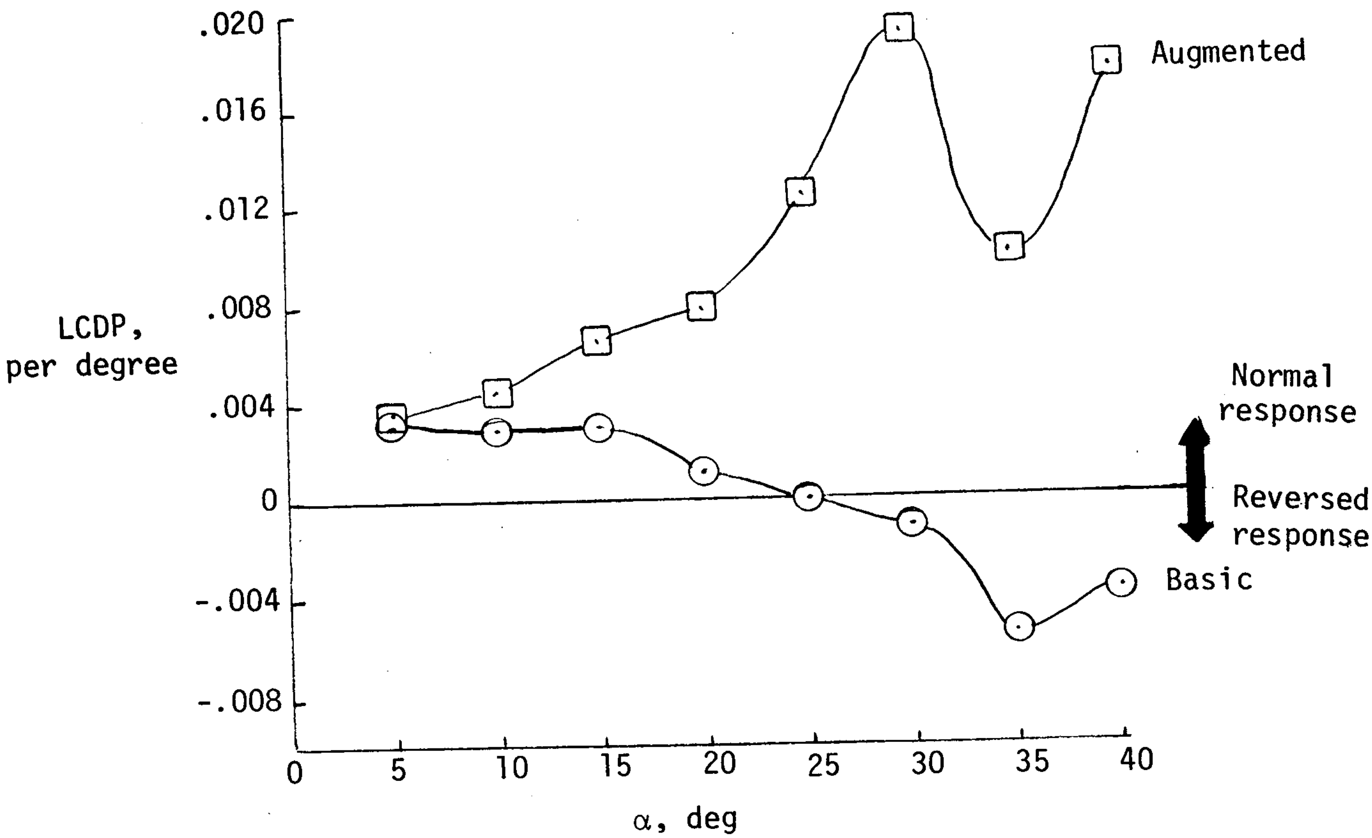

Figure 14.- Variation of lateral control divergence parameter (LCDP) with angle of attack for simulated configuration.

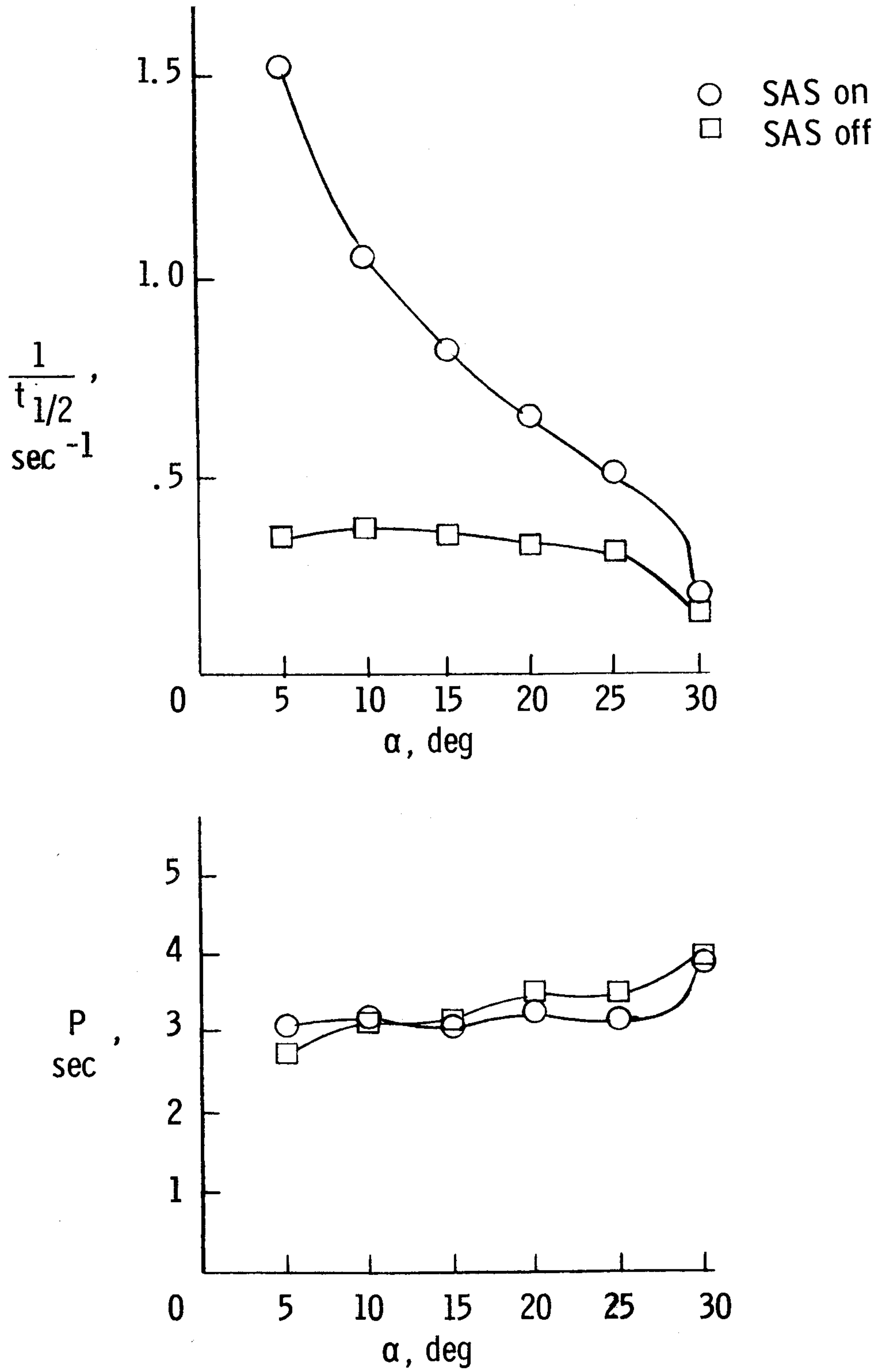

(a) Dutch roll mode.

Figure 15.- Variation of airplane dynamic lateral-directional stability with angle of attack for airplane with and without SAS. h = 9144 m (30 000 ft); velocity for 1g; level flight.

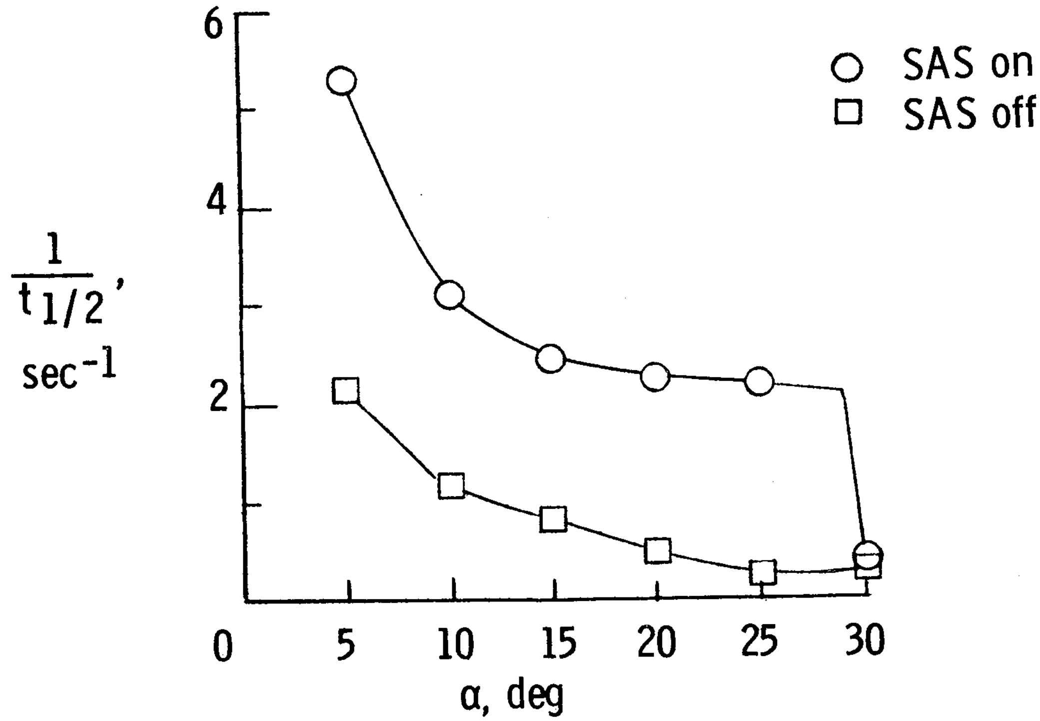

(b) Roll mode.

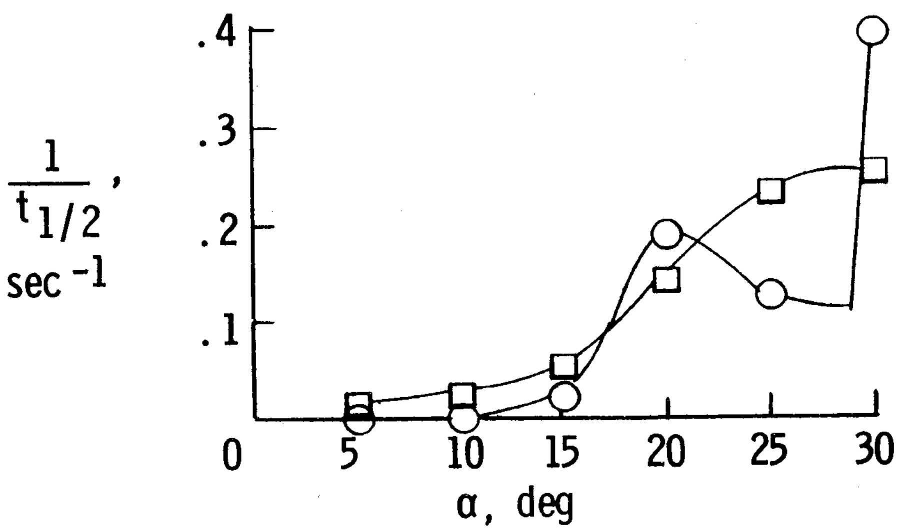

(c) Spiral mode.

Figure 15.- Concluded.

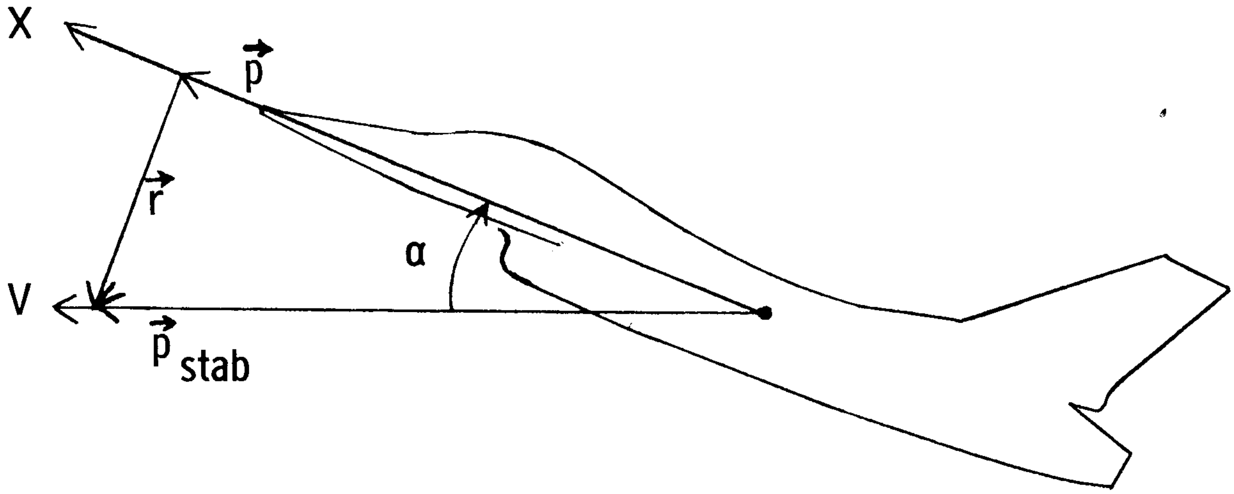

(a) $\phi = 0^{\circ}$.

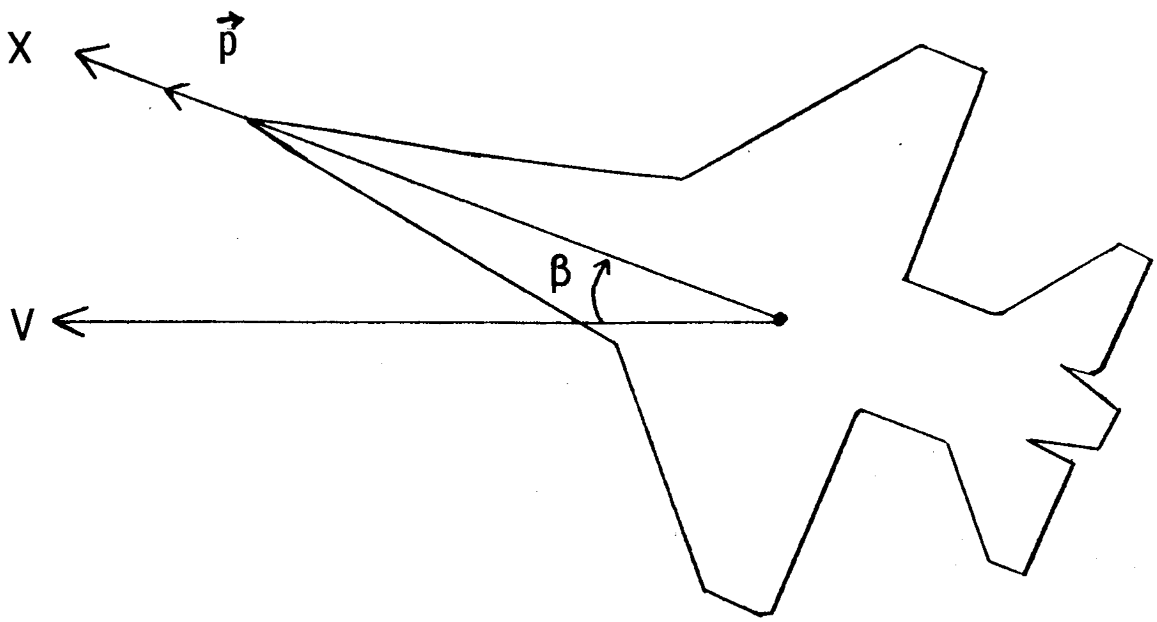

(b) $\phi = 90^{\circ}$.

Figure 16.- Illustration of kinematic coupling between angle of attack and sideslip.

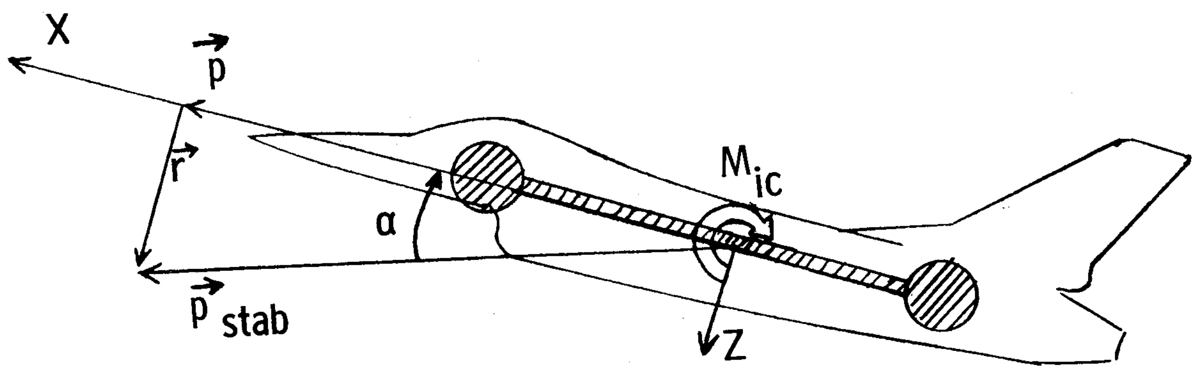

(a) Pitching moment created by roll and yaw rates.

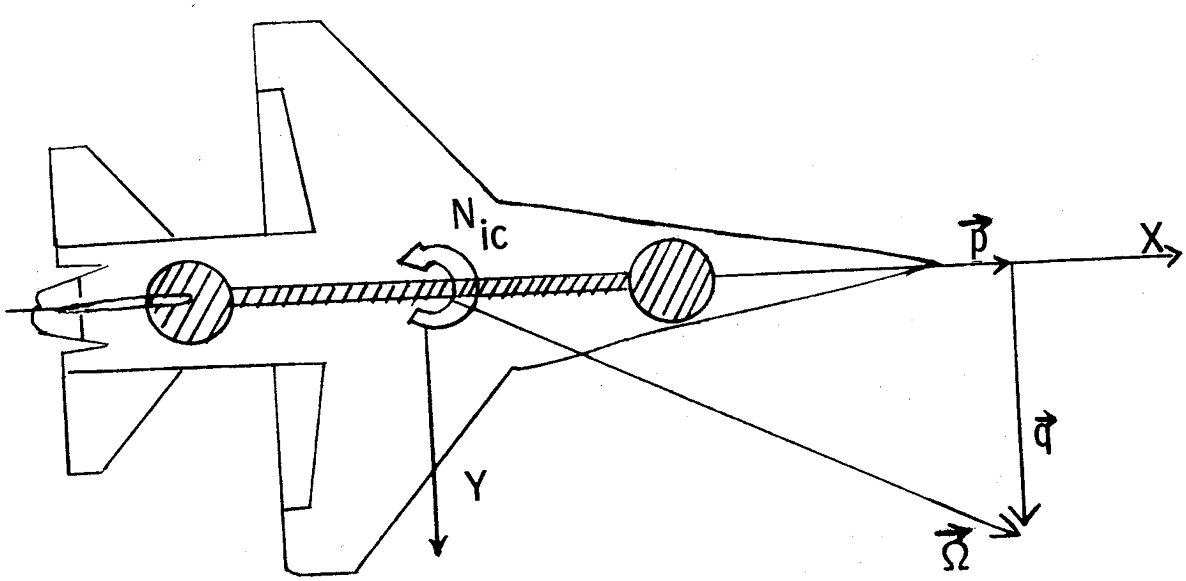

(b) Yawing moment created by roll and pitch rates.

Figure 17.- Illustration of inertia-coupling phenomena.

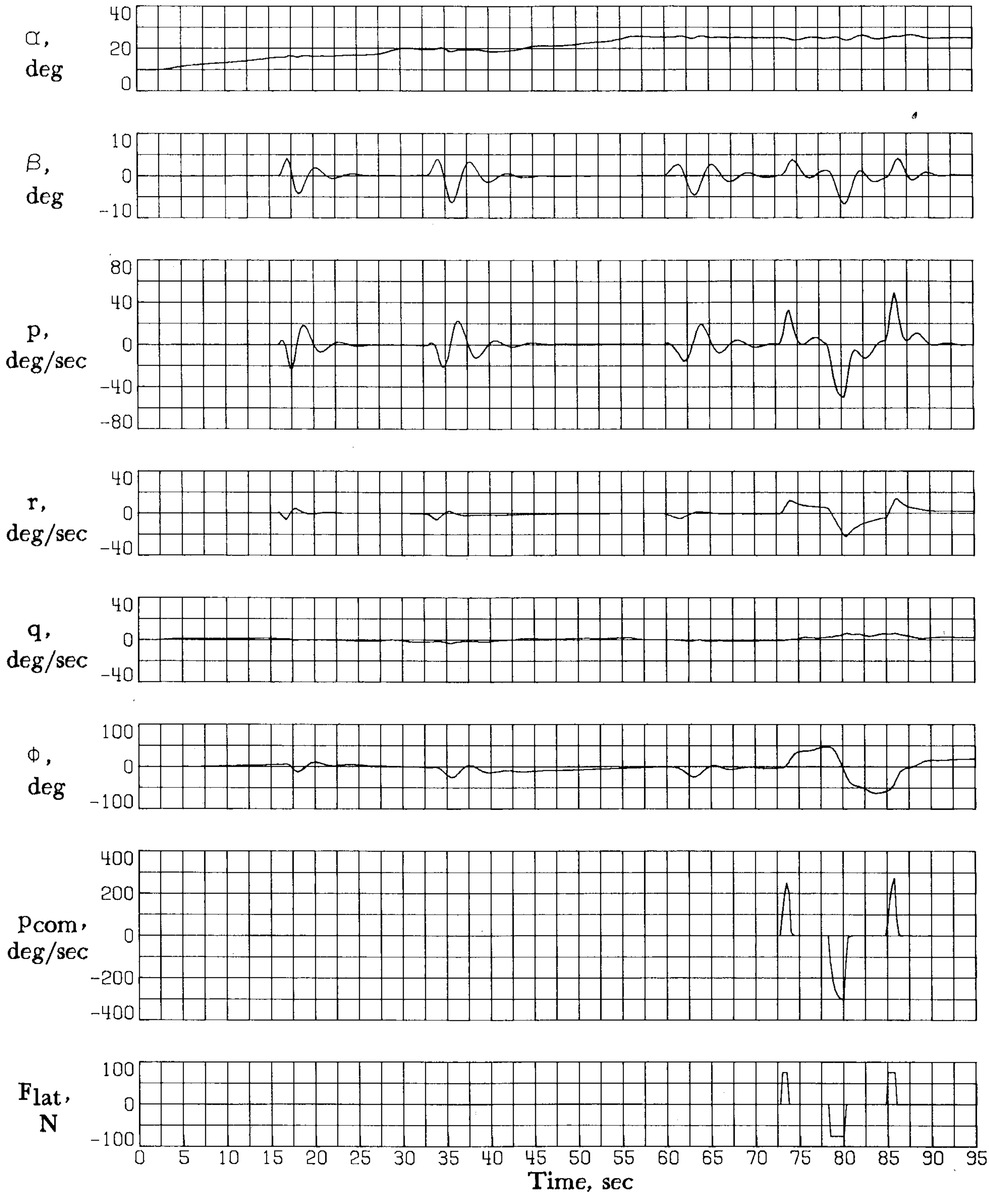

Figure 18.- Time histories of 1g stall to limit angle of attack. Control system A; h_o = 9144 m.

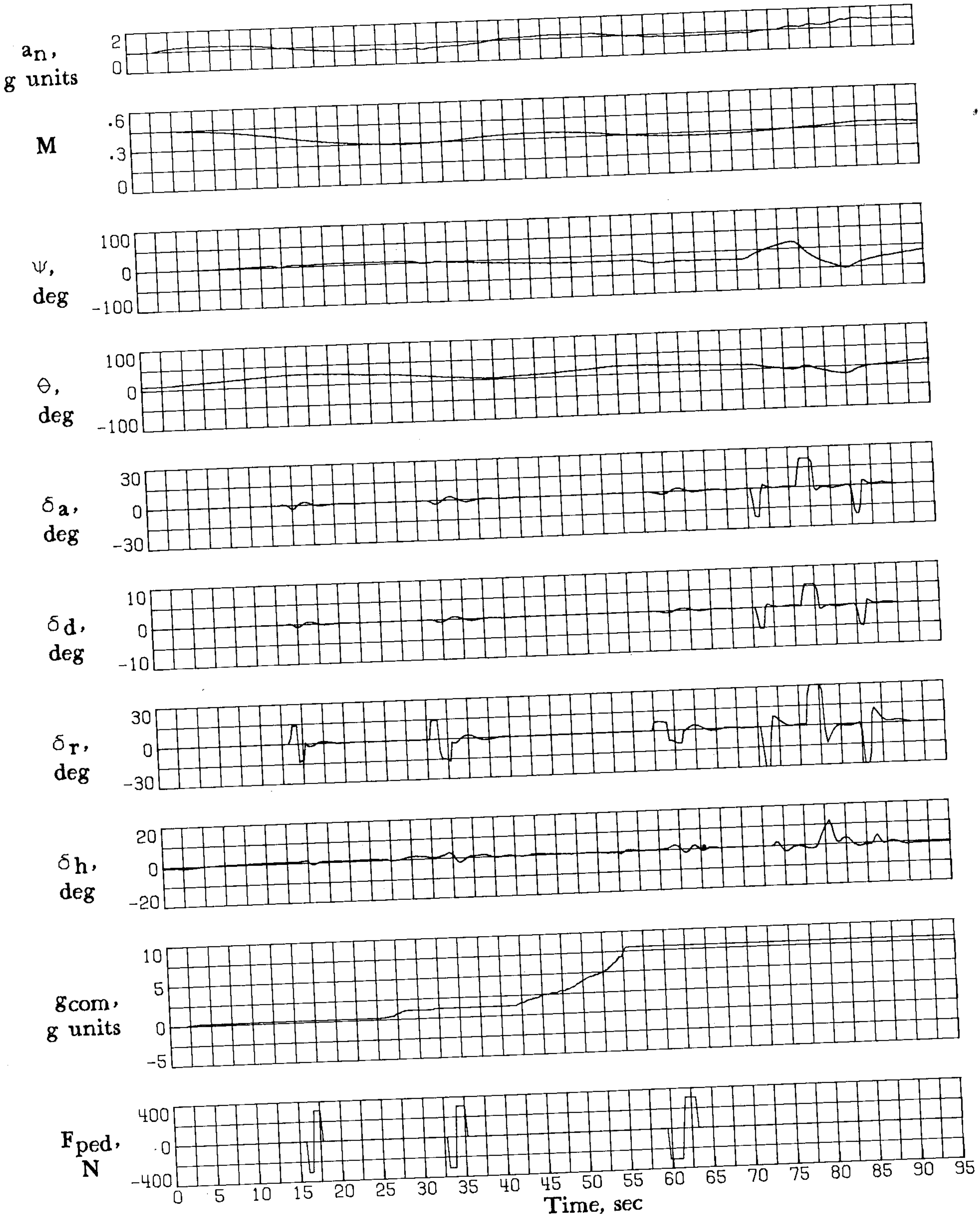

Figure 18.- Concluded.

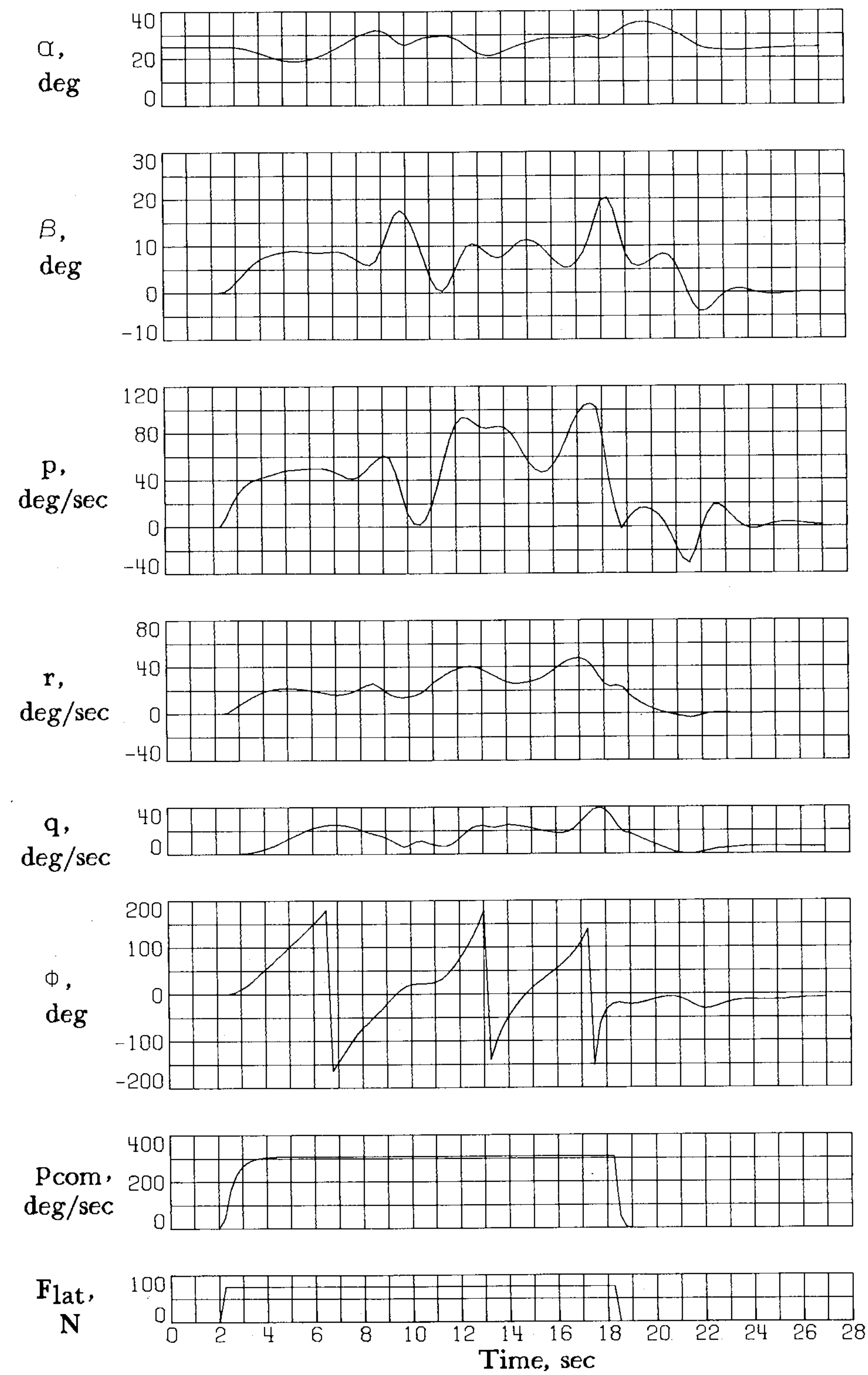

Figure 19.- Response to full cross-control input at $\alpha = 25^{\circ}$. Control system A; $h_o = 9144$ m.

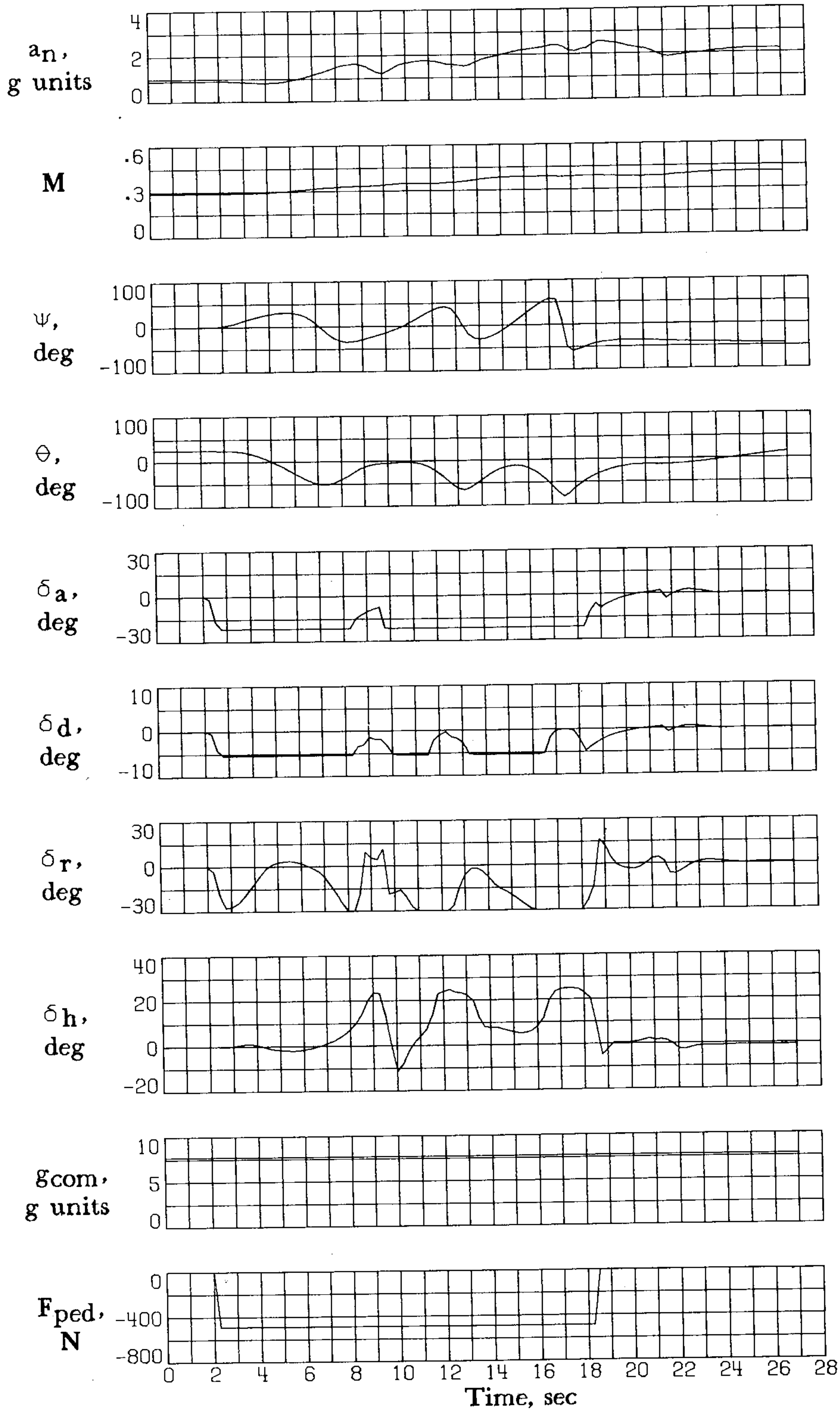

Figure 19.- Continued.

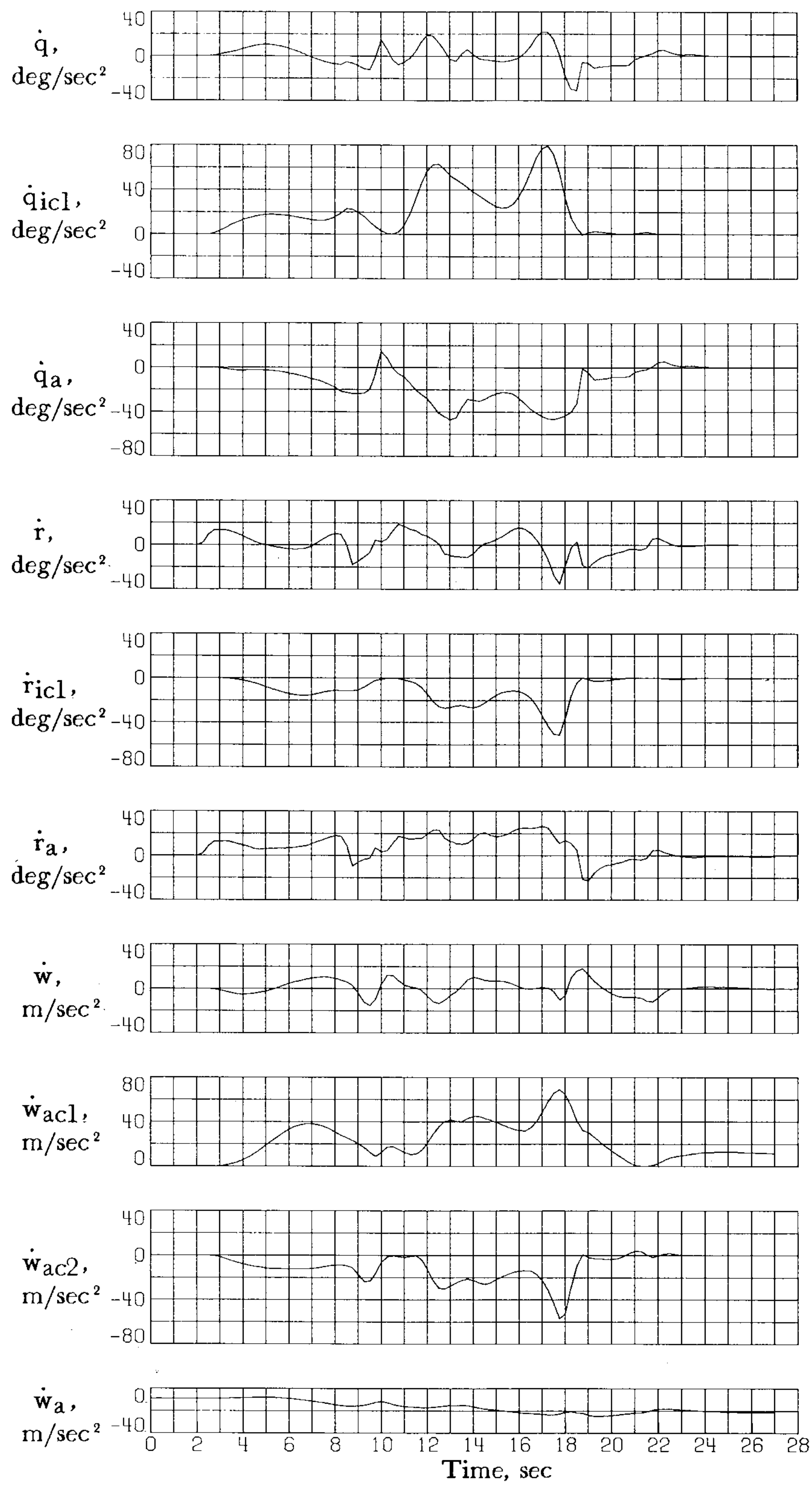

Figure 19.- Concluded.

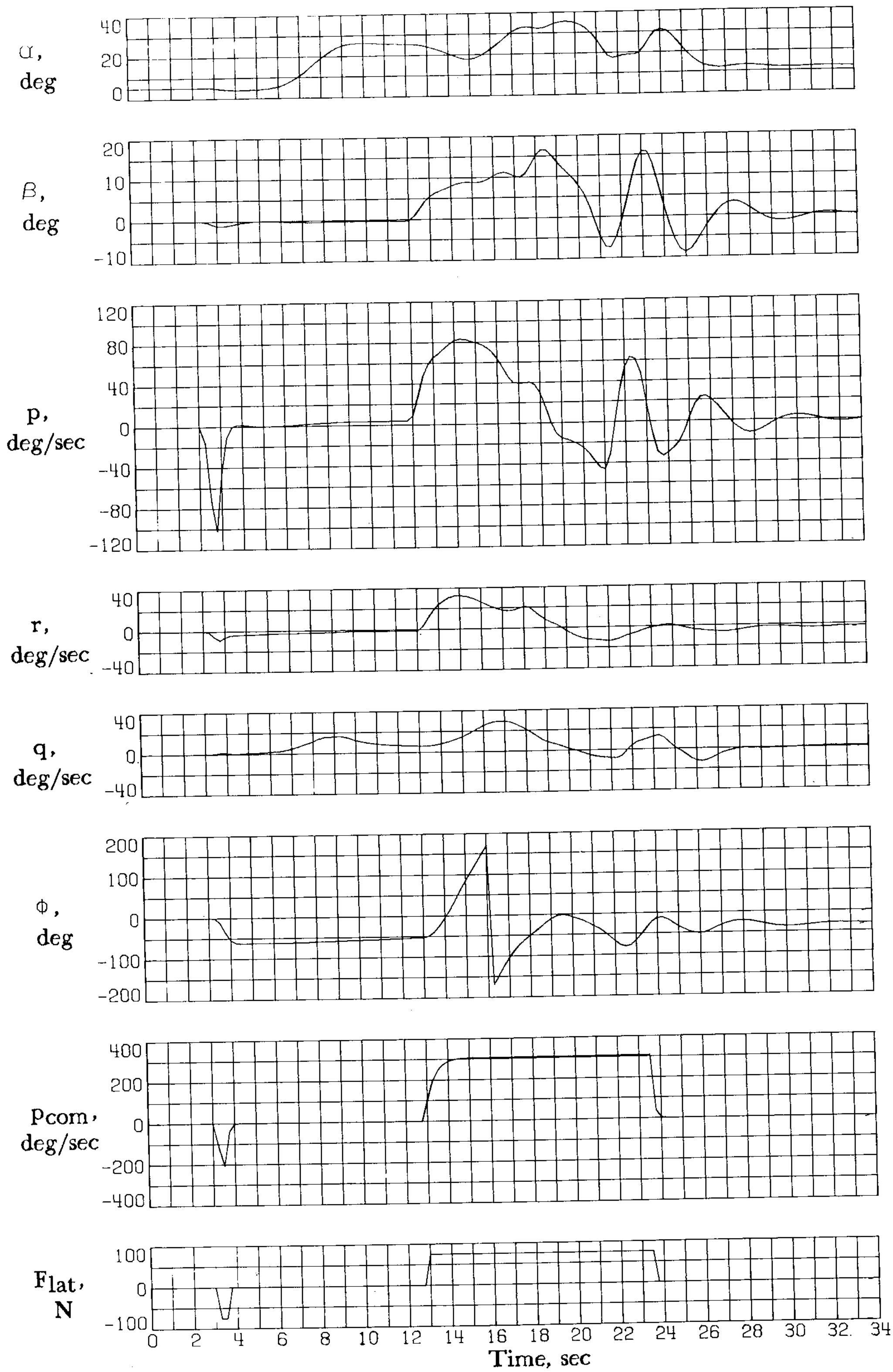

Figure 20.- Response to cross controls applied in accelerated turn at limit angle of attack. Control system A; h_o = 9144 m.

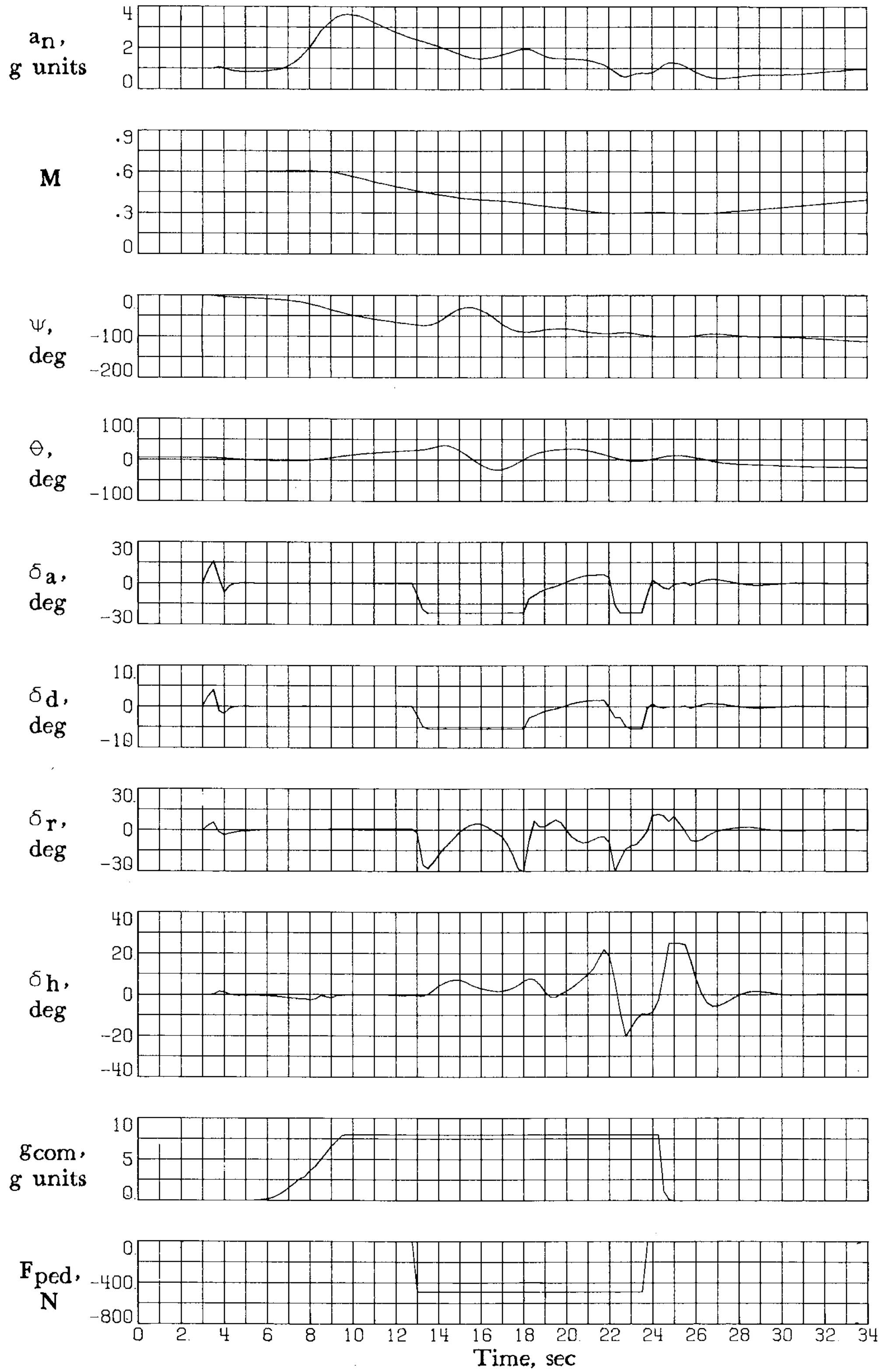

Figure 20.- Continued.

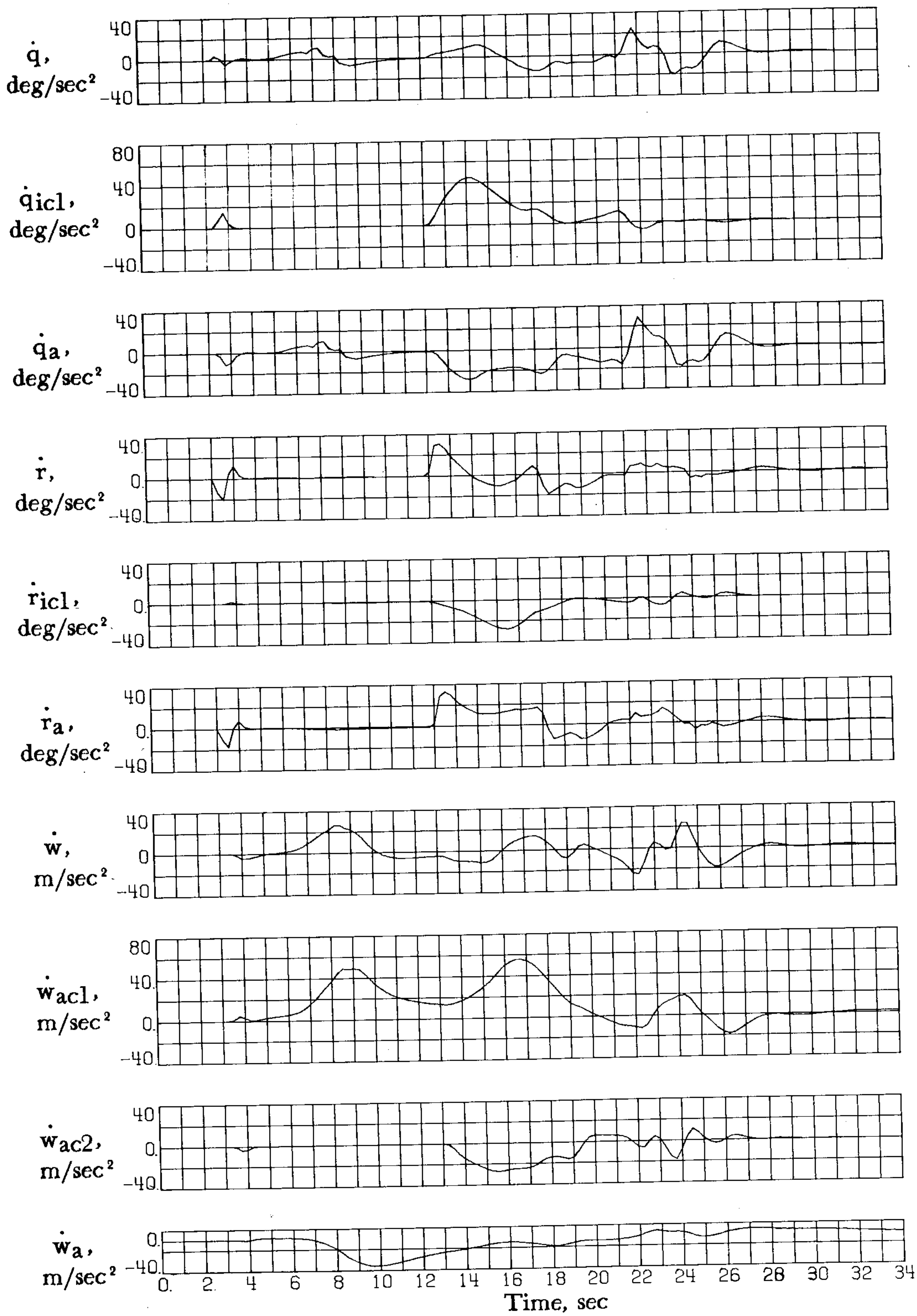

Figure 20.- Concluded.

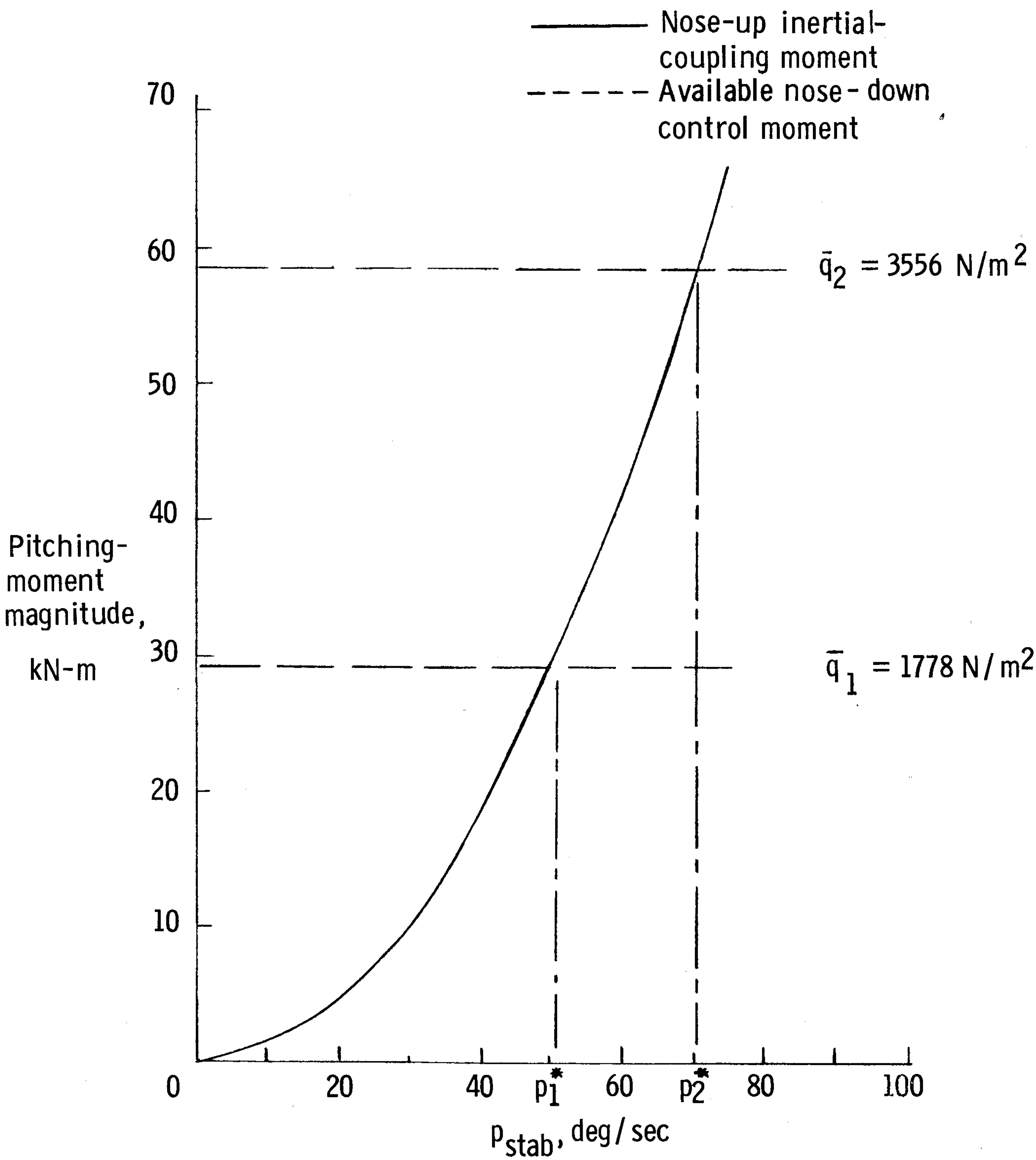

Figure 21.- Comparison of inertial-coupling moment for increasing roll rate with available pitch control moment at two values of dynamic pressure. $\alpha = 25^o$.

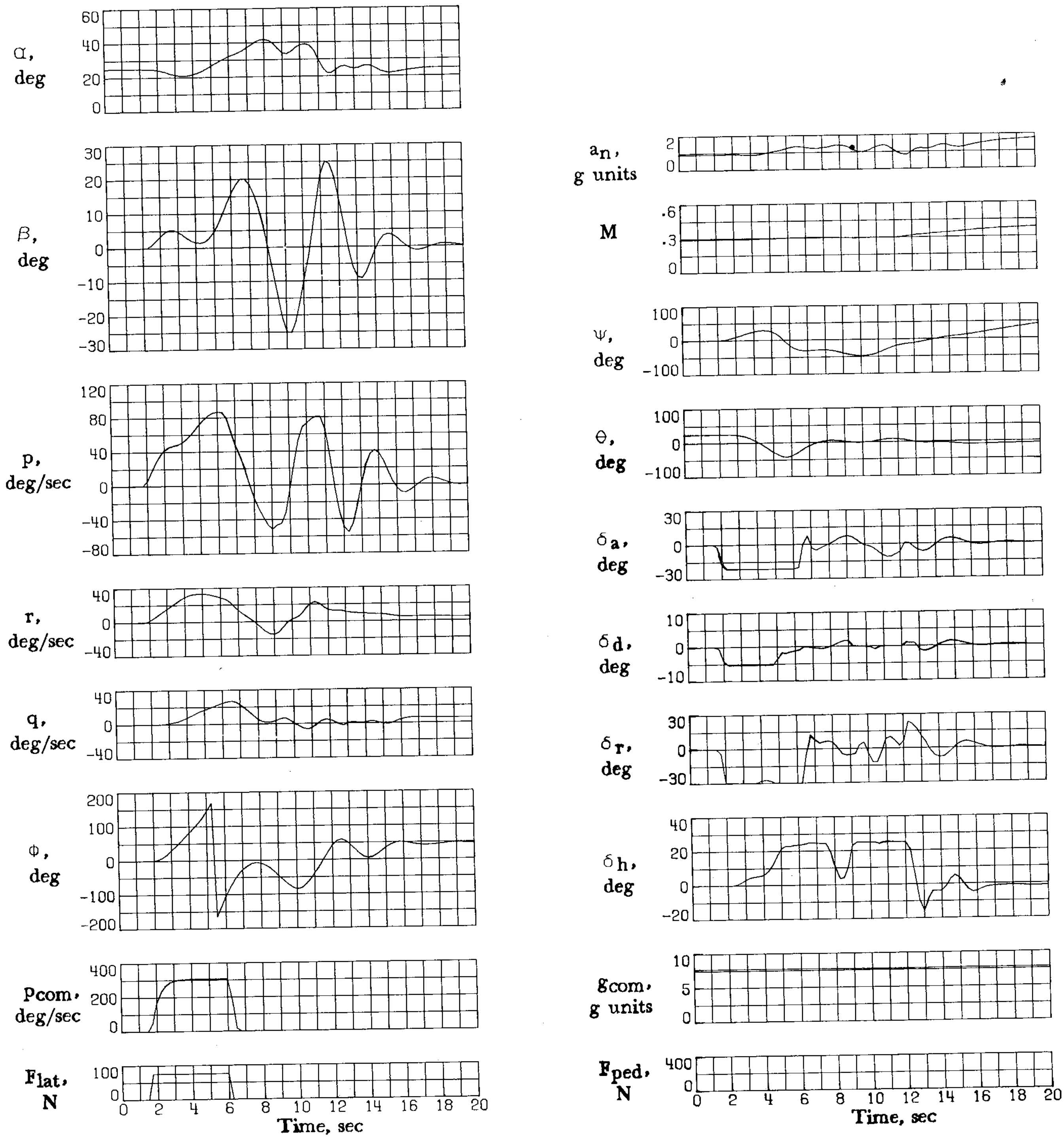

Figure 22.- A 360° roll attempt using full lateral stick input applied from 1g flight at $\alpha = 25^{\circ}$. Control system A; $h_o = 9144$ m.

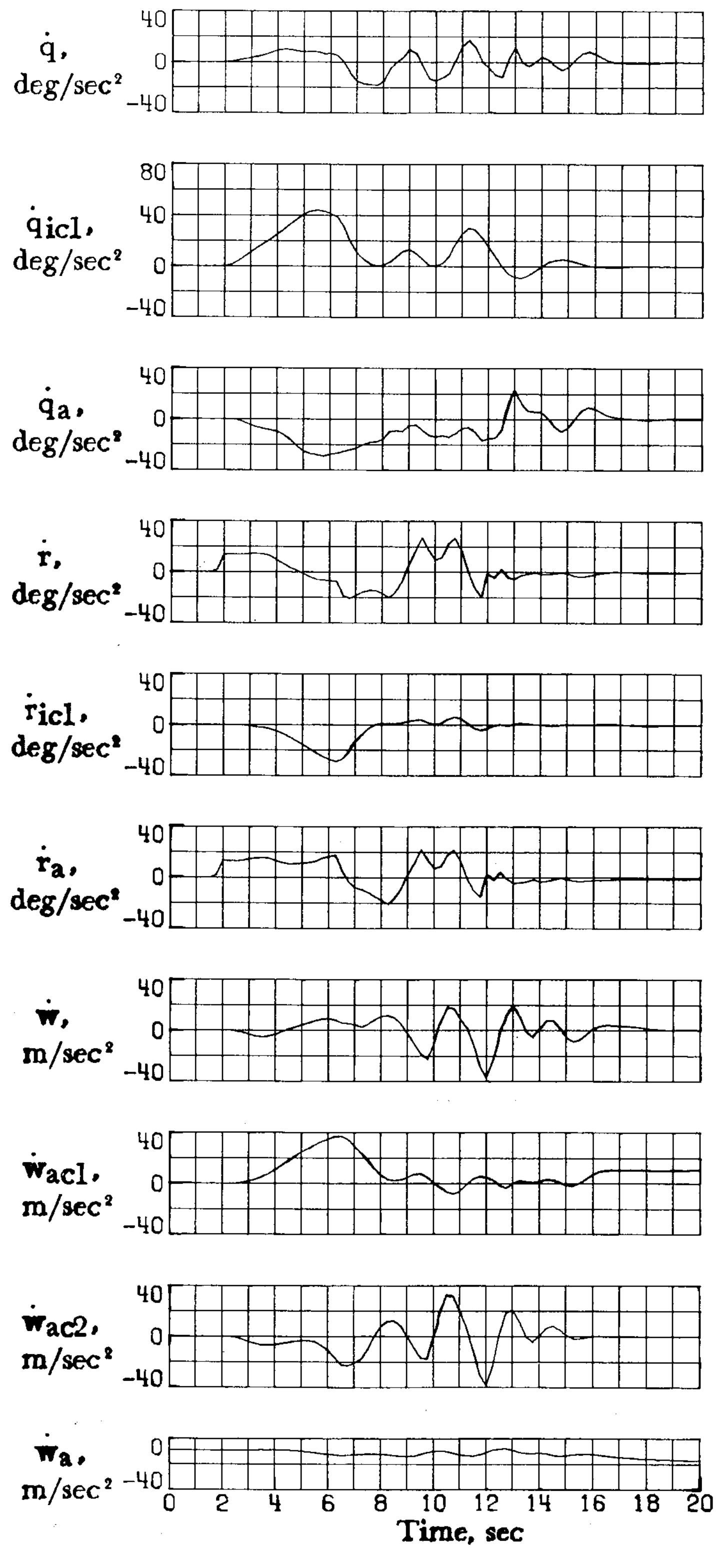

Figure 22.- Concluded.

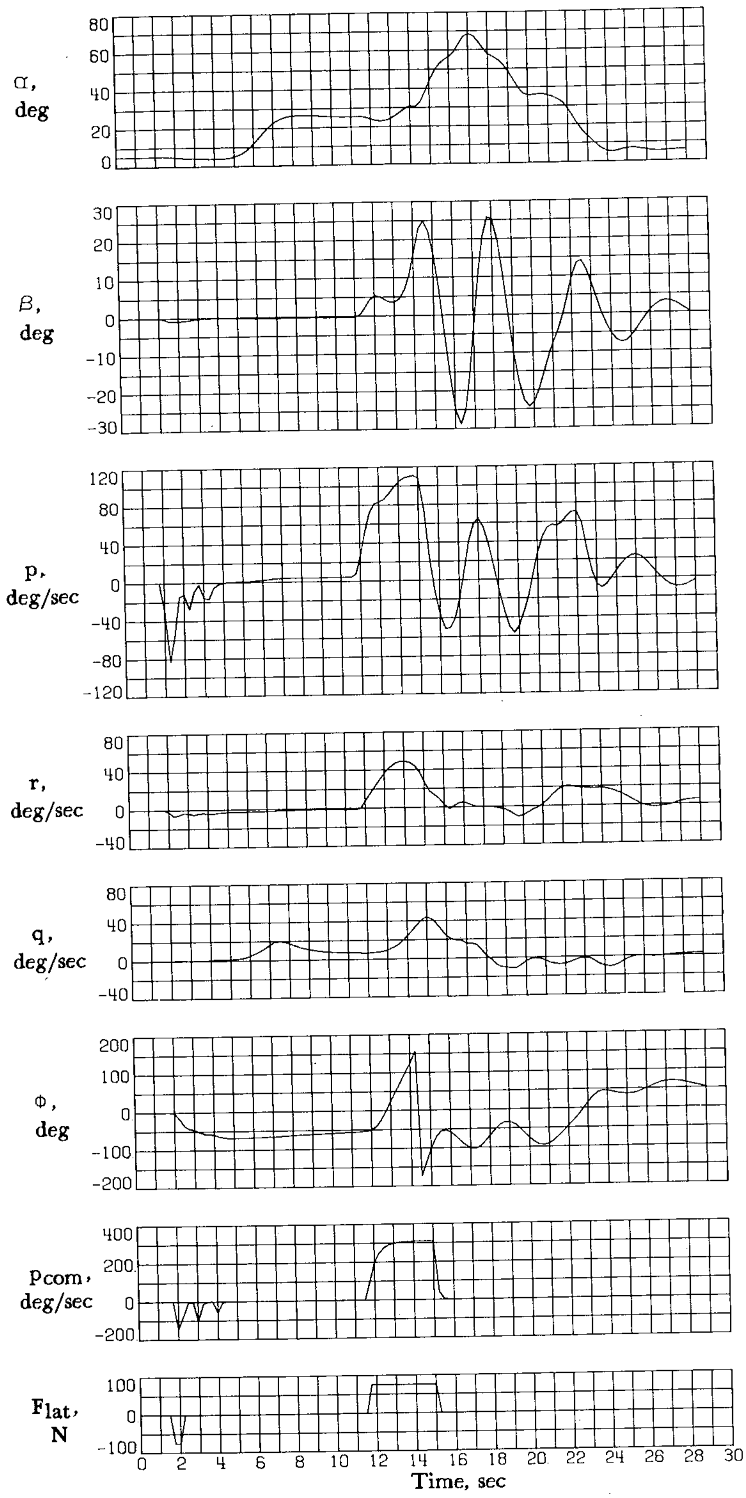

Figure 23.- A 360° roll attempt using full lateral stick input applied in an accelerated turn at limit α. Control system A; h_o = 9144 m.

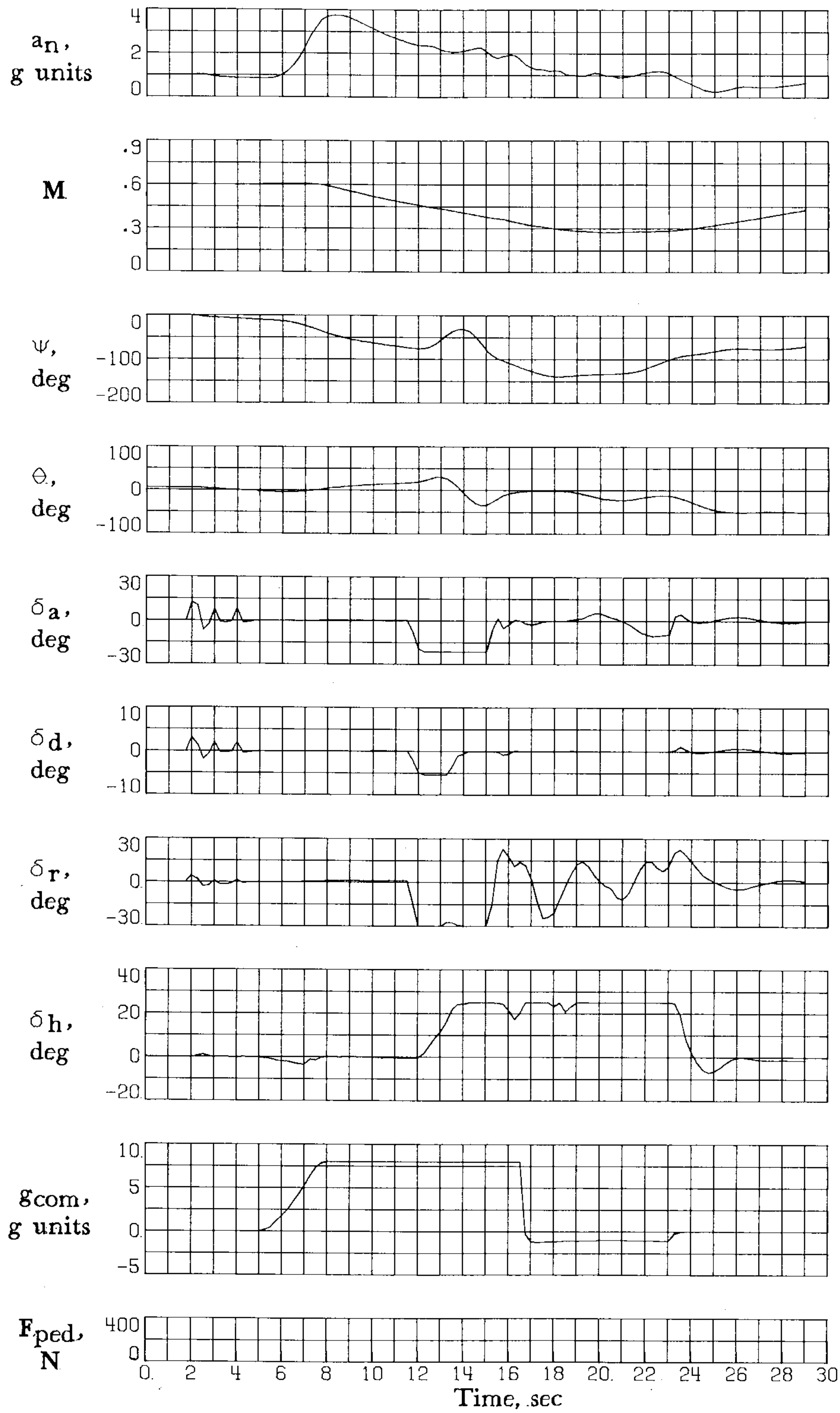

Figure 23.- Concluded.

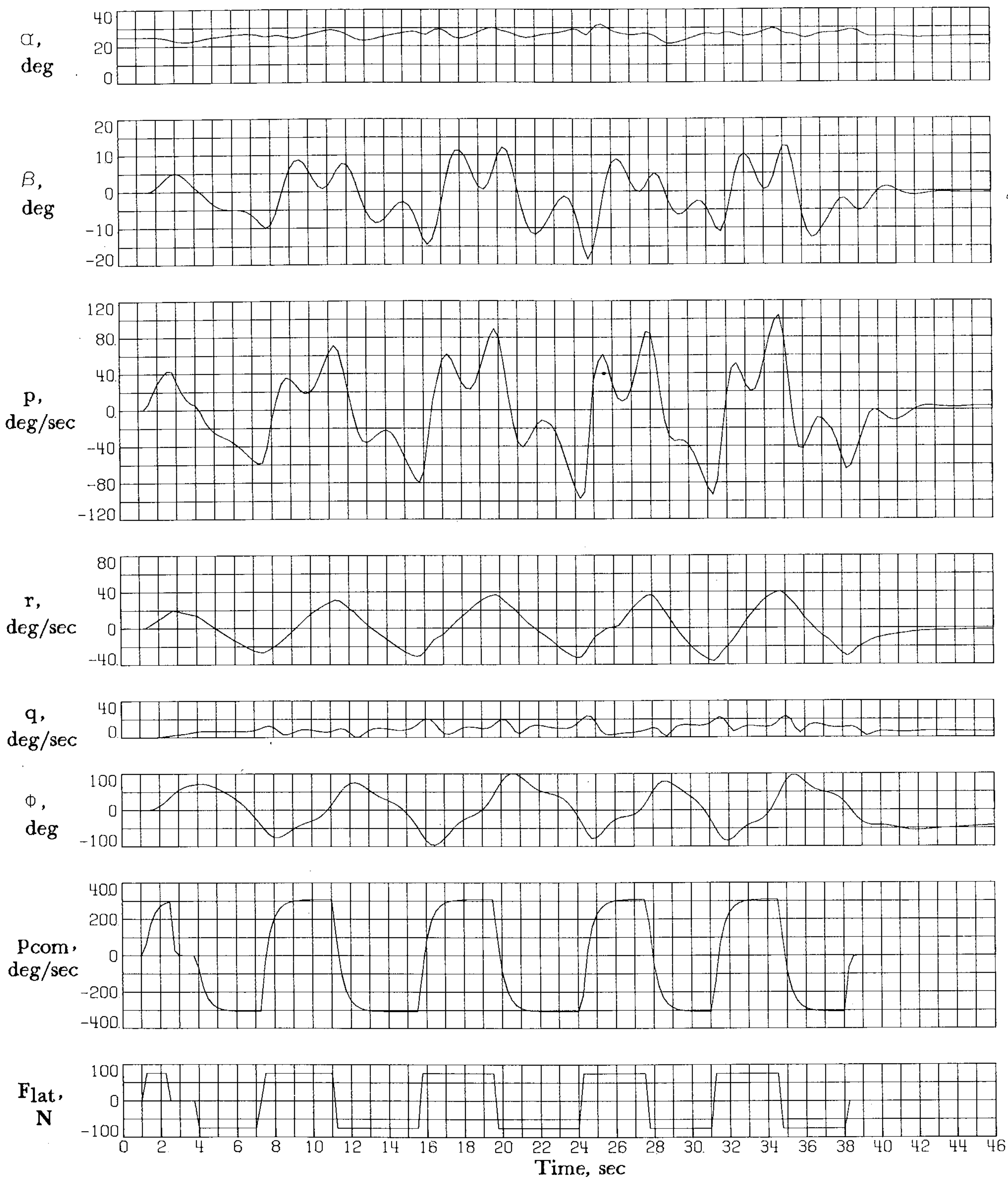

Figure 24.- Bank-to-bank reversals using maximum lateral stick inputs applied from 1g flight at $\alpha = 25^{\circ}$. Control system A; $h_o = 9144$ m.

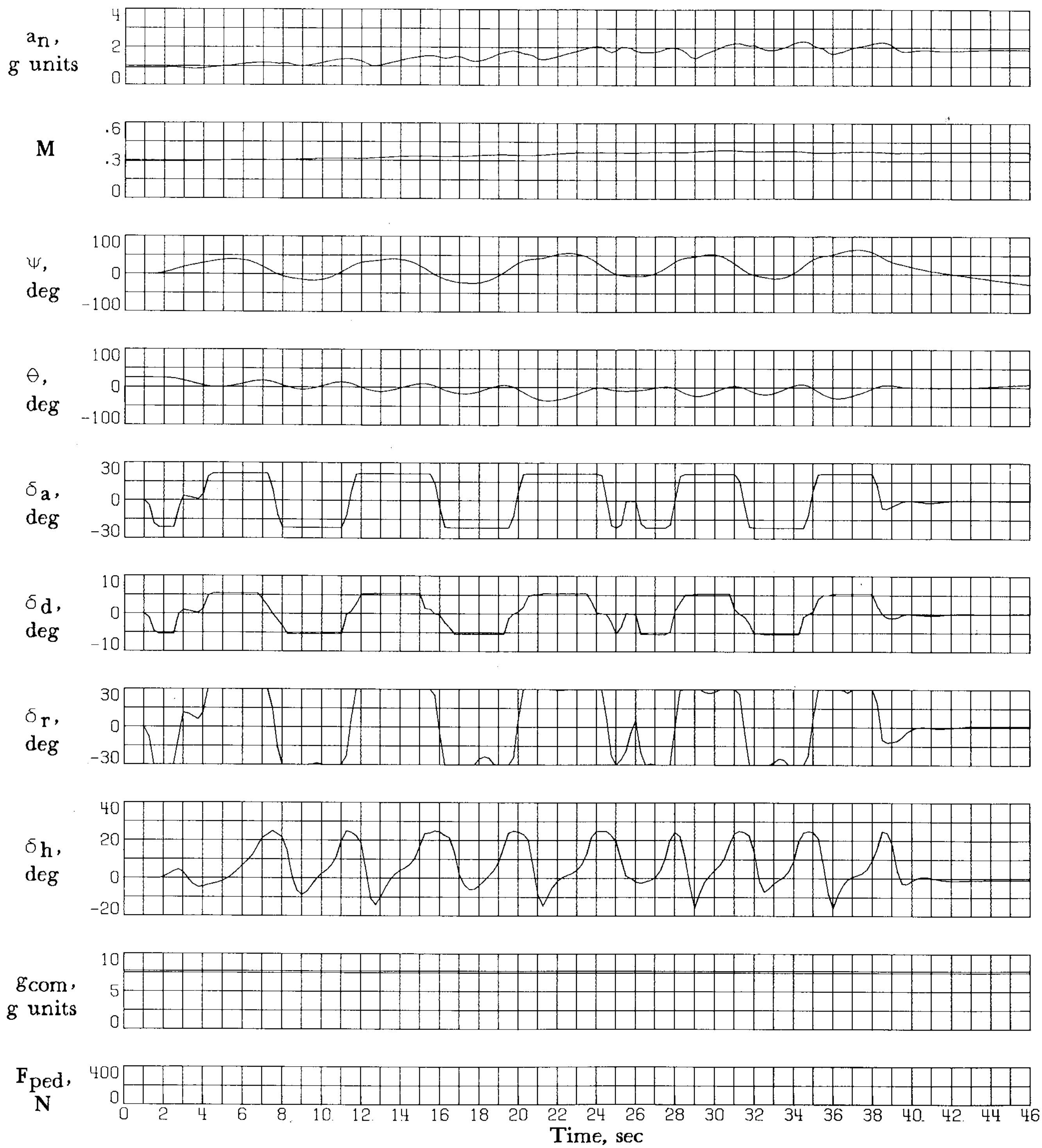

Figure 24.- Continued.

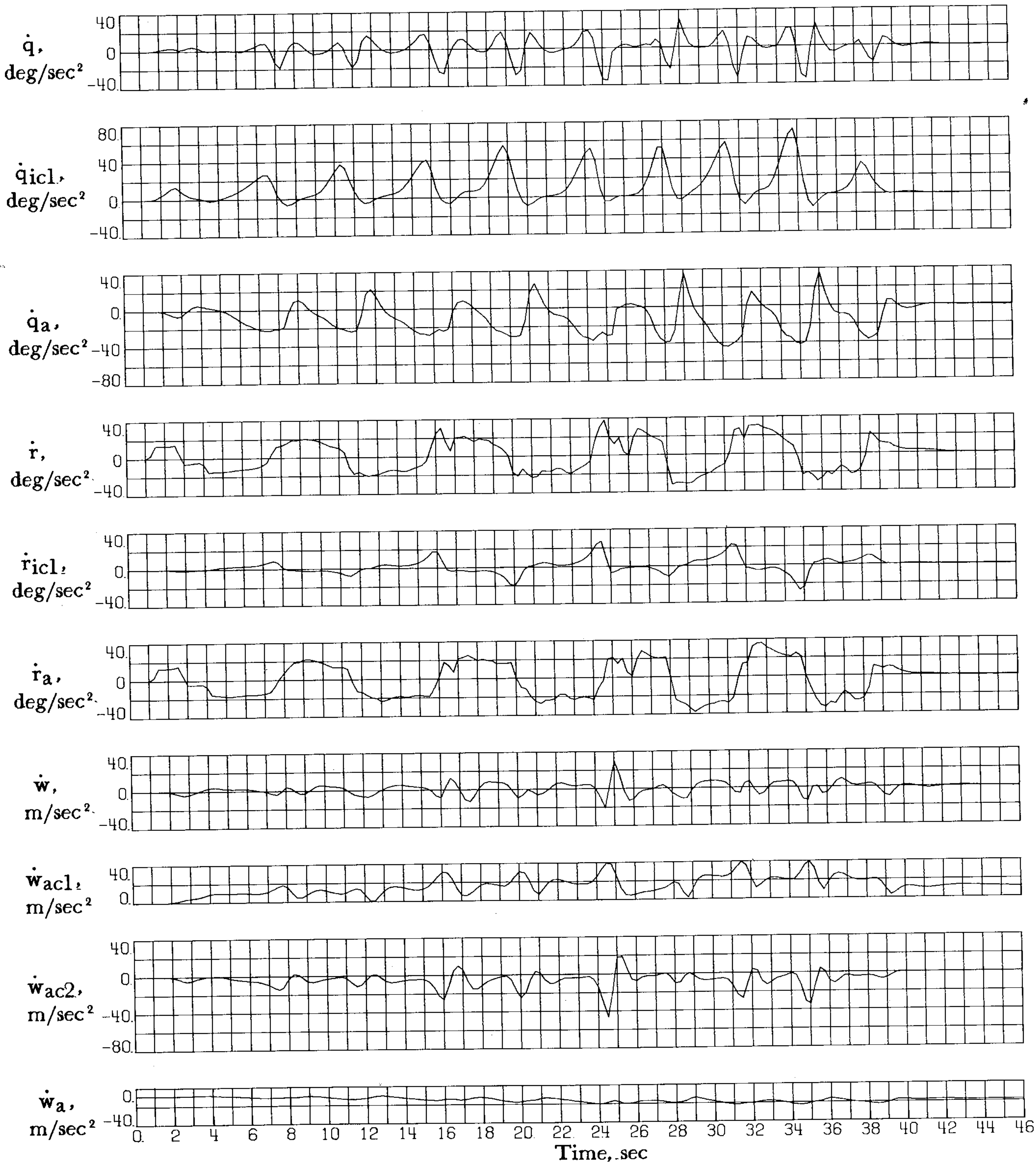

Figure 24.- Concluded.

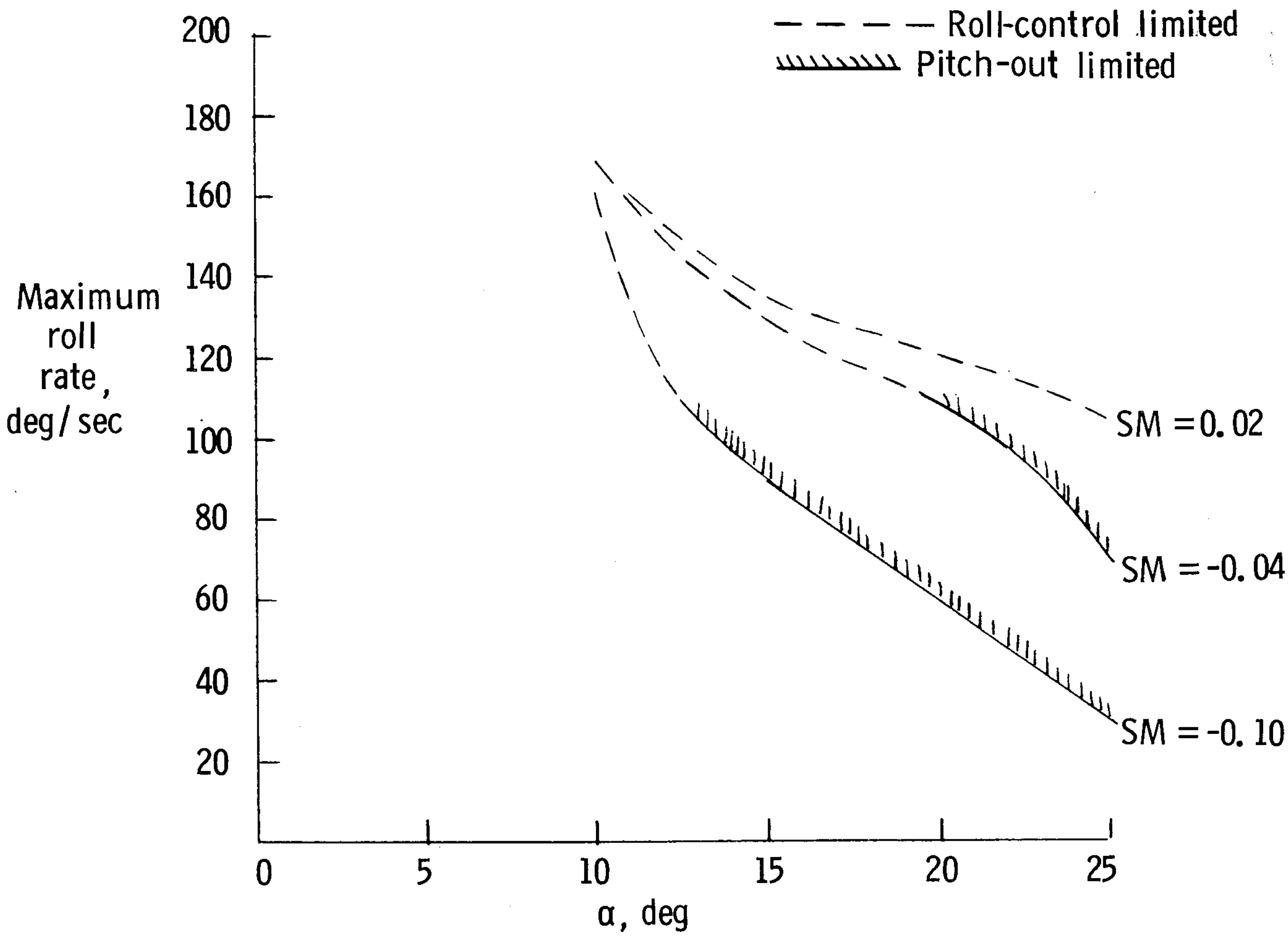

Figure 25.- Variation of maximum roll rate with α for various levels of static margin. 1g flight; 360° roll; h_o = 9144 m.

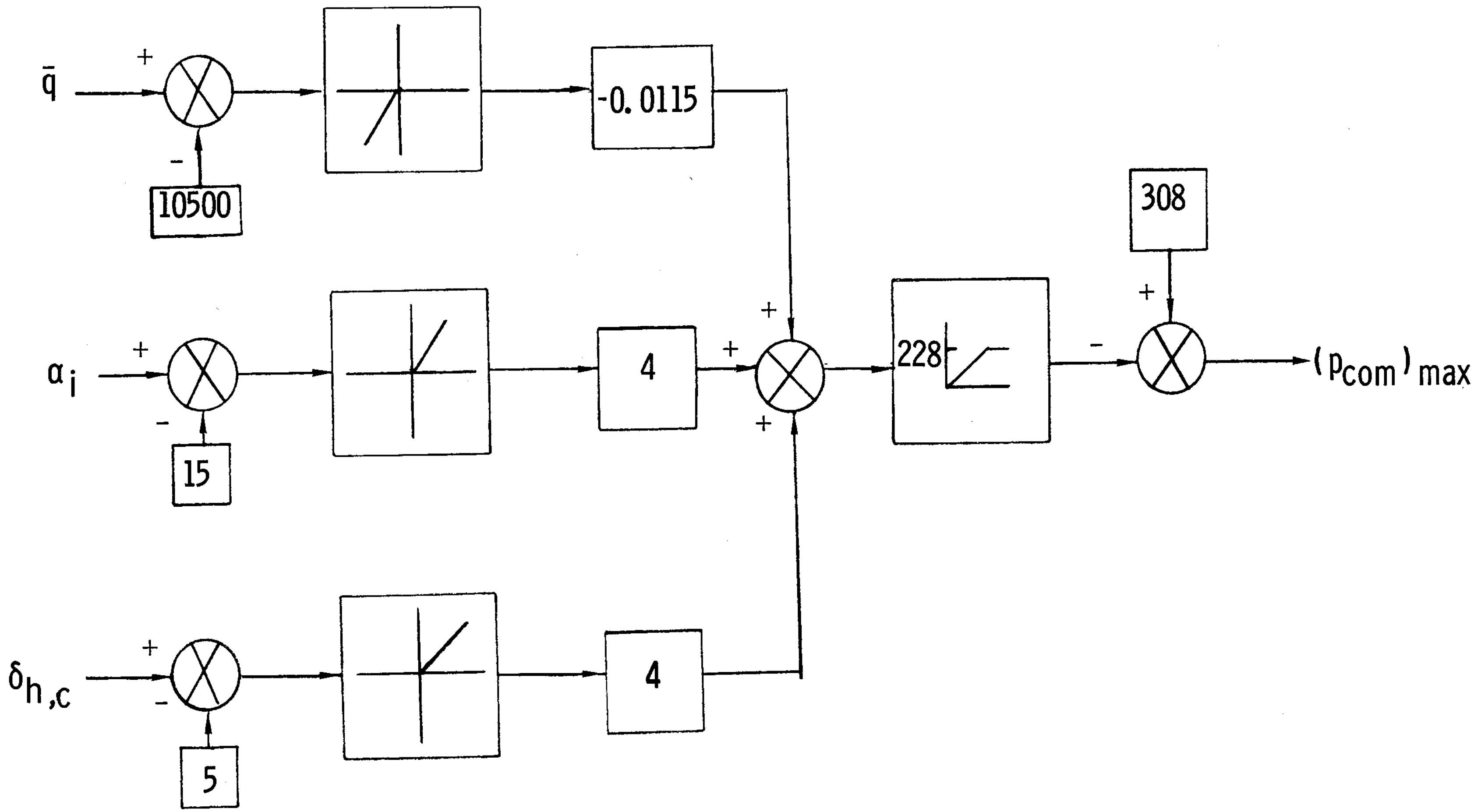

Figure 26.- Roll-rate limiting scheme used in control system B.

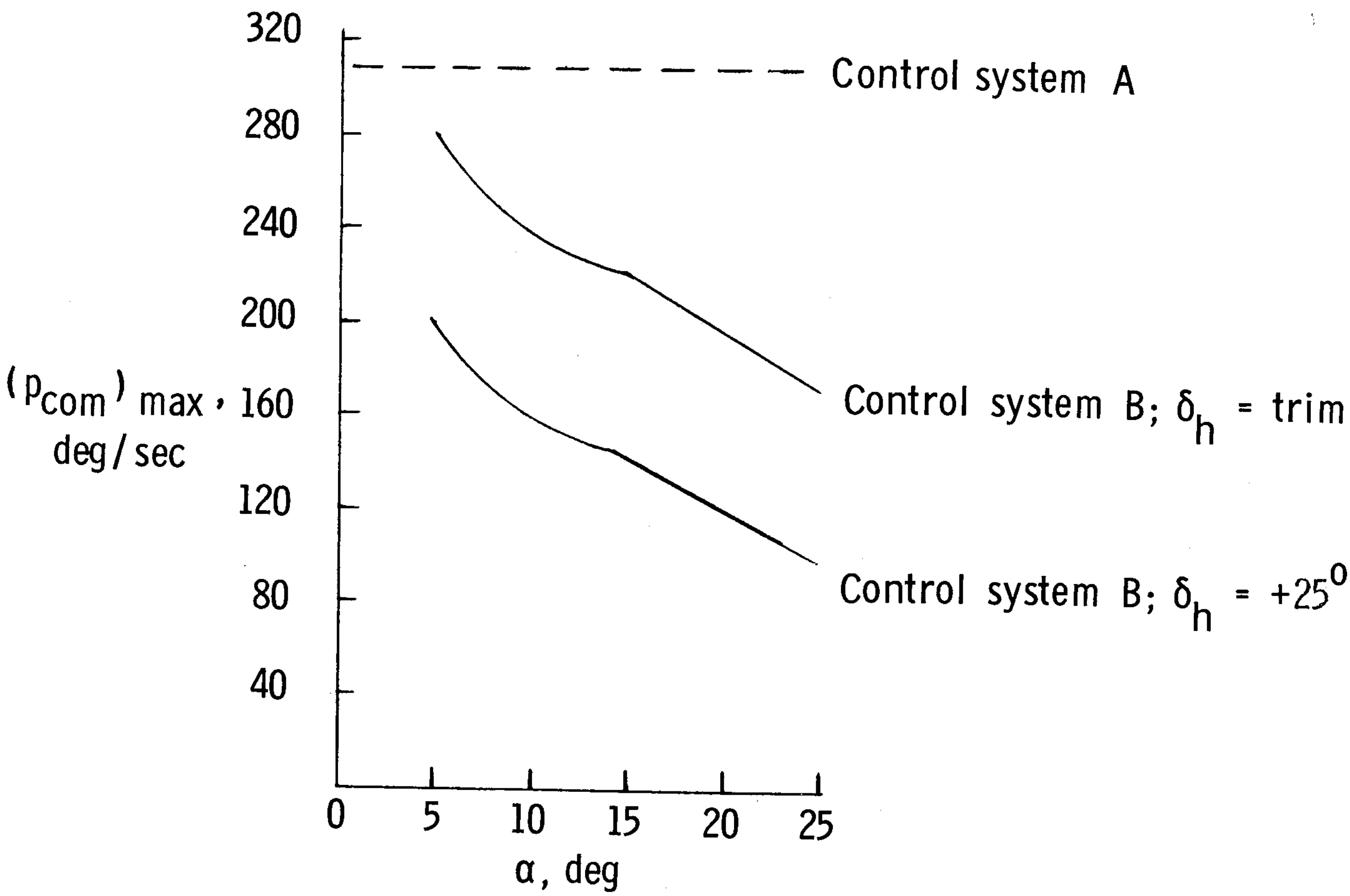

Figure 27.- Variation of maximum commandable roll rate with α for 1g trim.

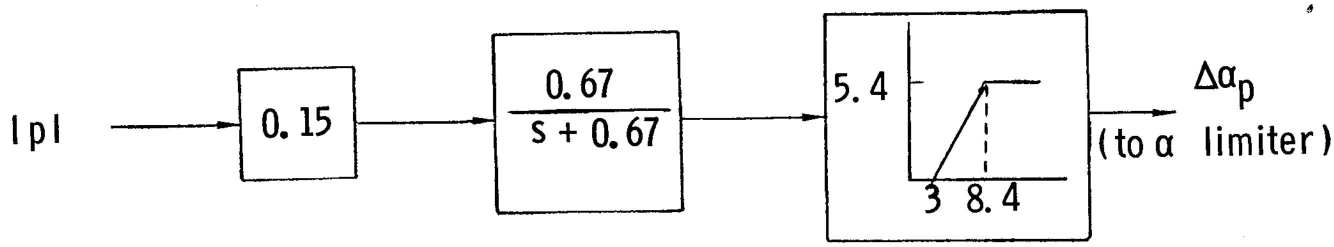

Figure 28.- Pitch-axis modification used in control system B.

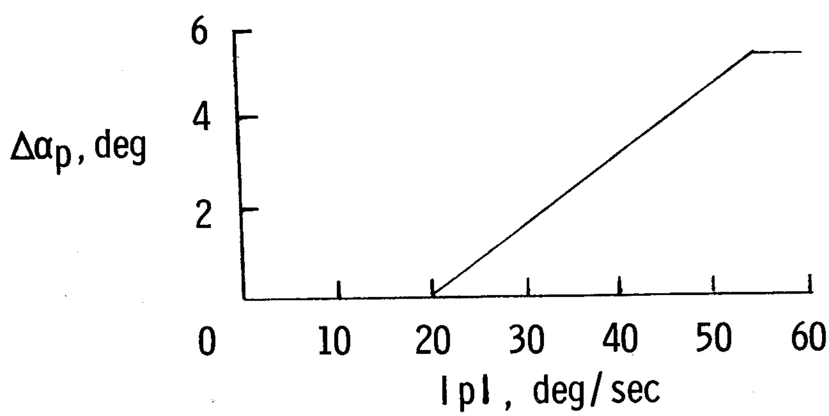

Figure 29.- Variation of $\Delta\alpha_p$ with roll-rate magnitude for control system B.

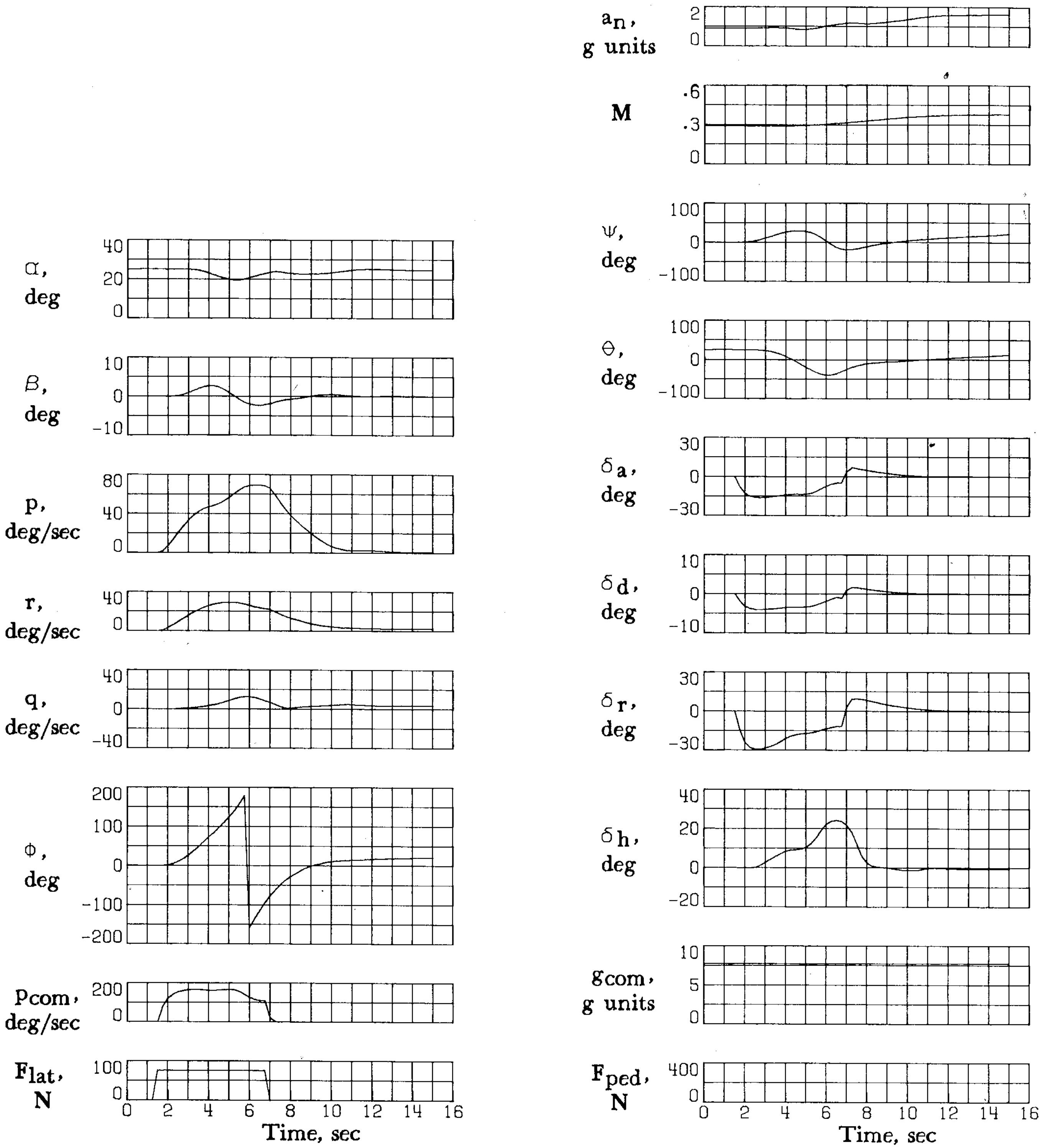

Figure 30.- A 360° roll initiated from 1g trim at $\alpha = 25^\circ$ using maximum lateral stick input. Control system B; $h_o = 9144$ m.

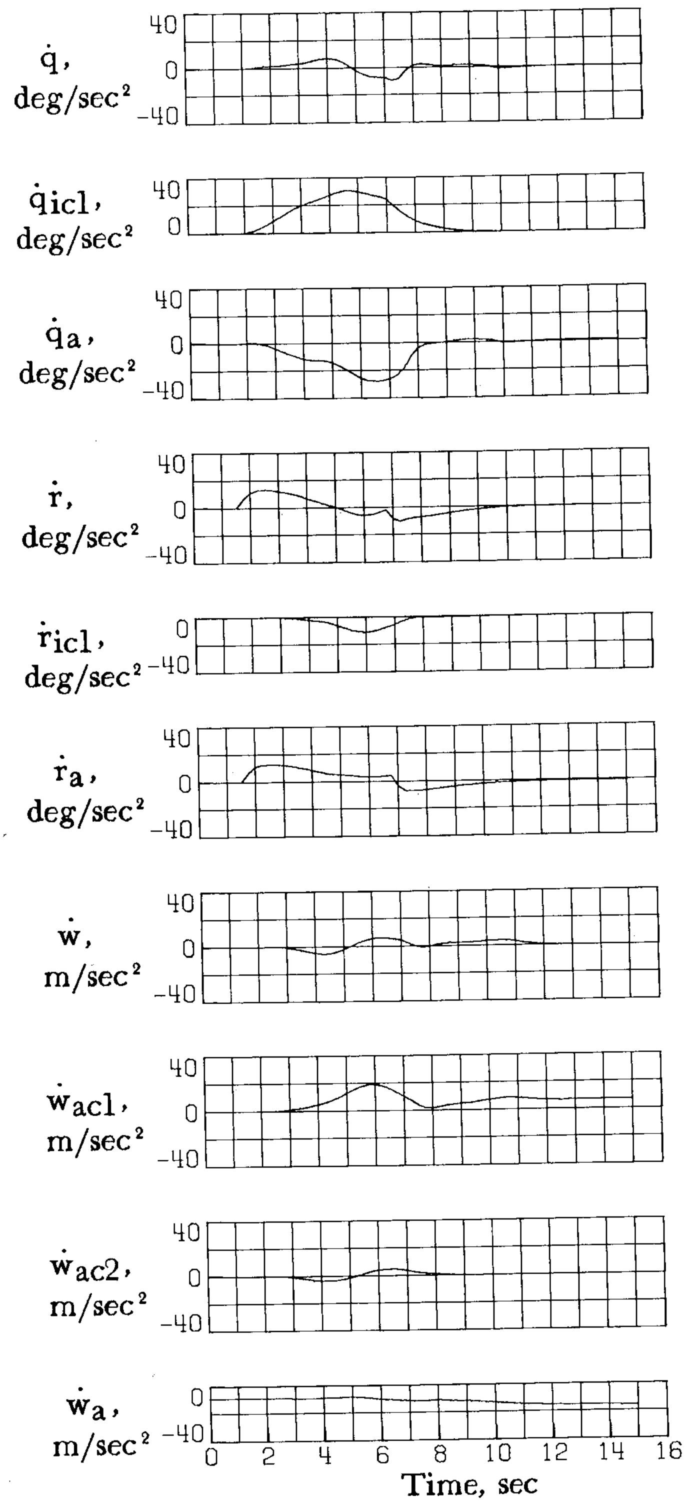

Figure 30.- Concluded.

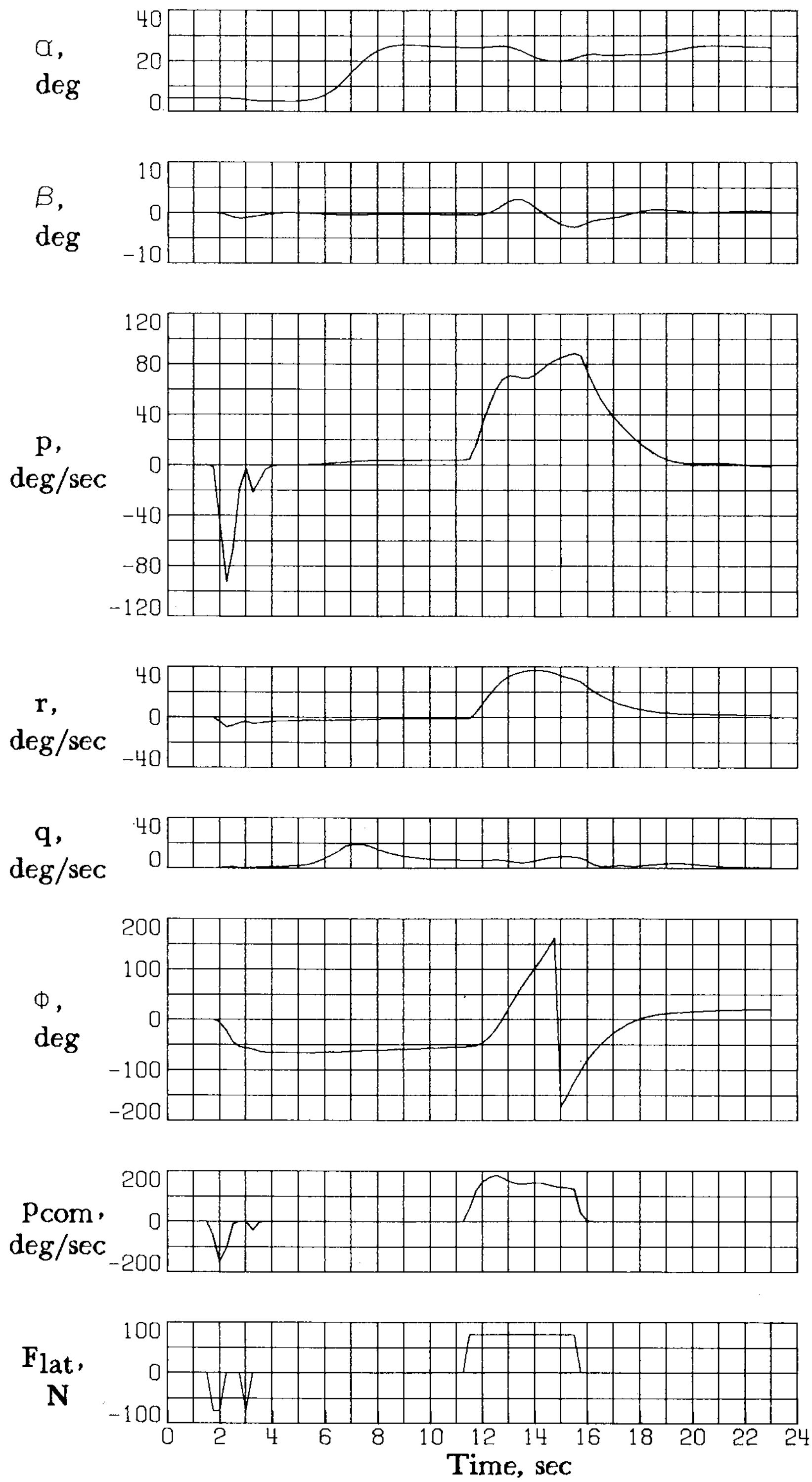

Figure 31.- A 360° roll initiated from accelerated turn at limit α using full lateral stick input. Control system B; h_o = 9144 m.

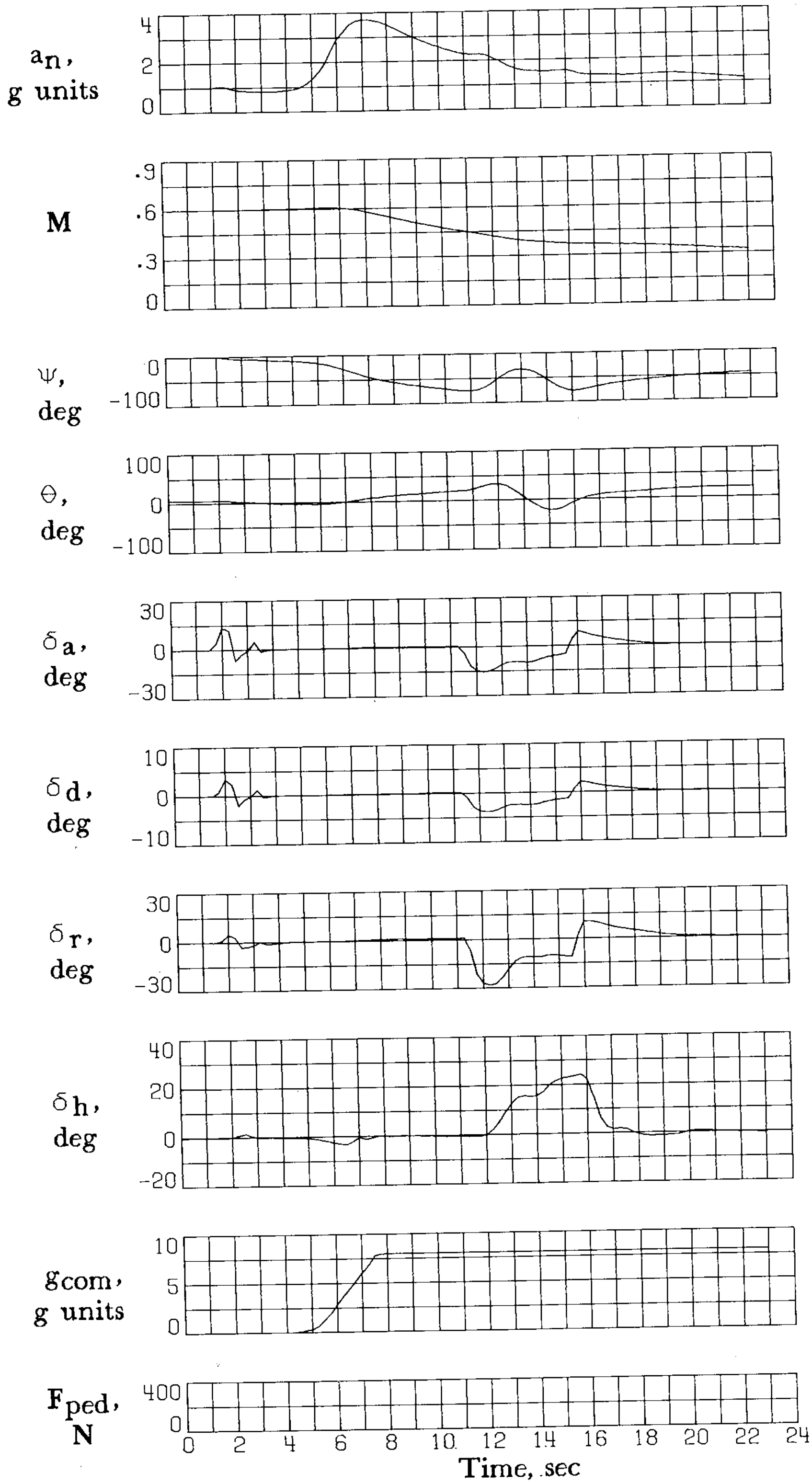

Figure 31.- Continued.

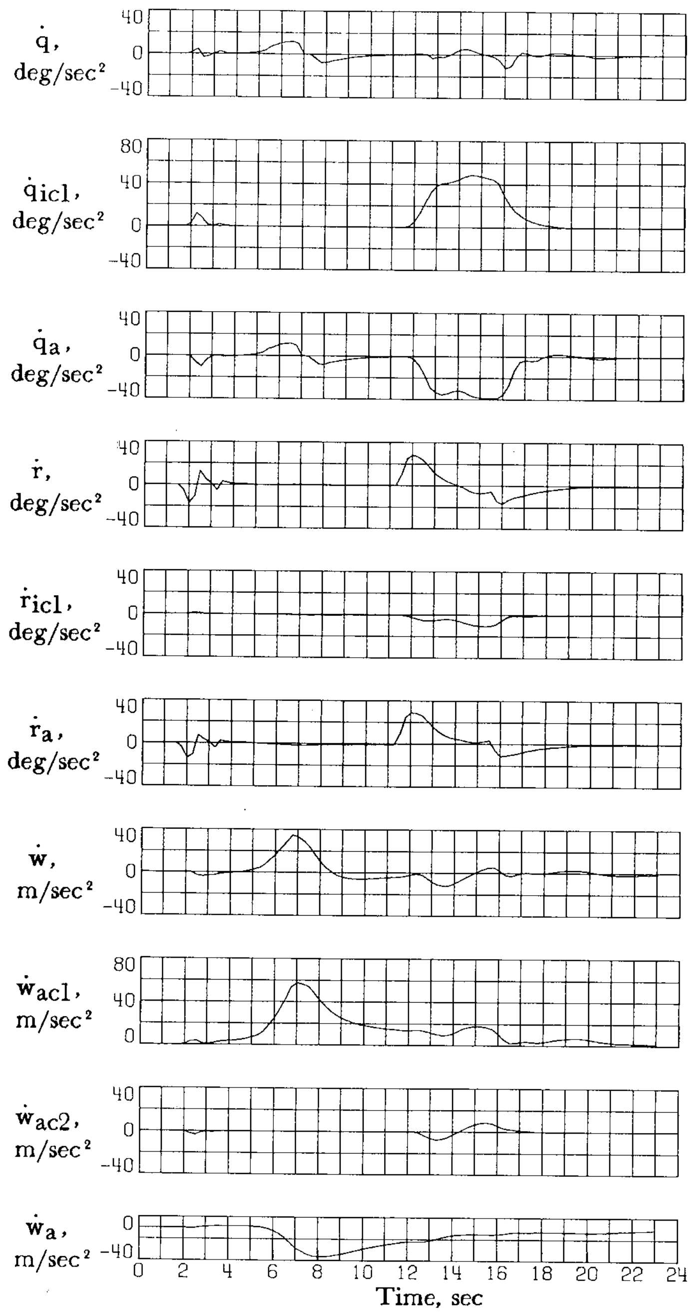

Figure 31.- Concluded.

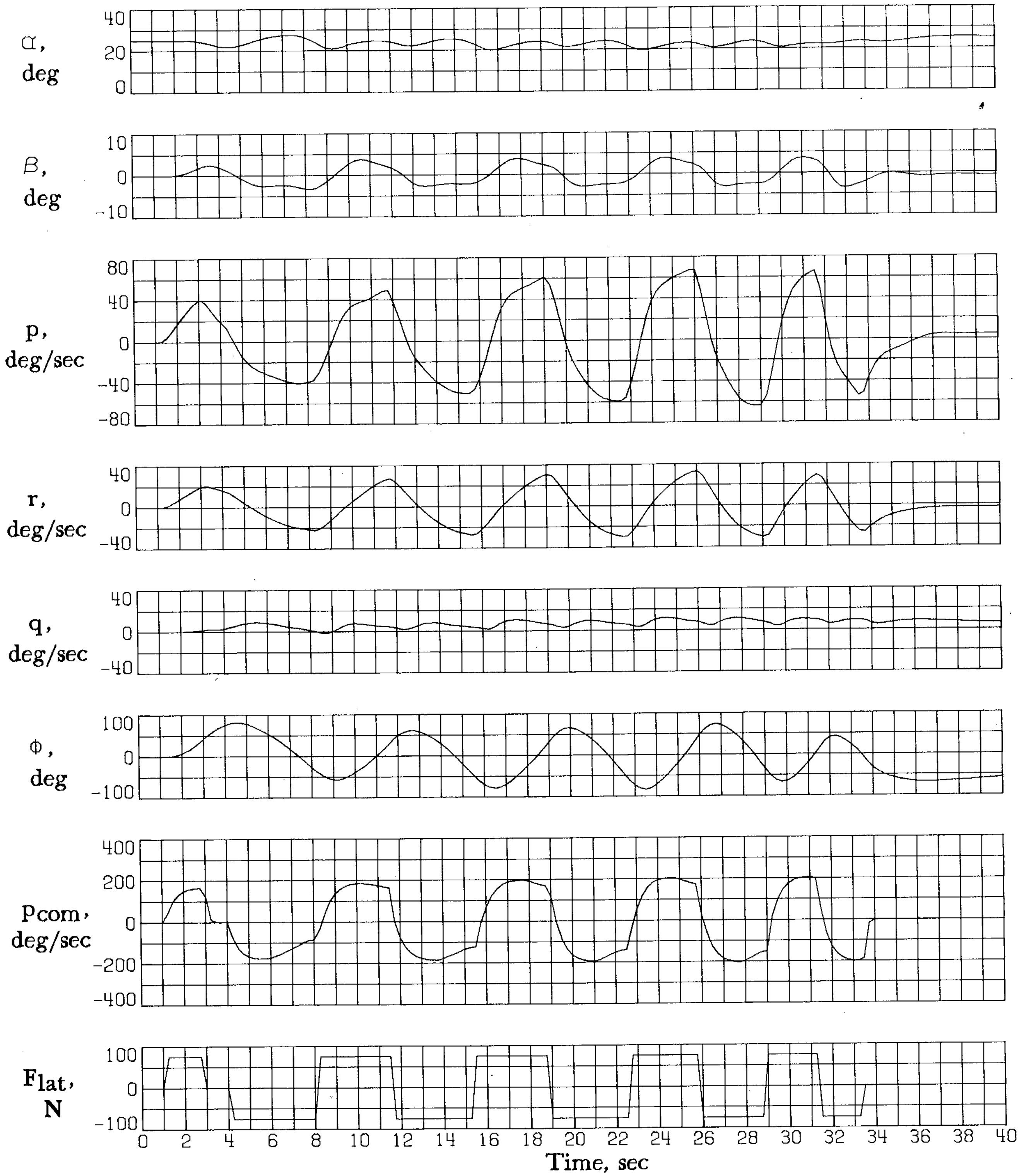

Figure 32.- Bank-to-bank reversals using full lateral stick inputs initiated from 1g trim at $\alpha = 25^{\circ}$. Control system B; $h_o = 9144$ m.

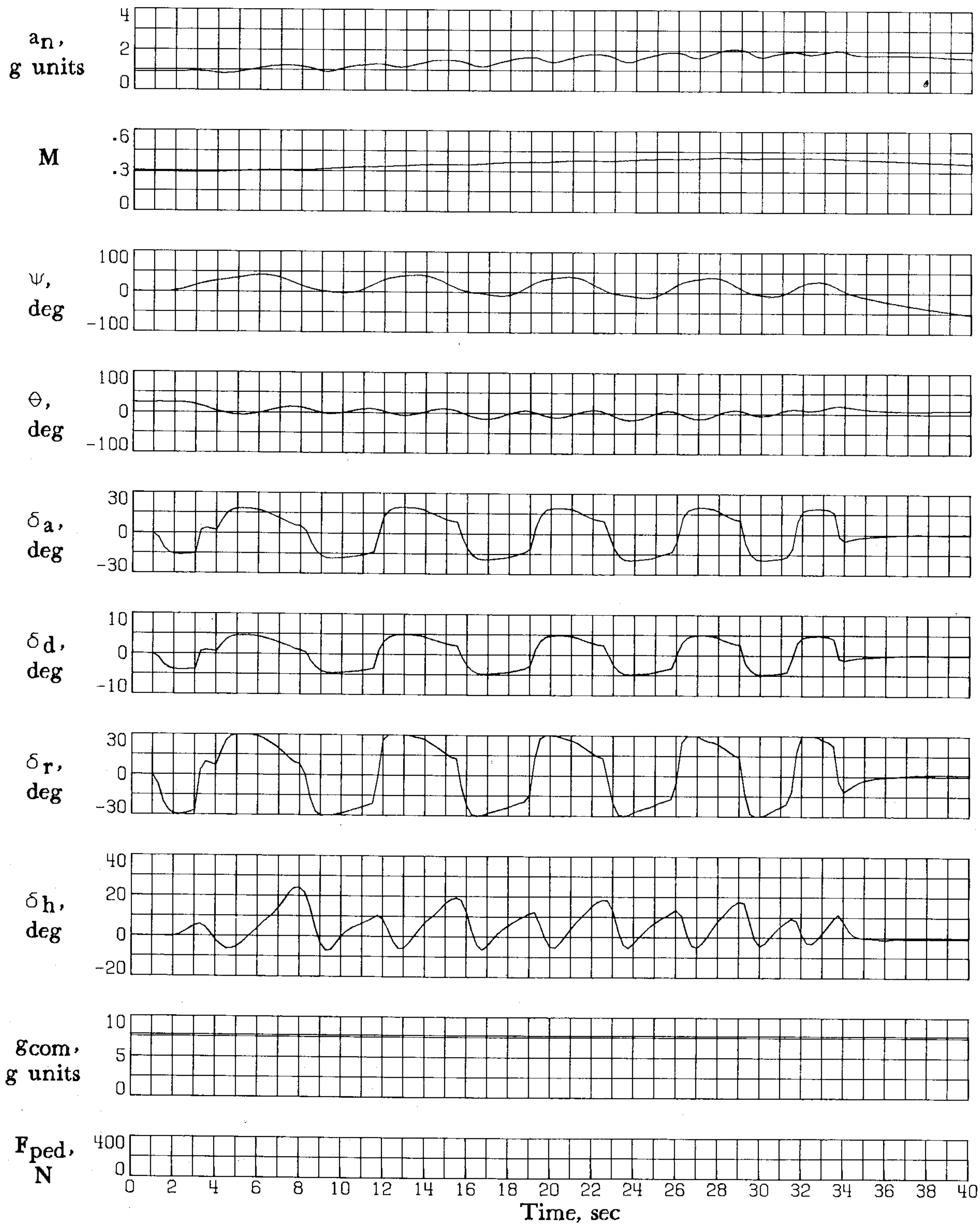

Figure 32.- Continued.

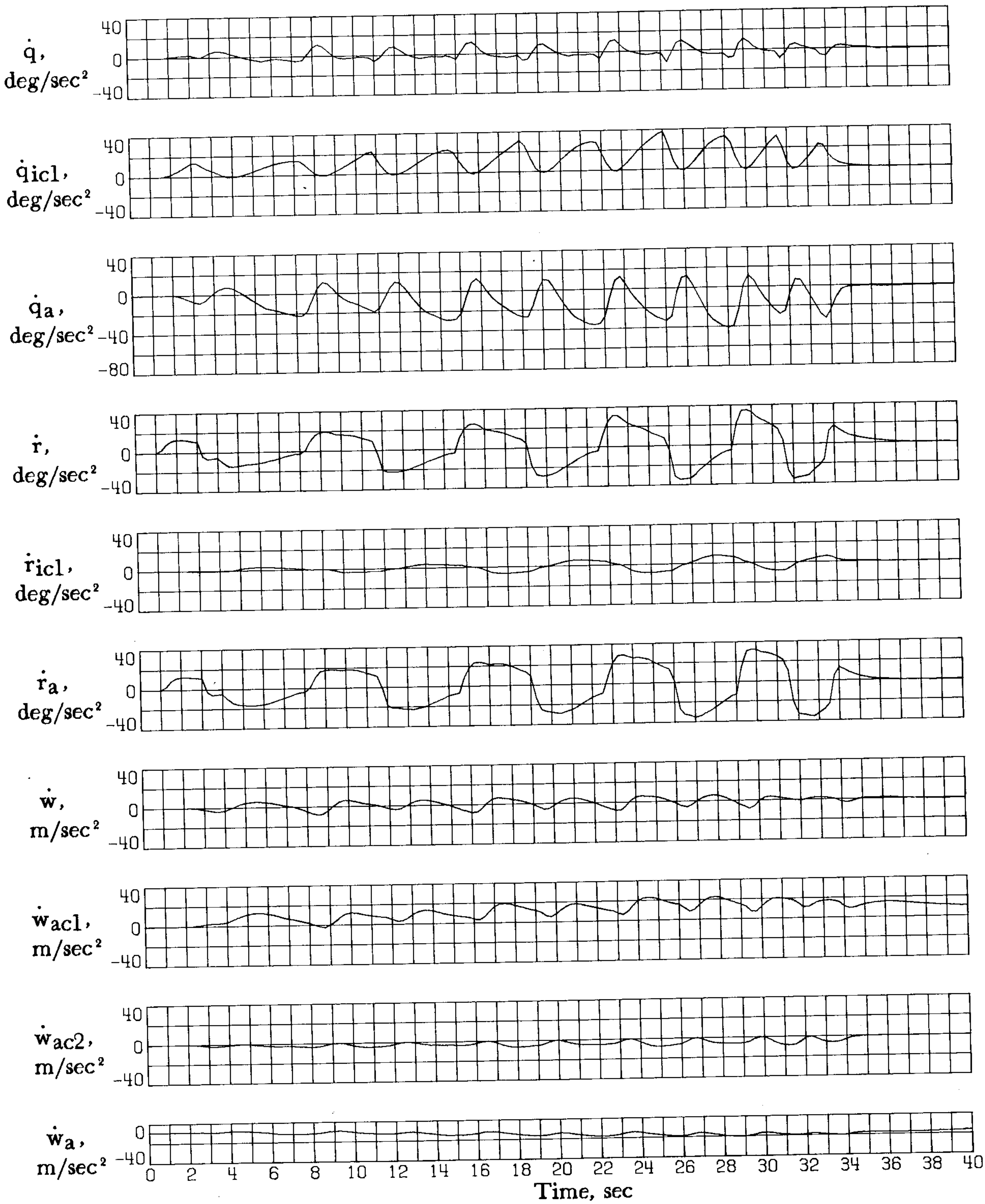

Figure 32.- Concluded.

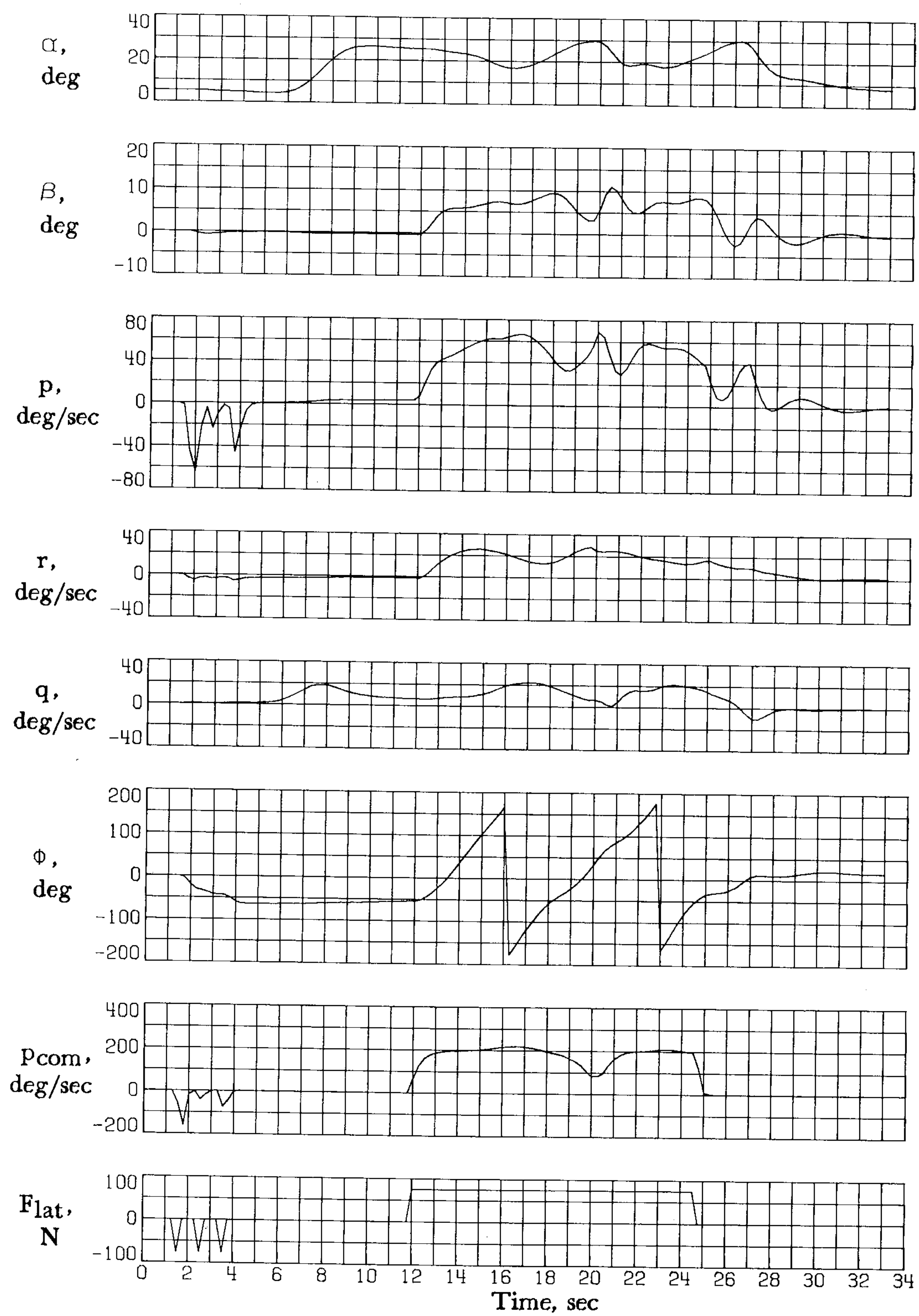

Figure 33.- Response to full cross controls applied in accelerated turn at limit α. Control system B; h_o = 9144 m.

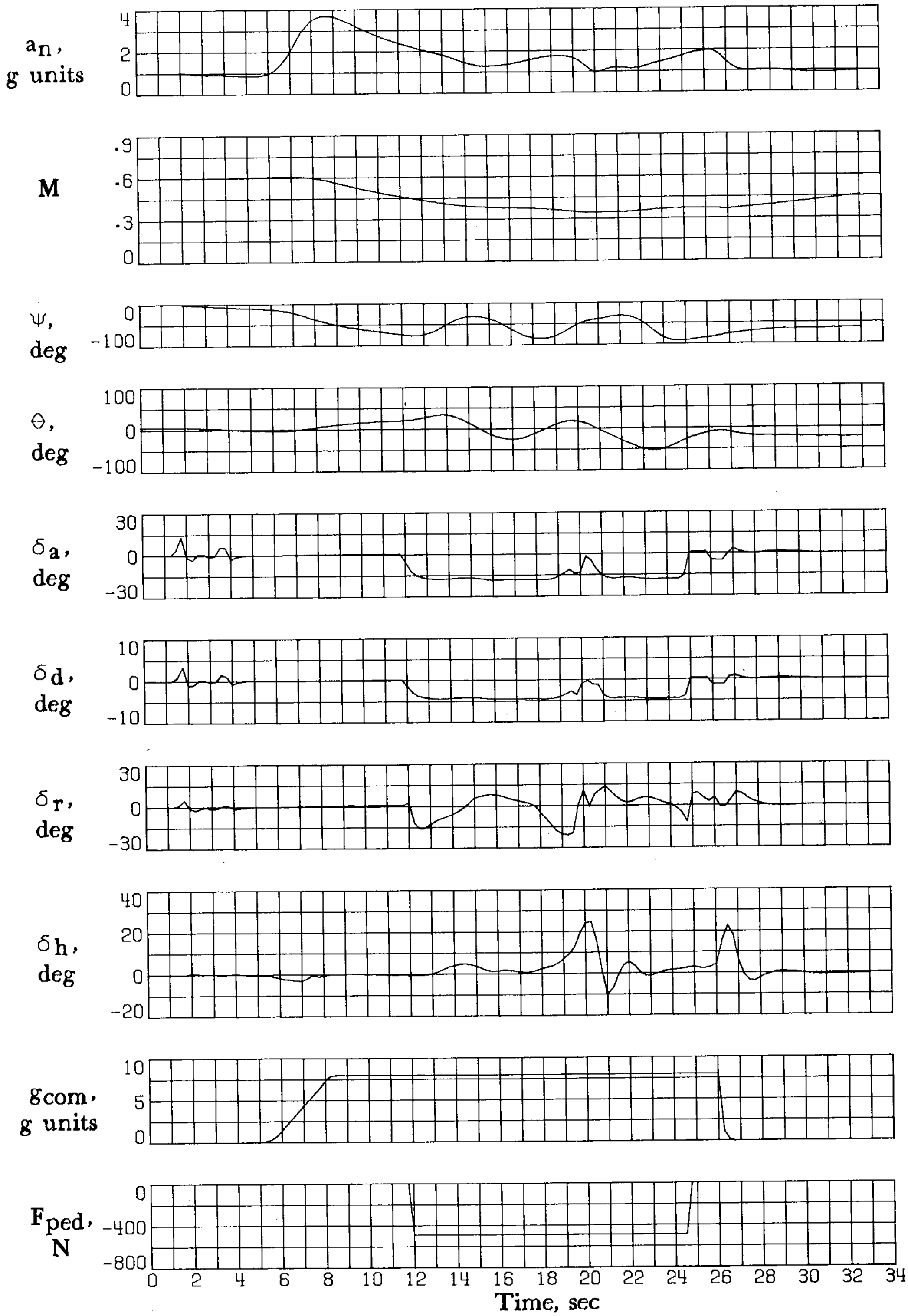

Figure 33.- Continued.

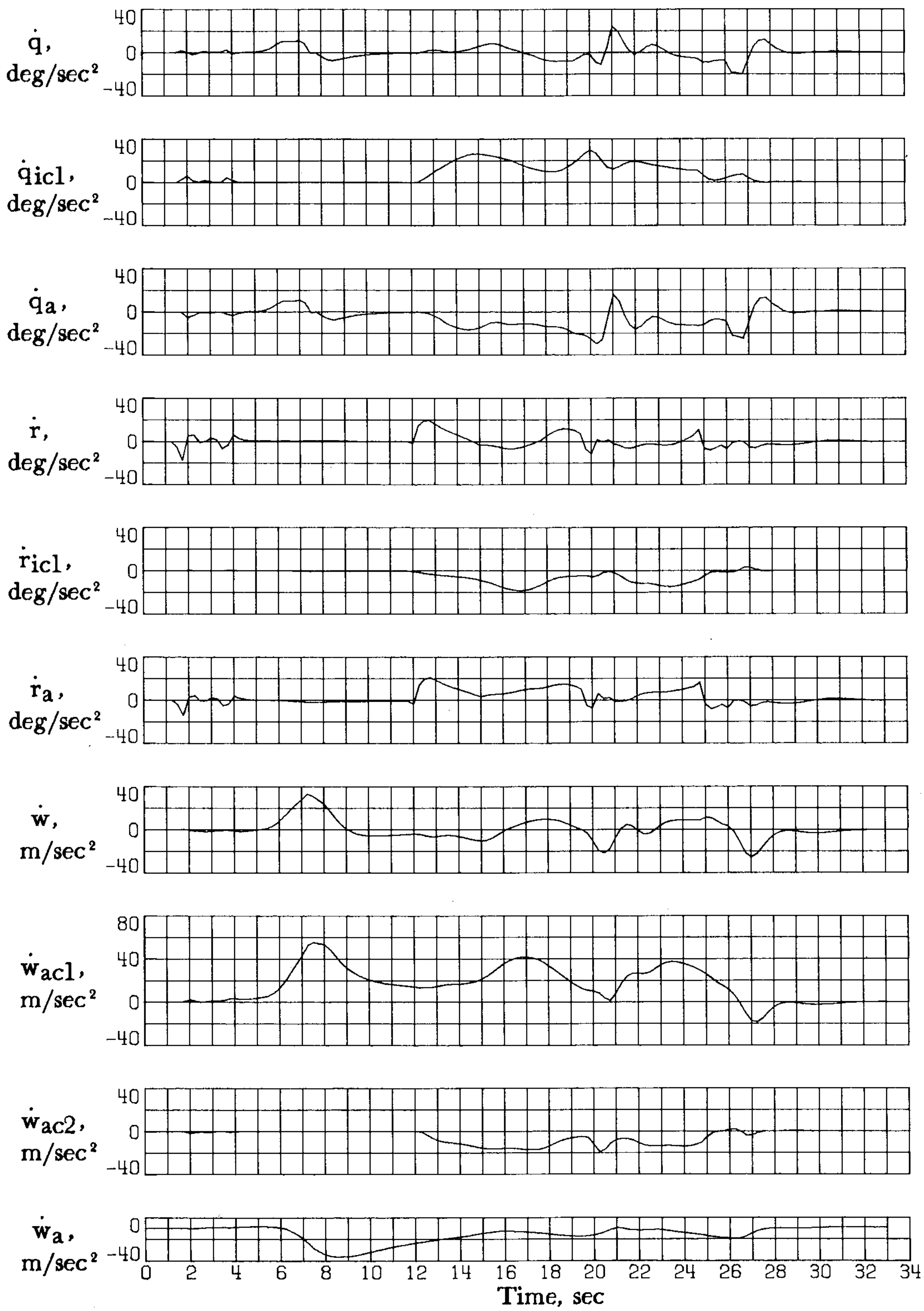

Figure 33.- Concluded.

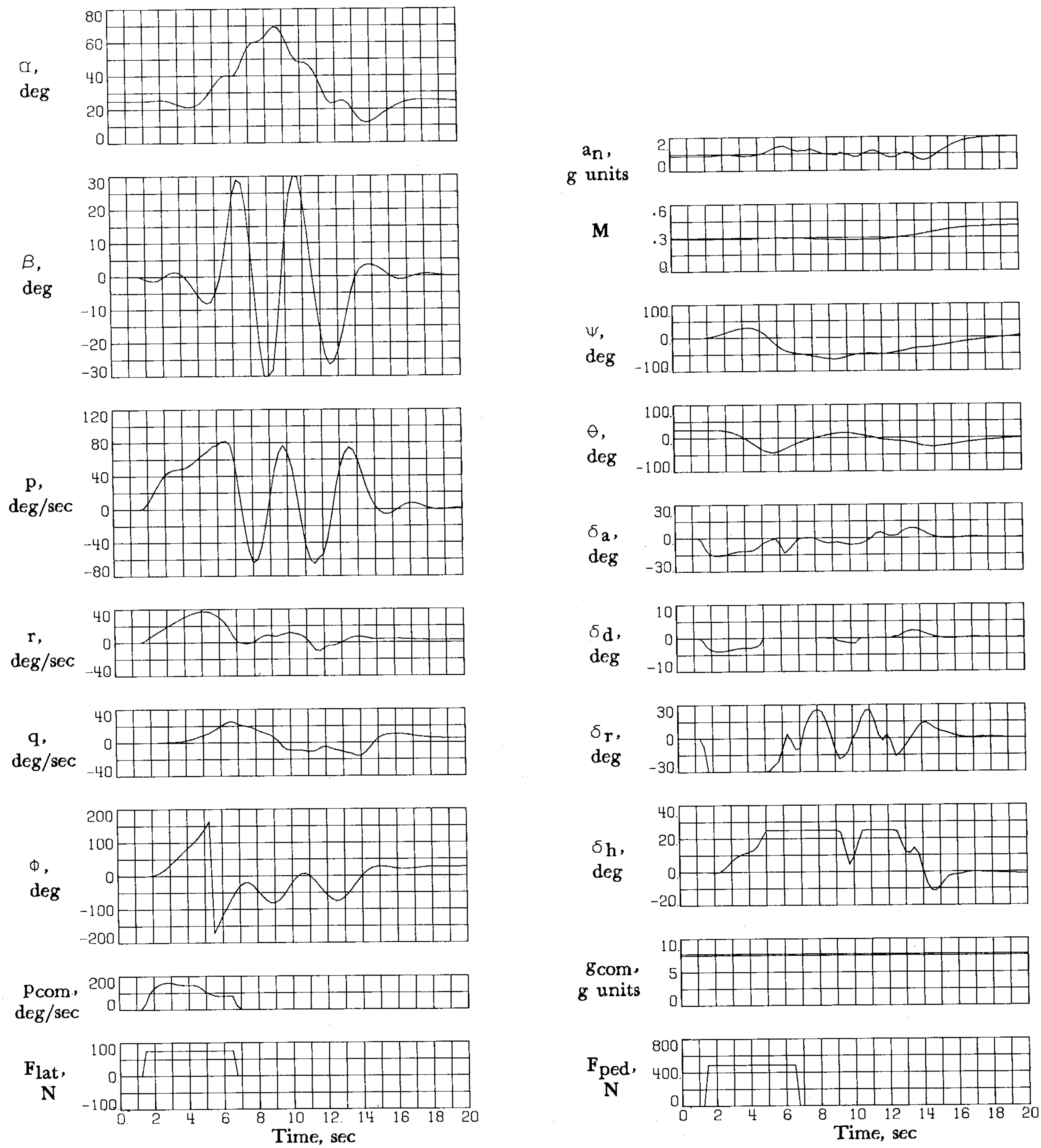

Figure 34.- A 360° roll attempt applied in 1g flight at $\alpha = 25^{\circ}$ using full coordinated stick and pedal inputs. Control system B; $h_o = 9144$ m.

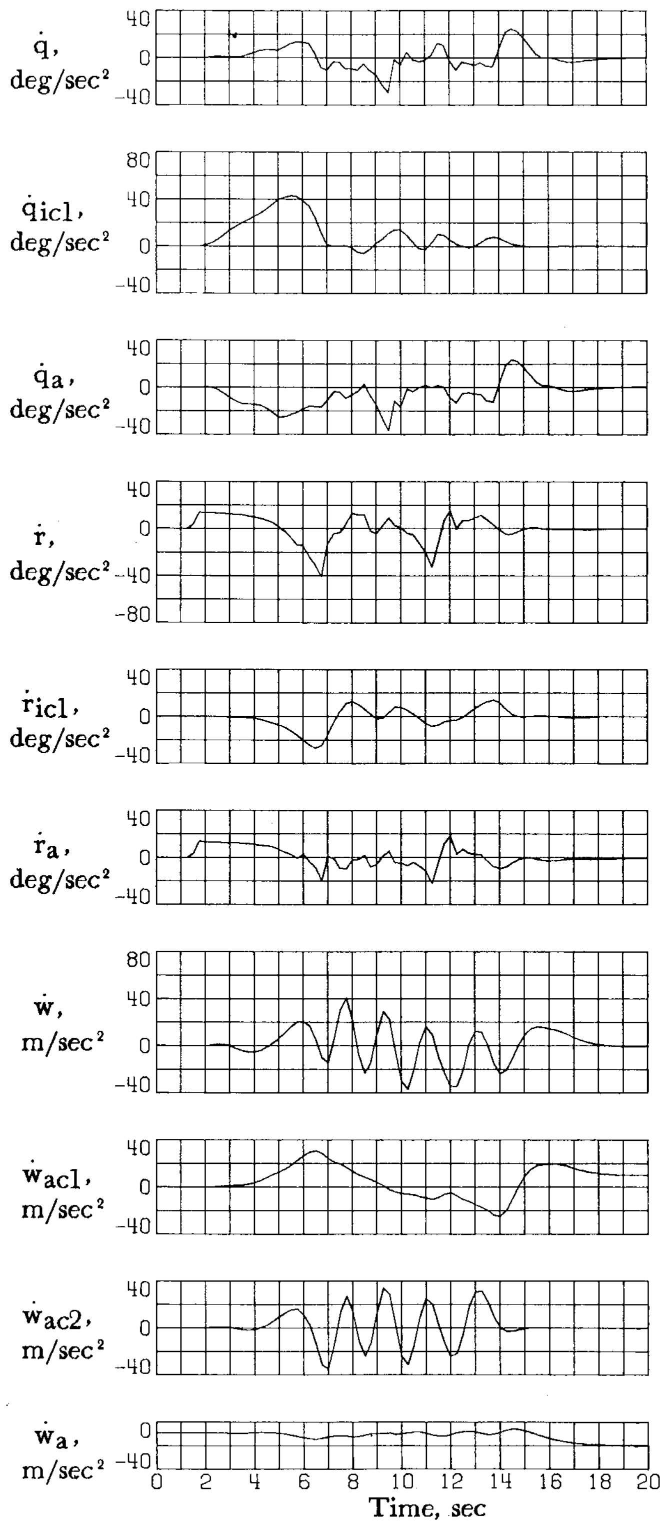

Figure 34.- Concluded.

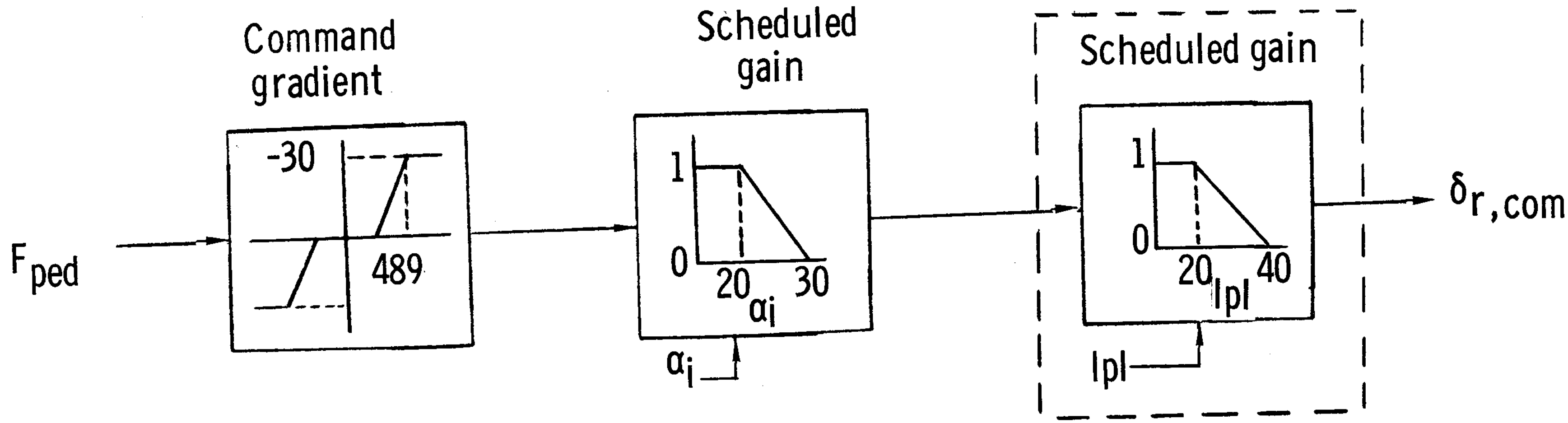

(a) Yaw-axis modification.

Figure 35.- Modifications to yaw and roll axes incorporated in going from control system B to C (modifications enclosed in dashed lines).

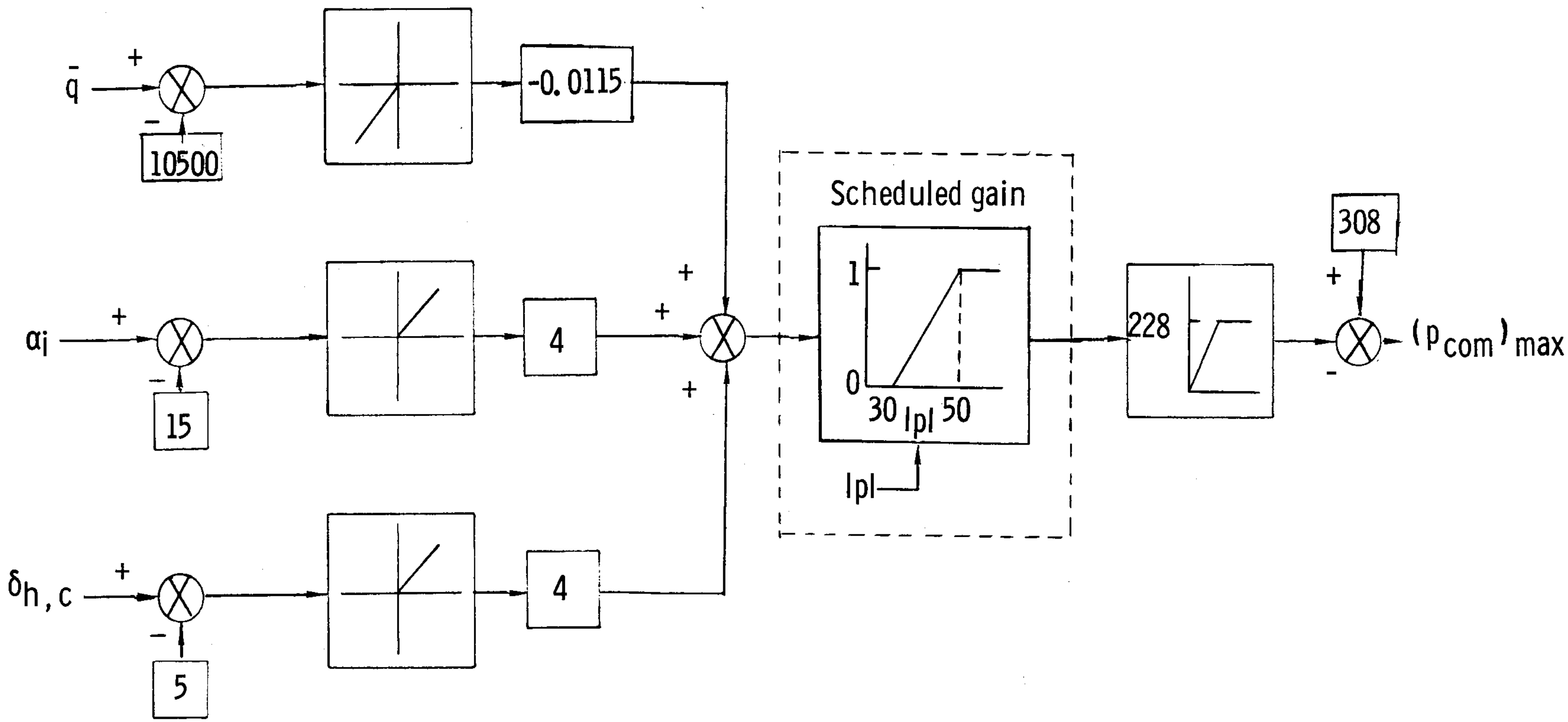

(b) Roll-axis modification.

Figure 35.- Concluded.

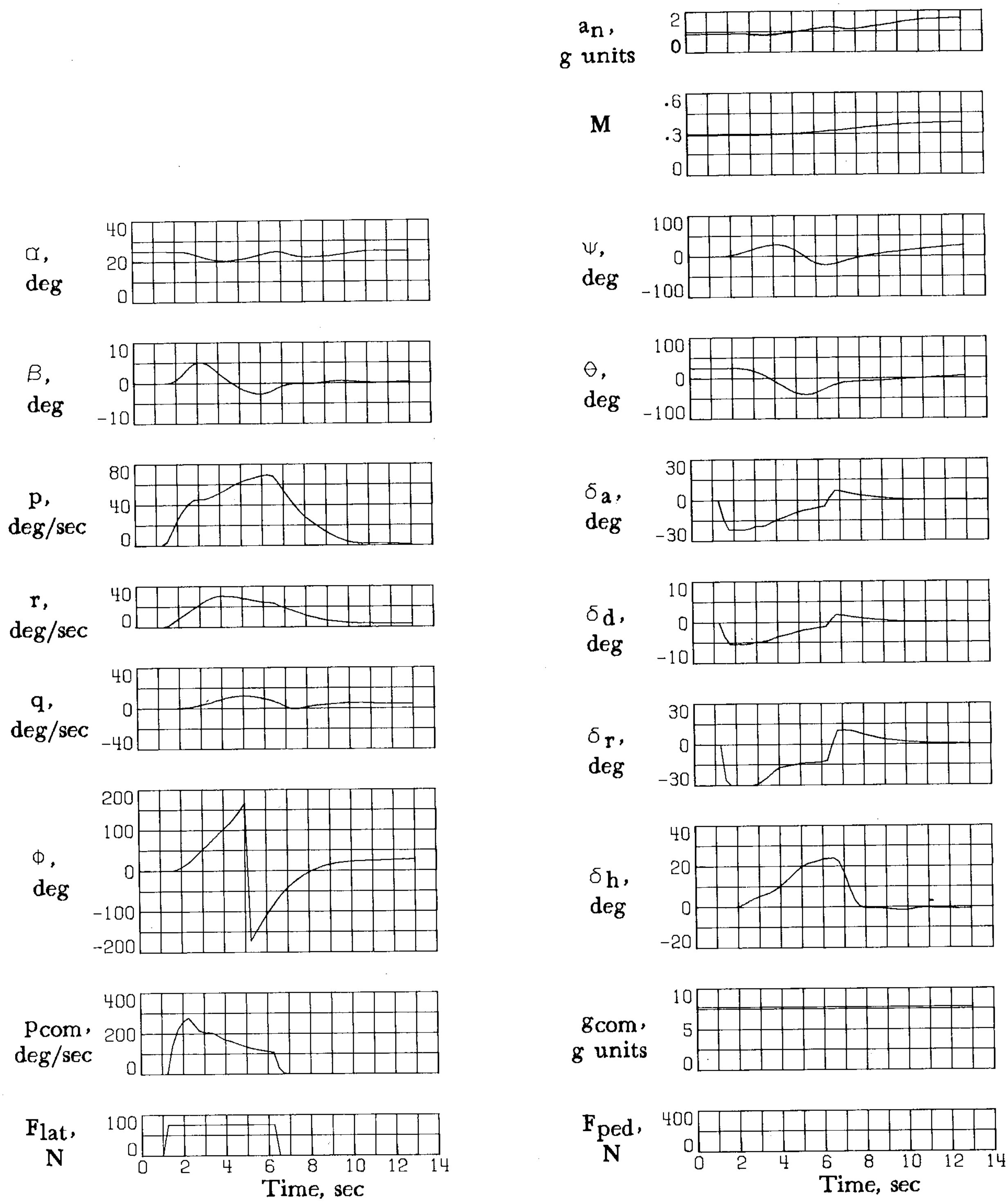

Figure 36.- A 360° roll initiated from 1g trim flight at $\alpha = 25^{\circ}$ using full lateral stick. Control system C; $h_o = 9144$ m.

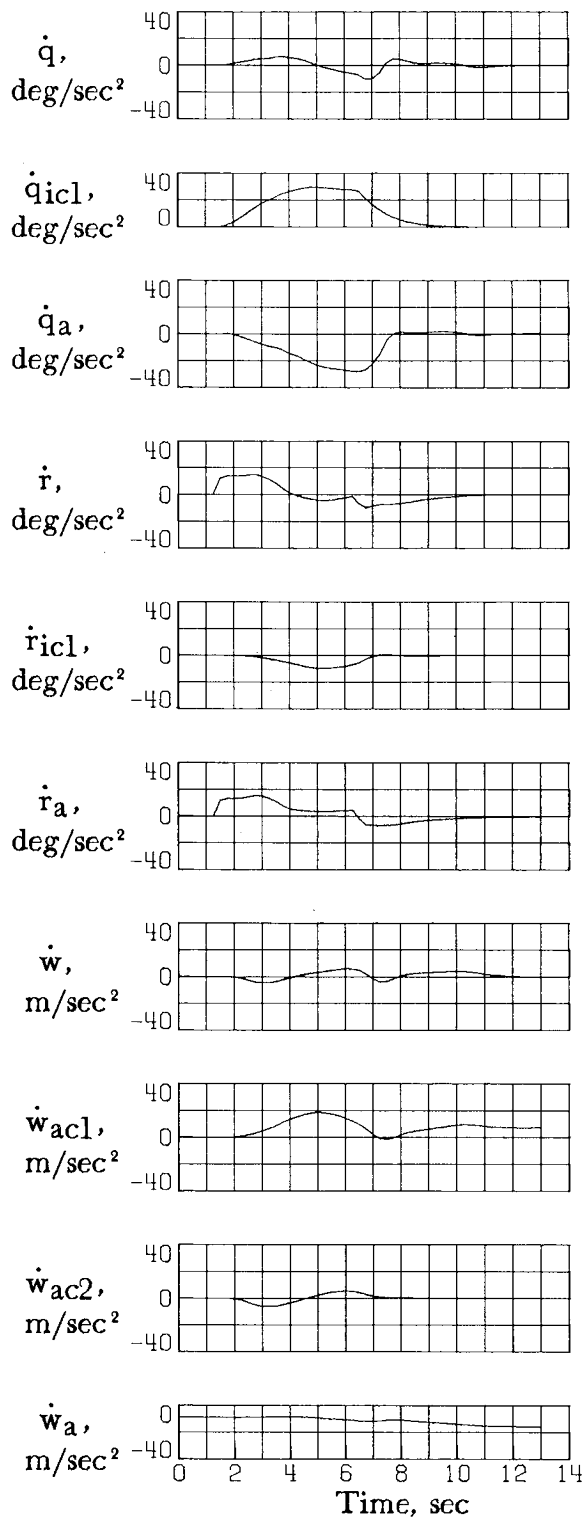

Figure 36.- Concluded.

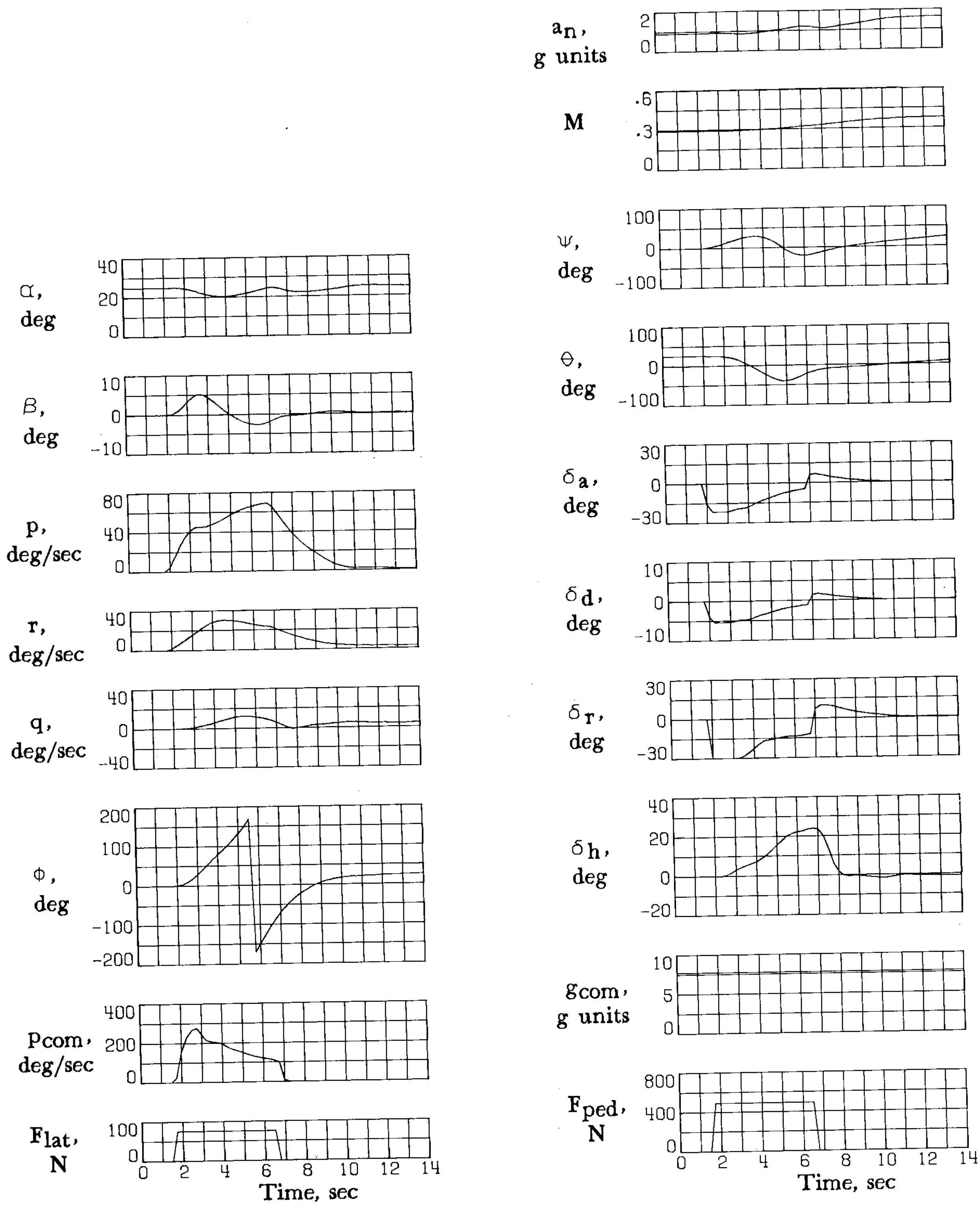

Figure 37.- A 360° roll initiated from 1g flight at $\alpha = 25^{\circ}$ using full coordinated stick and pedal. Control system C; $h_o = 9144$ m.

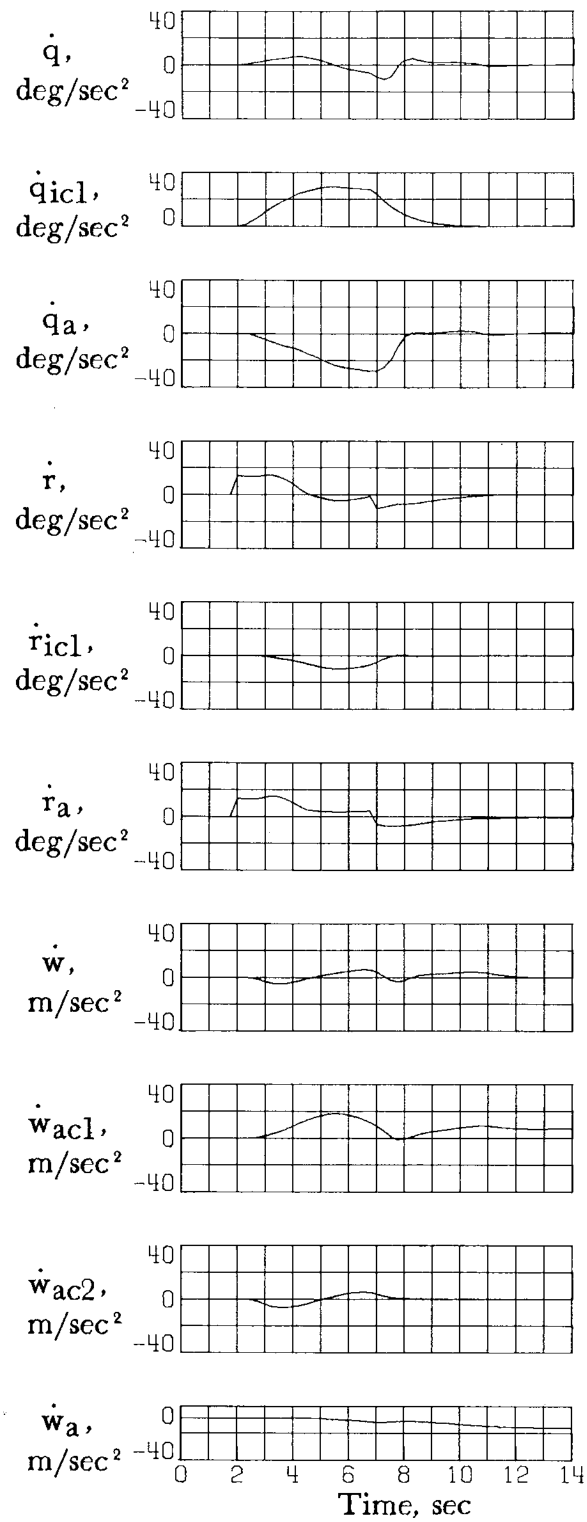

Figure 37.- Concluded.

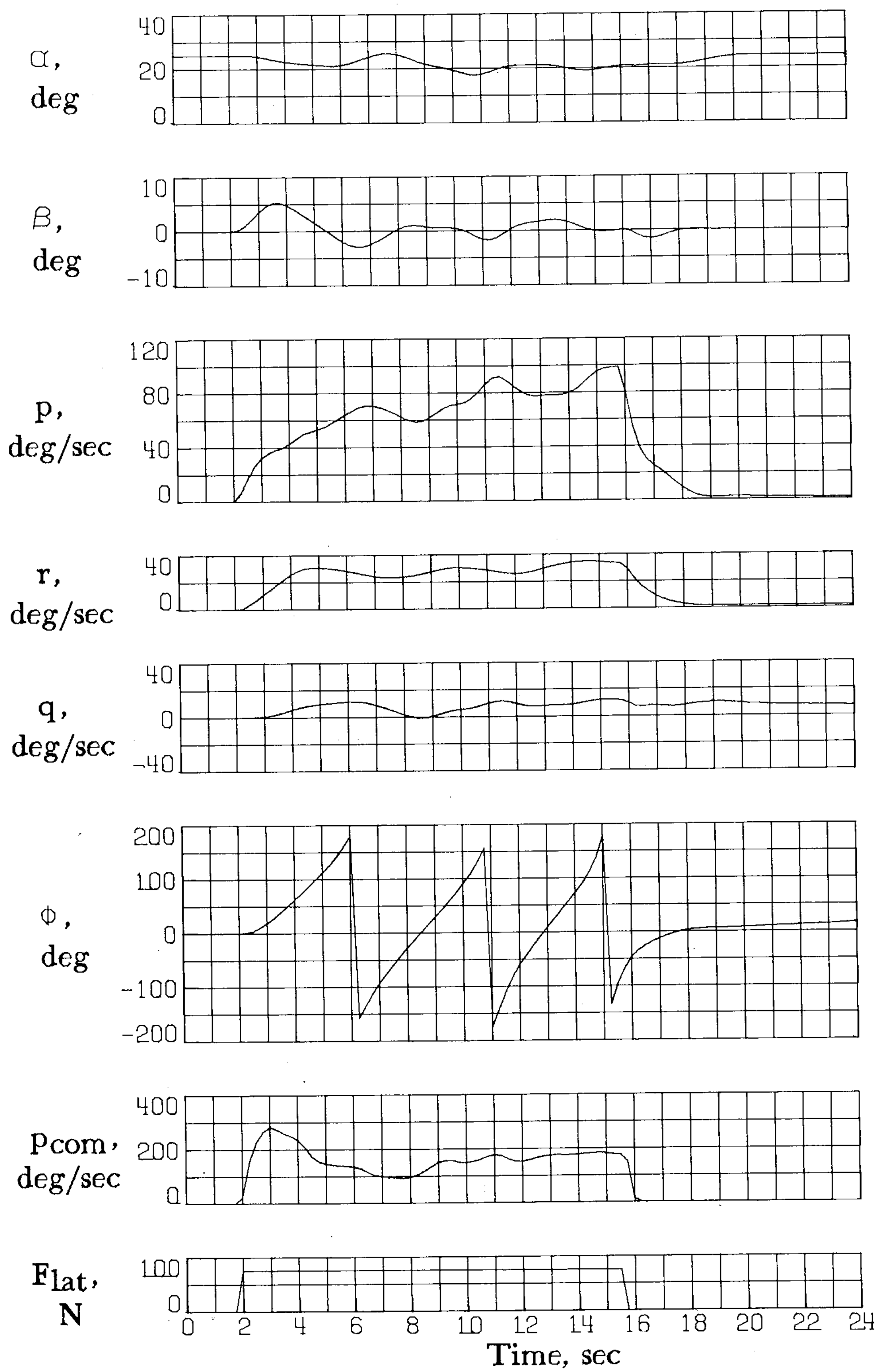

Figure 38.- Response to full cross controls applied in lg trim flight at $\alpha = 25^{\circ}$. Control system C; h_o = 9144 m.

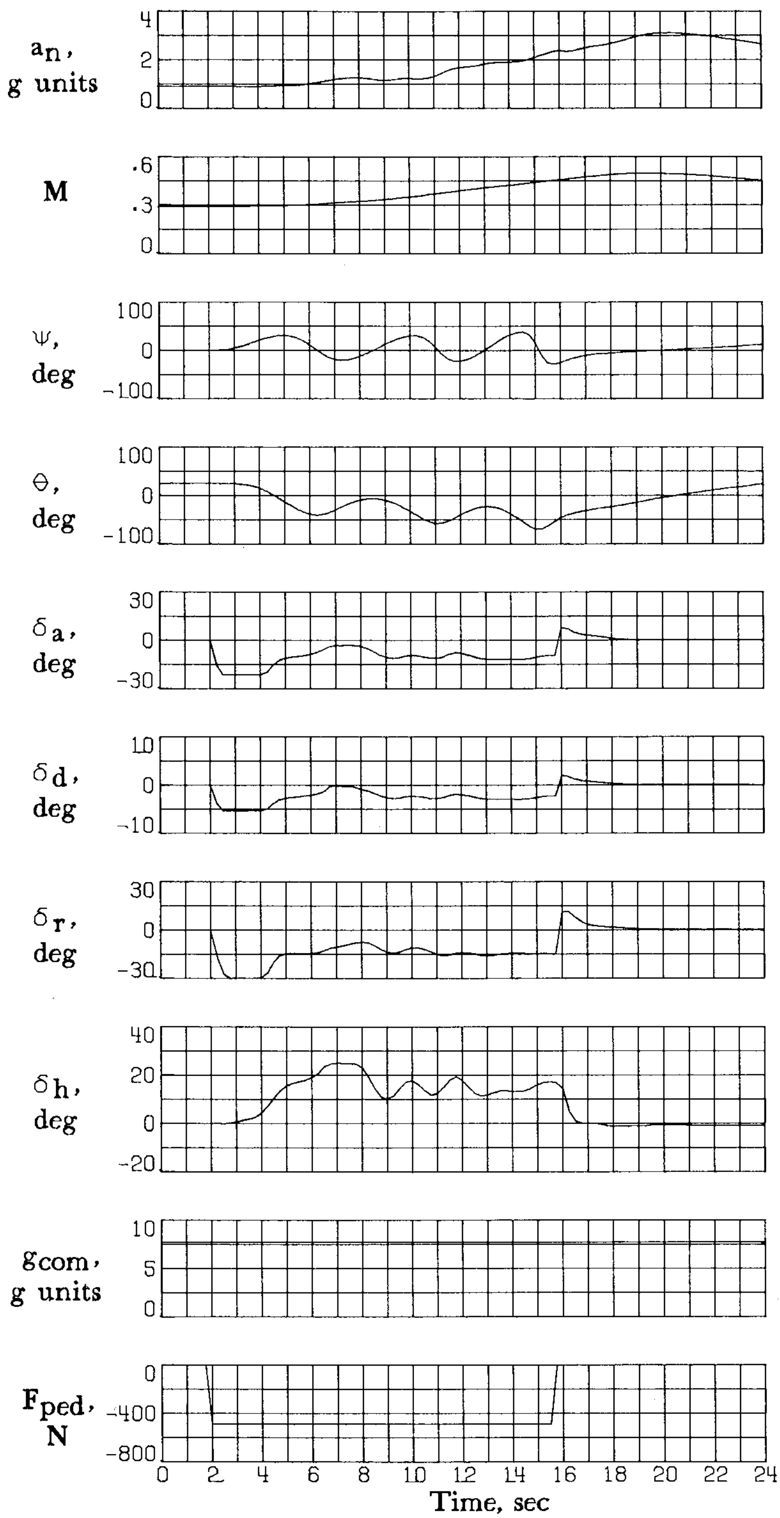

Figure 38.- Continued.

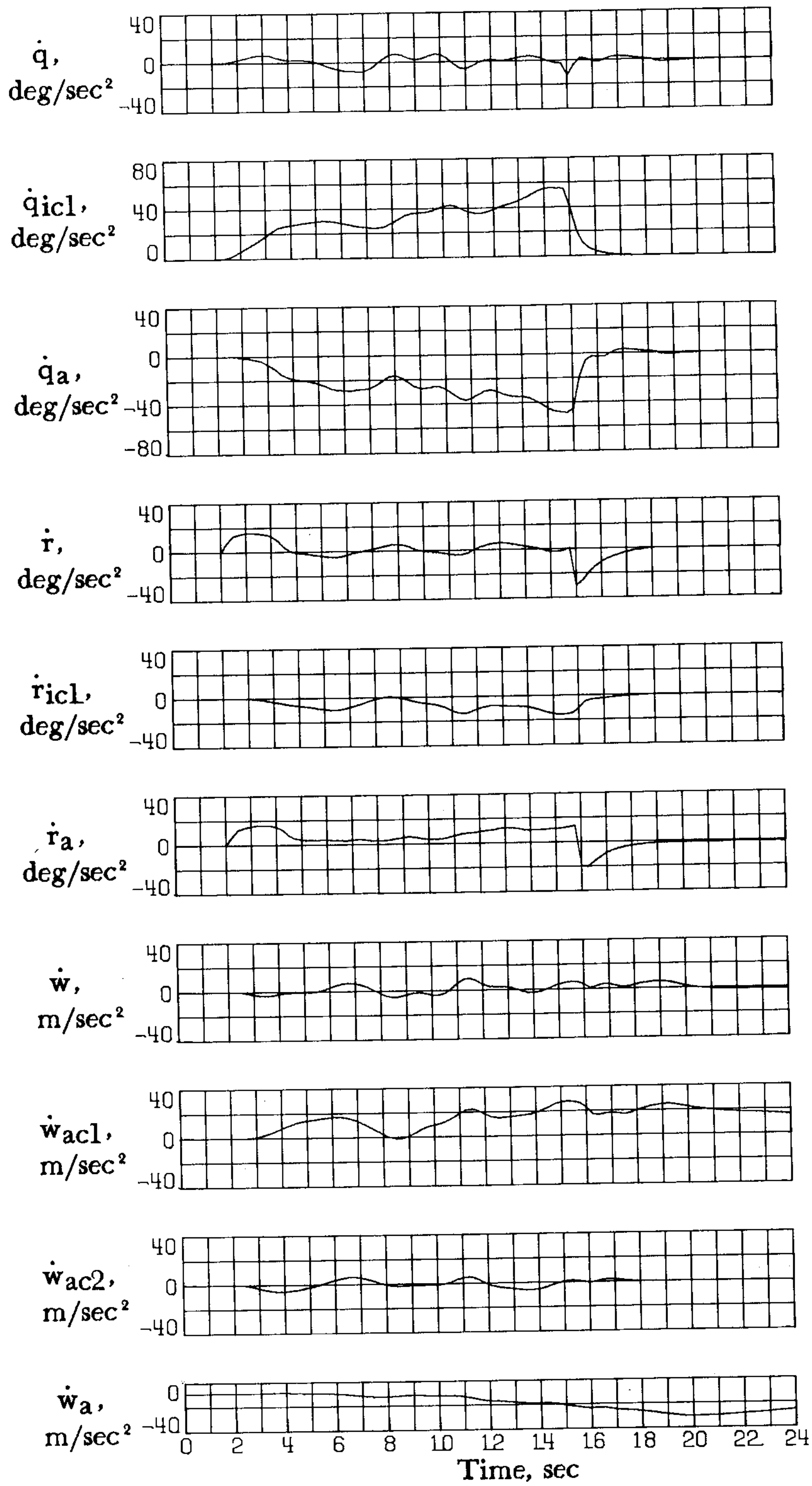

Figure 38.- Concluded.

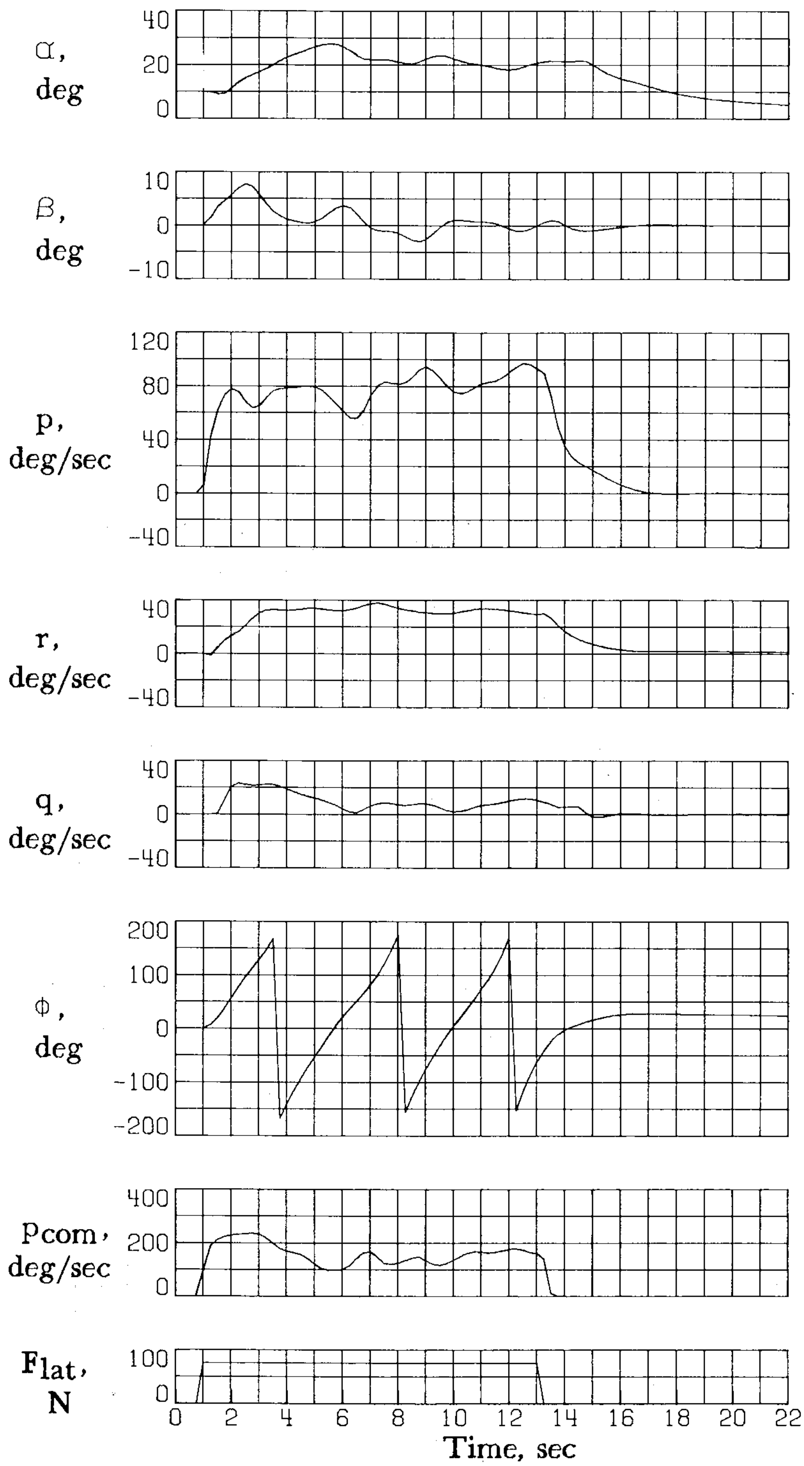

Figure 39.- Response to full cross controls applied in 1g trim at $\alpha = 10^{\circ}$, followed by rapid full aft stick application. Control system C; $h_o = 9144$ m.

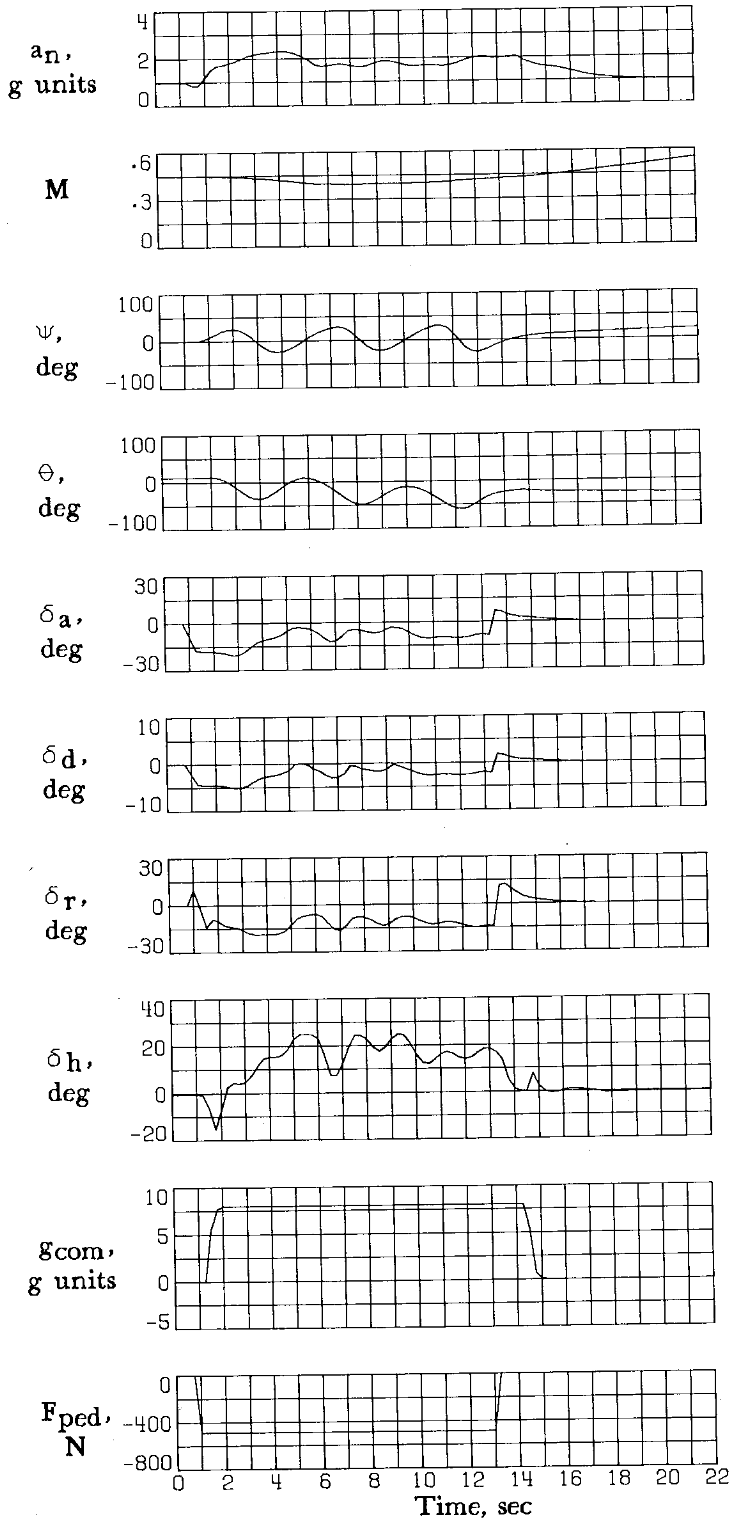

Figure 39.- Continued.

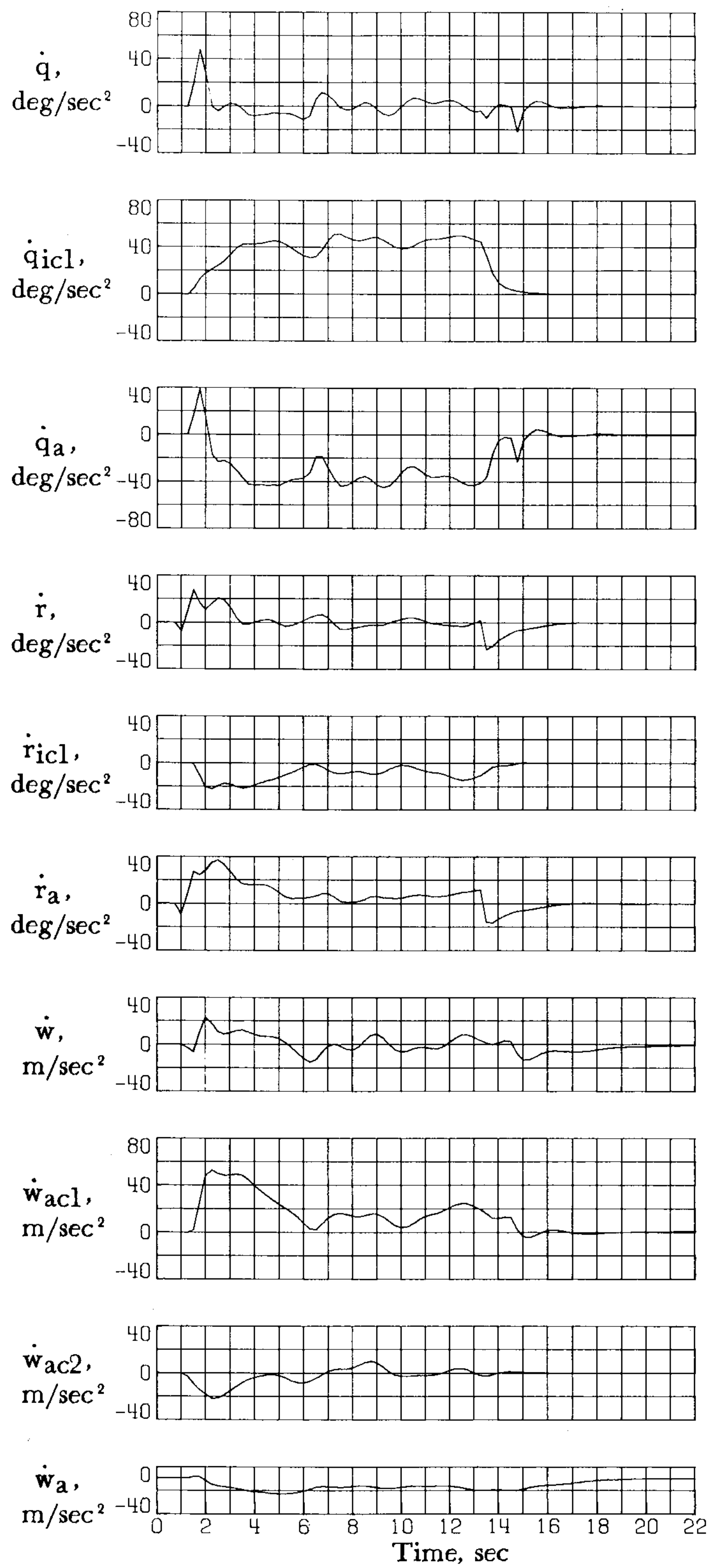

Figure 39.- Concluded.

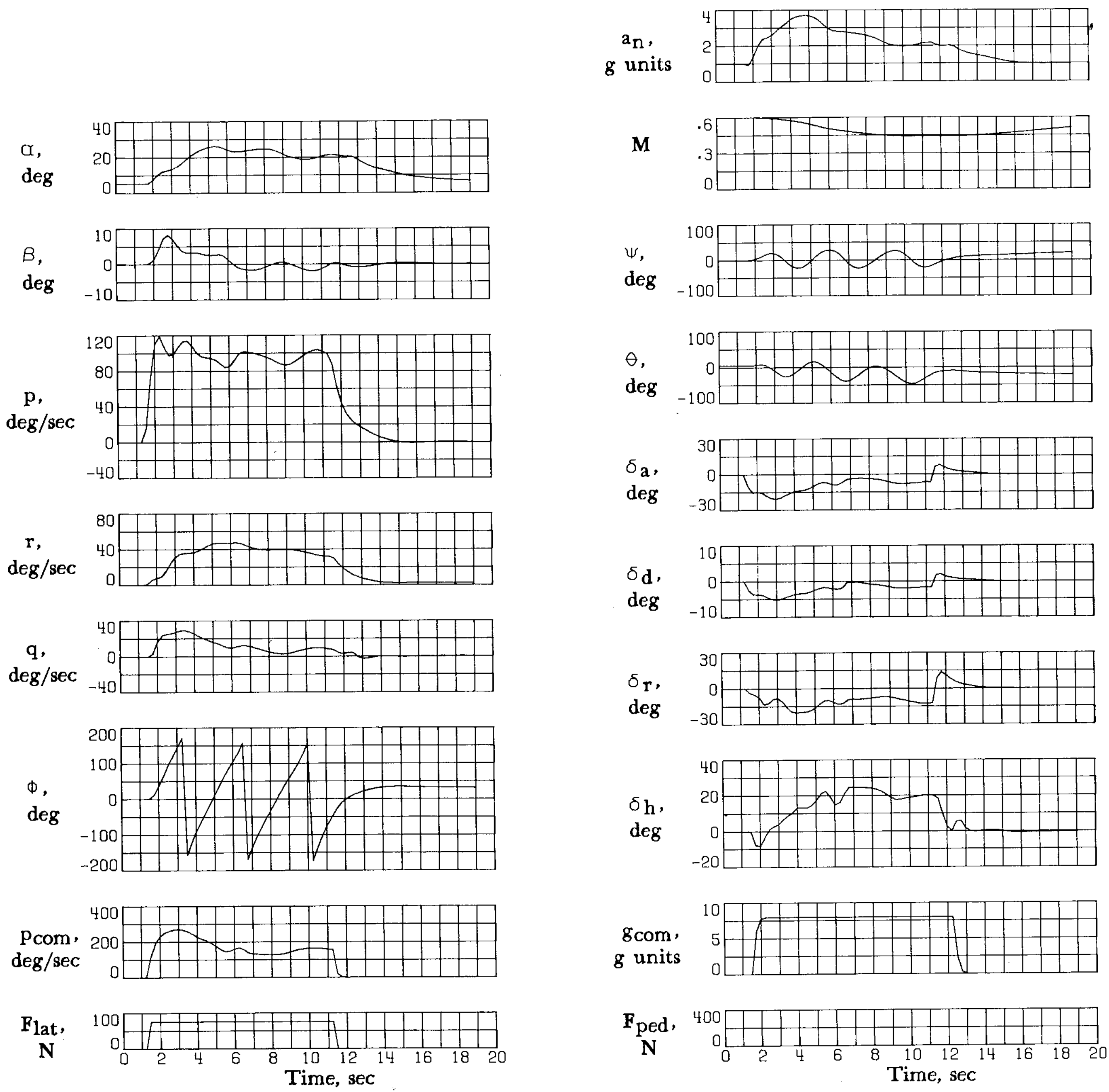

Figure 40.- Response to maximum inertia-coupling maneuver. Control system C; h_o = 9144 m.

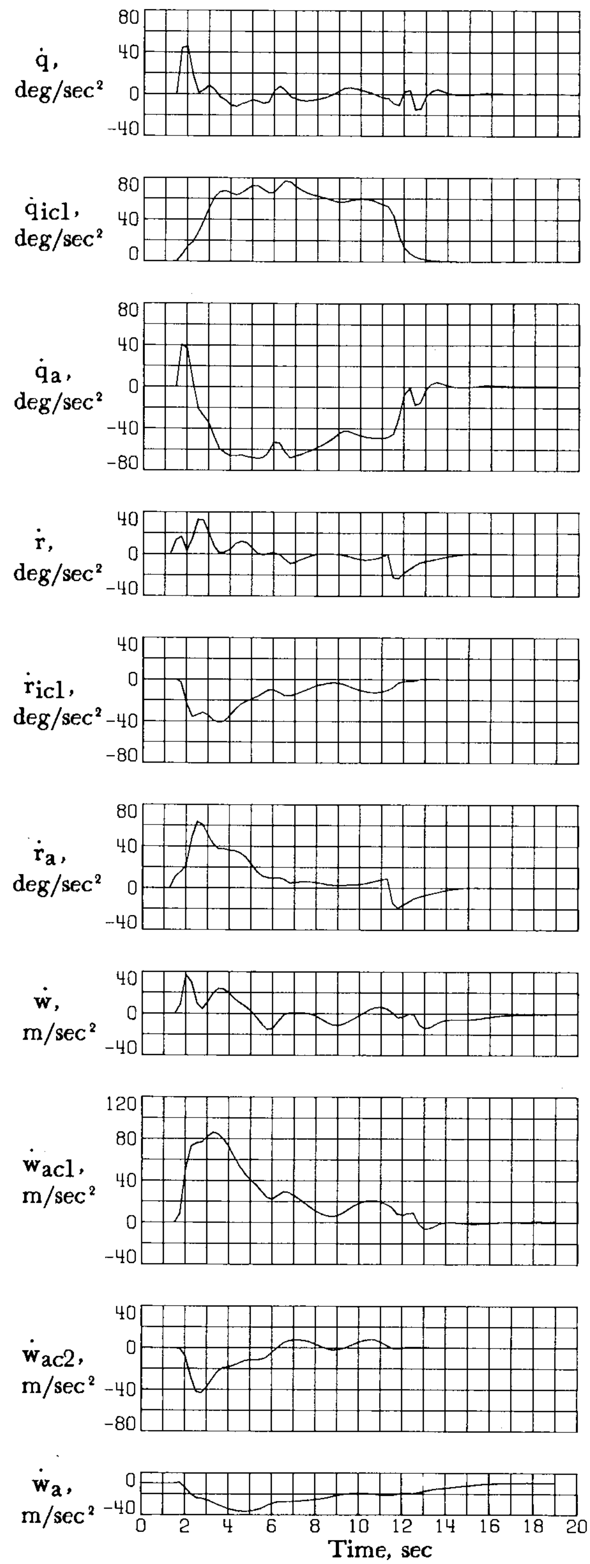

Figure 40.- Concluded.

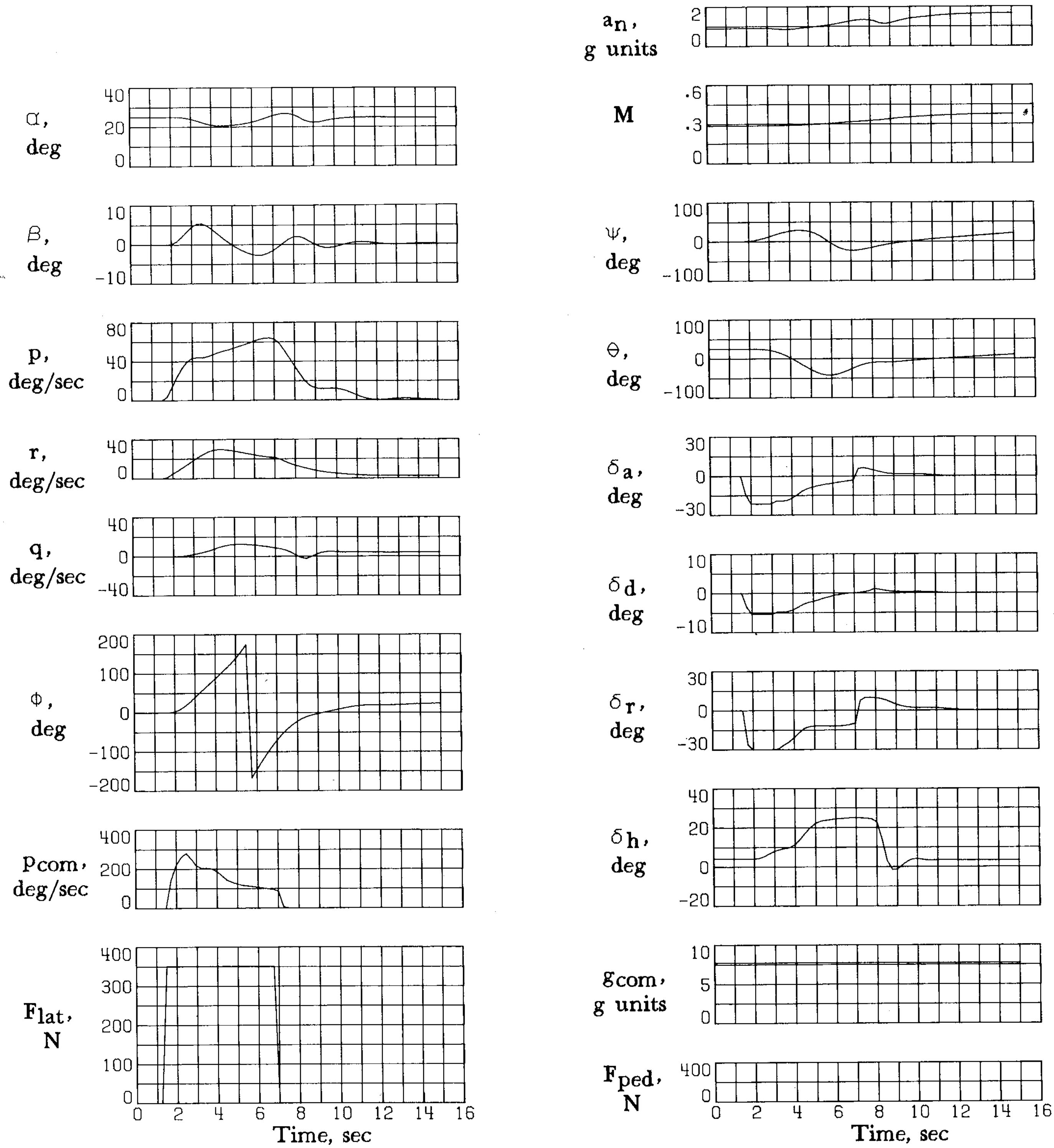

Figure 41.- A 360° roll from 1g trim flight at $\alpha = 25^{\circ}$ using full lateral stick input at a center-of-gravity location of $0.375\bar{c}$. Control system C; $h_o = 9144$ m.

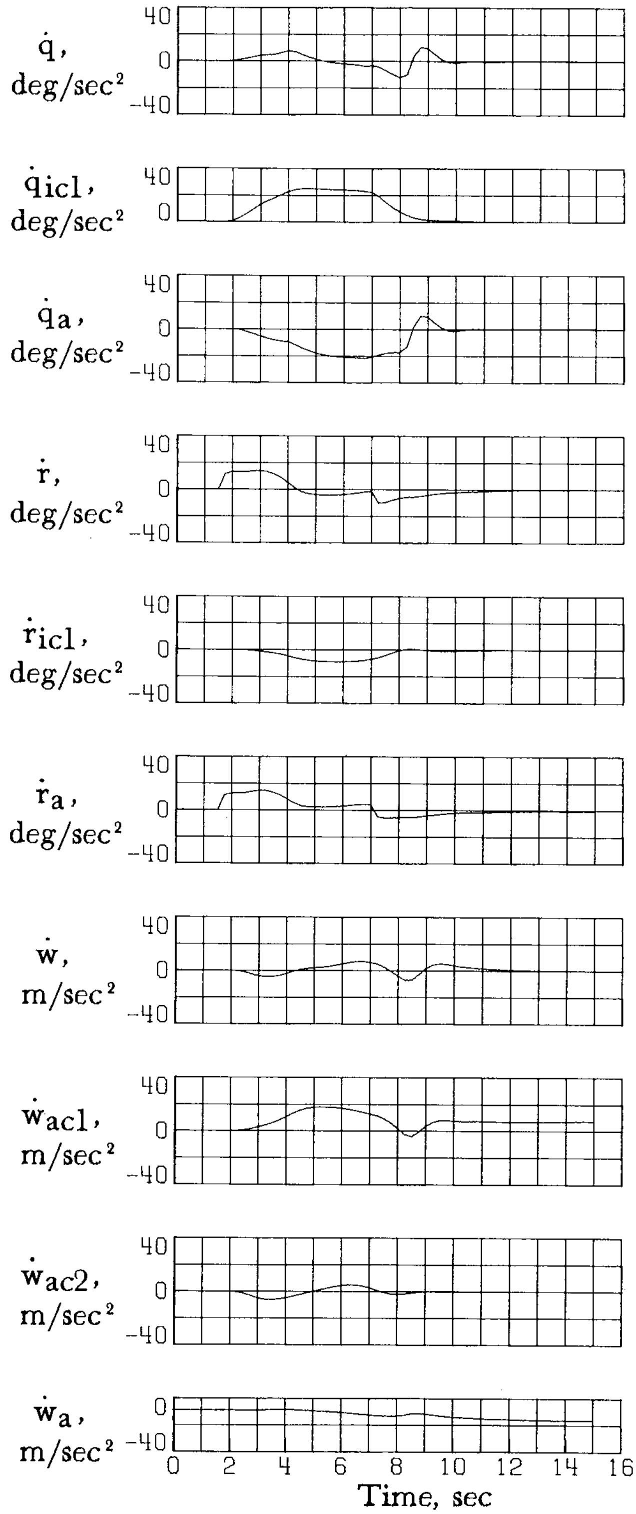

Figure 41.- Concluded.

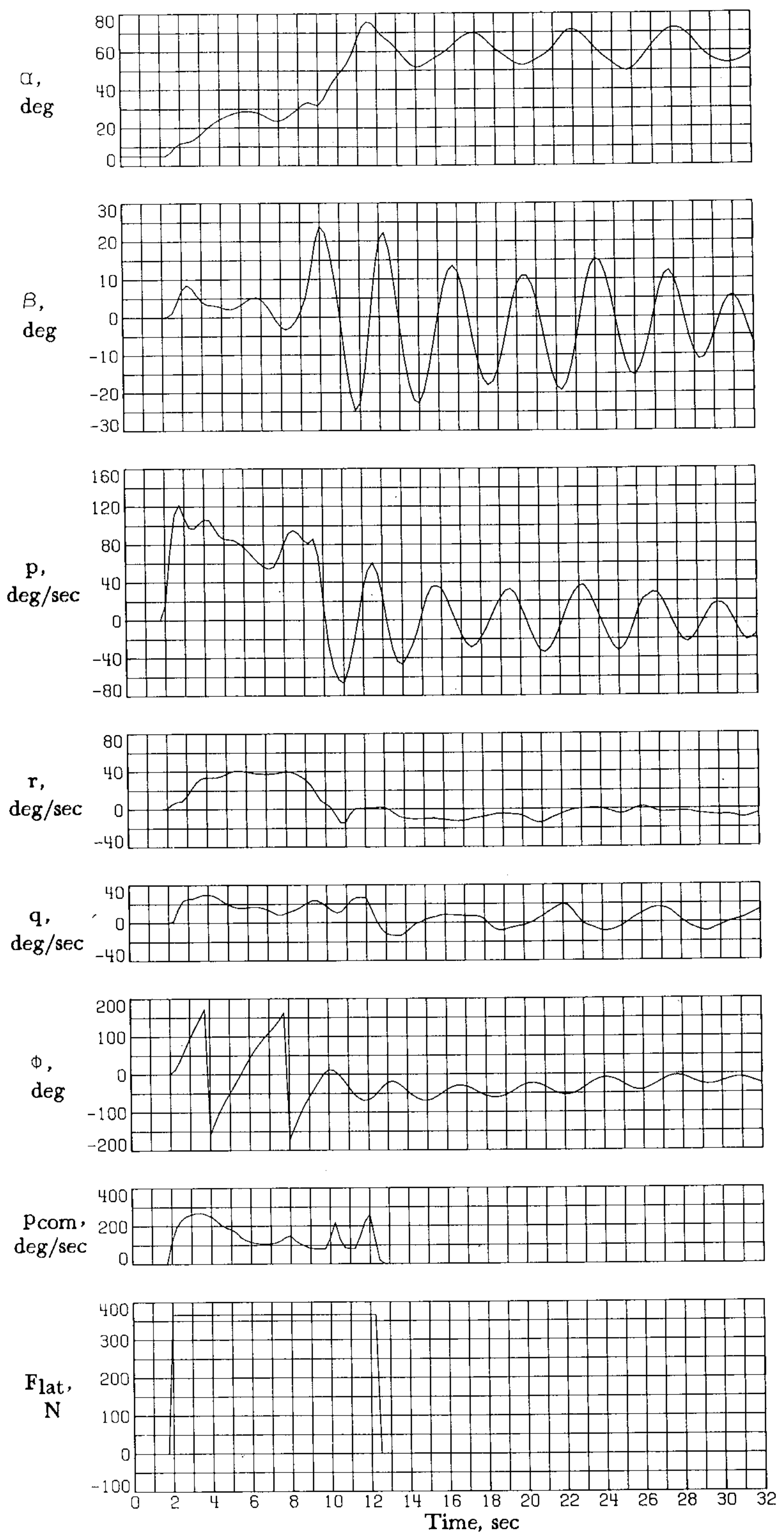

Figure 42.- Response to maximum inertia-coupling maneuver at a center-of-gravity location of $0.375\bar{c}$. Control system C; h_o = 9144 m.

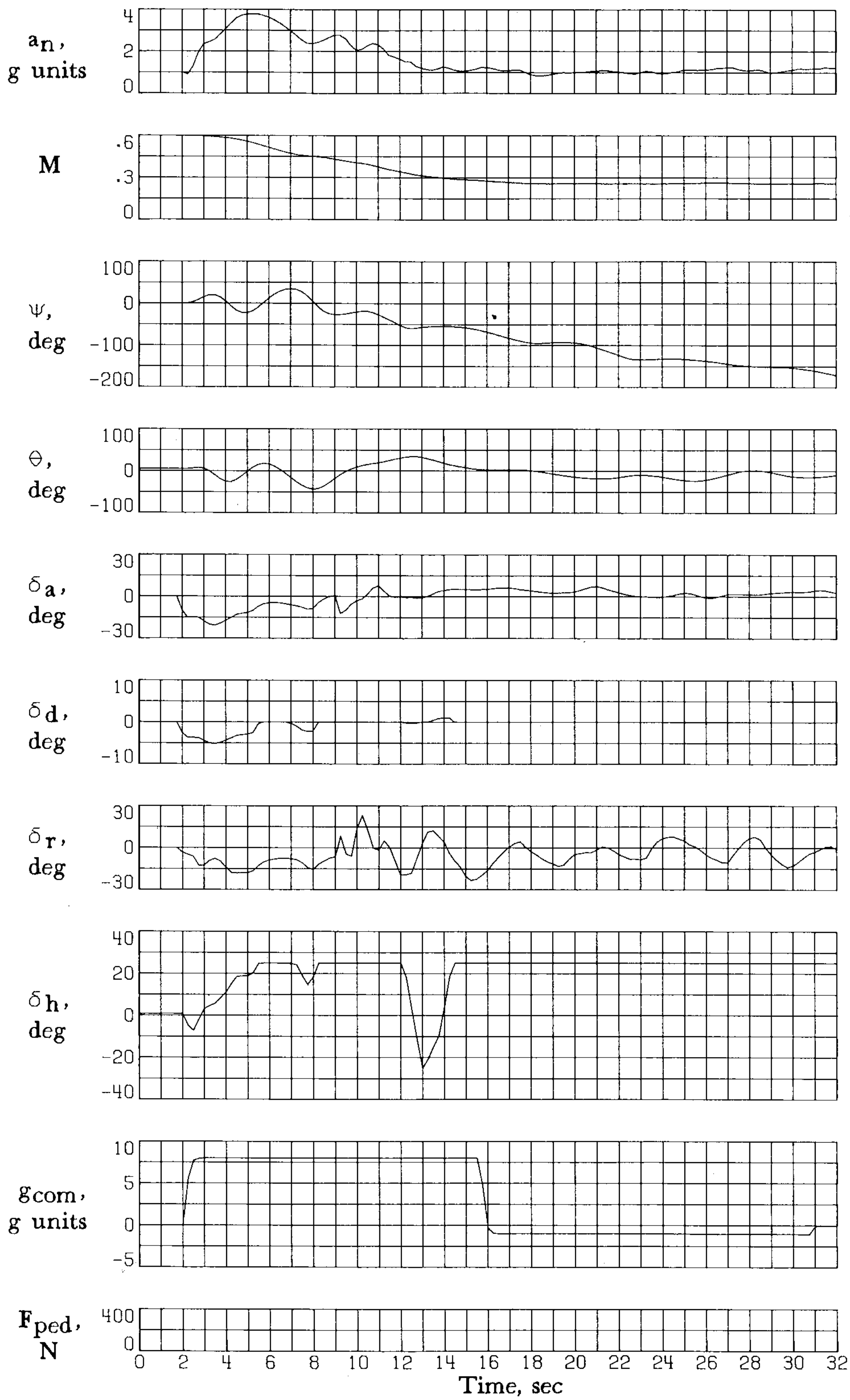

Figure 42.- Continued.

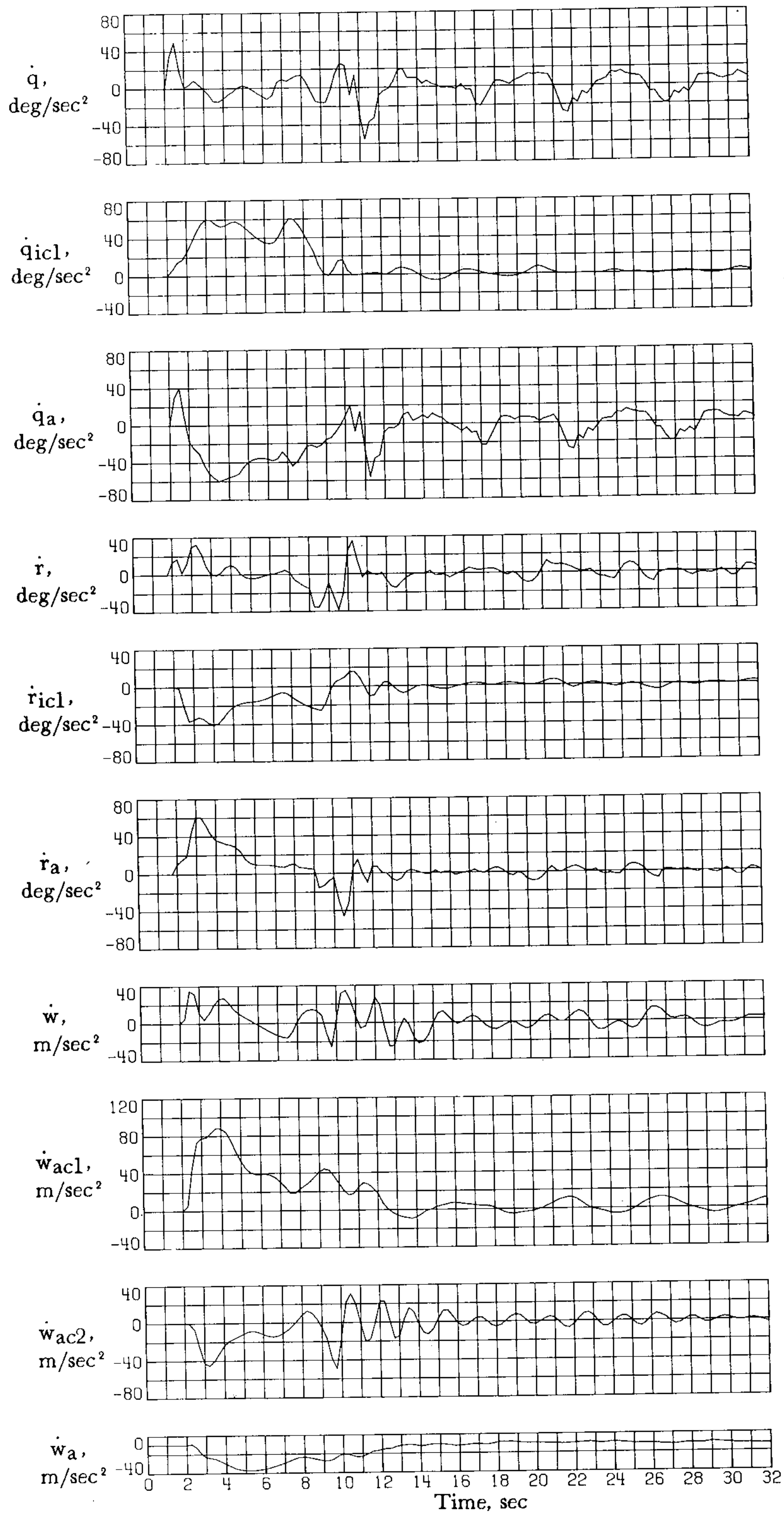

Figure 42.- Concluded.

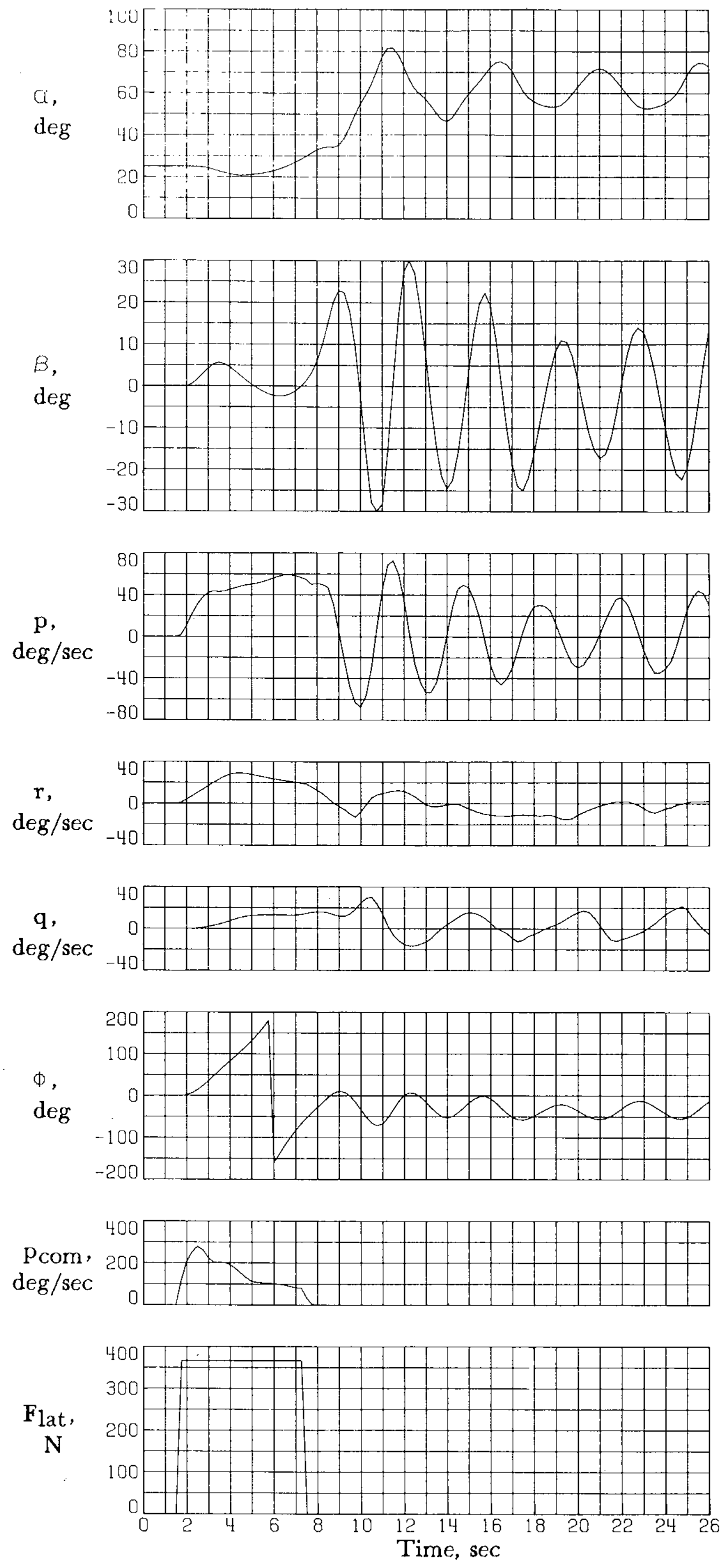

Figure 43.- A 360° roll attempt initiated in 1g trim flight at $\alpha = 25^{\circ}$ using full lateral stick input at a center-of-gravity location of $0.39\bar{c}$. Control system C; $h_o = 9144$ m.

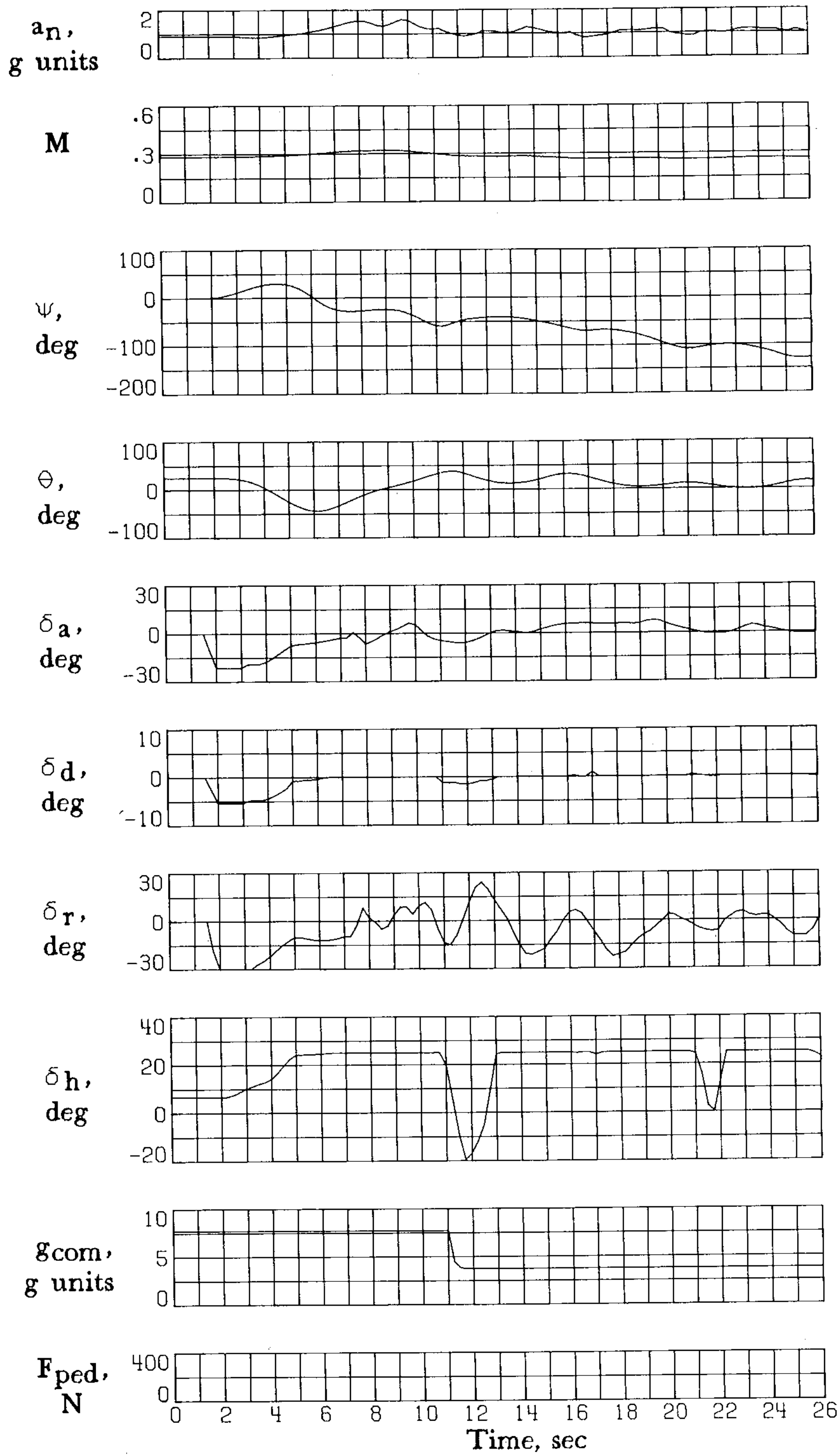

Figure 43.- Continued.

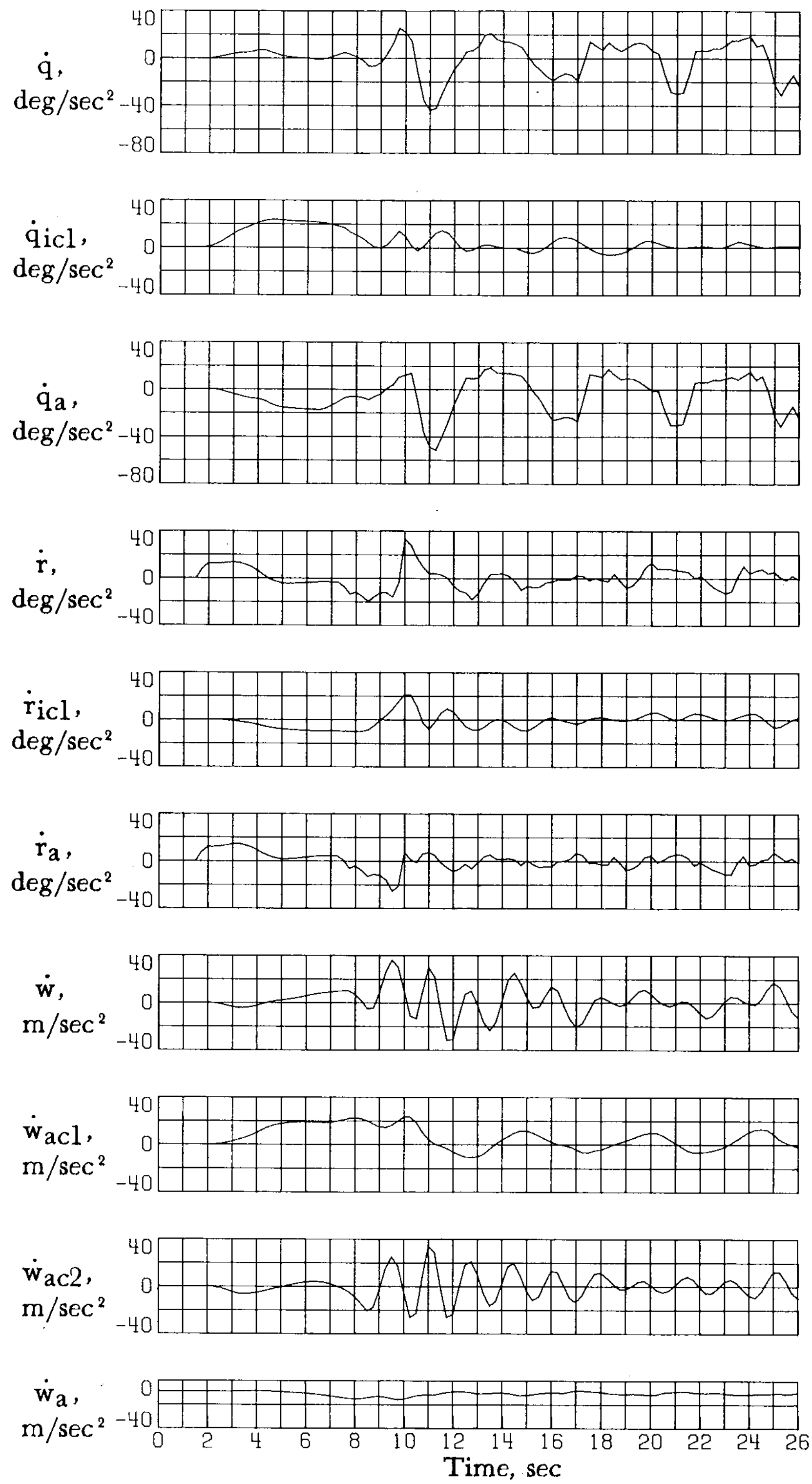

Figure 43.- Concluded.

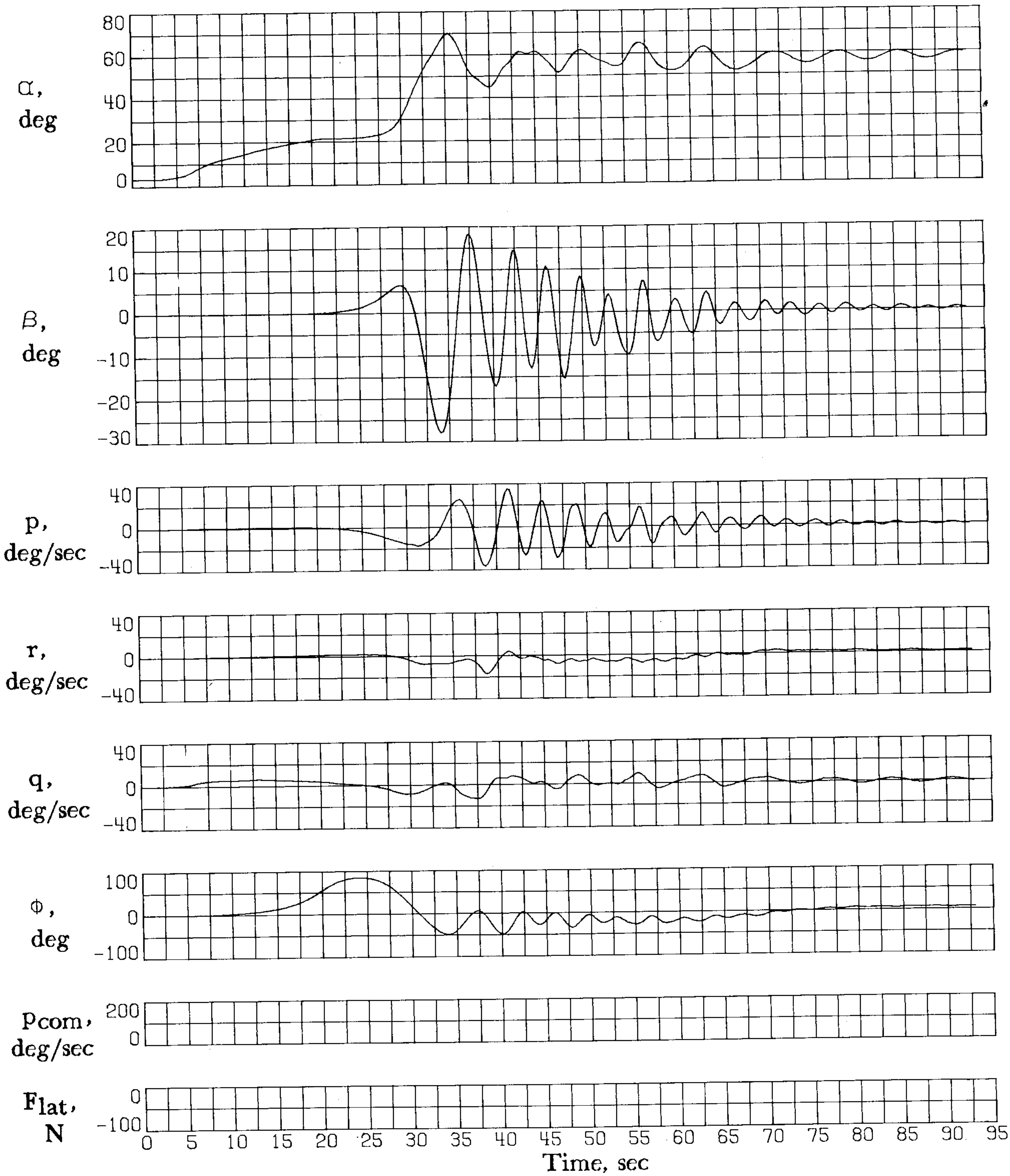

Figure 44.- Deep-stall entry at a center-of-gravity location of $0.35\bar{c}$. Asymmetries not modeled; $h_o = 9144$ m.

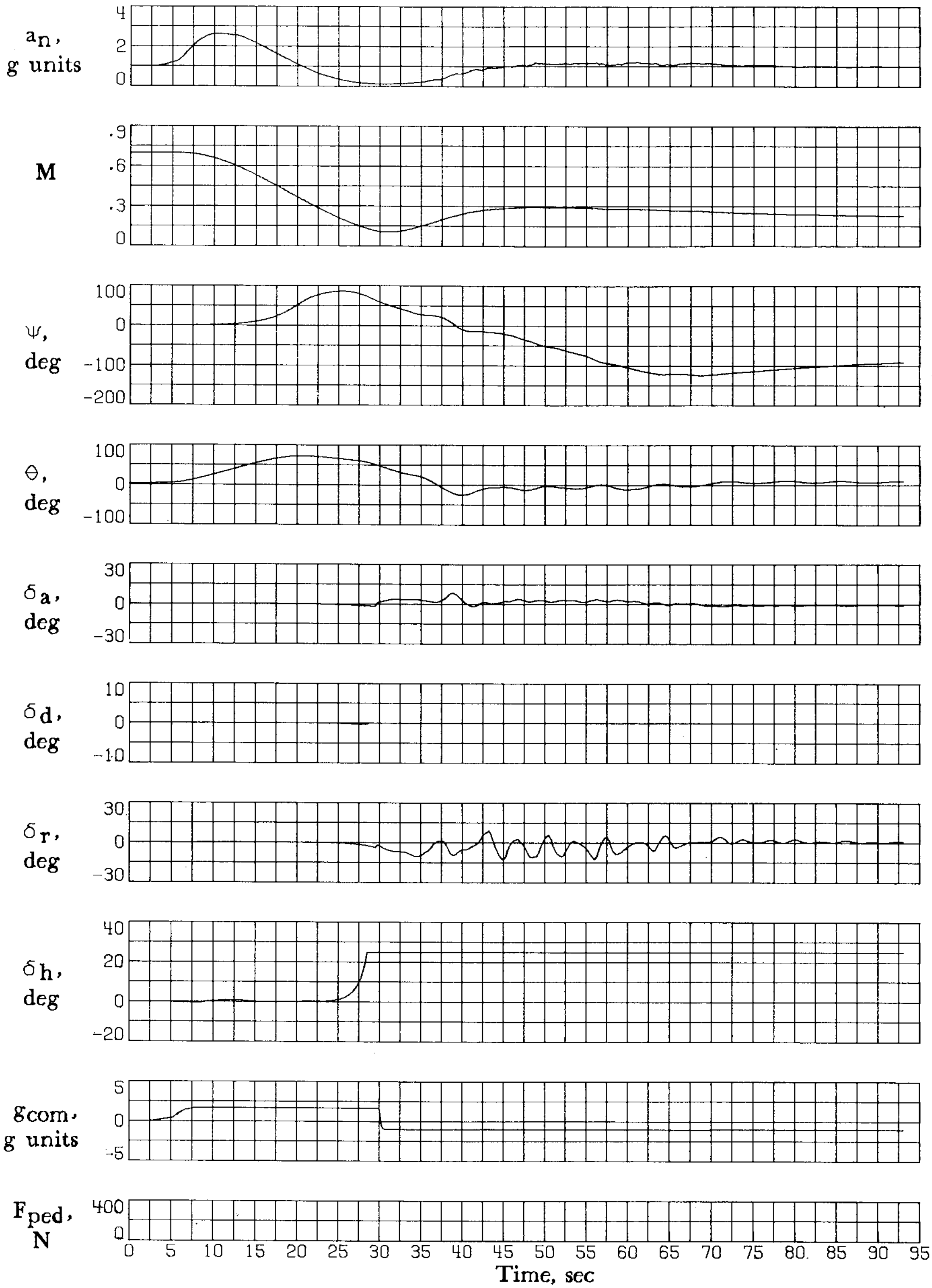

Figure 44.- Continued.

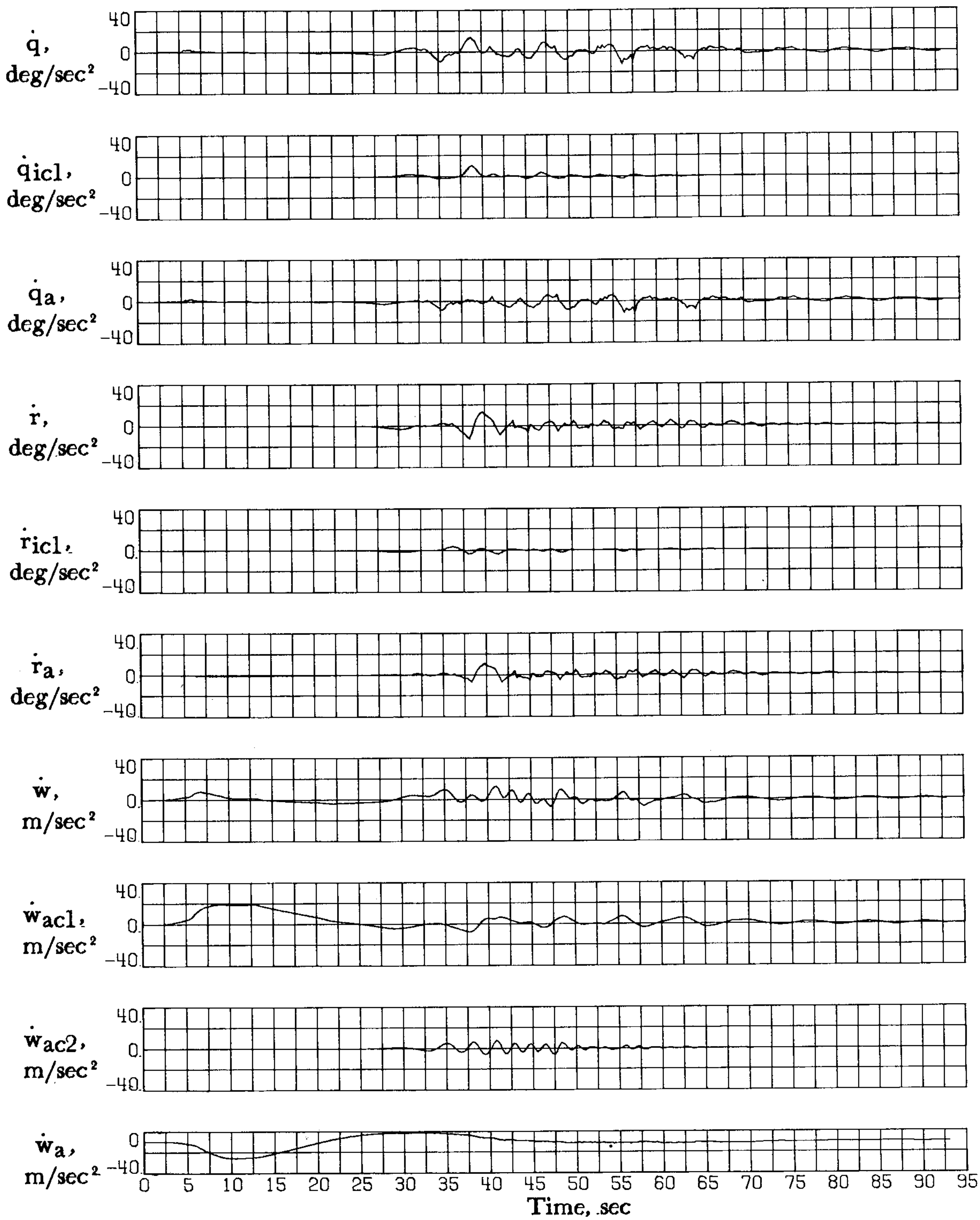

Figure 44.- Concluded.

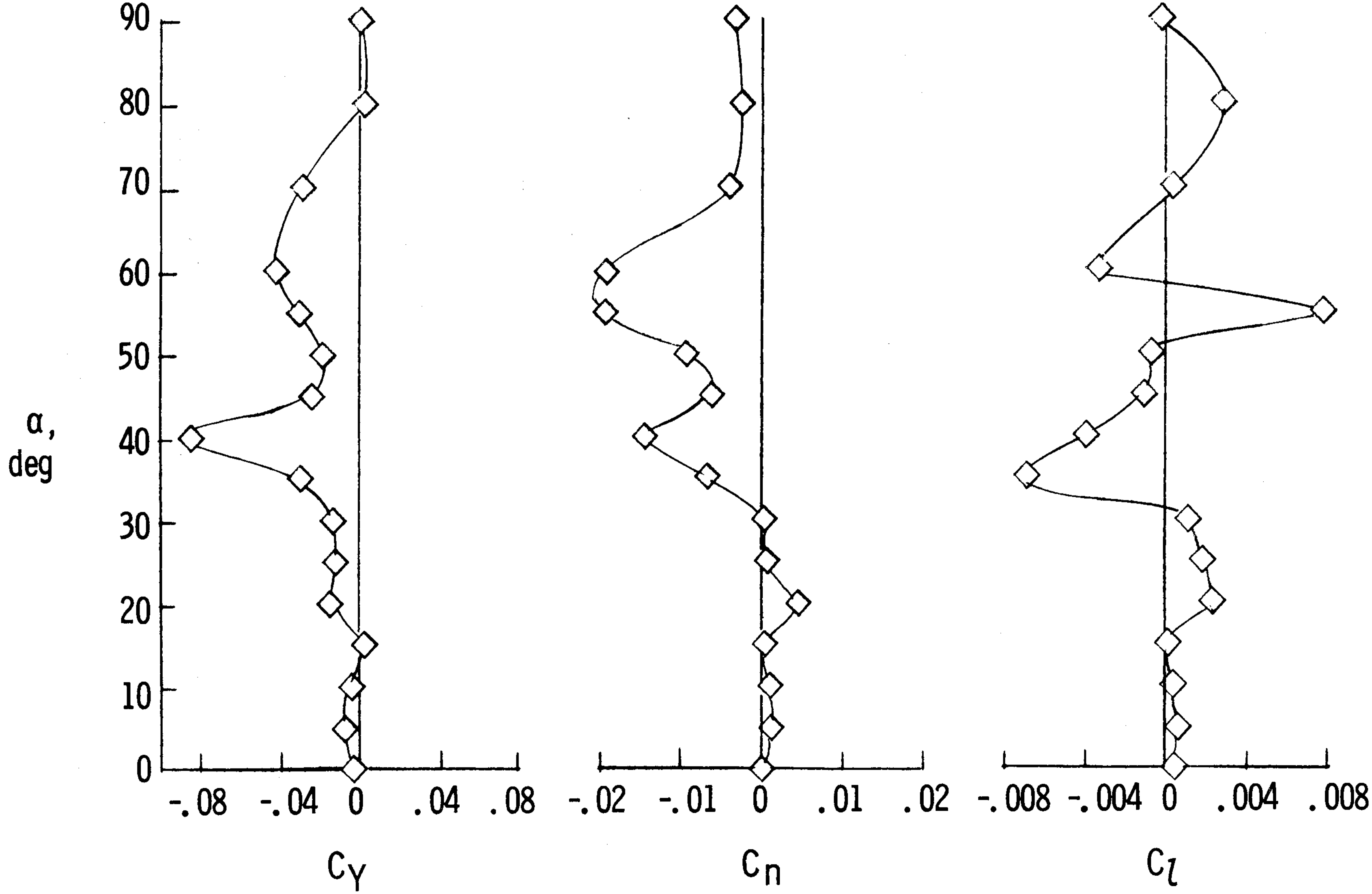

Figure 45.- Variation of measured aerodynamic asymmetries with angle of attack. $\delta_{lef} = 25^{\circ}$.

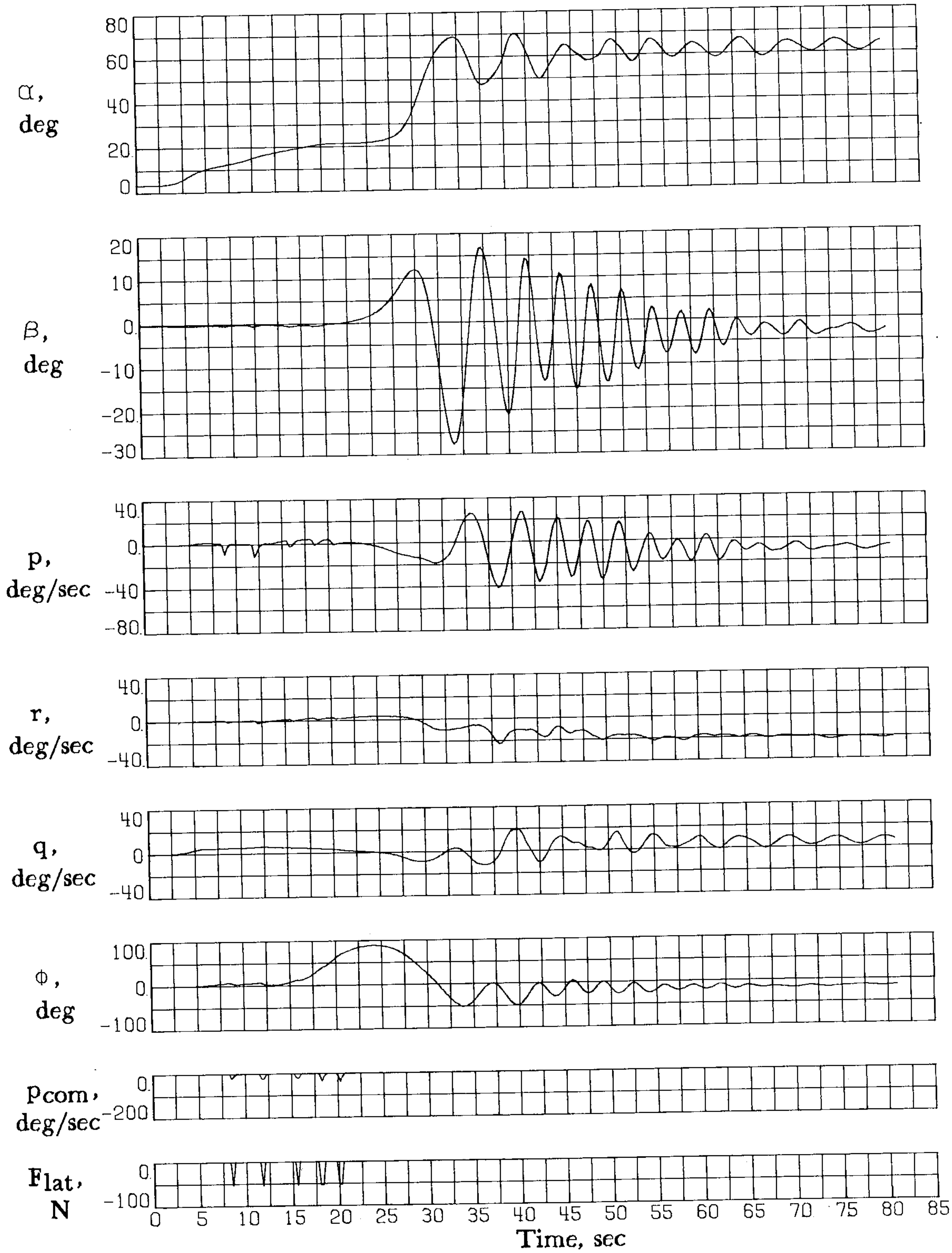

Figure 46.- Deep-stall entry at a center-of-gravity location of $0.35\bar{c}$. Asymmetries modeled; h_o = 9144 m.

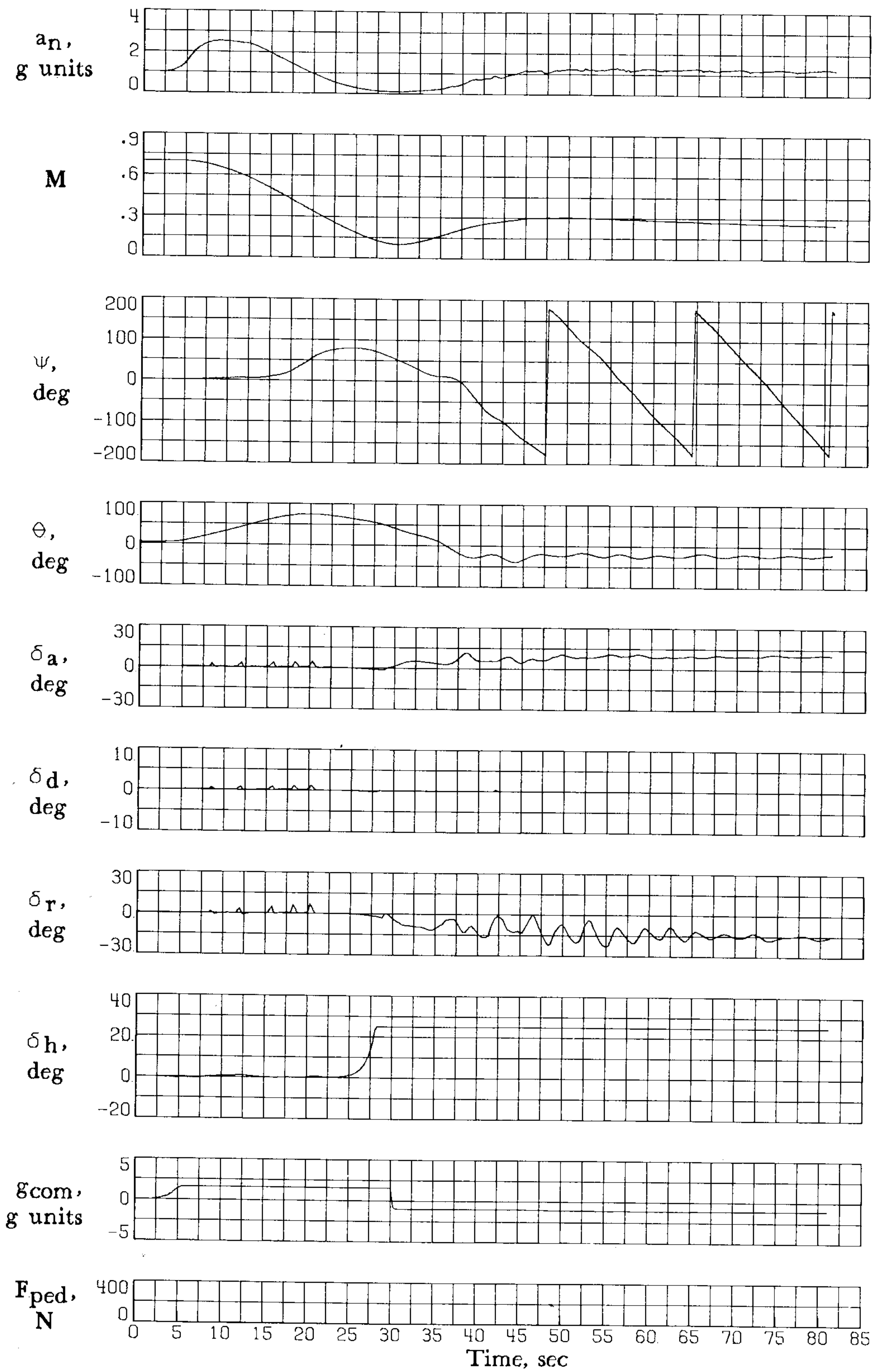

Figure 46.- Continued.

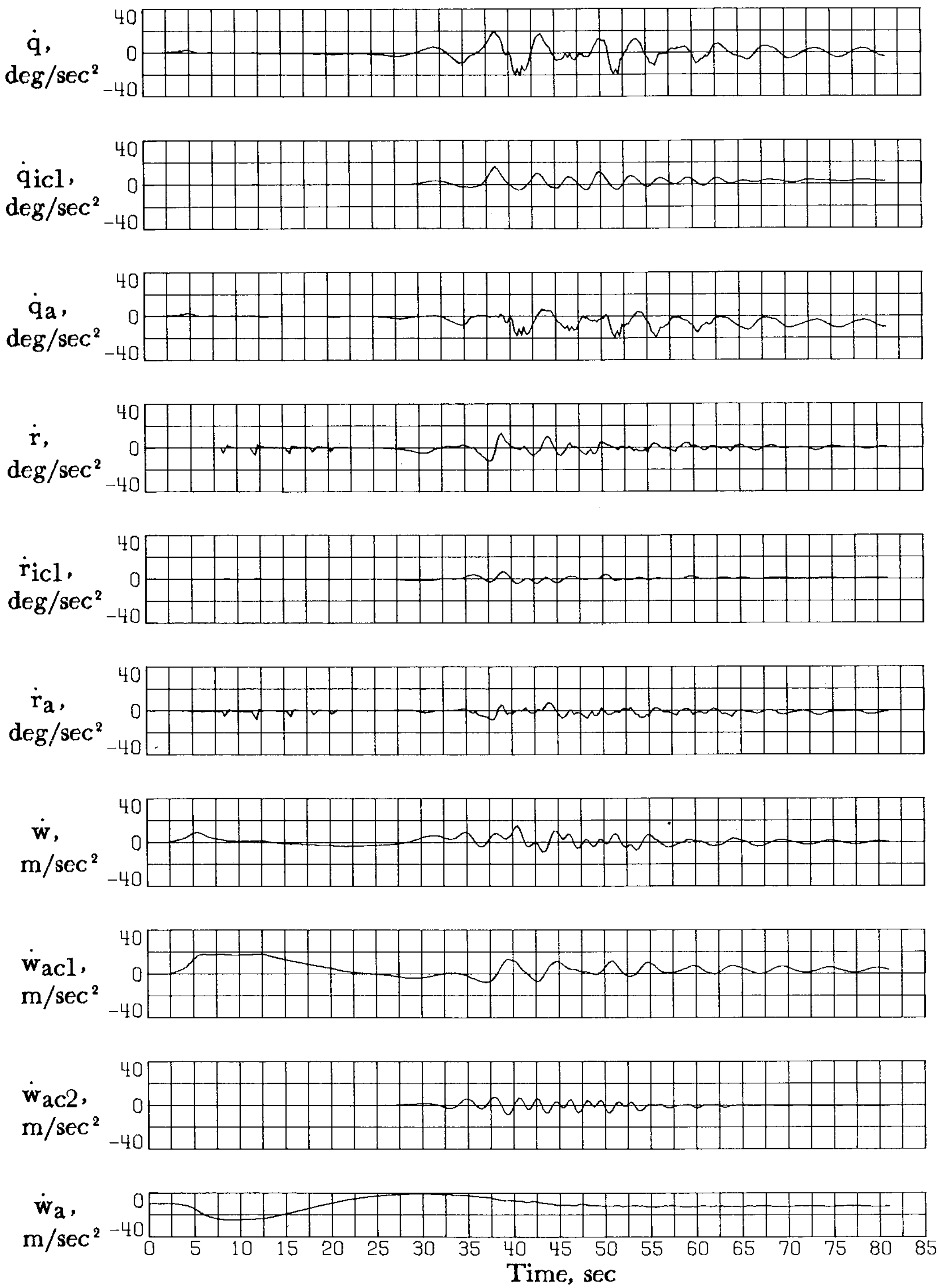

Figure 46.- Concluded.

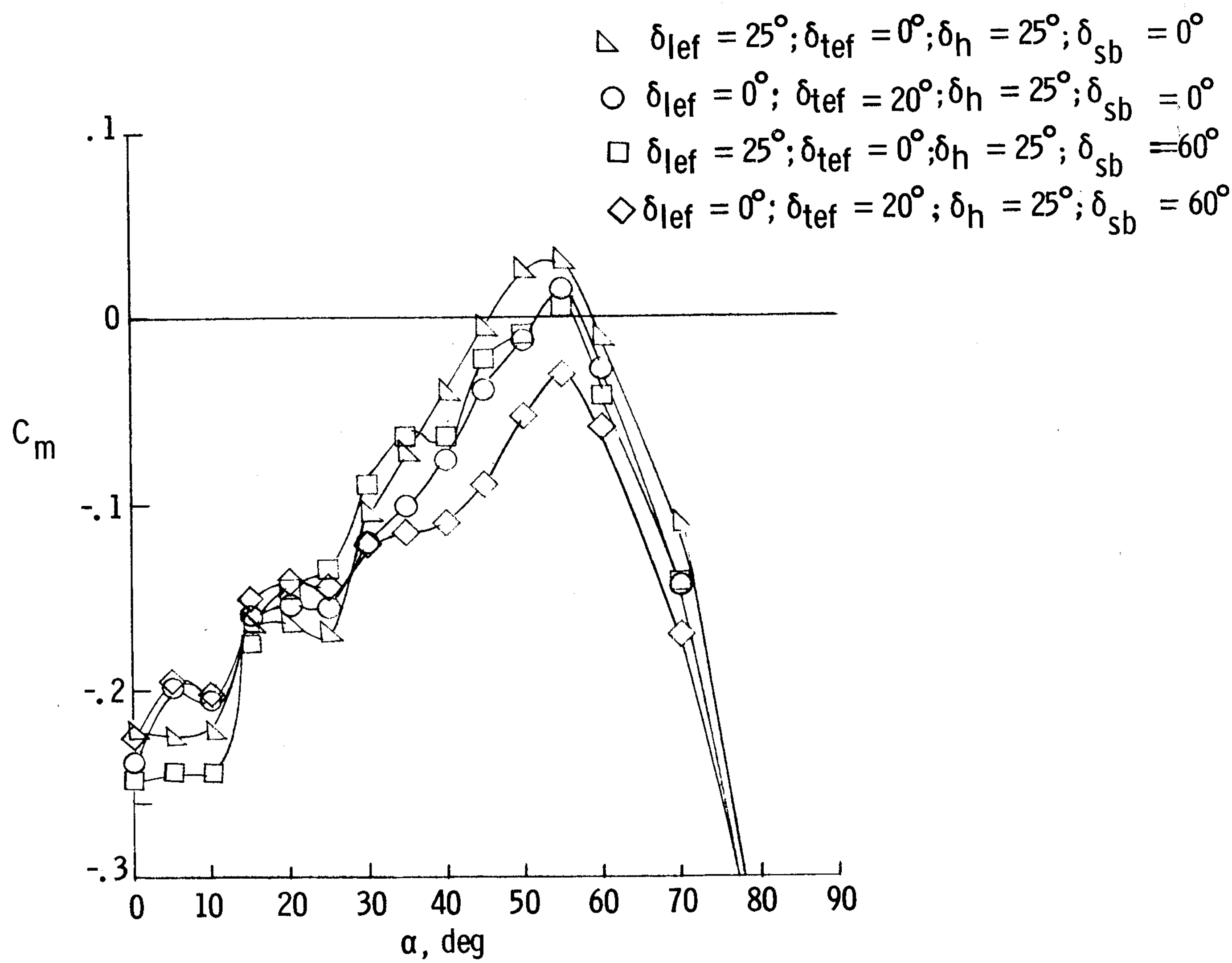

Figure 47.- Effect of flaps and speed brake on pitching-moment variation with angle of attack at a center-of-gravity location of $0.35\bar{c}$. $\delta_h = 25°$.

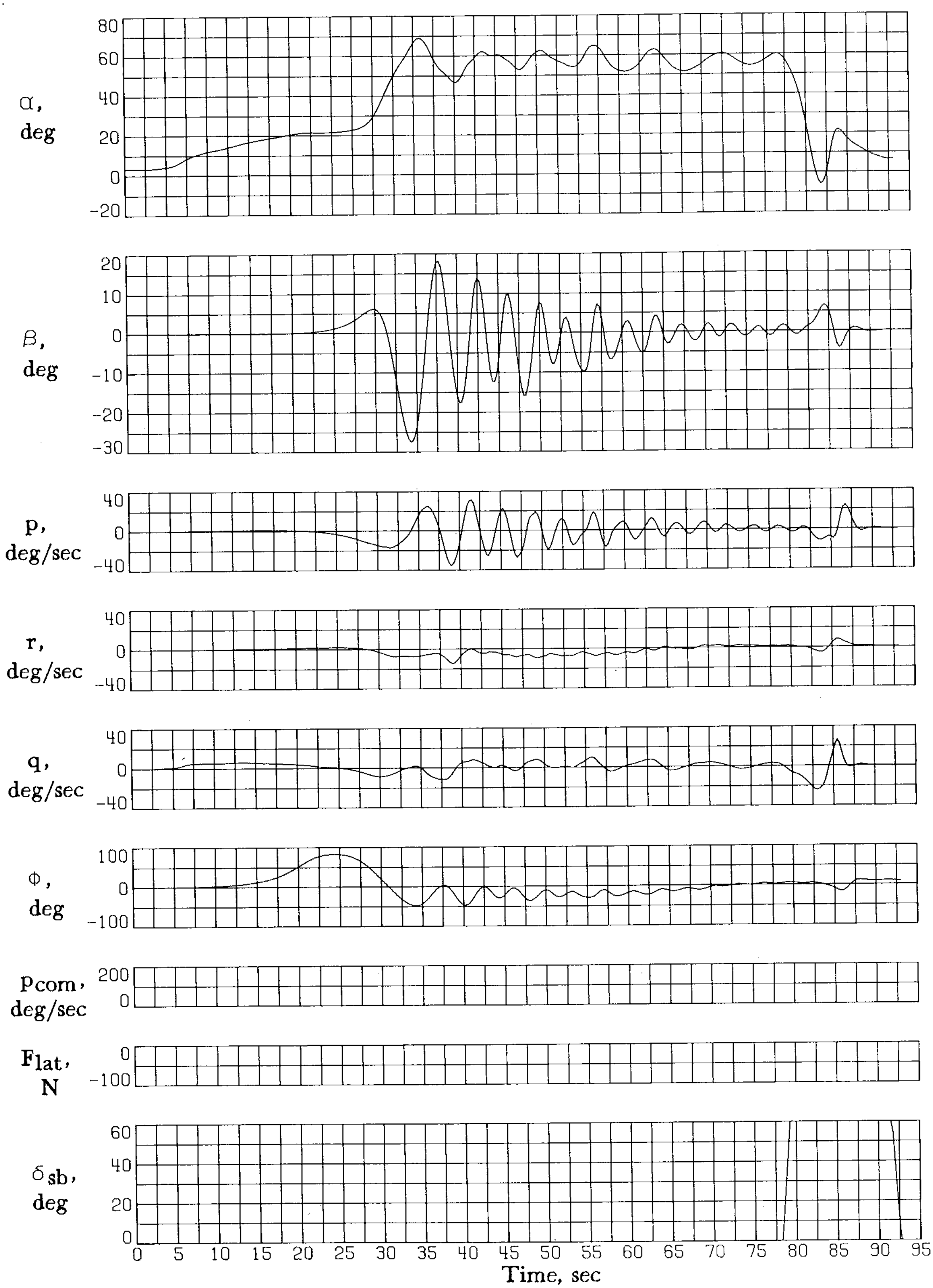

Figure 48.- Deep-stall recovery using speed brake and flaps at a center-of-gravity location of $0.35\bar{c}$. Asymmetries not modeled; h_o = 9144 m.

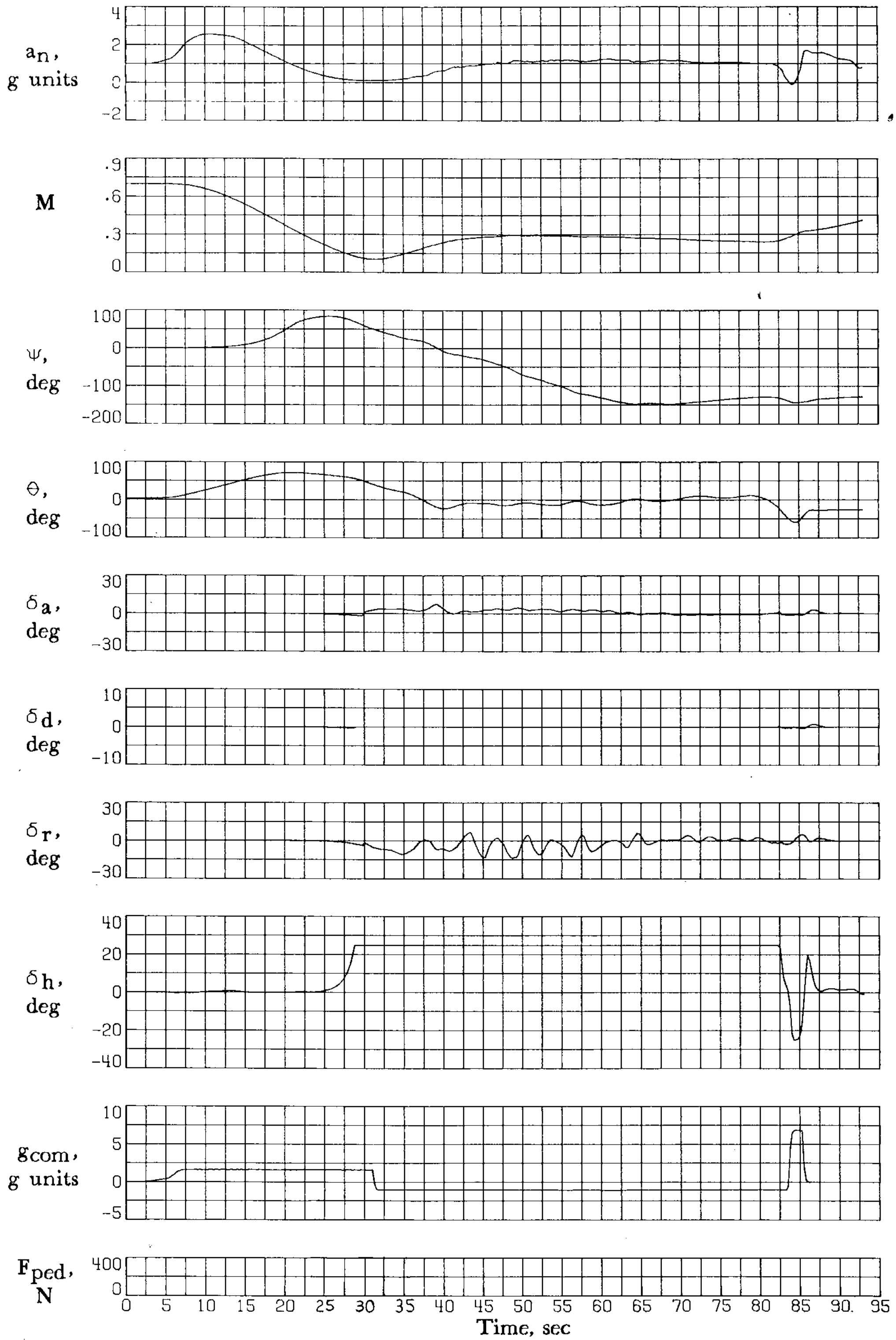

Figure 48.- Continued.

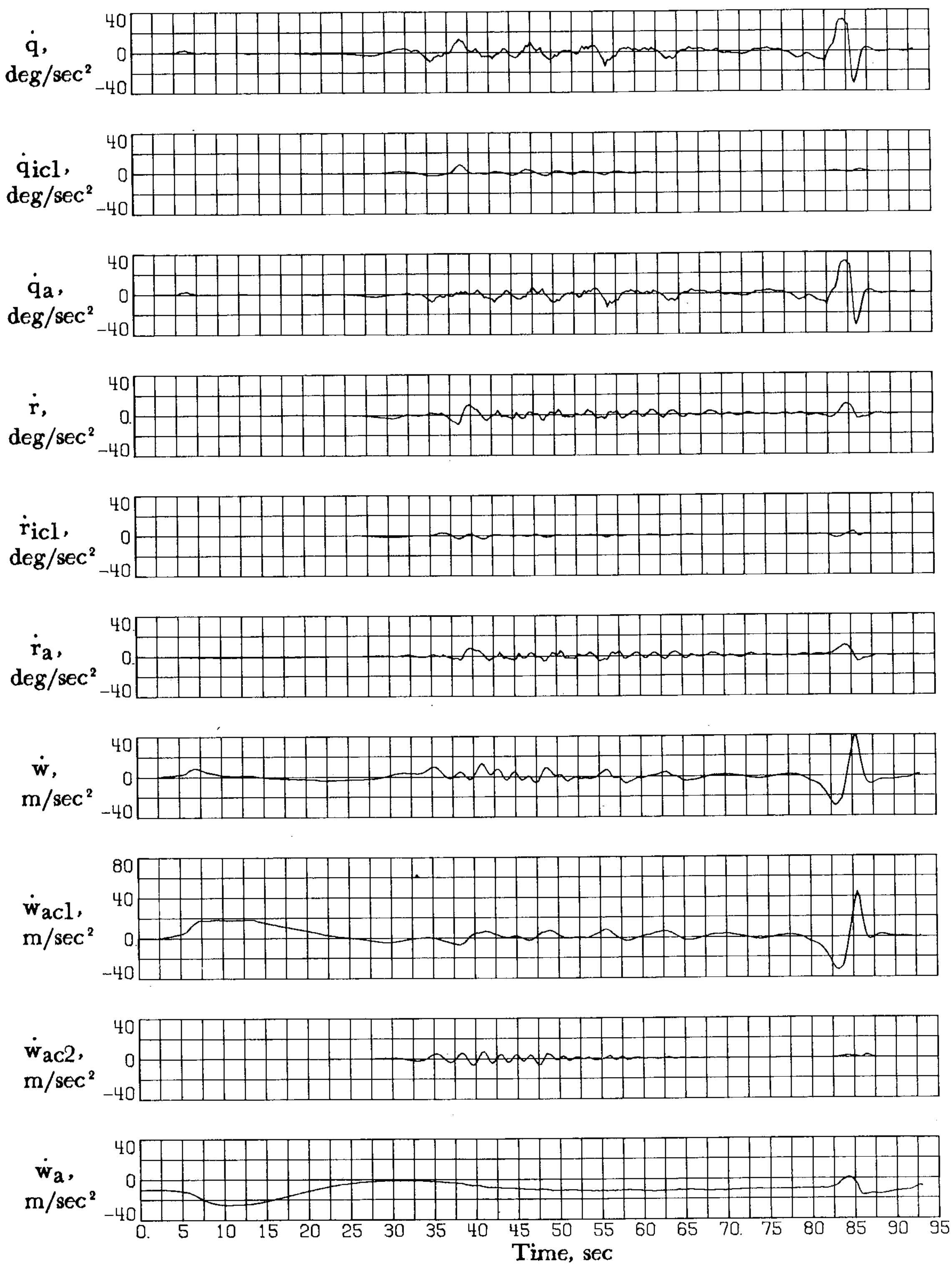

Figure 48.- Concluded.

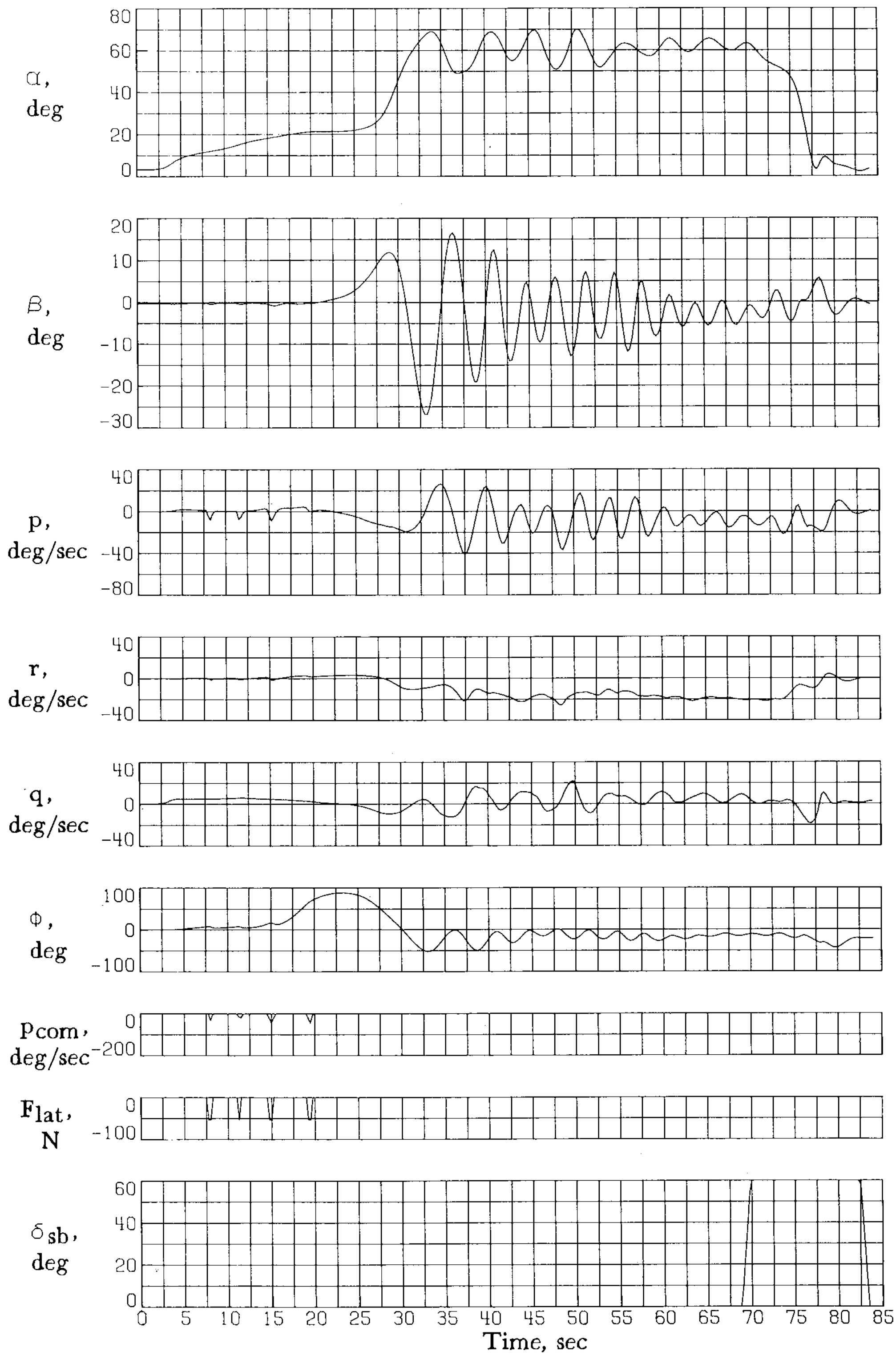

Figure 49.- Deep-stall recovery using speed brake and flaps at a center-of-gravity location of $0.35\bar{c}$. Asymmetries modeled; $h_o = 9144$ m.

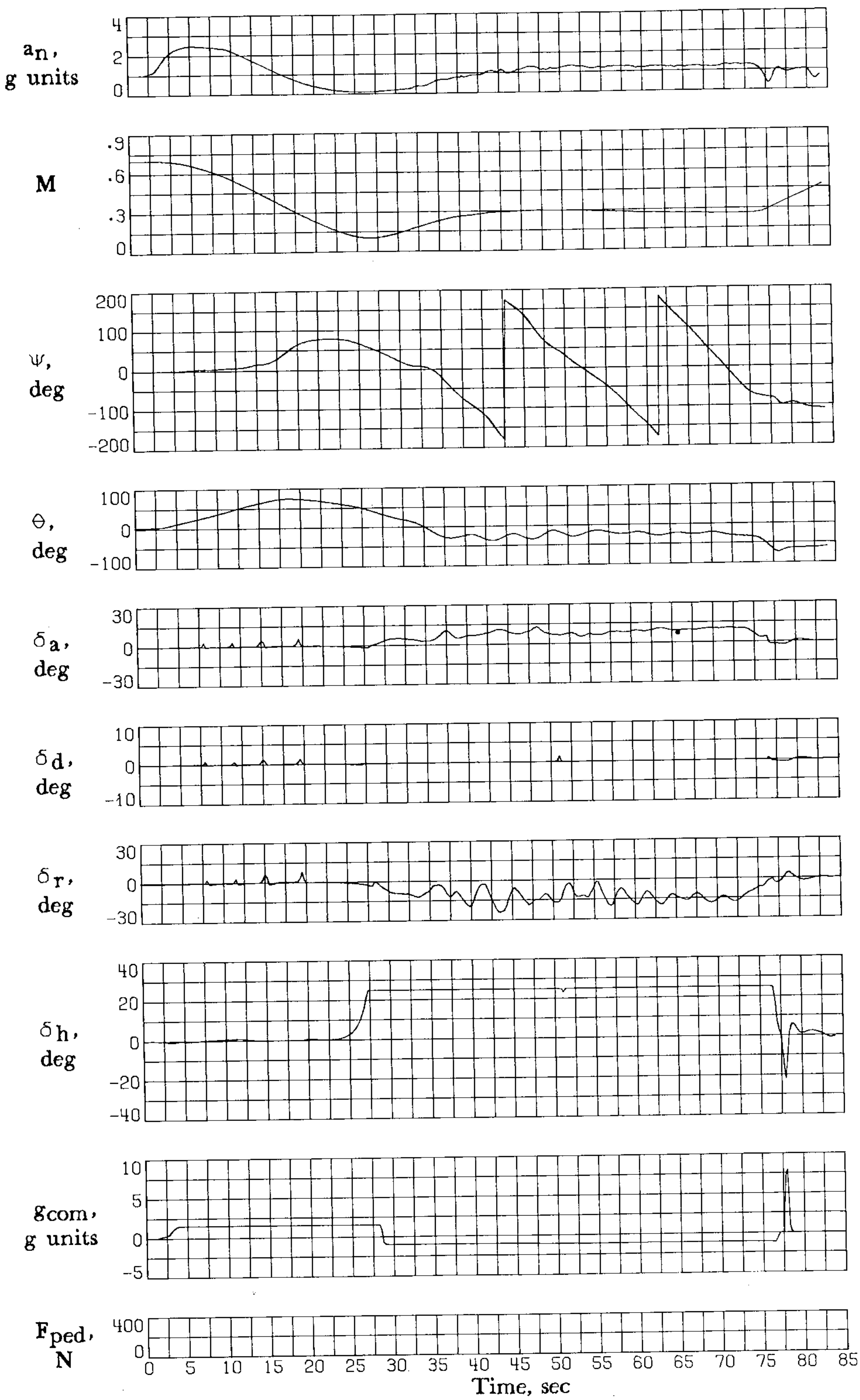

Figure 49.- Continued.

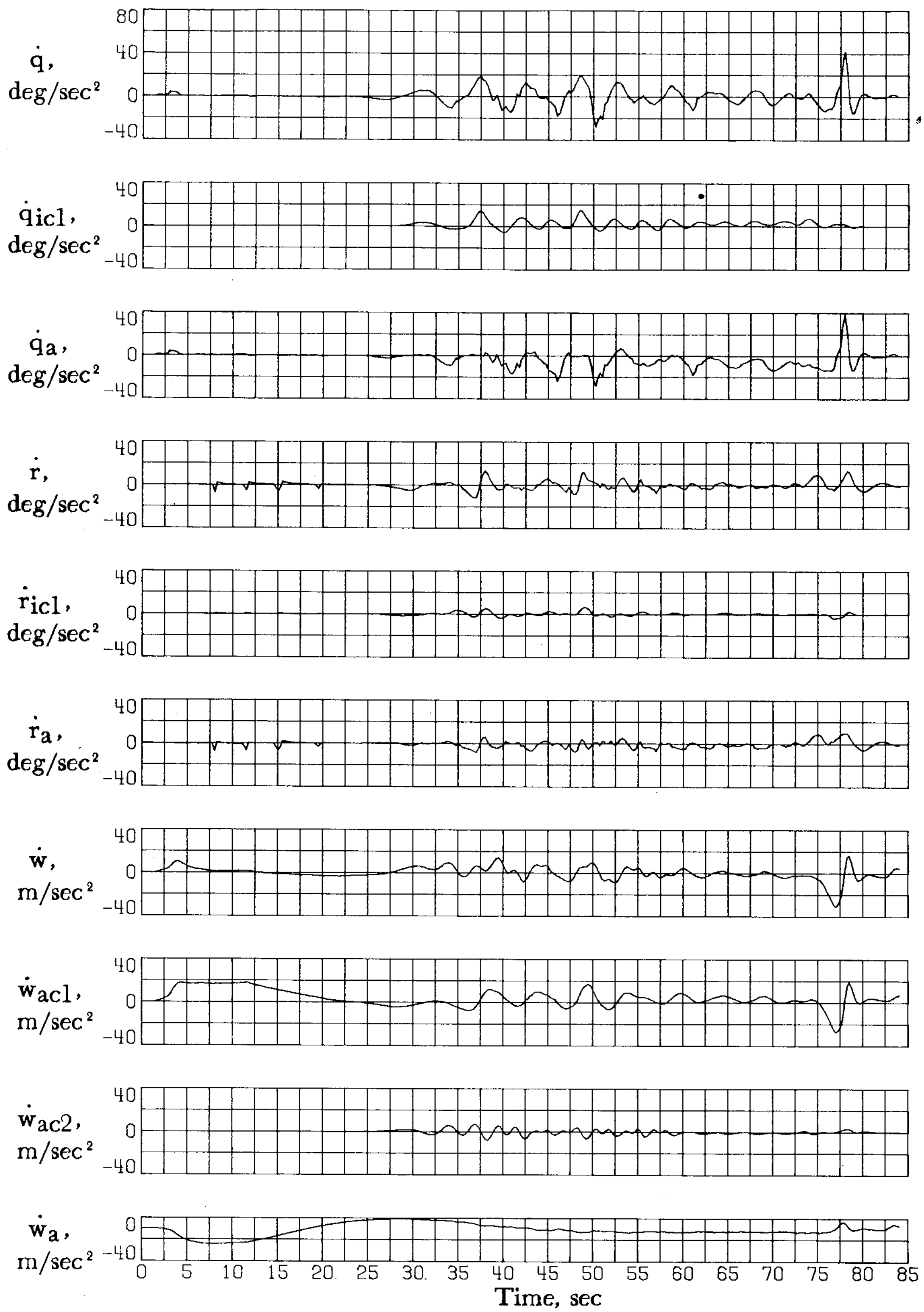

Figure 49.- Concluded.

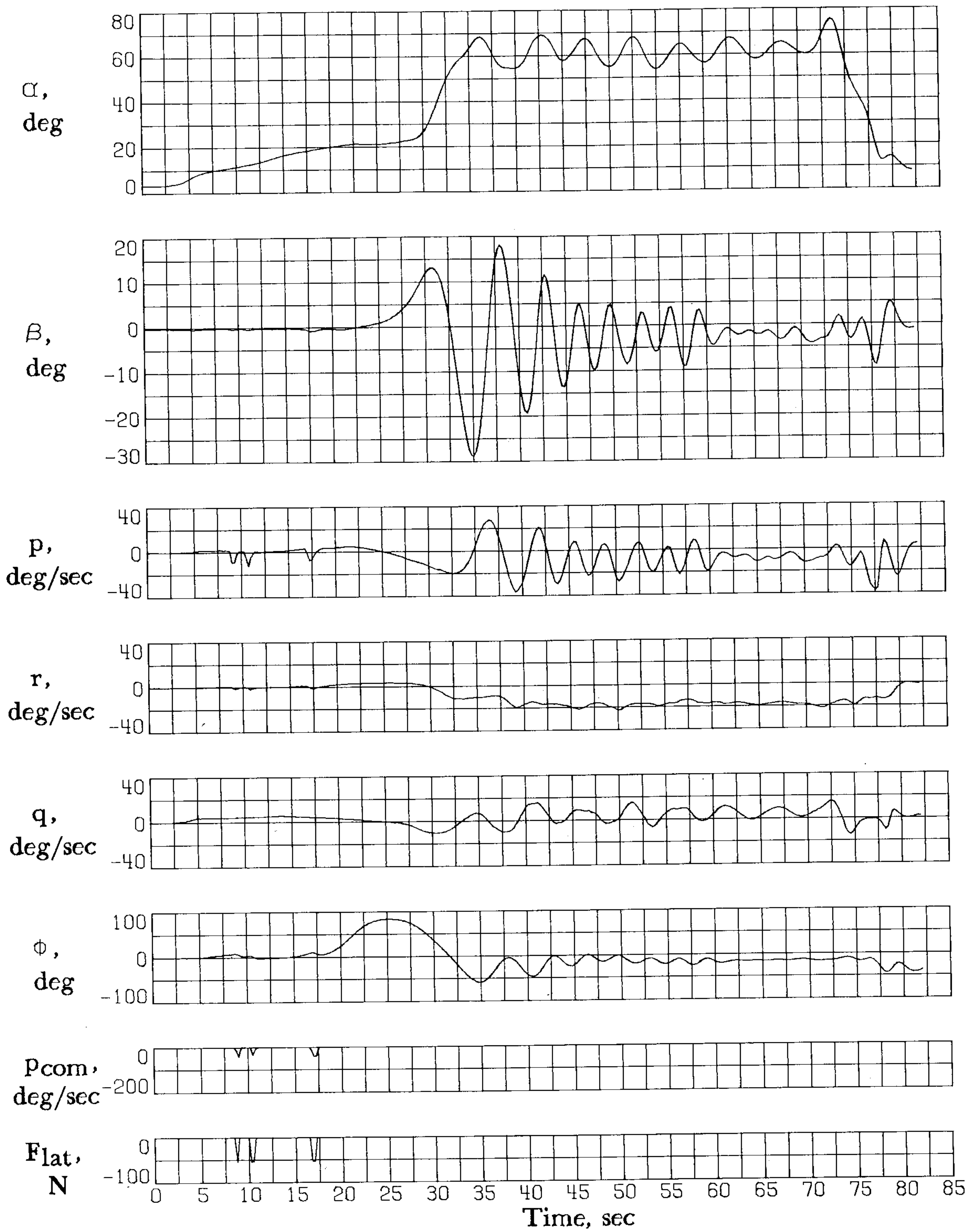

Figure 50.- Deep-stall recovery using pitch-rocking technique at a center-of-gravity location of $0.35\bar{c}$. Asymmetries modeled; h_o = 9144 m.

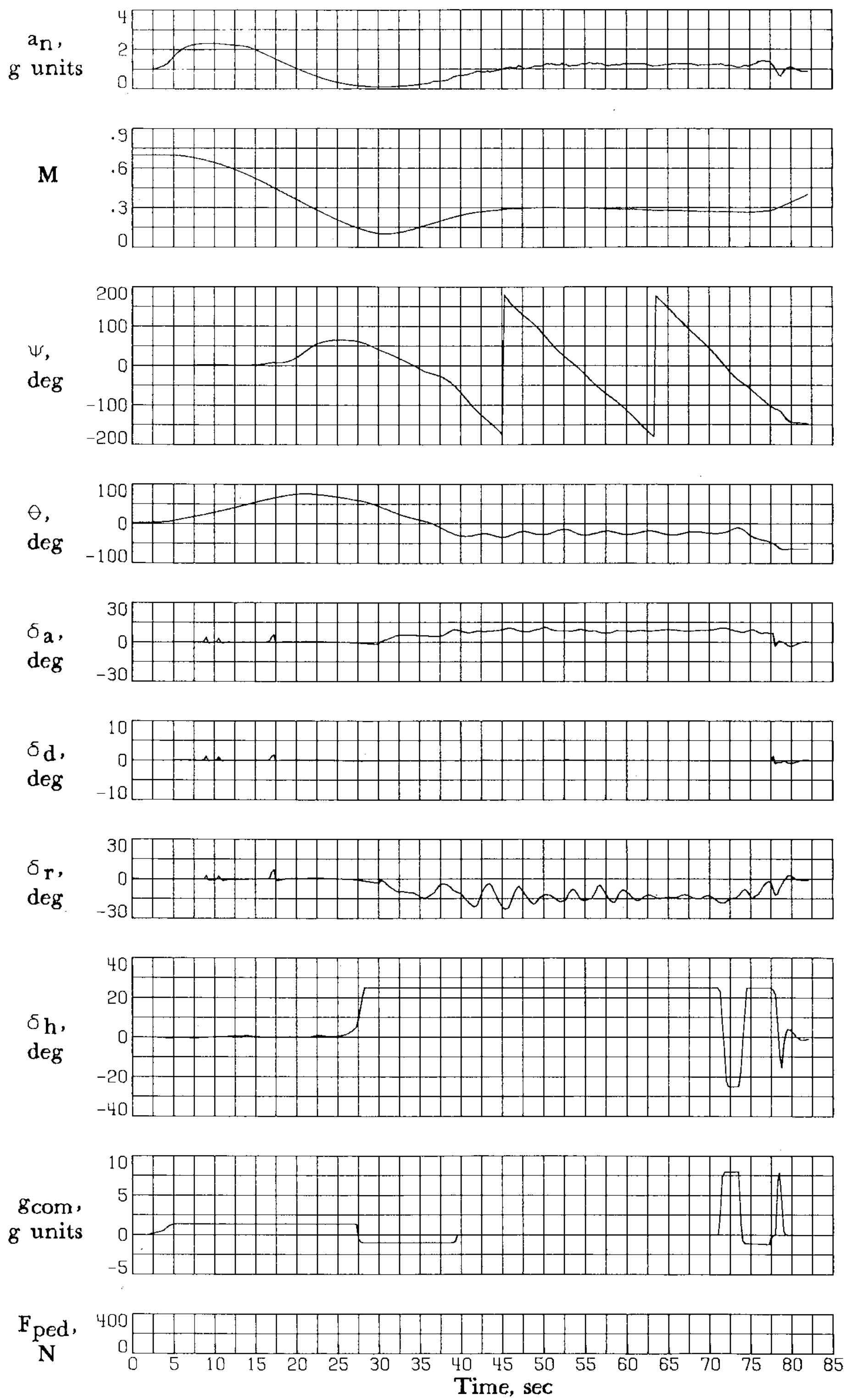

Figure 50.- Continued.

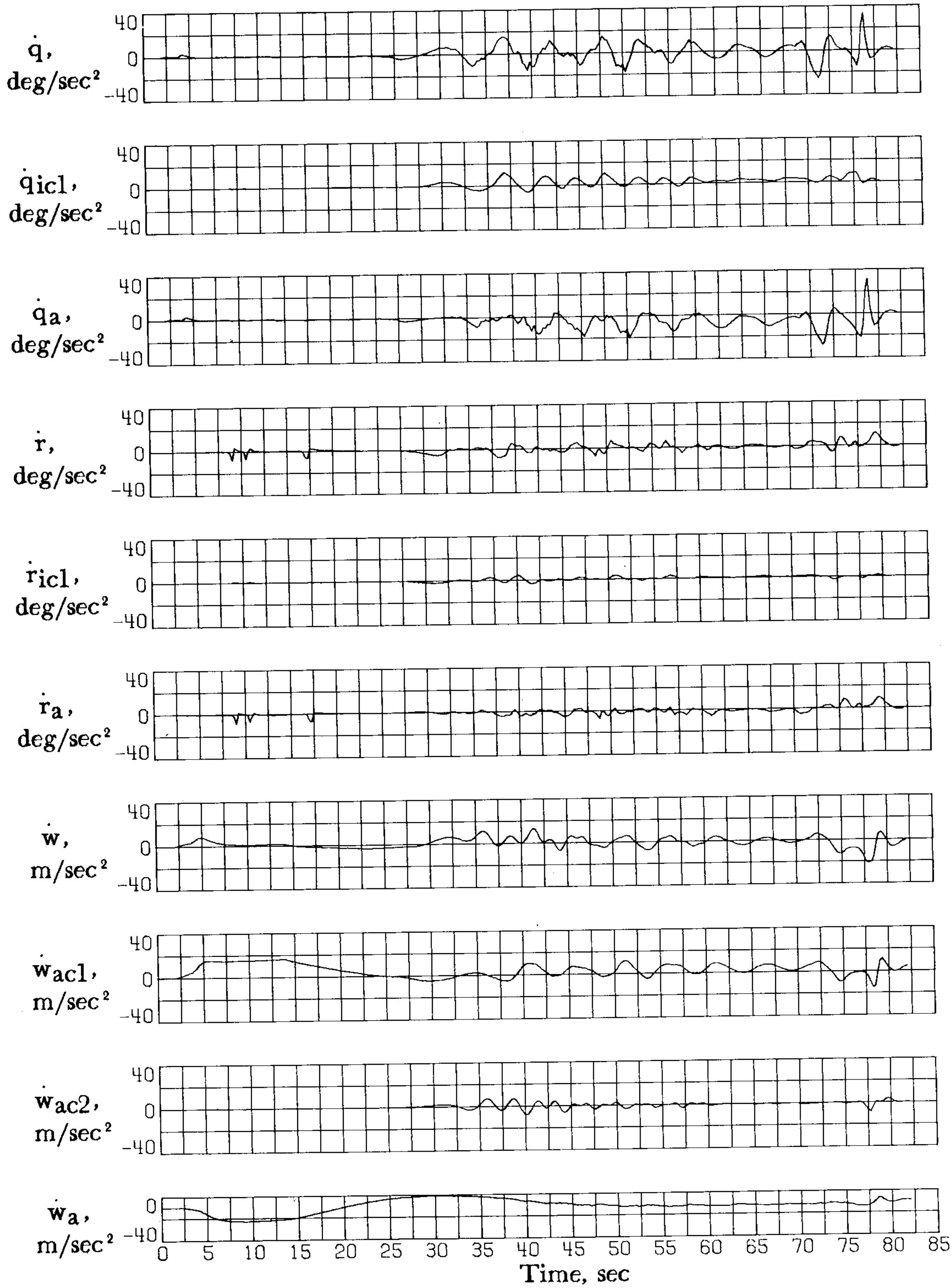

Figure 50.- Concluded.

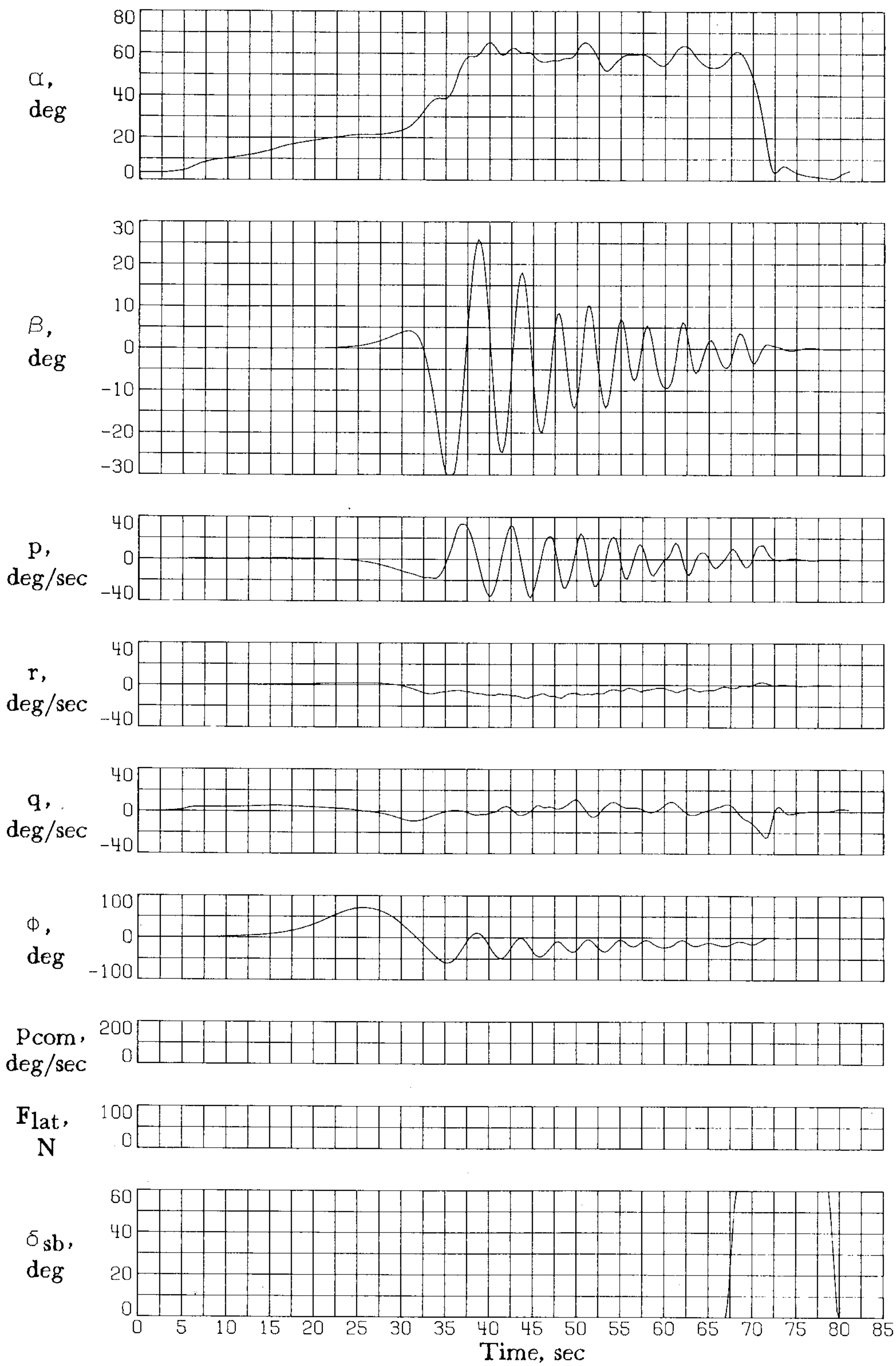

Figure 51.- Deep-stall recovery using speed brake and flaps at a center-of-gravity location of $0.375\bar{c}$. Asymmetries not modeled; $h_o = 9144$ m.

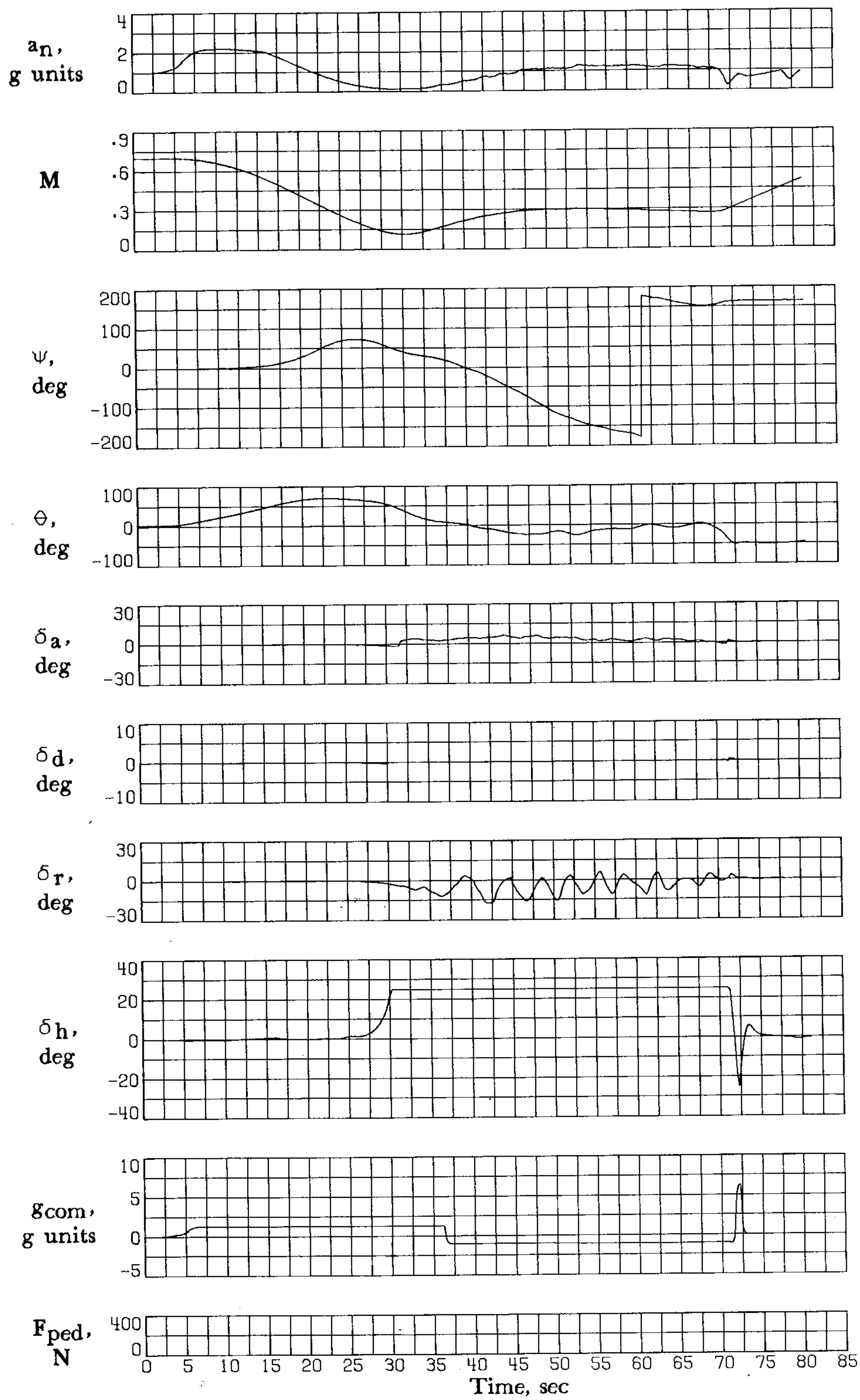

Figure 51.- Continued.

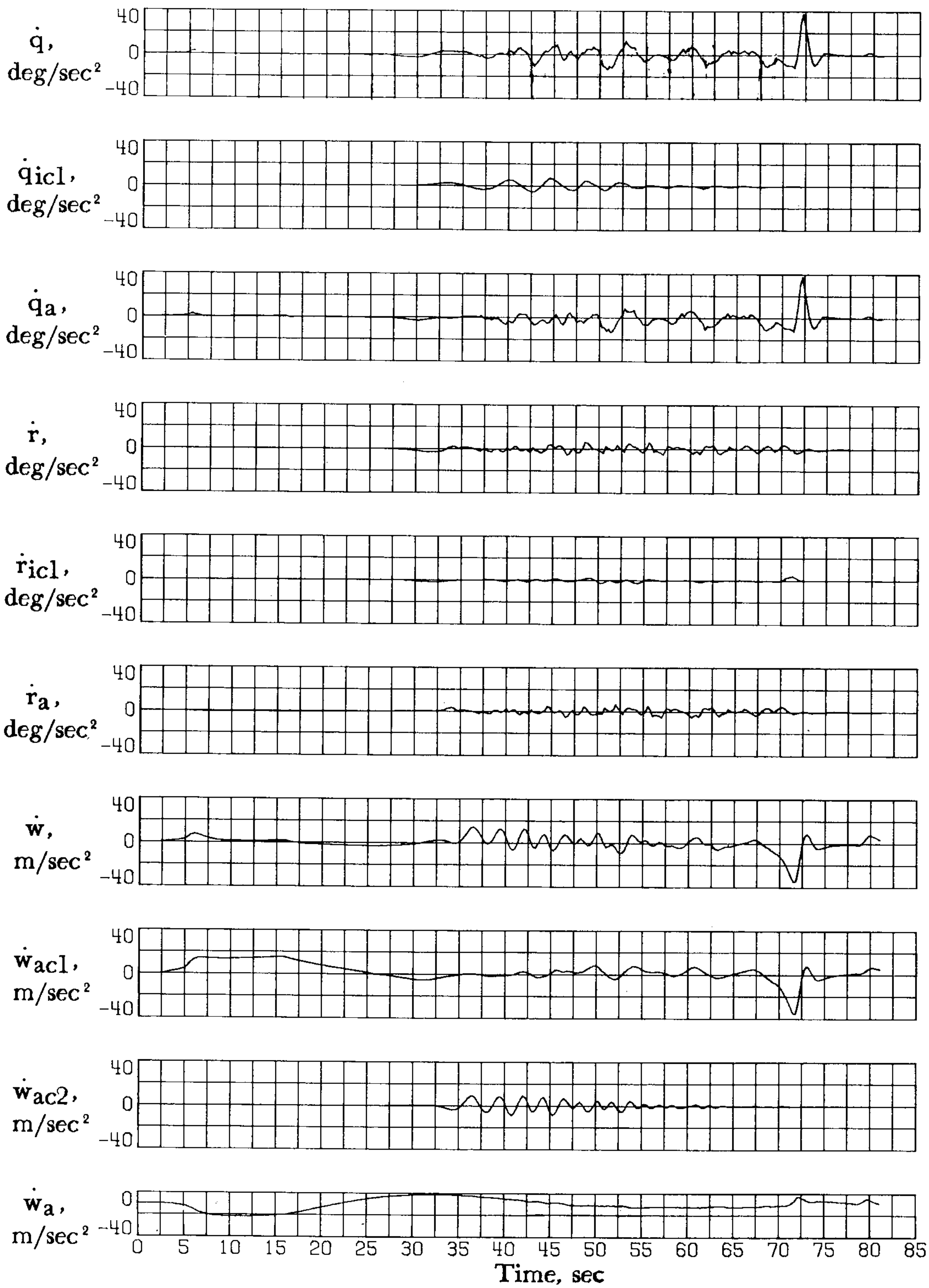

Figure 51.- Concluded.

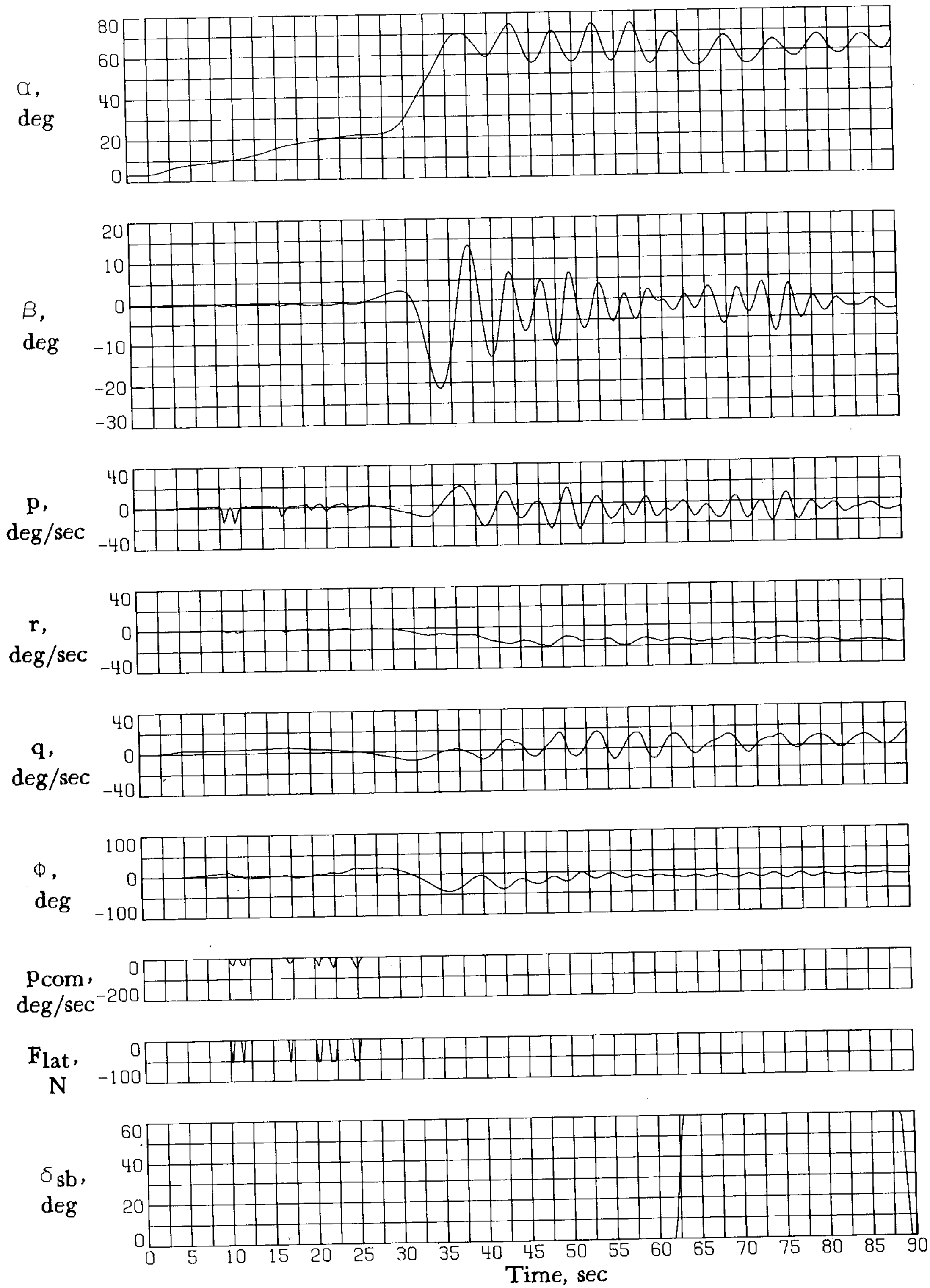

Figure 52.- Deep-stall recovery attempt using speed brake and flap at a center-of-gravity location of $0.375\bar{c}$. Asymmetries modeled; h_o = 9144 m.

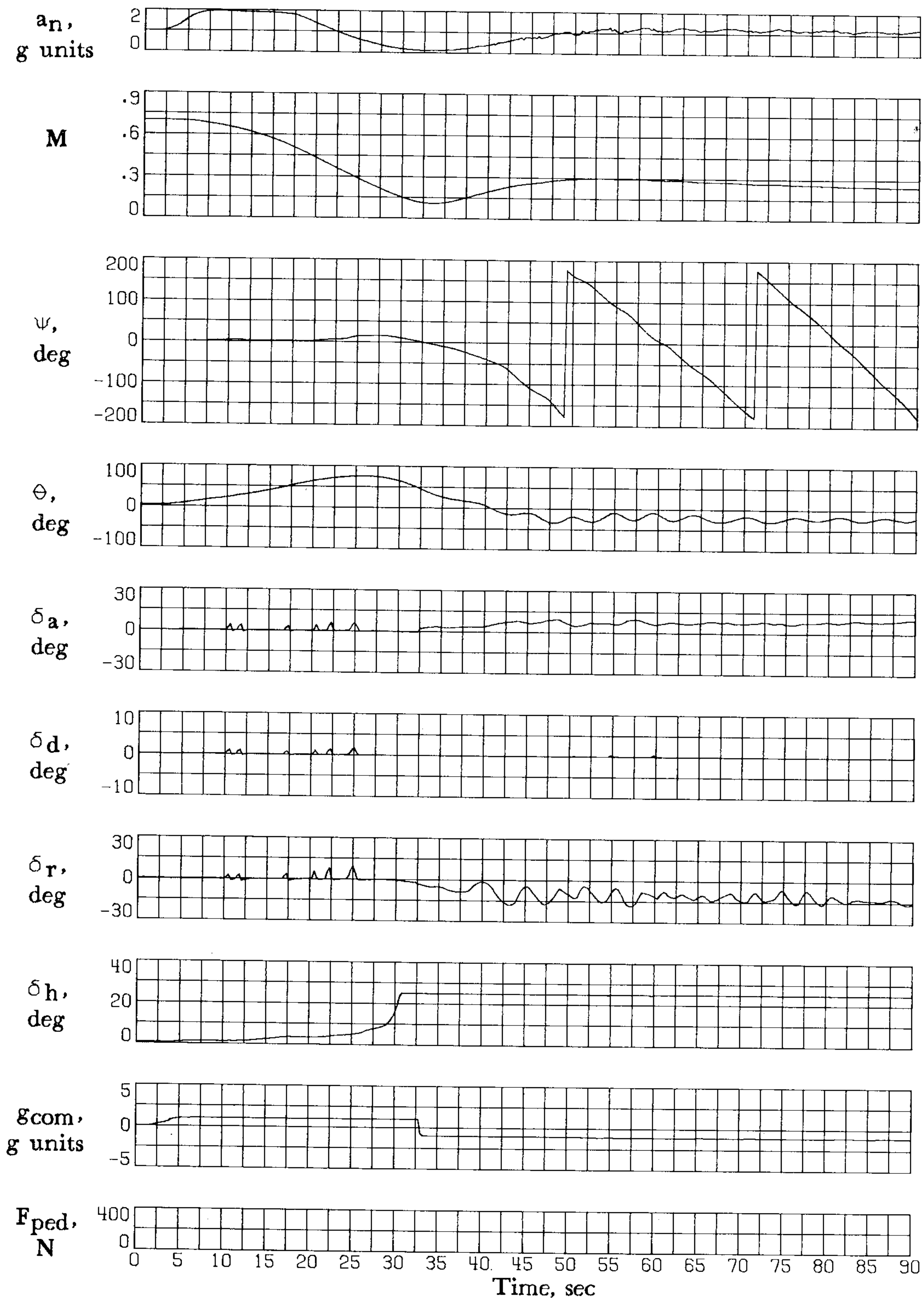

Figure 52.- Continued.

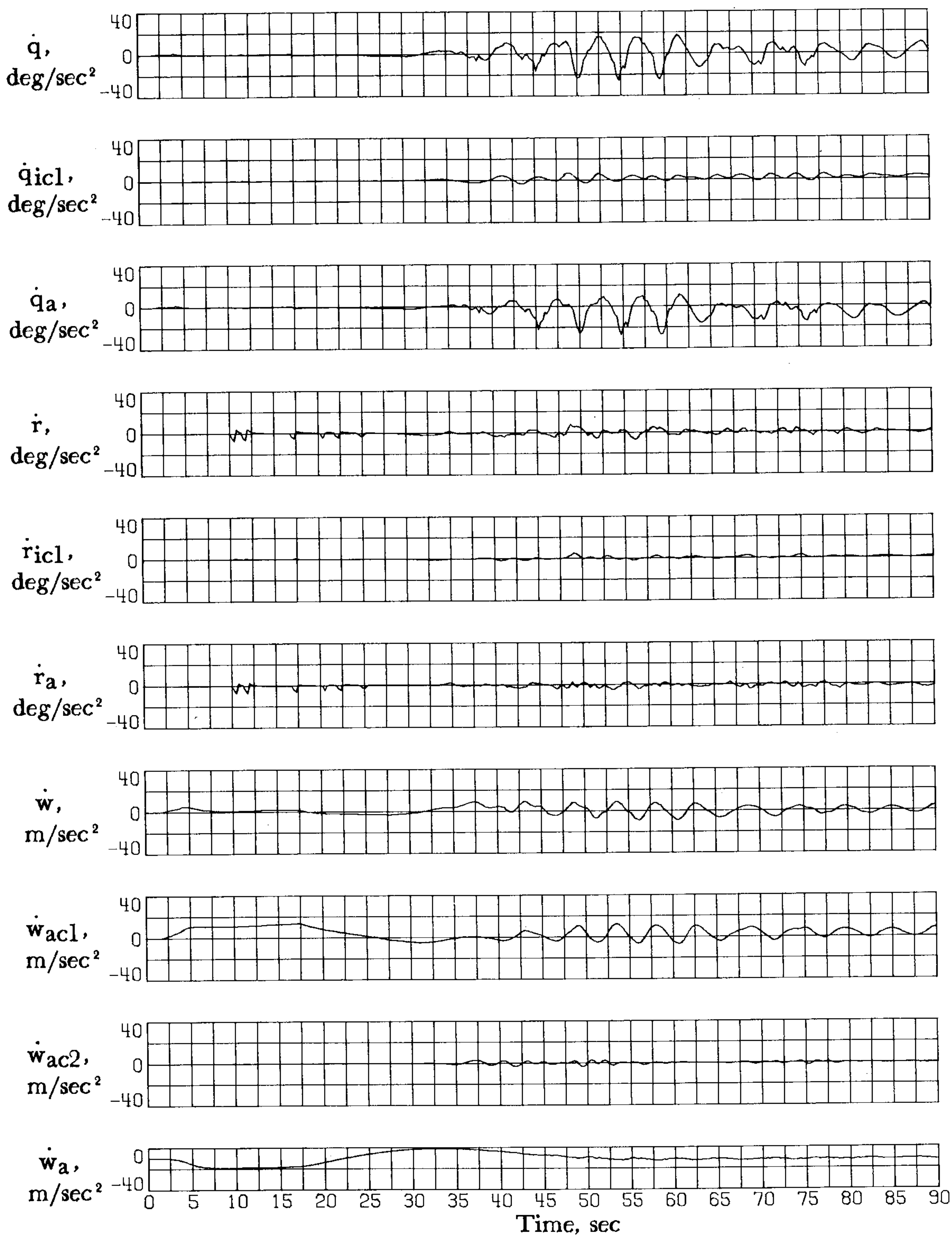

Figure 52.- Concluded.

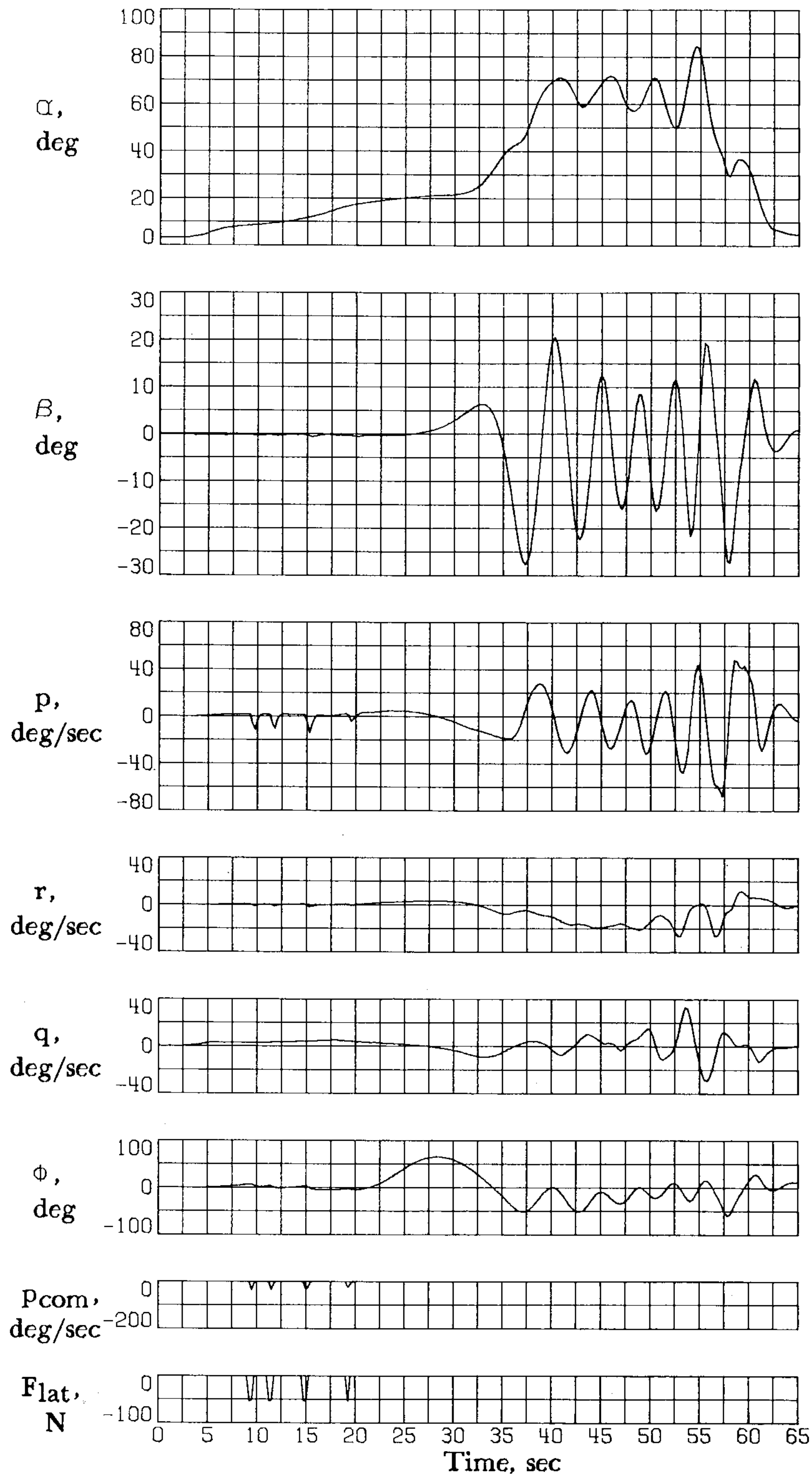

Figure 53.- Deep-stall recovery using pitch-rocking technique at a center-of-gravity location of $0.375\bar{c}$. Asymmetries modeled; $h_o = 9144$ m.

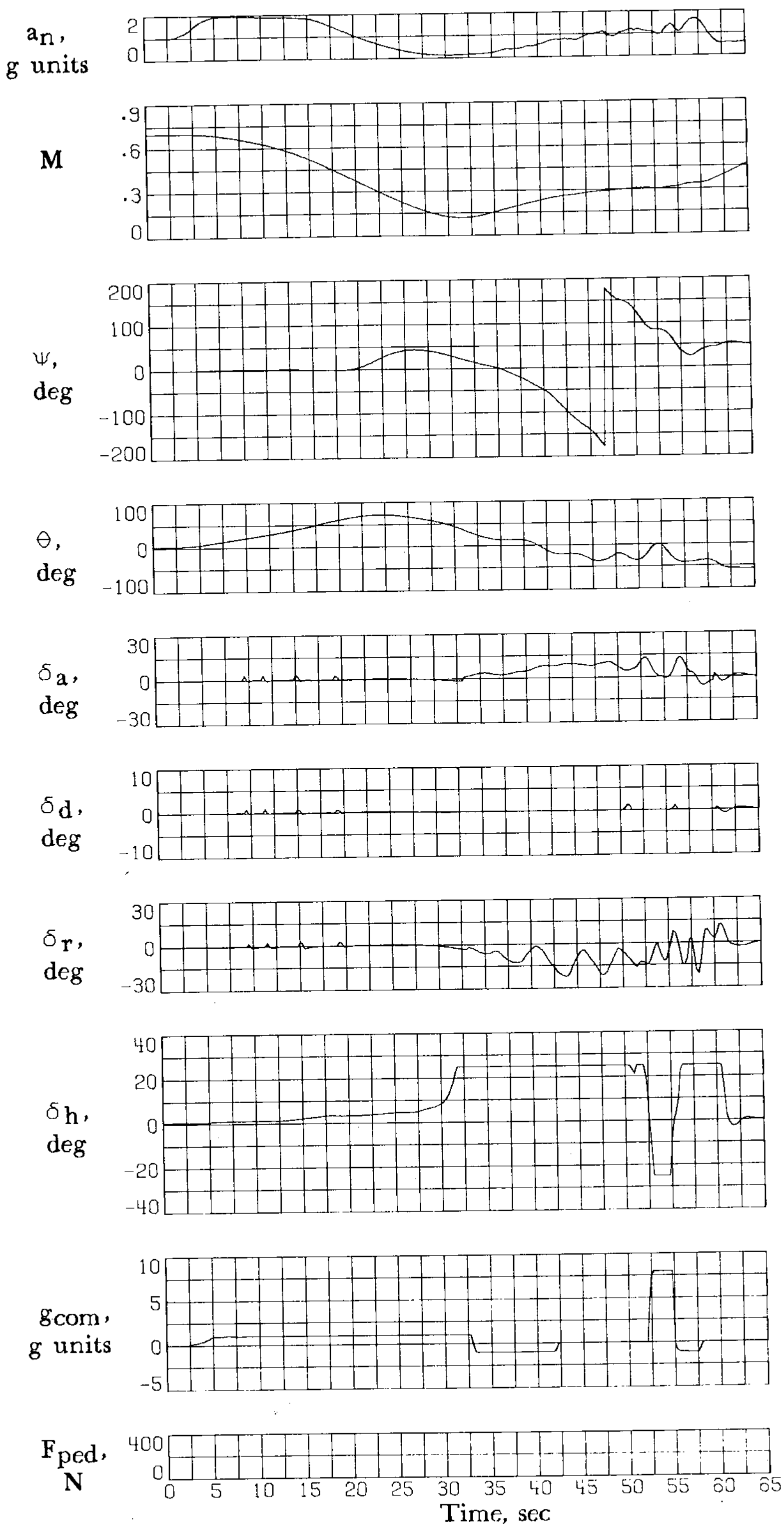

Figure 53.- Continued.

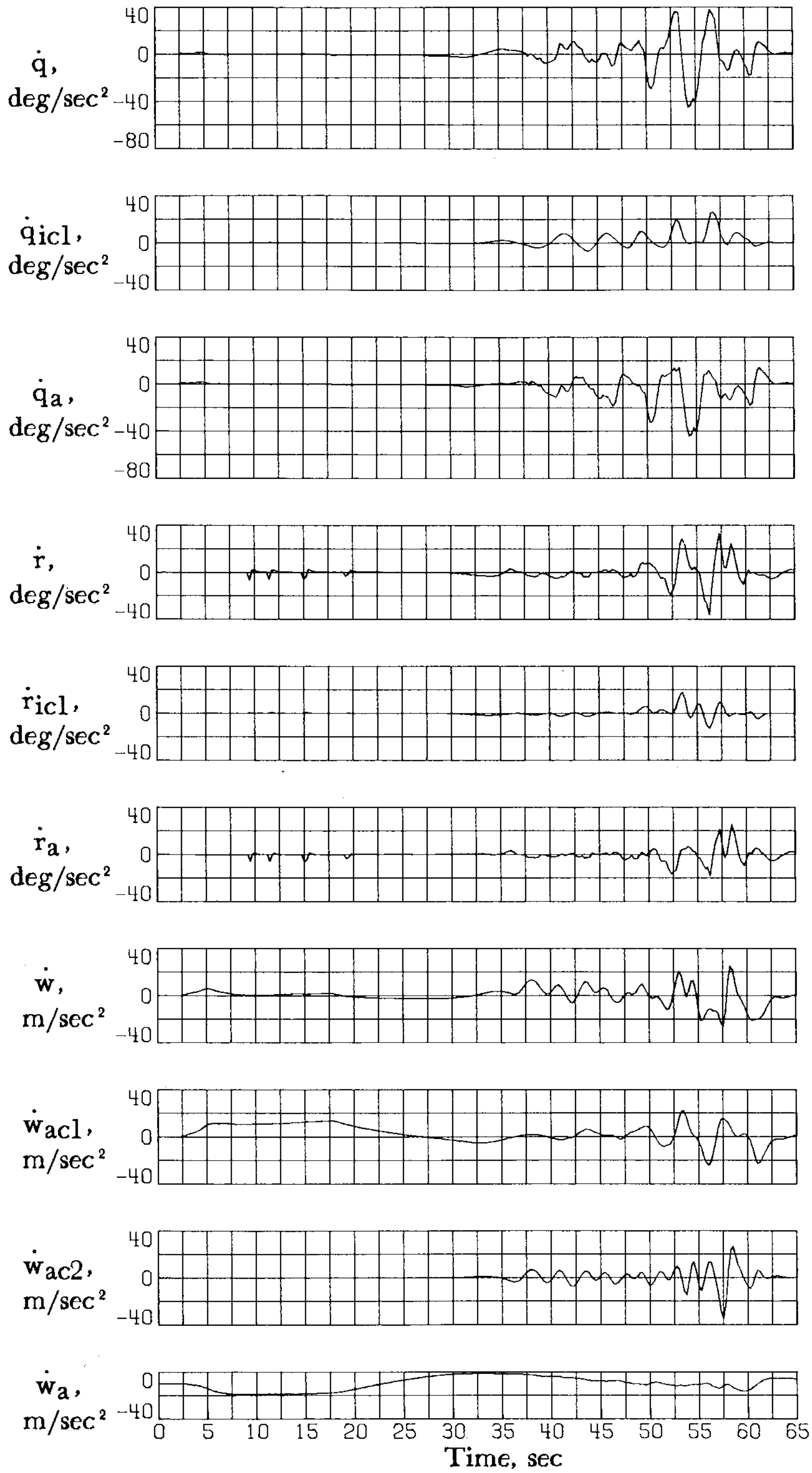

Figure 53.- Concluded.

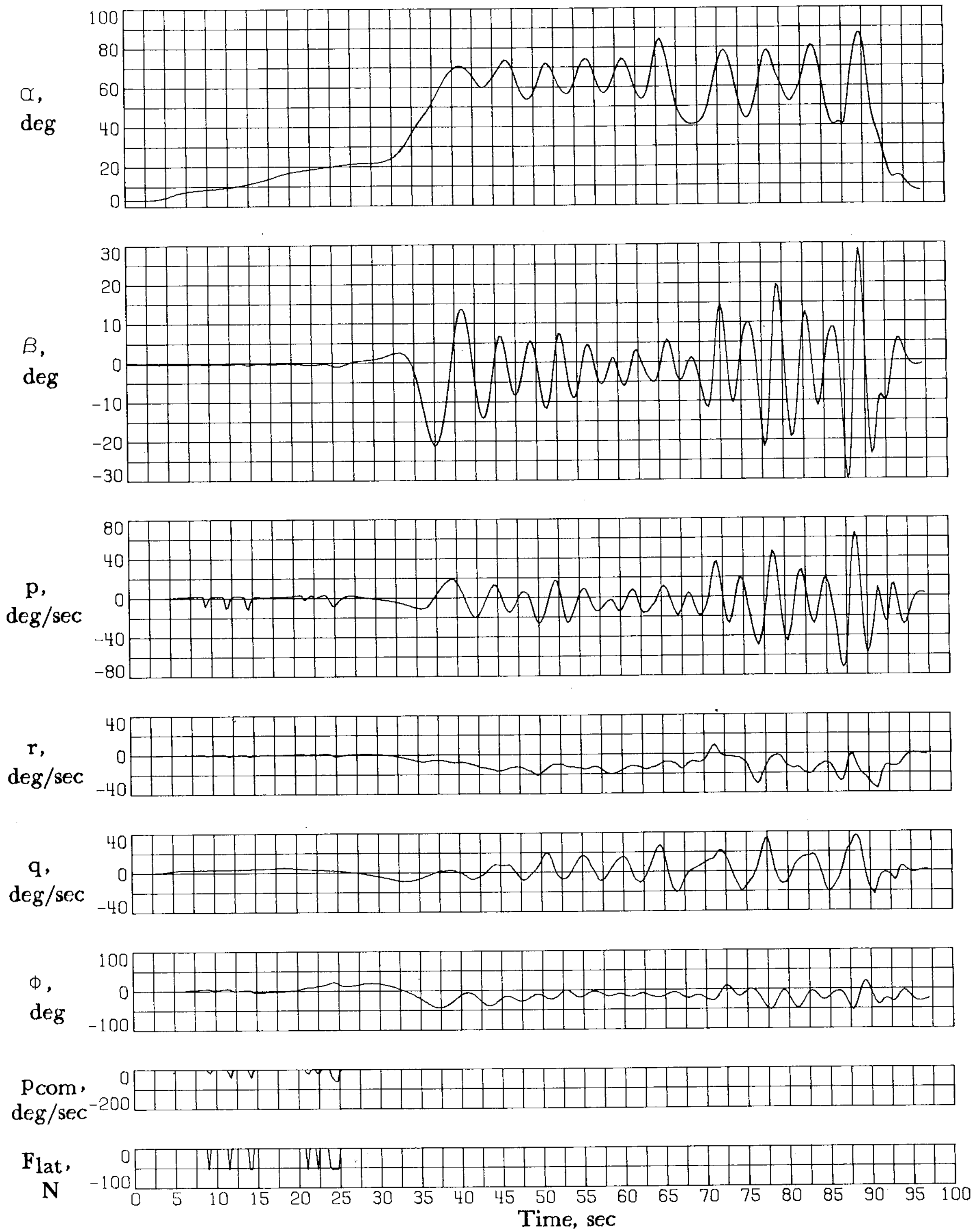

Figure 54.- Deep-stall recovery using pitch-rocking techniques at a center-of-gravity location of $0.375\bar{c}$. Asymmetries modeled; h_o = 9144 m.

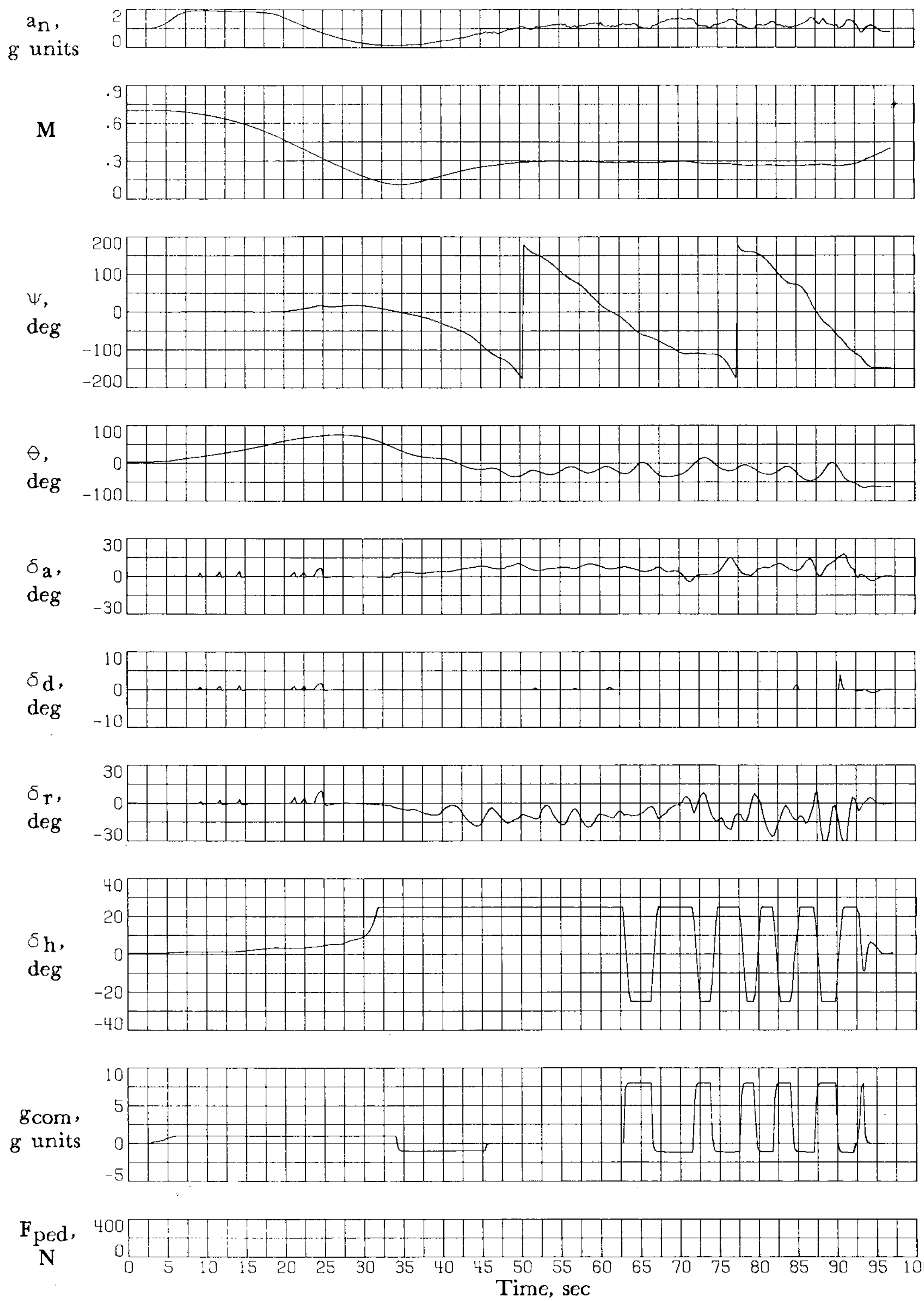

Figure 54.- Continued.

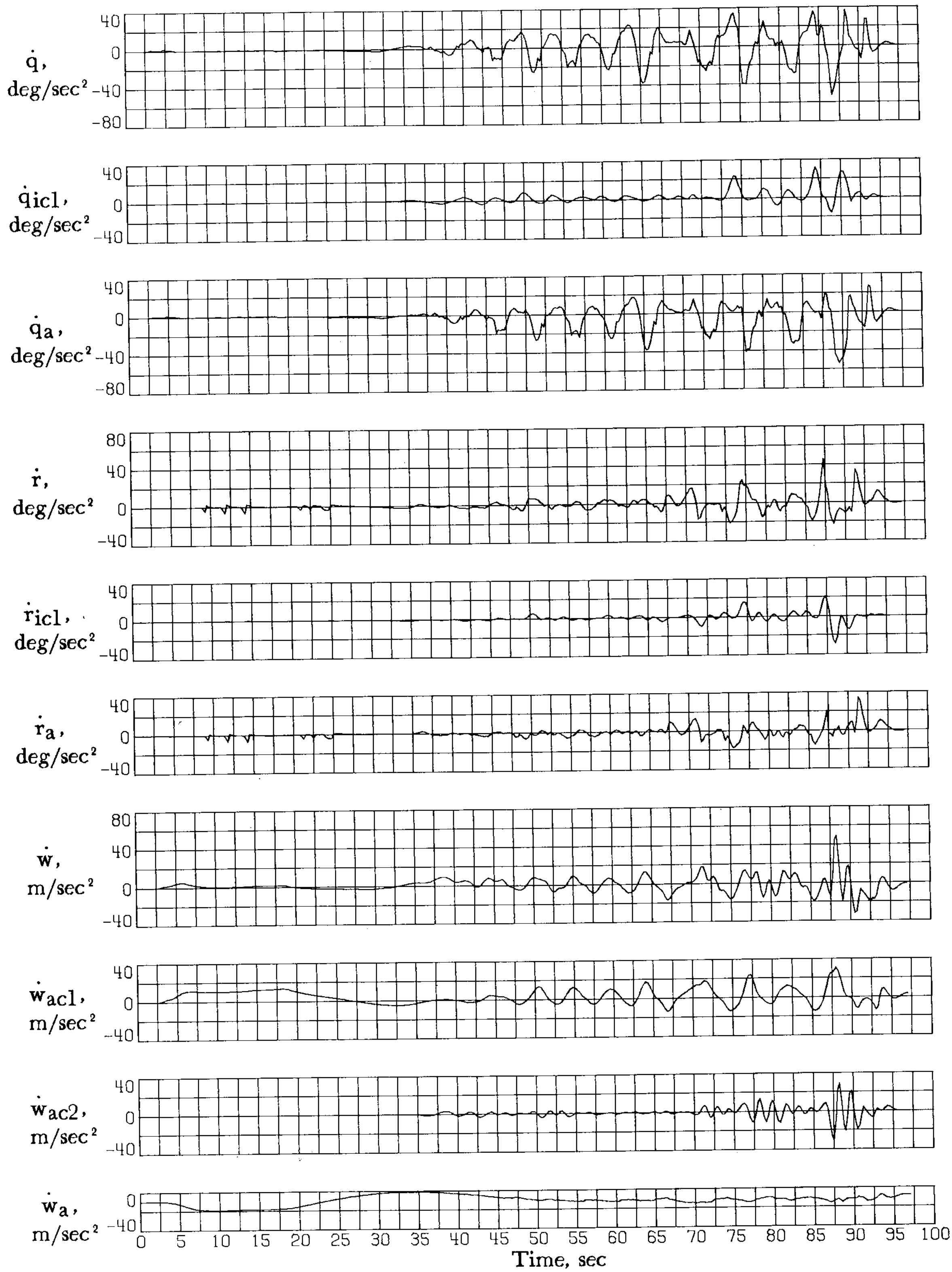

Figure 54.- Concluded.

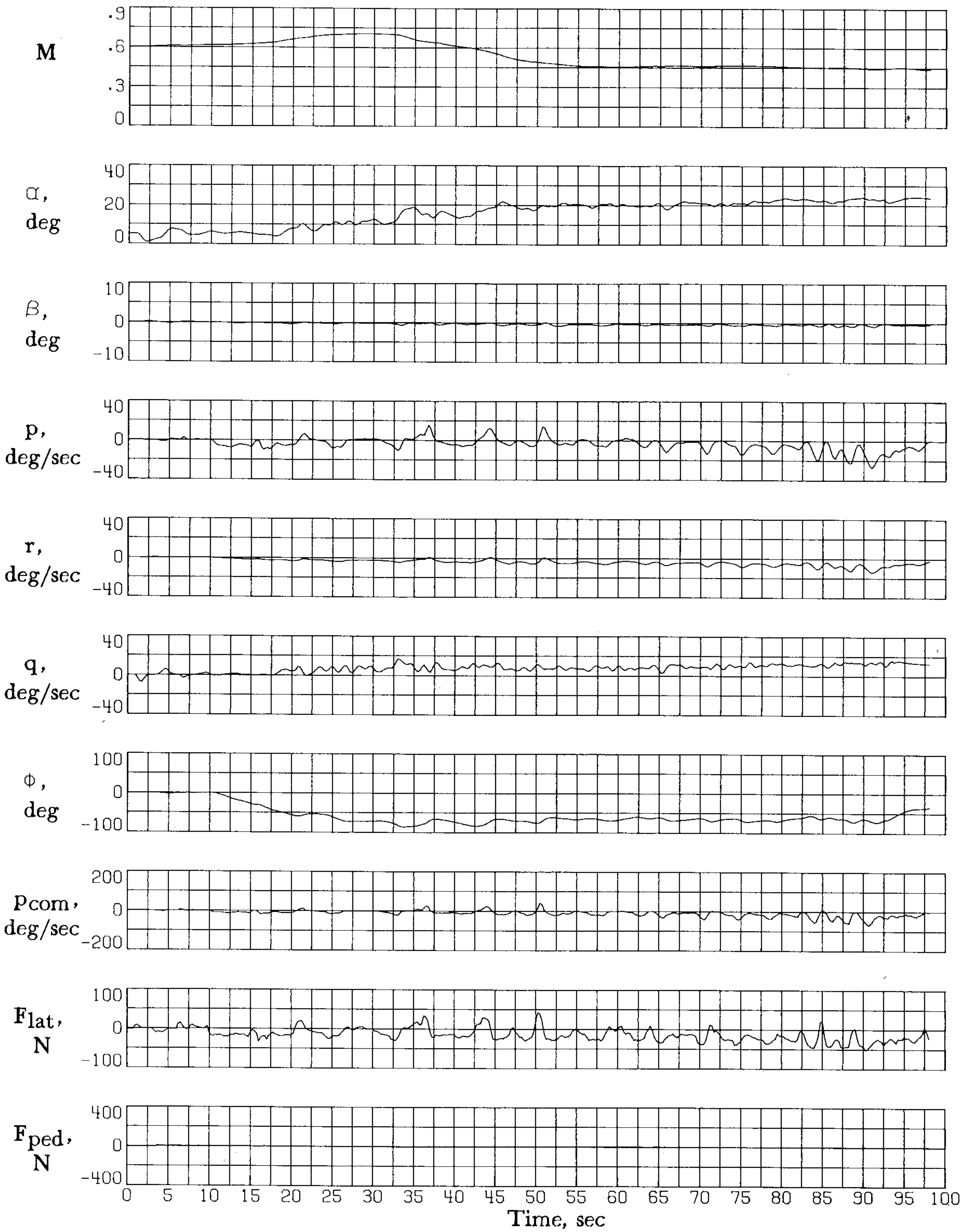

Figure 55.- Performance of airplane with control system A in wind-up turn task. h_o = 9144 m.

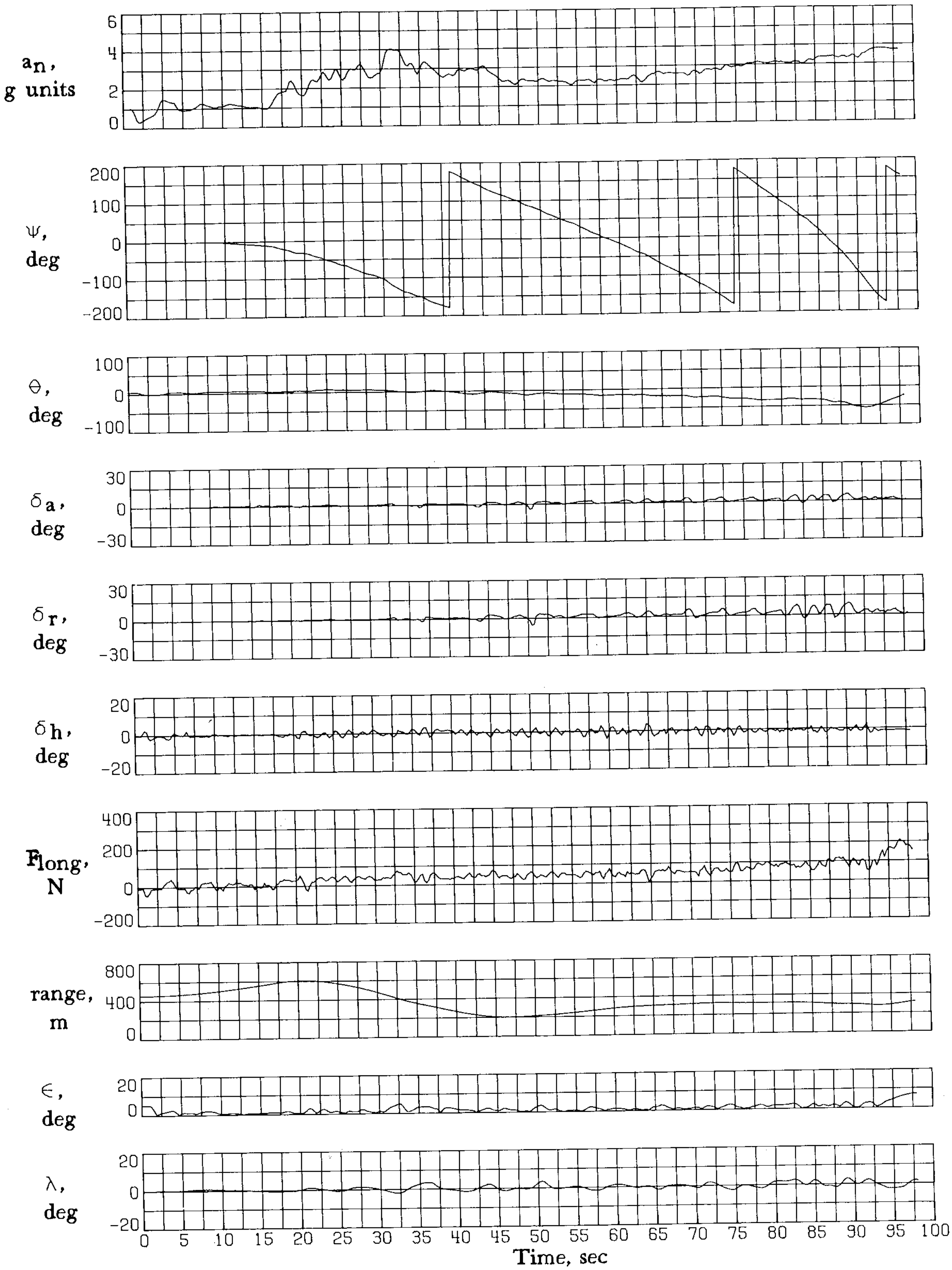

Figure 55.- Concluded.

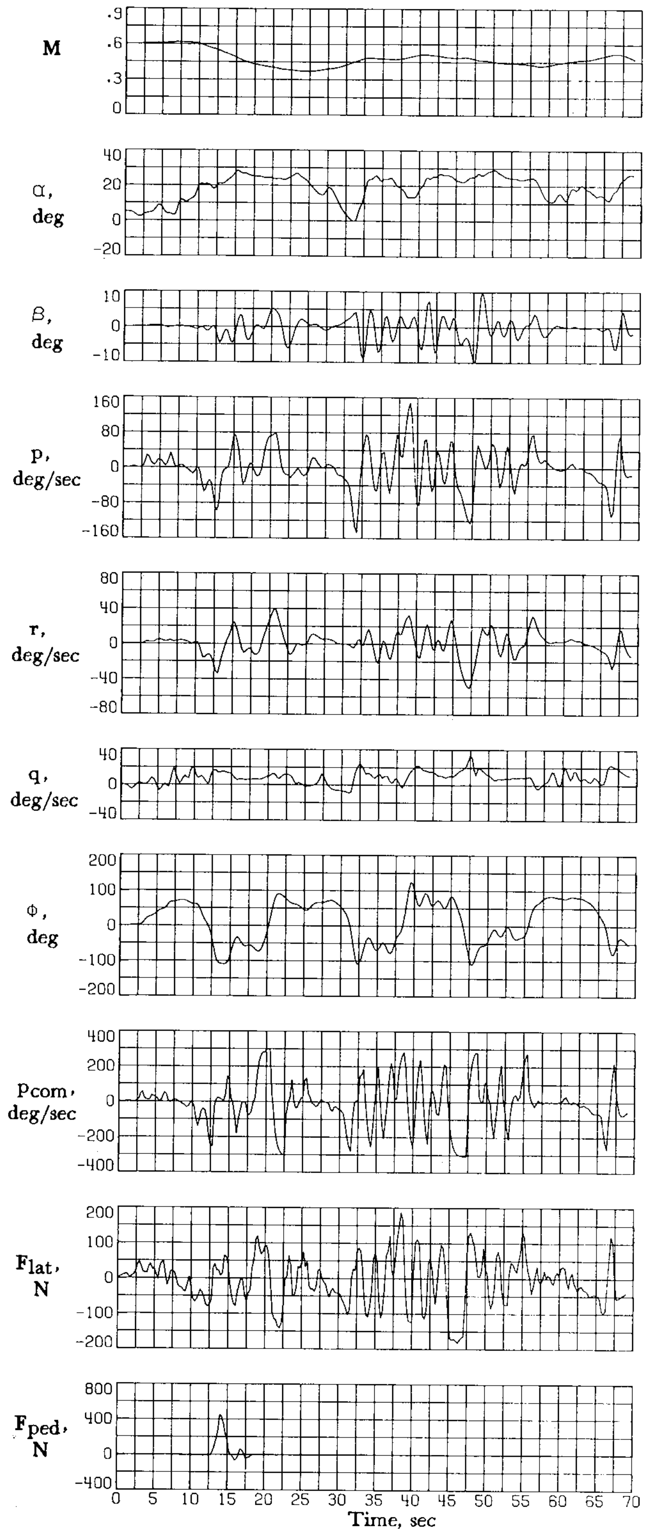

Figure 56.- Performance of airplane with control system A in bank-to-bank task.

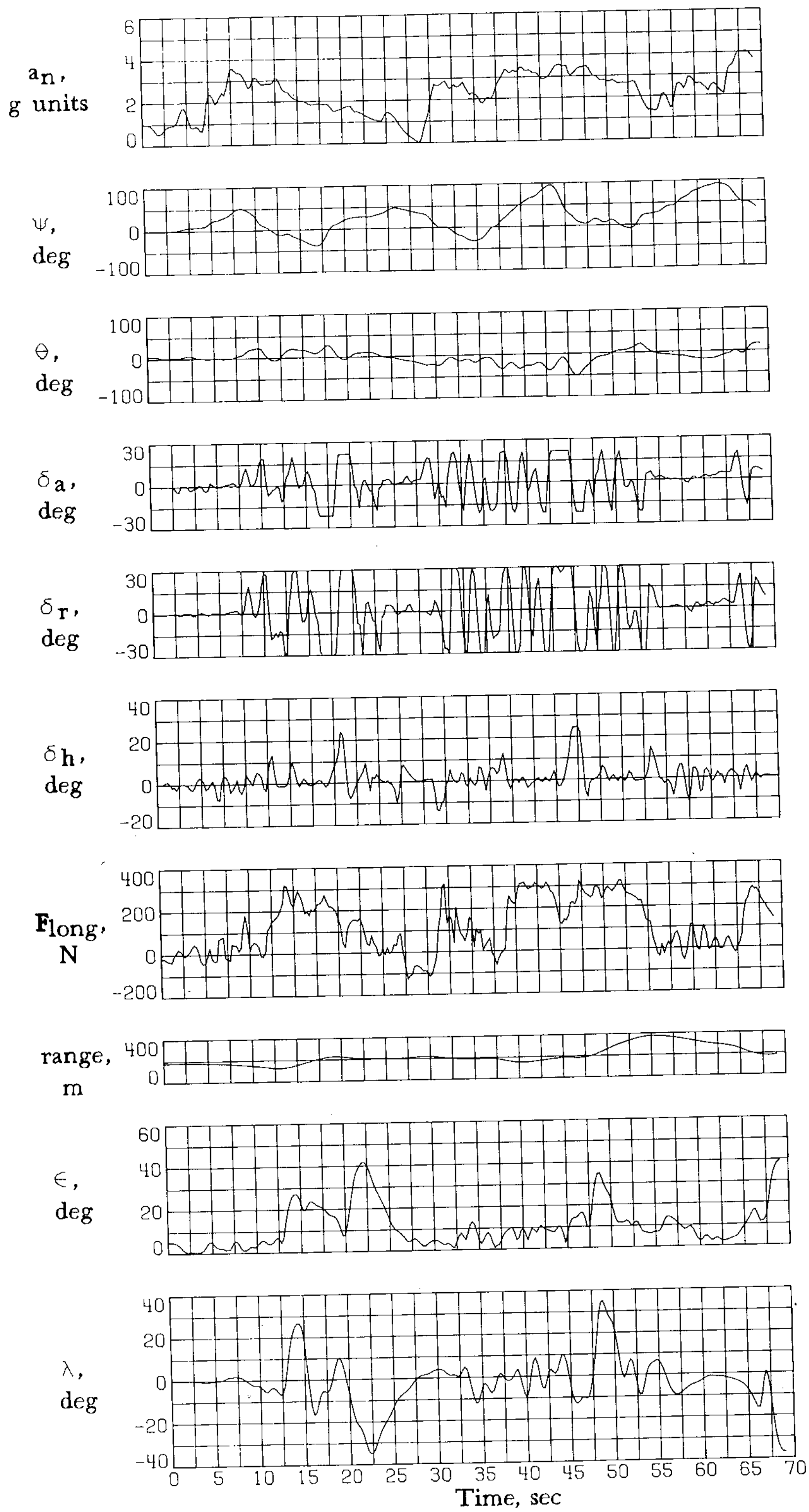

Figure 56.- Concluded.

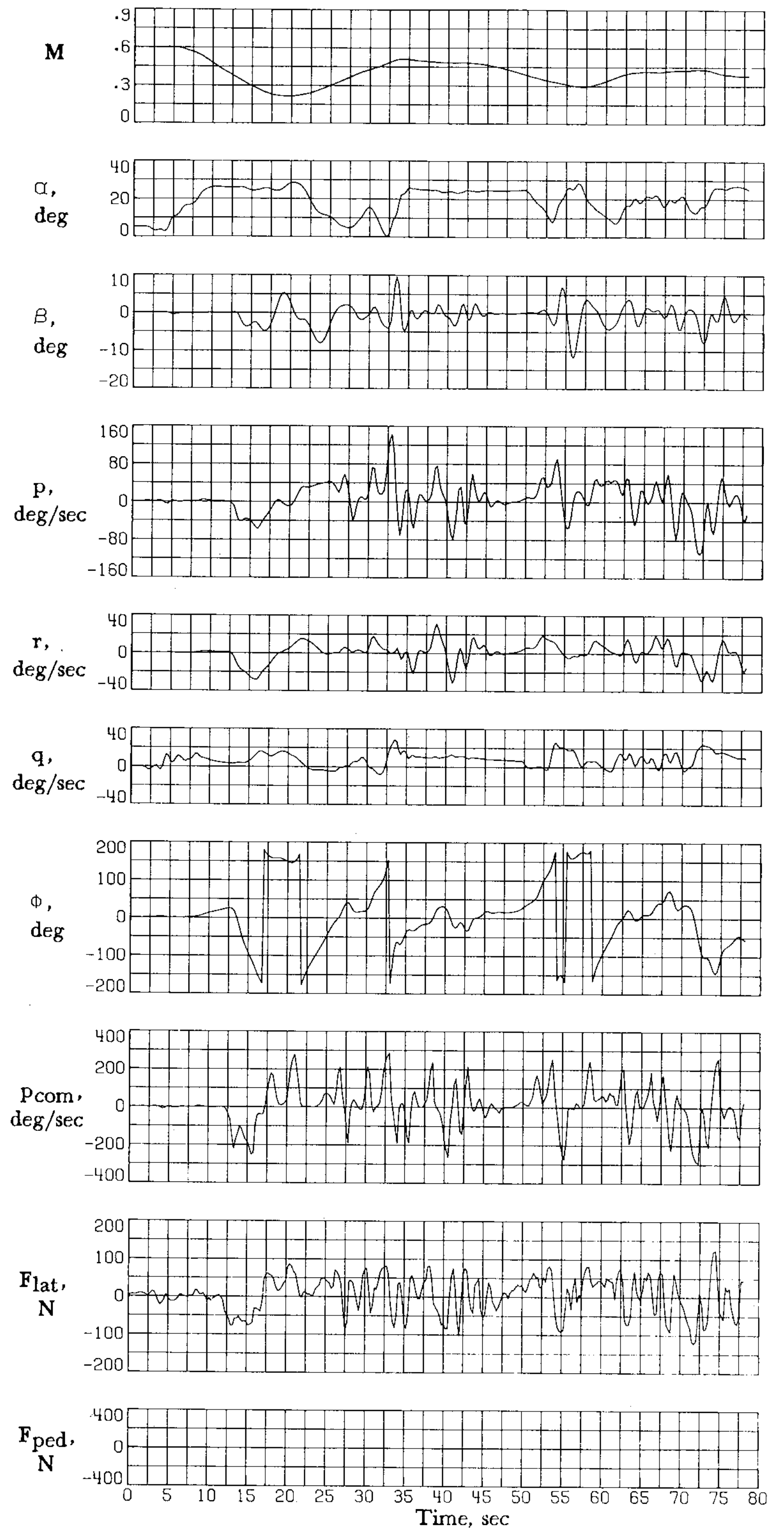

Figure 57.- Performance of airplane with control system A in ACM task.

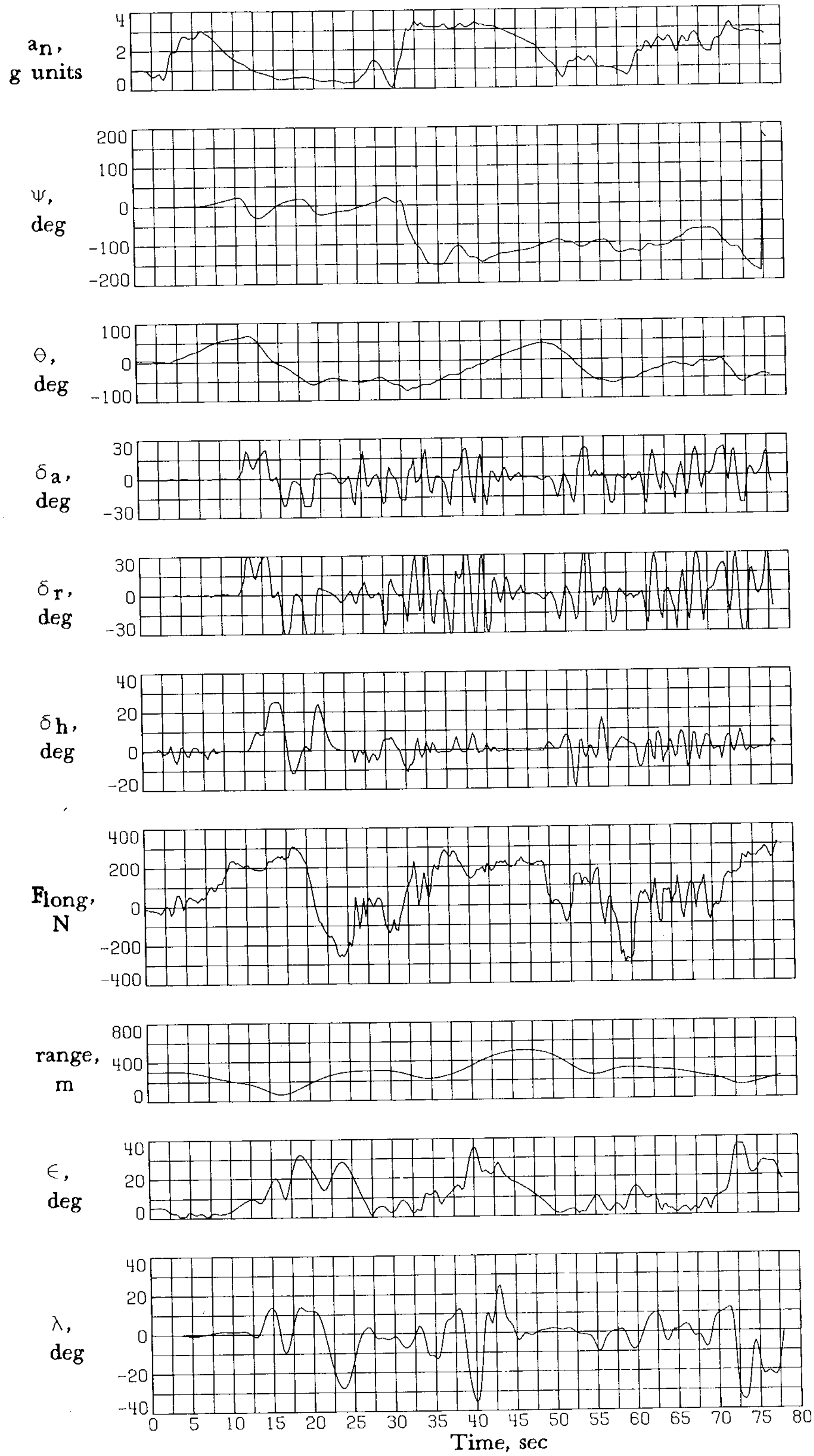

Figure 57.- Concluded.

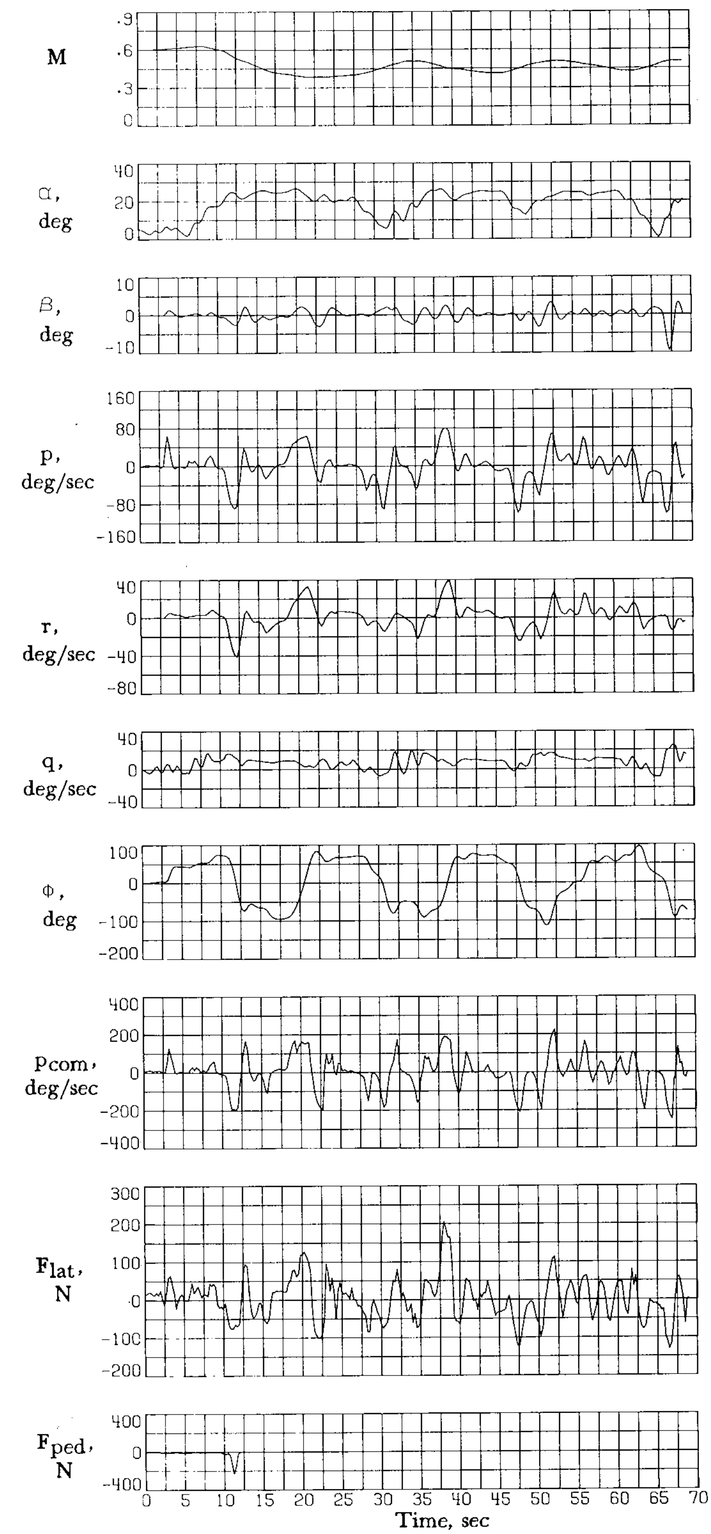

Figure 58.- Performance of airplane with control system B in bank-to-bank task.

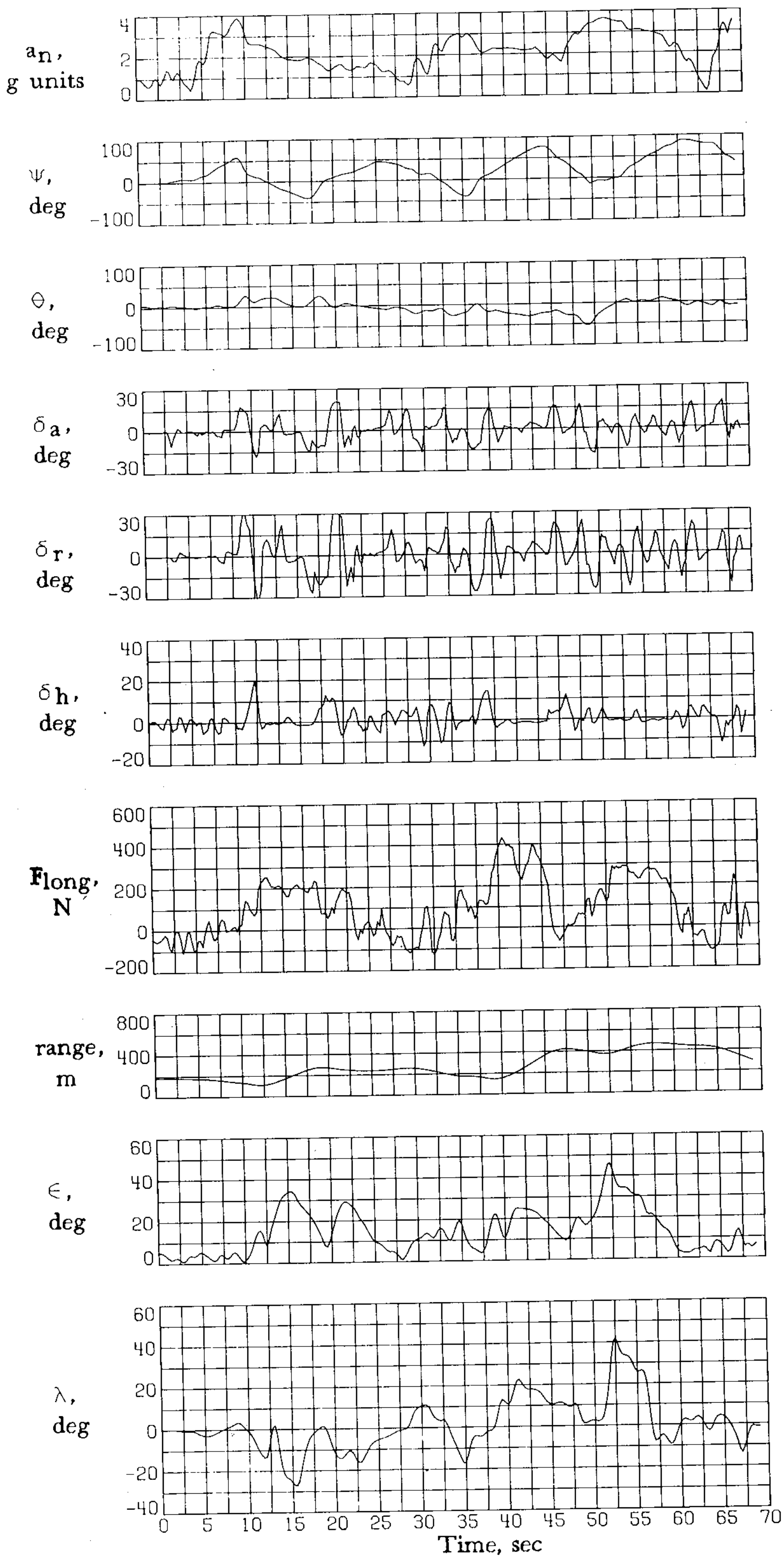

Figure 58.- Concluded.

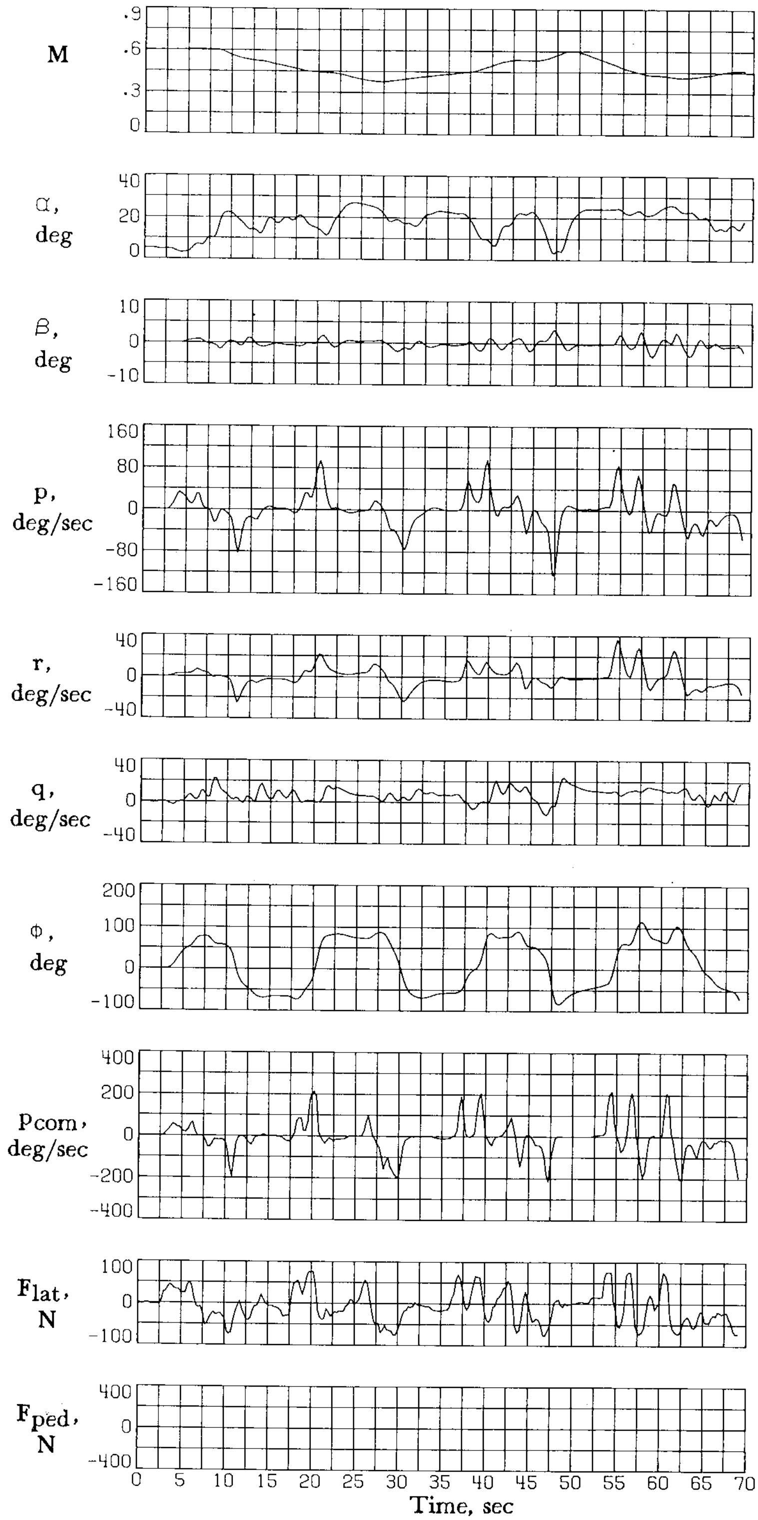

Figure 59.- Performance of airplane with control system C in bank-to-bank task.

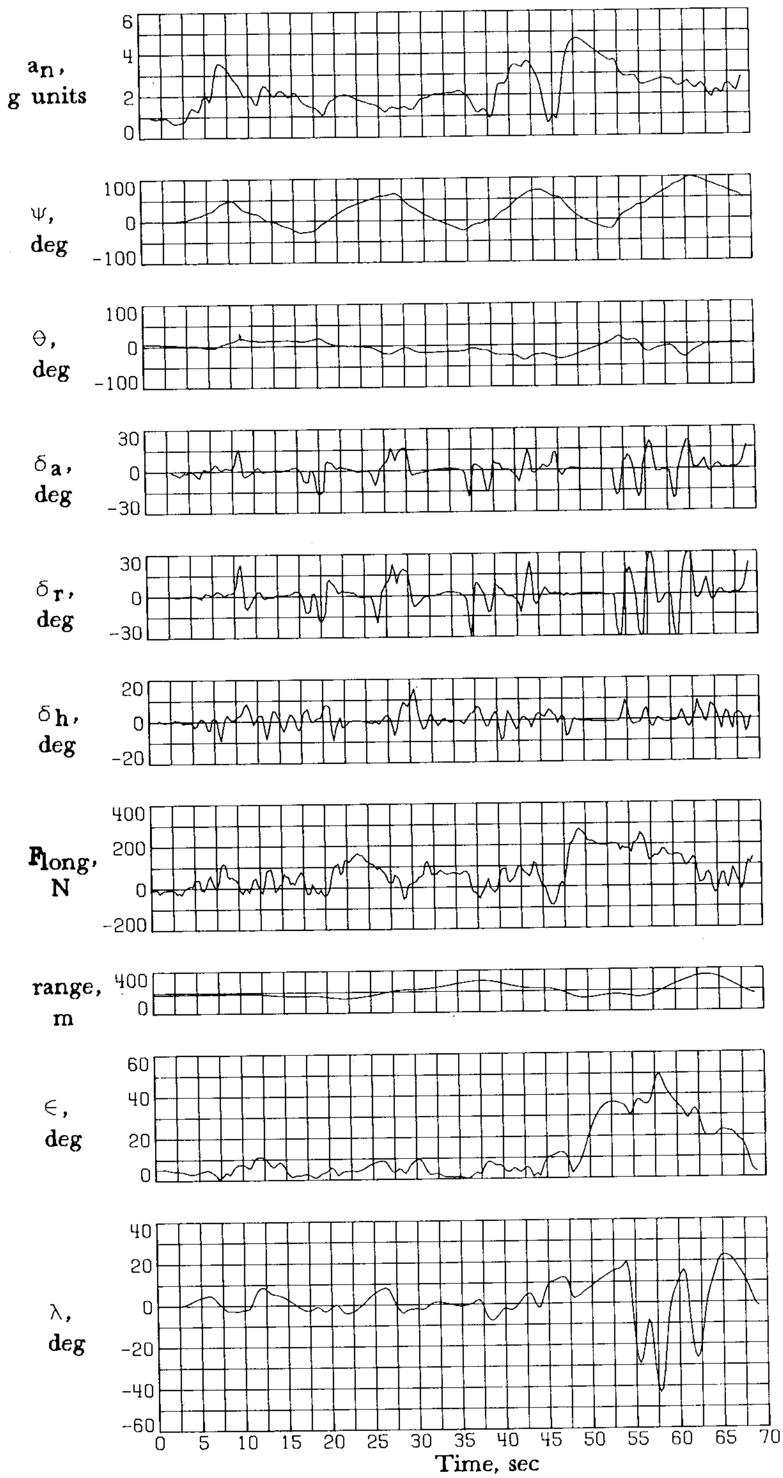

Figure 59.- Concluded.

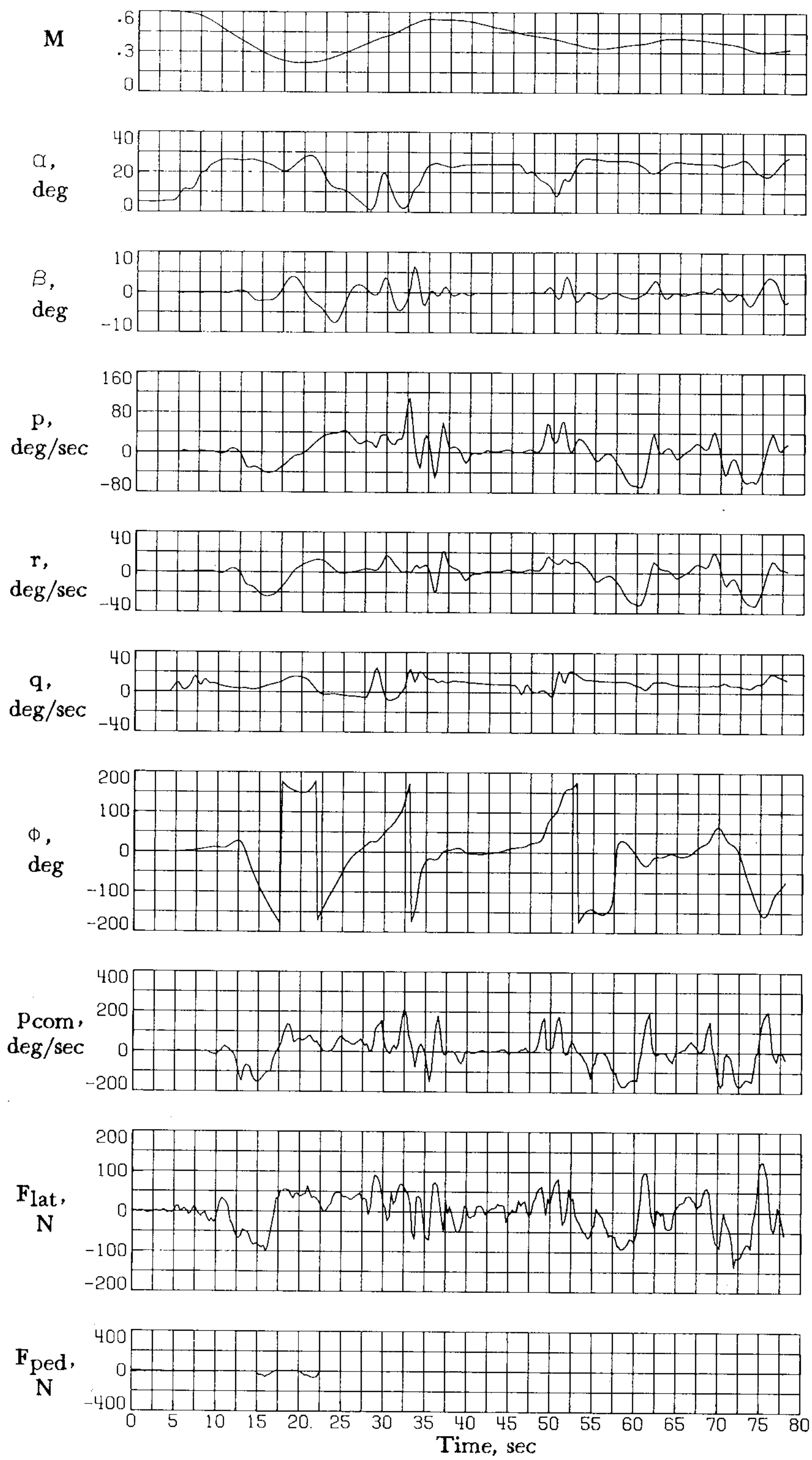

Figure 60.- Performance of airplane with control system B in ACM task.

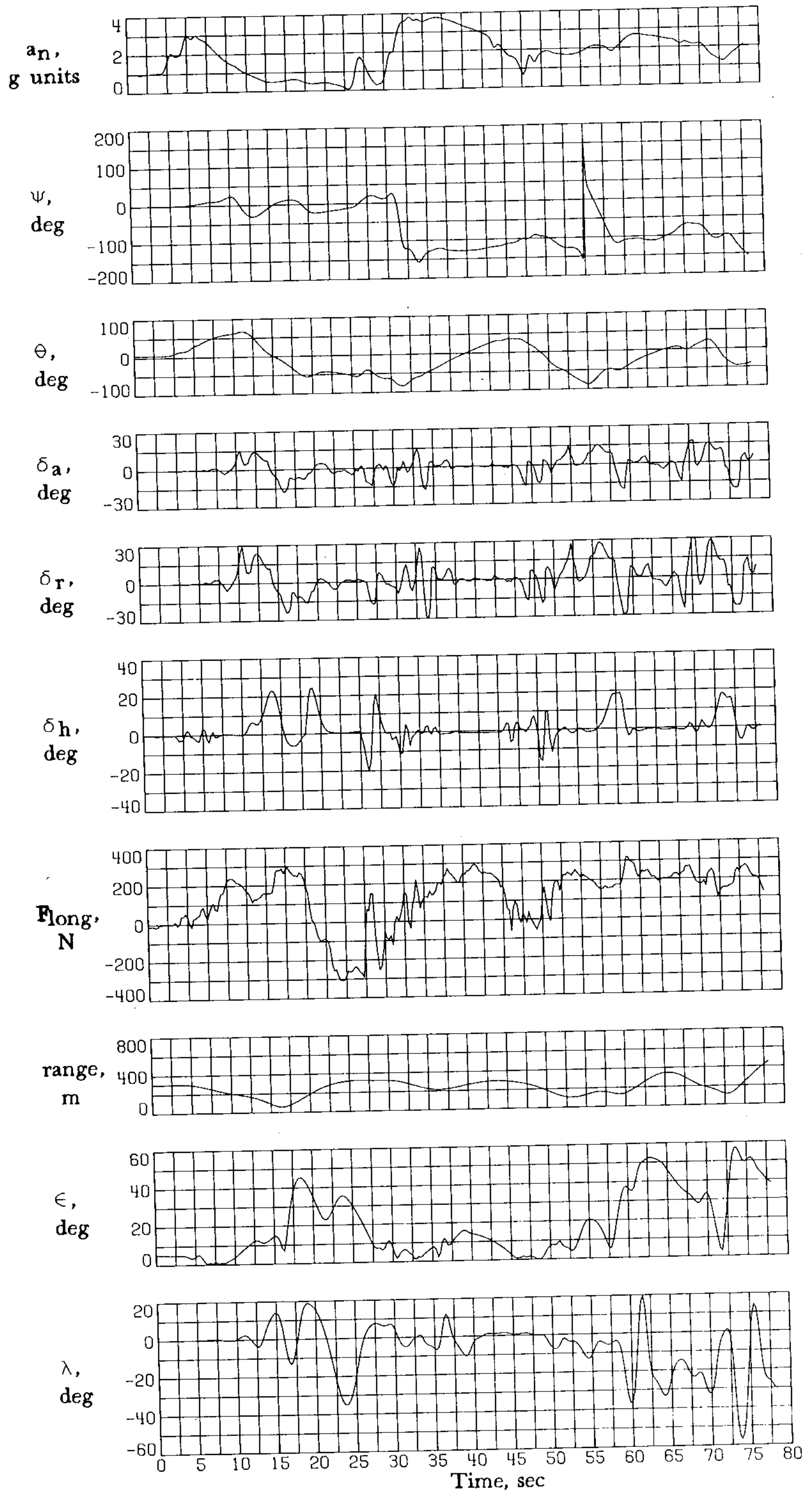

Figure 60.- Concluded.

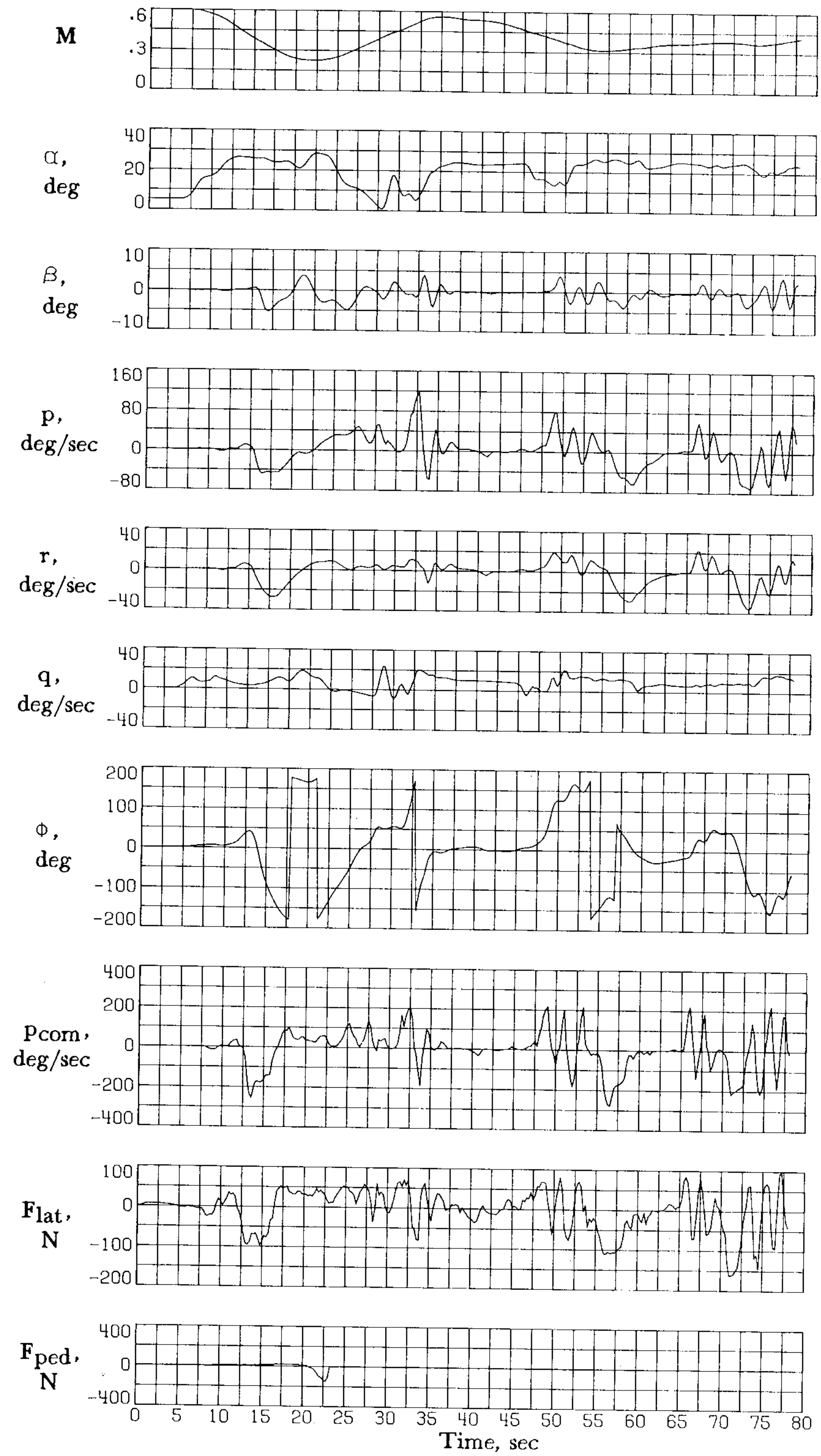

Figure 61.- Performance of airplane with control system C in ACM task.

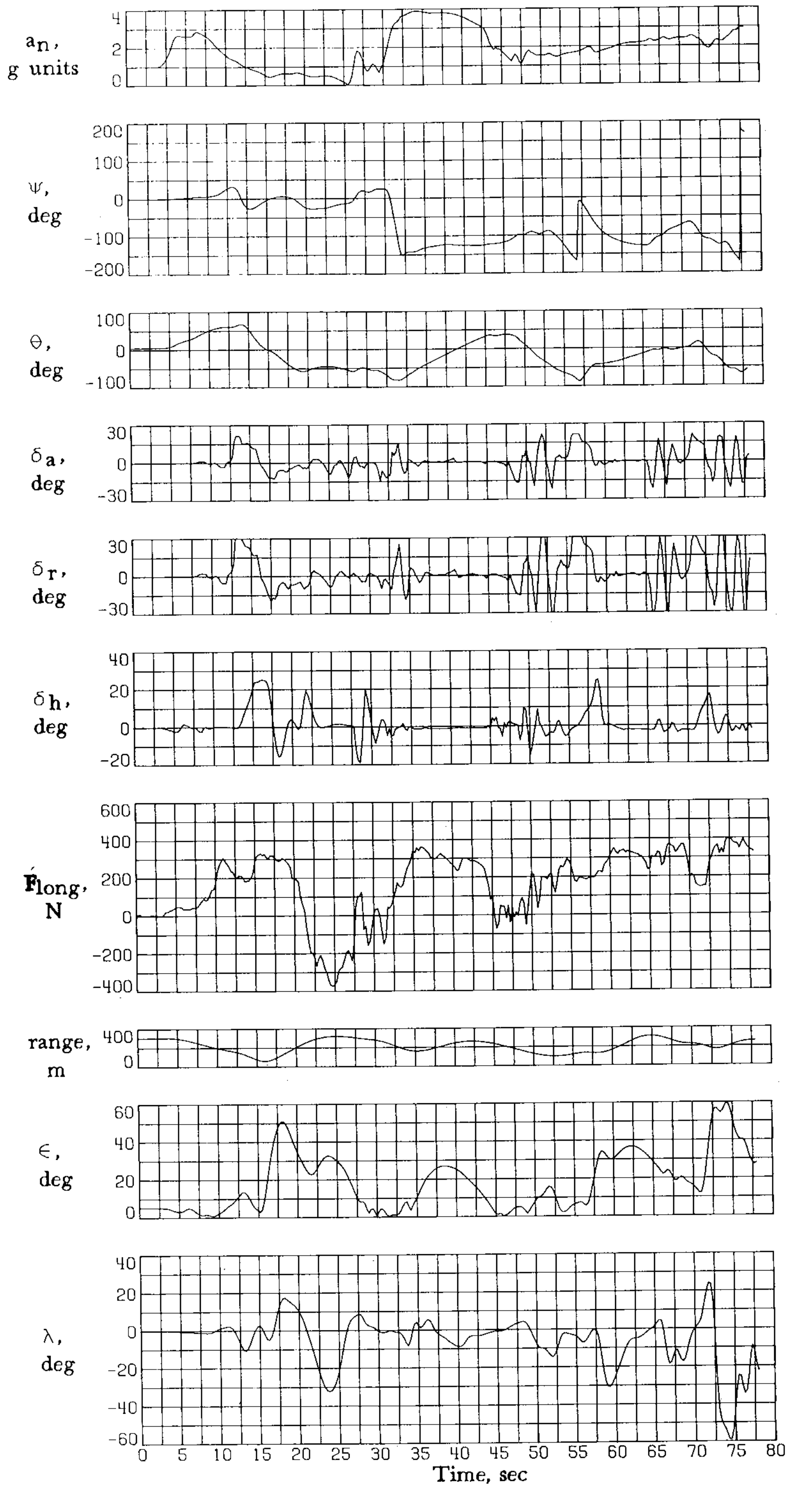

Figure 61.- Concluded.

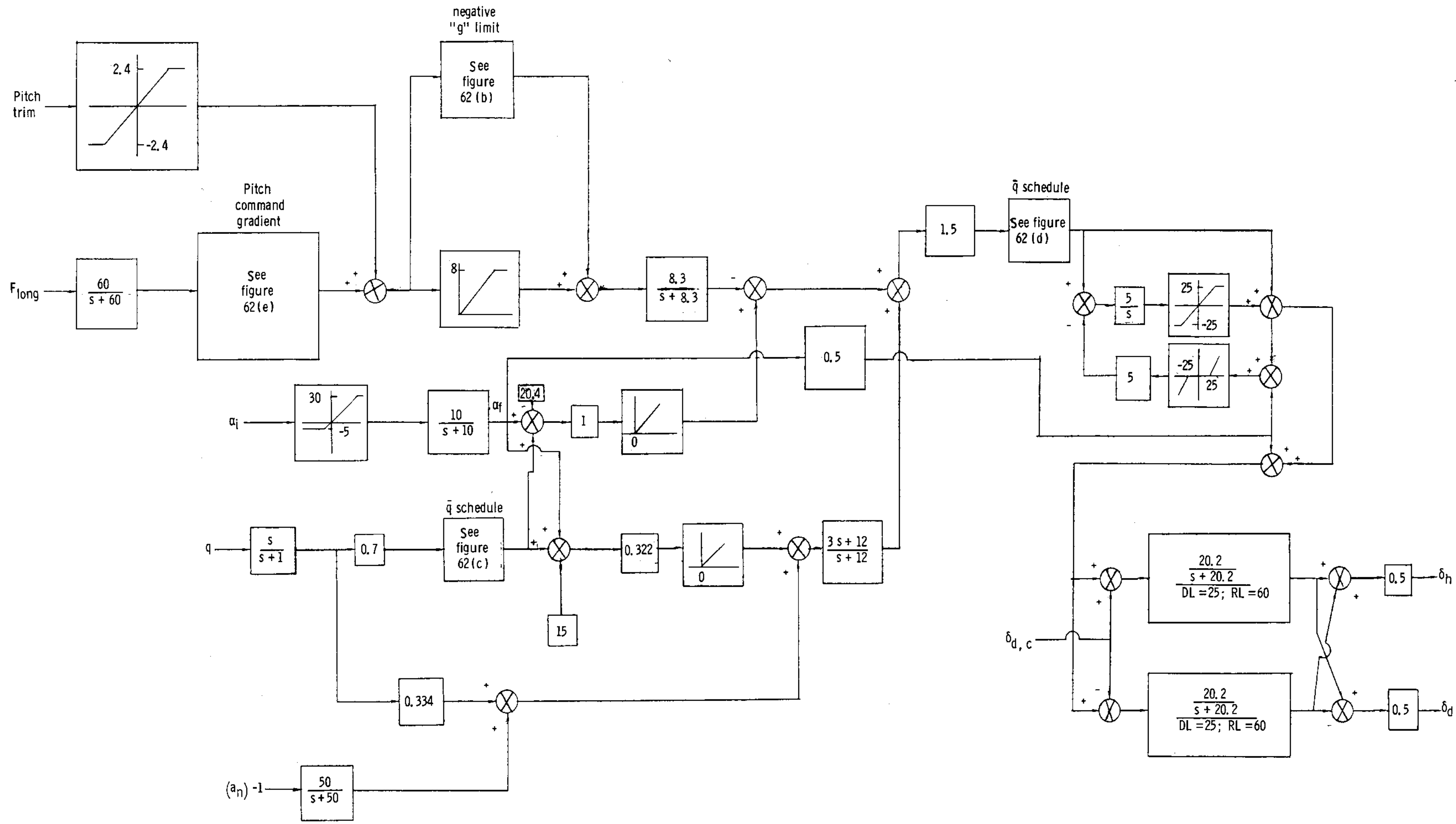

(a) Schematic of overall system.

Figure 62.- Simulated basic pitch control system (control system A).

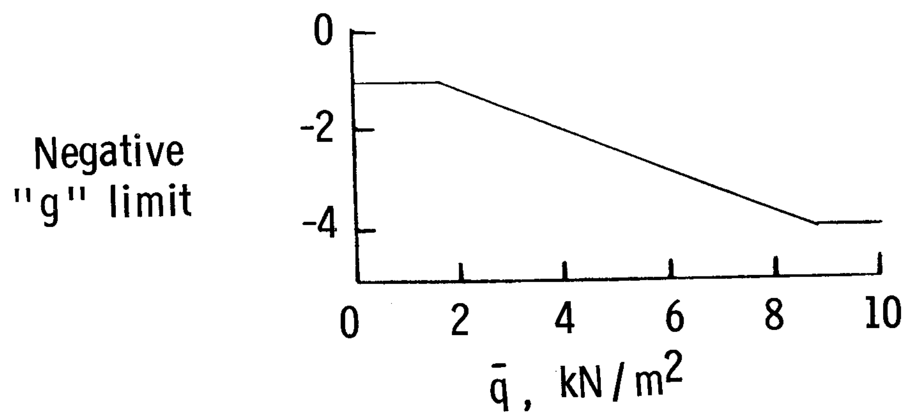

(b) Schedule of negative "g" limit with $\bar{q}$.

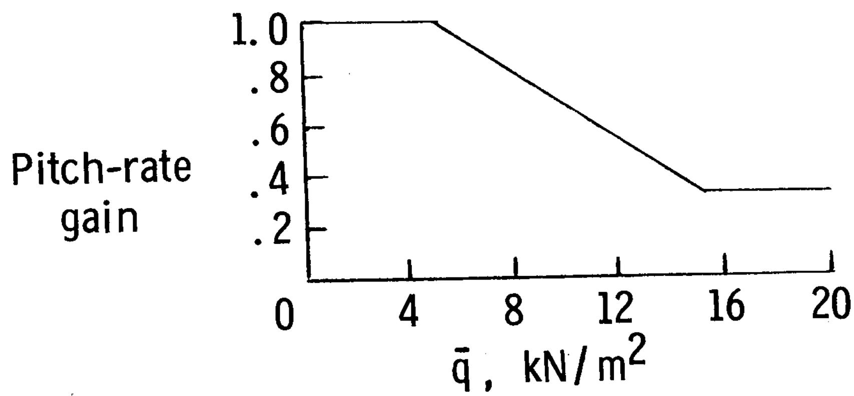

(c) Schedule of pitch-rate gain with $\bar{q}$.

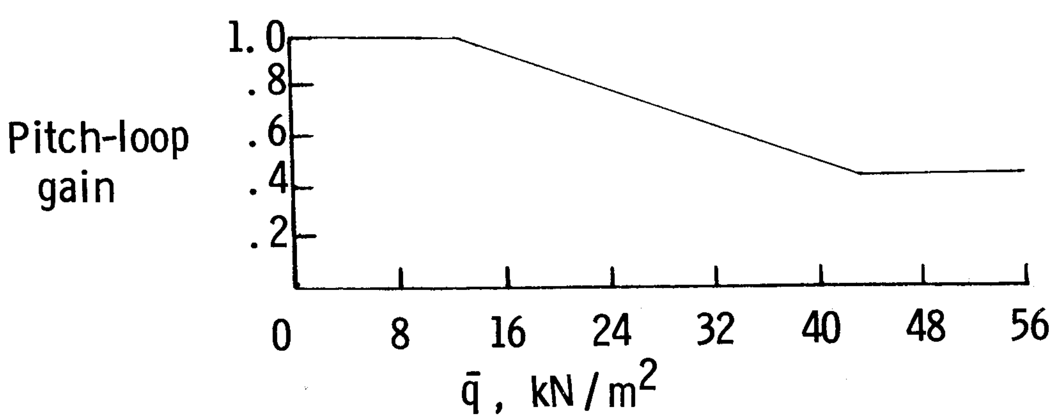

(d) Schedule of pitch-loop gain with $\bar{q}$.

Figure 62.- Continued.

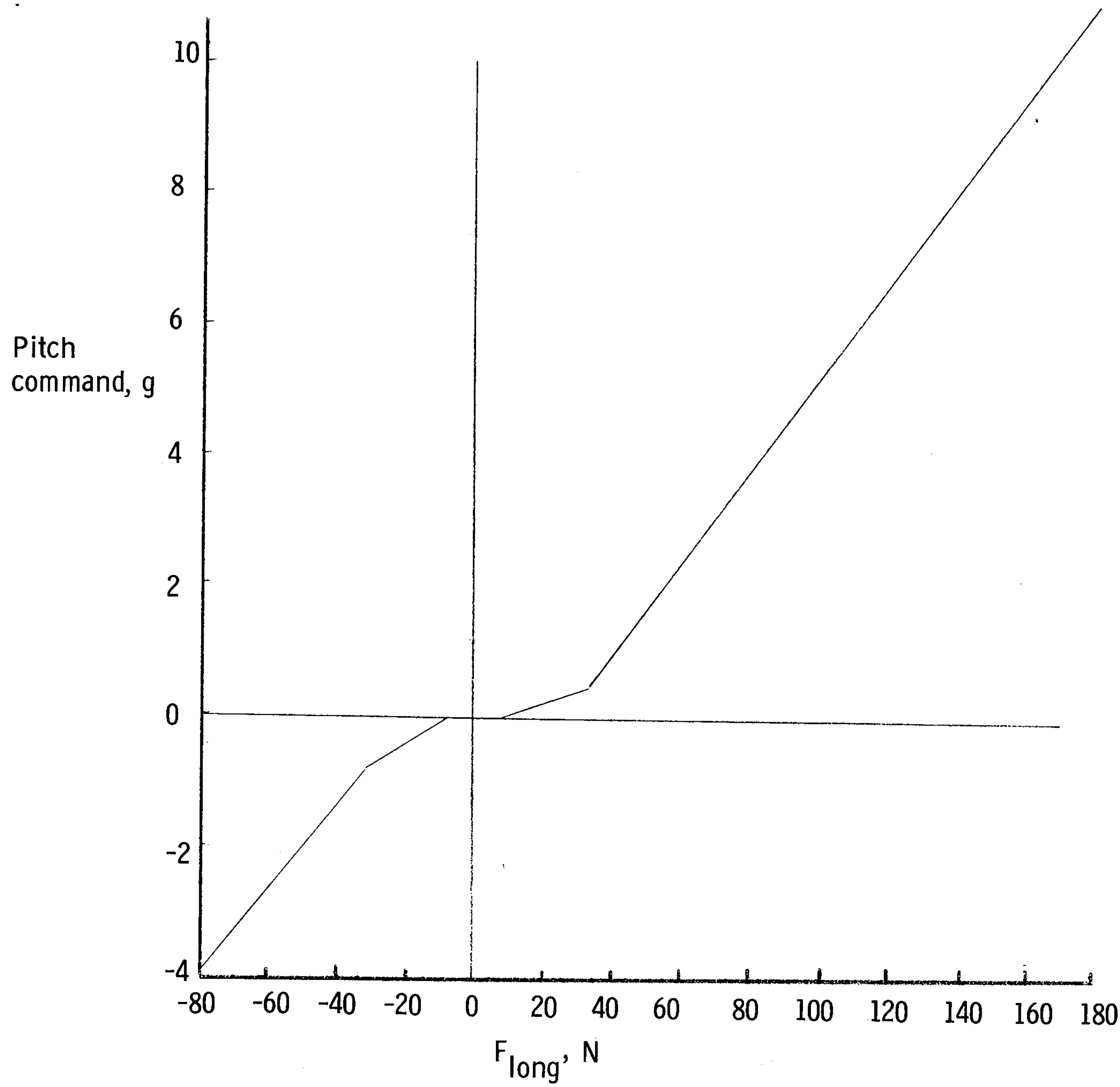

(e) Pitch command gradient.

Figure 62.- Concluded.

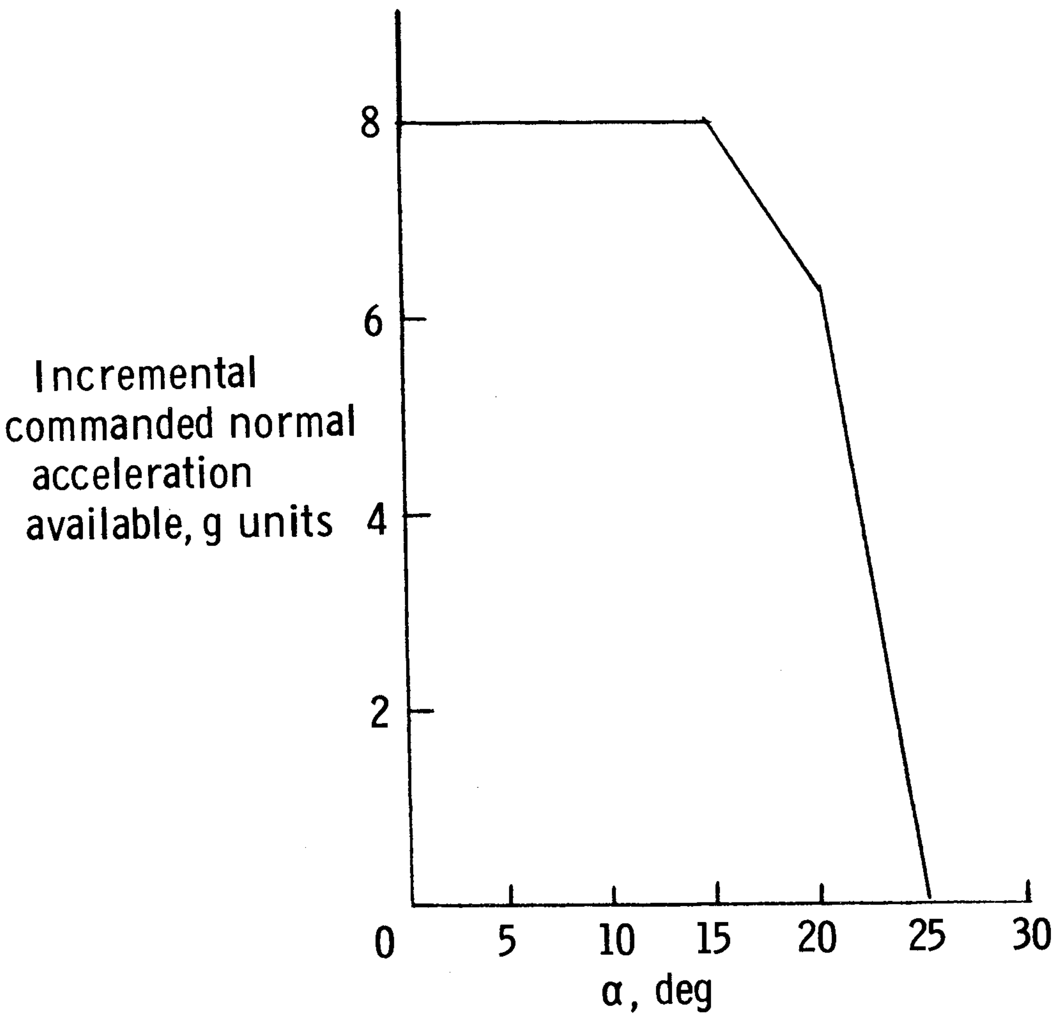

Figure 63.- Variation of maximum commandable incremental normal acceleration with angle of attack.

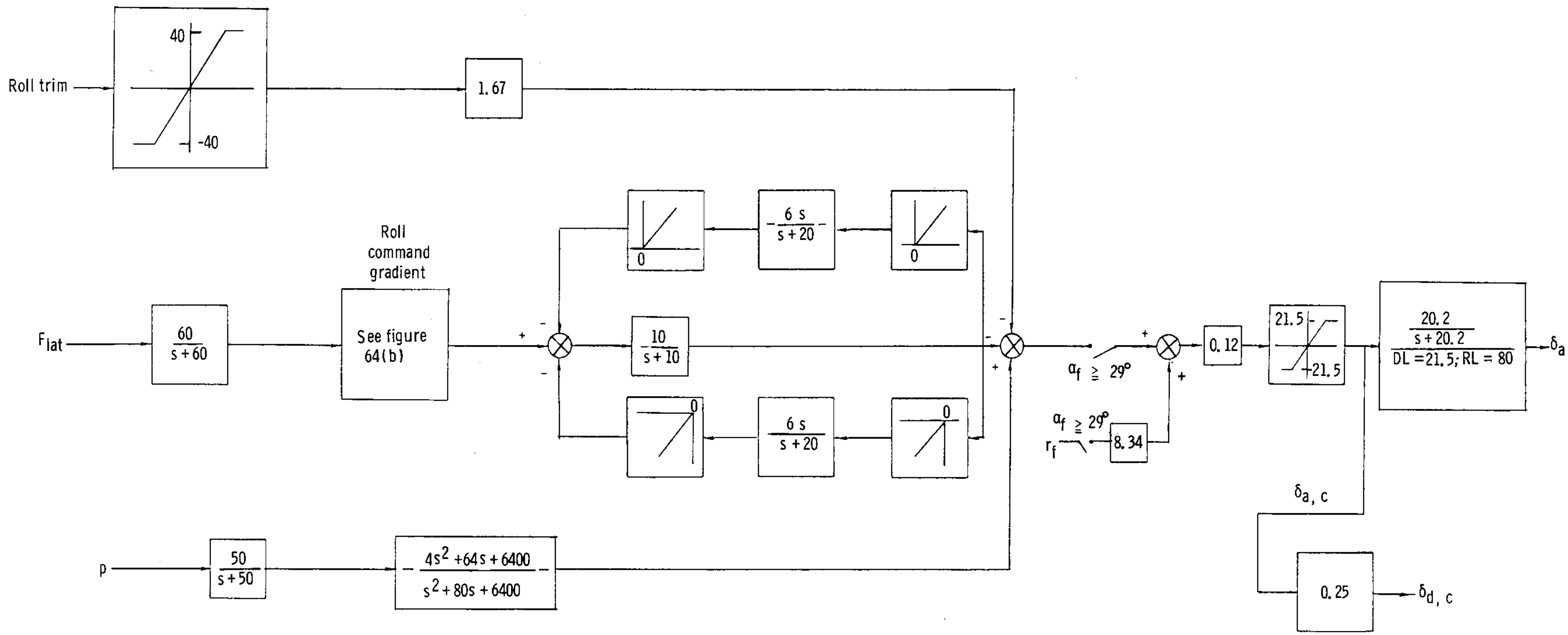

(a) Schematic of overall system.

Figure 64.- Schematic of roll axis of basic control system (control system A).

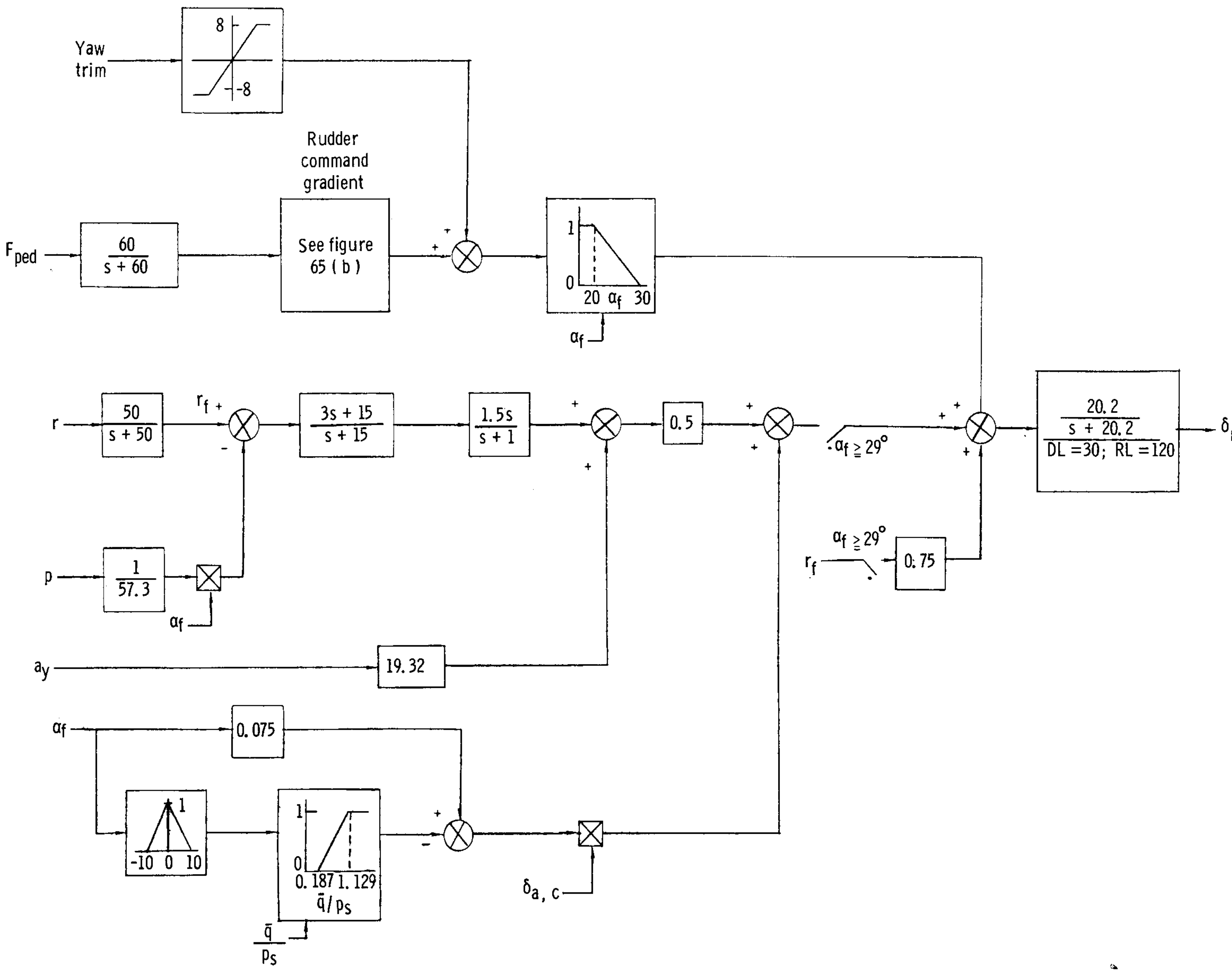

(a) Schematic of overall system.

Figure 65.- Schematic of yaw axis of basic control system (control system A).

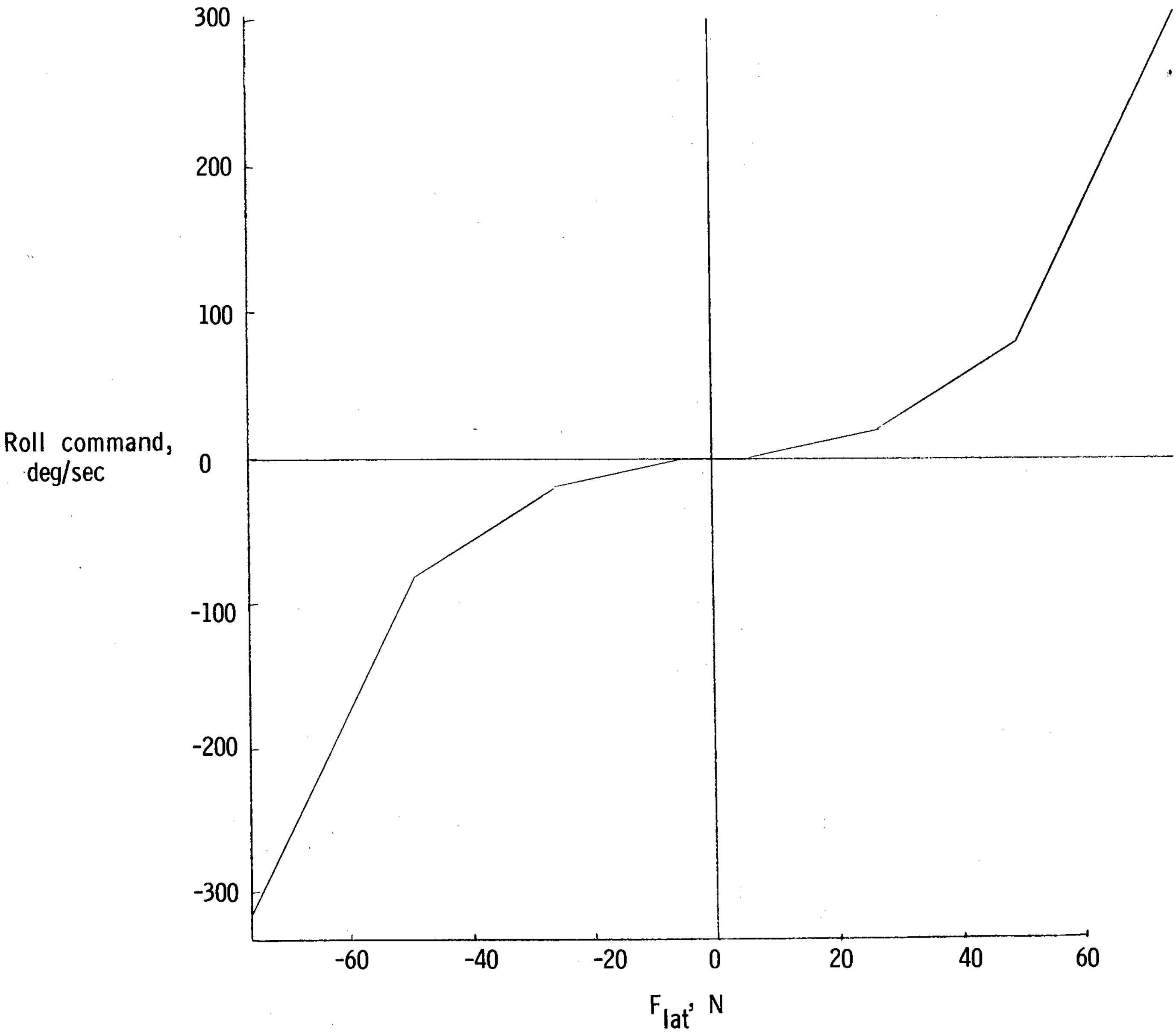

(b) Roll command gradient.

Figure 64.- Concluded.

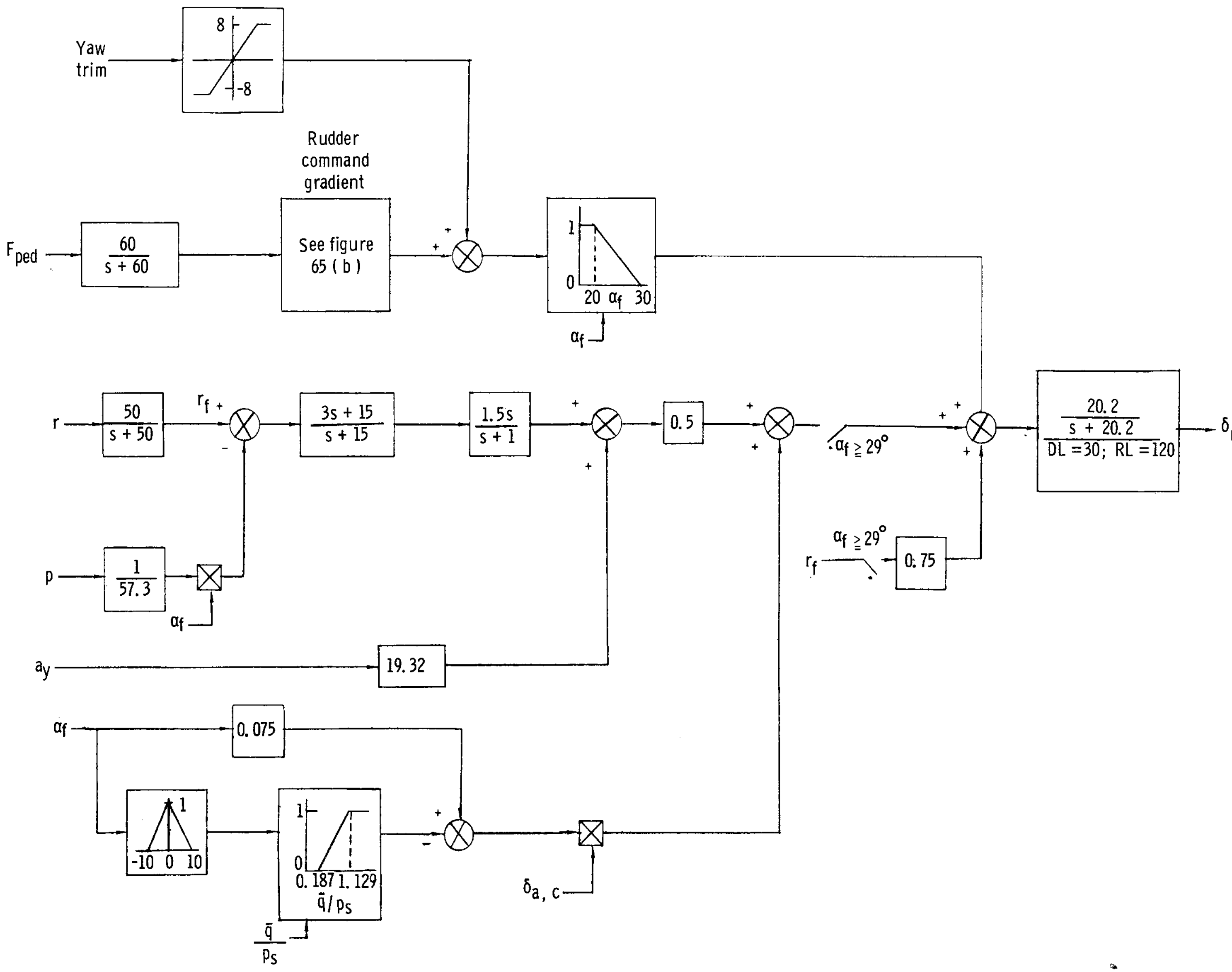

(a) Schematic of overall system.

Figure 65.- Schematic of yaw axis of basic control system (control system A).

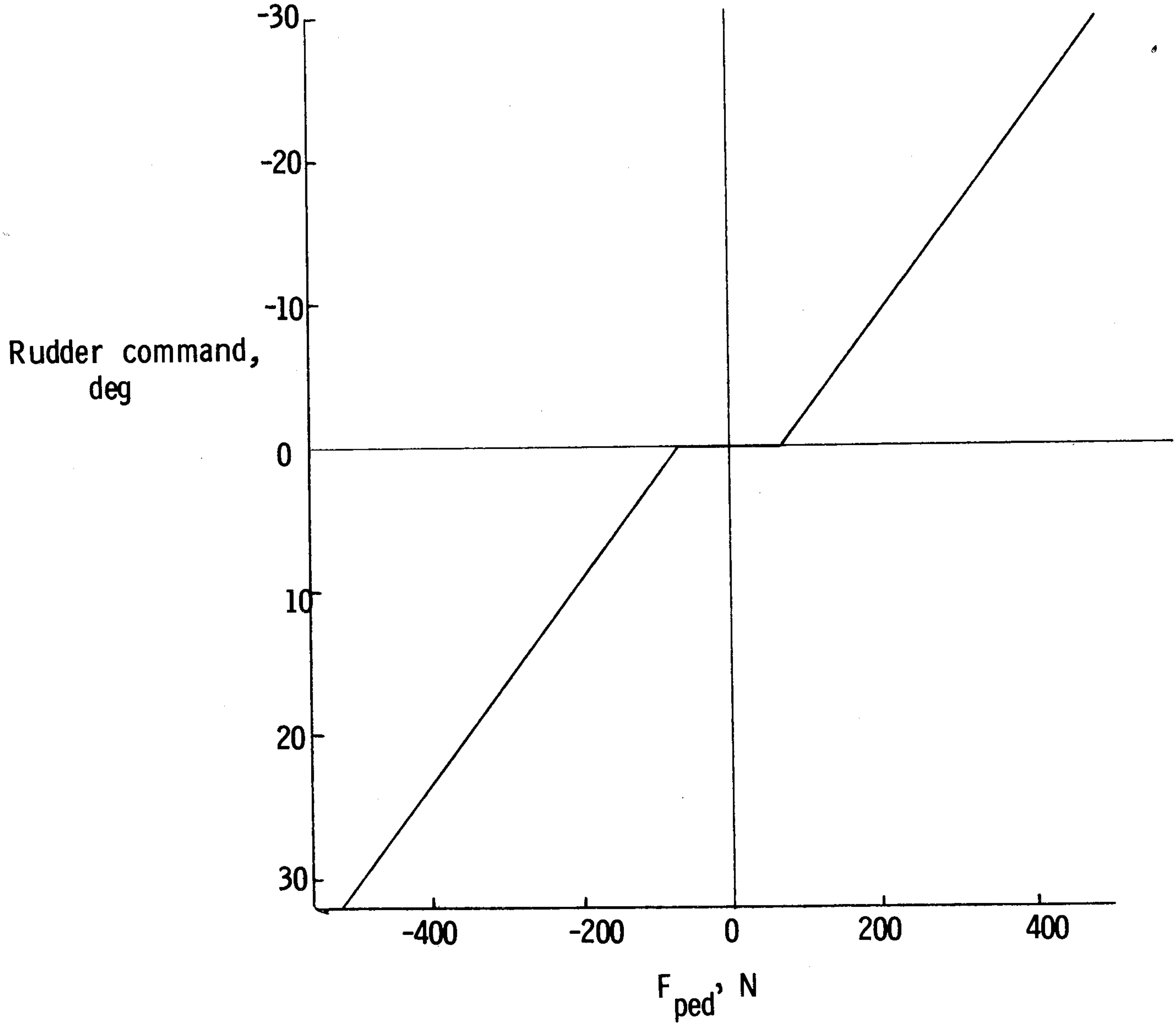

(b) Rudder command gradient.

Figure 65.- Concluded.

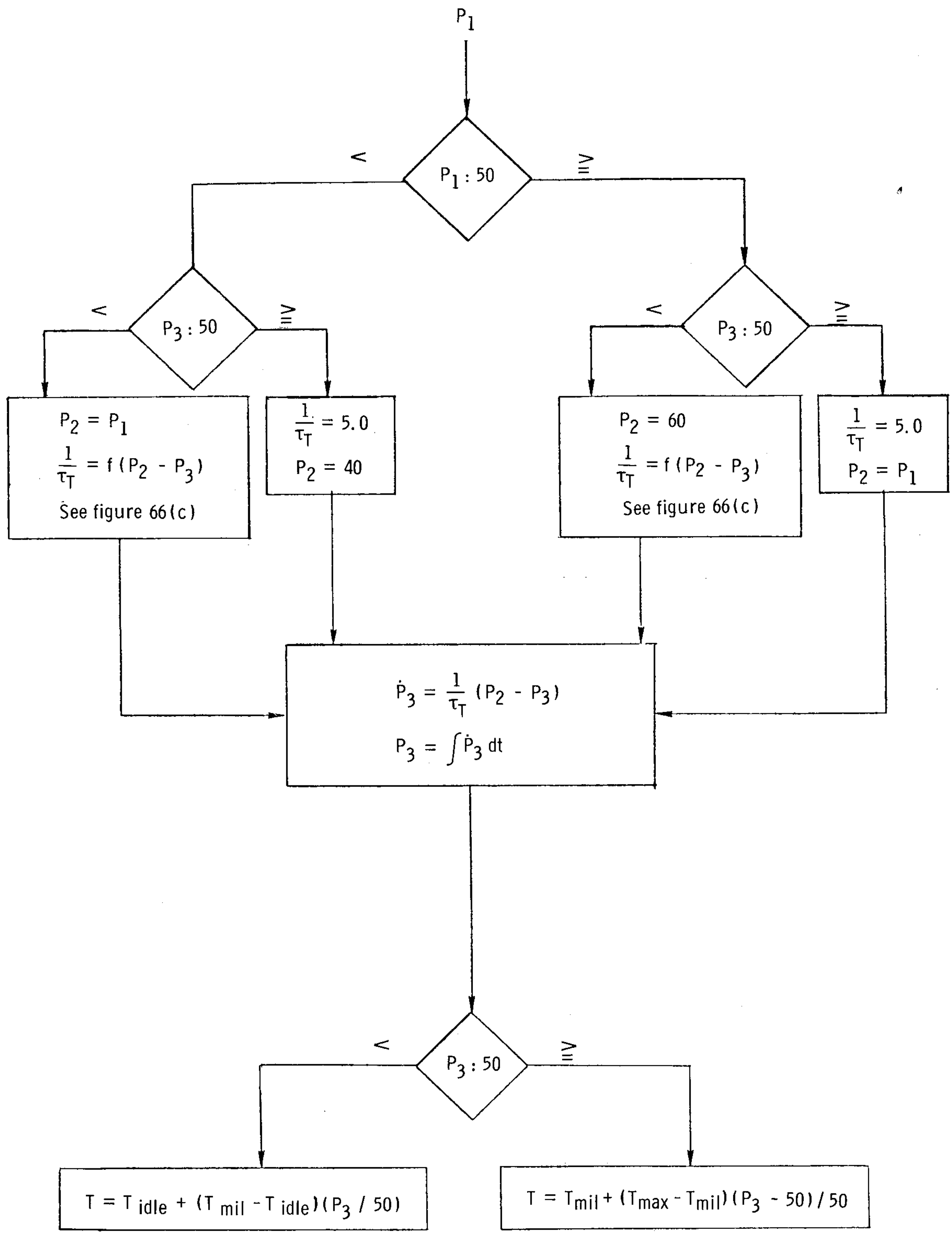

(a) Logic diagram for thrust dynamic model.

Figure 66.- Simulated powerplant characteristics.

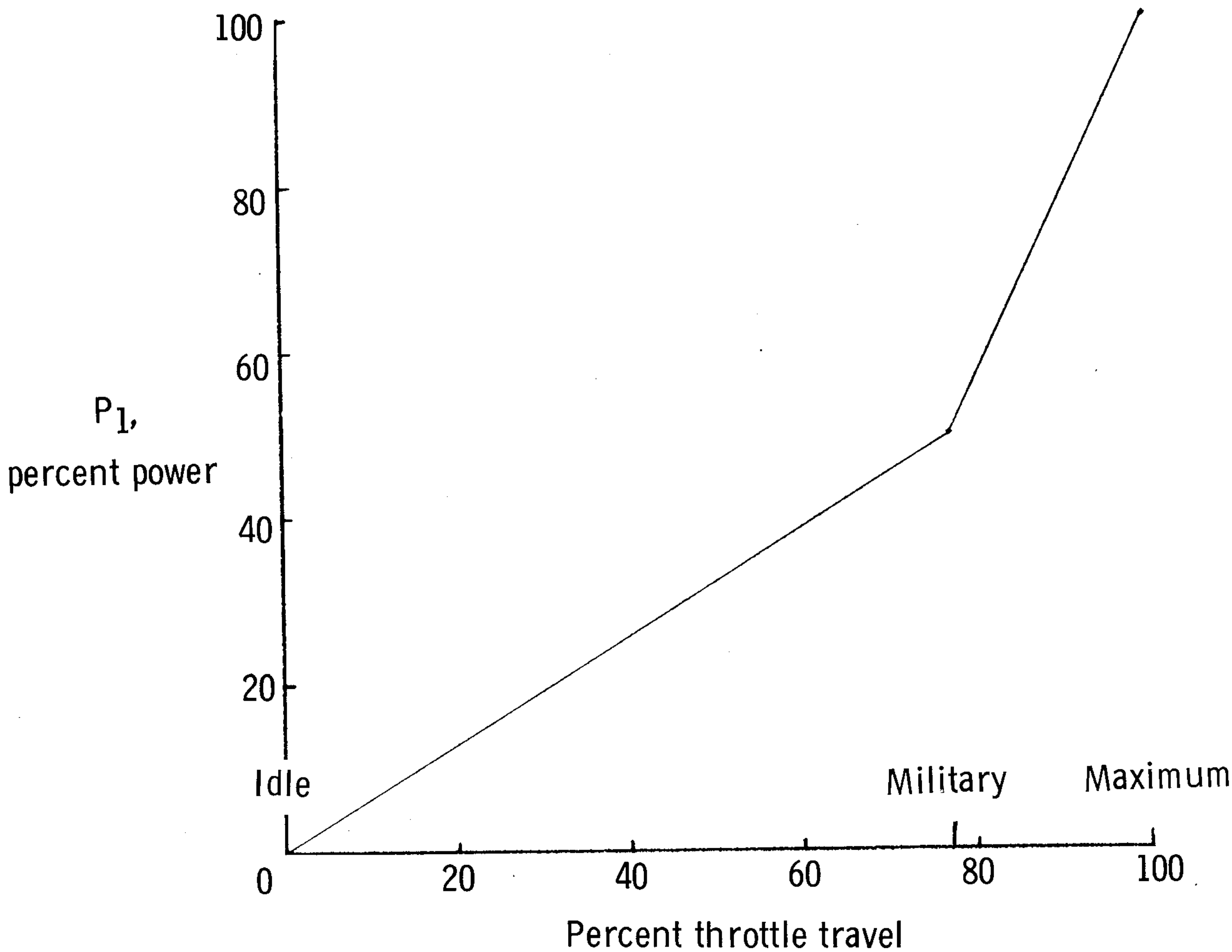

(b) Power variation with throttle position.

Figure 66.- Continued.

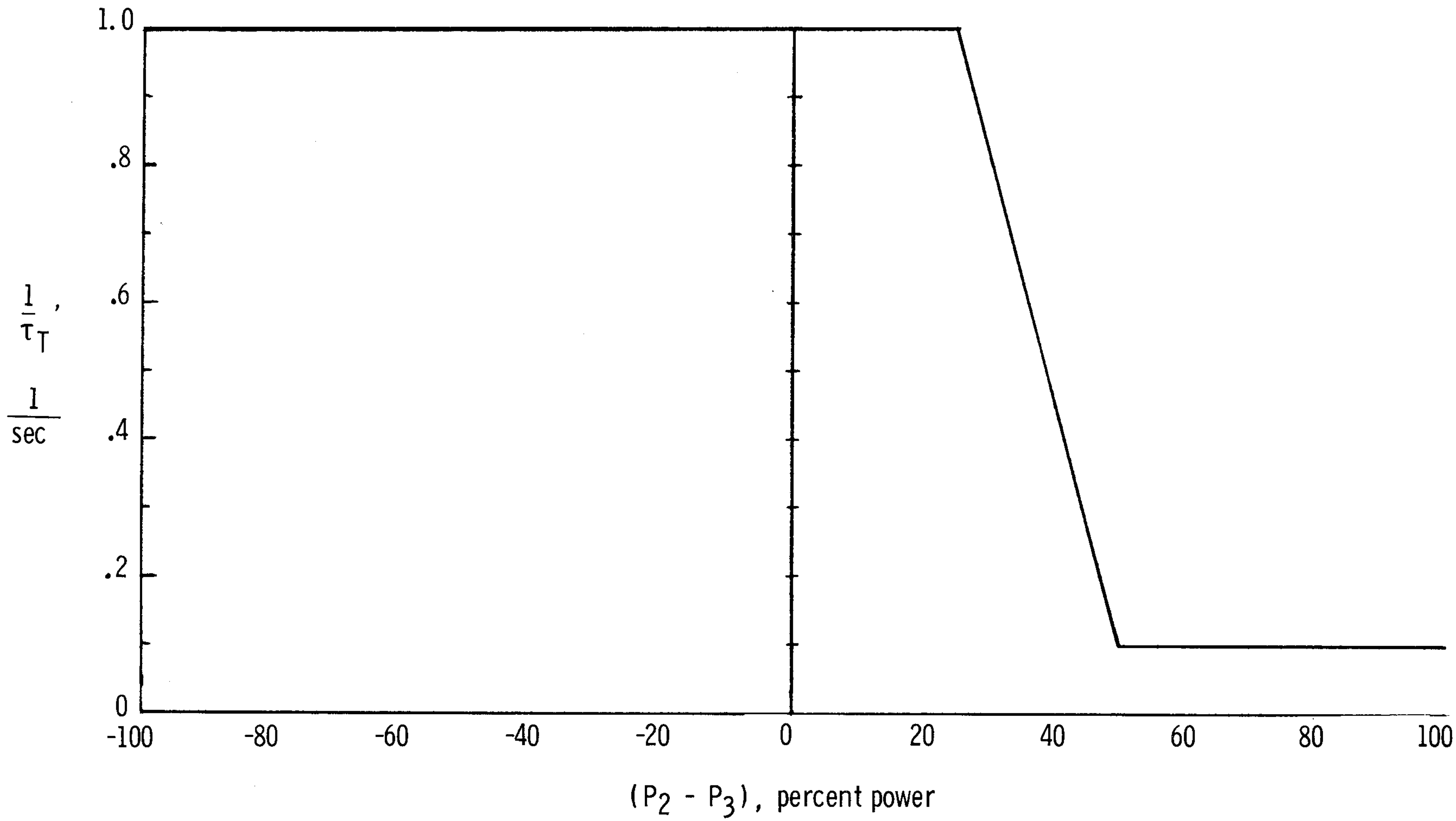

(c) Variation of inverse of thrust time constant with incremental power command.

Figure 66.- Concluded.

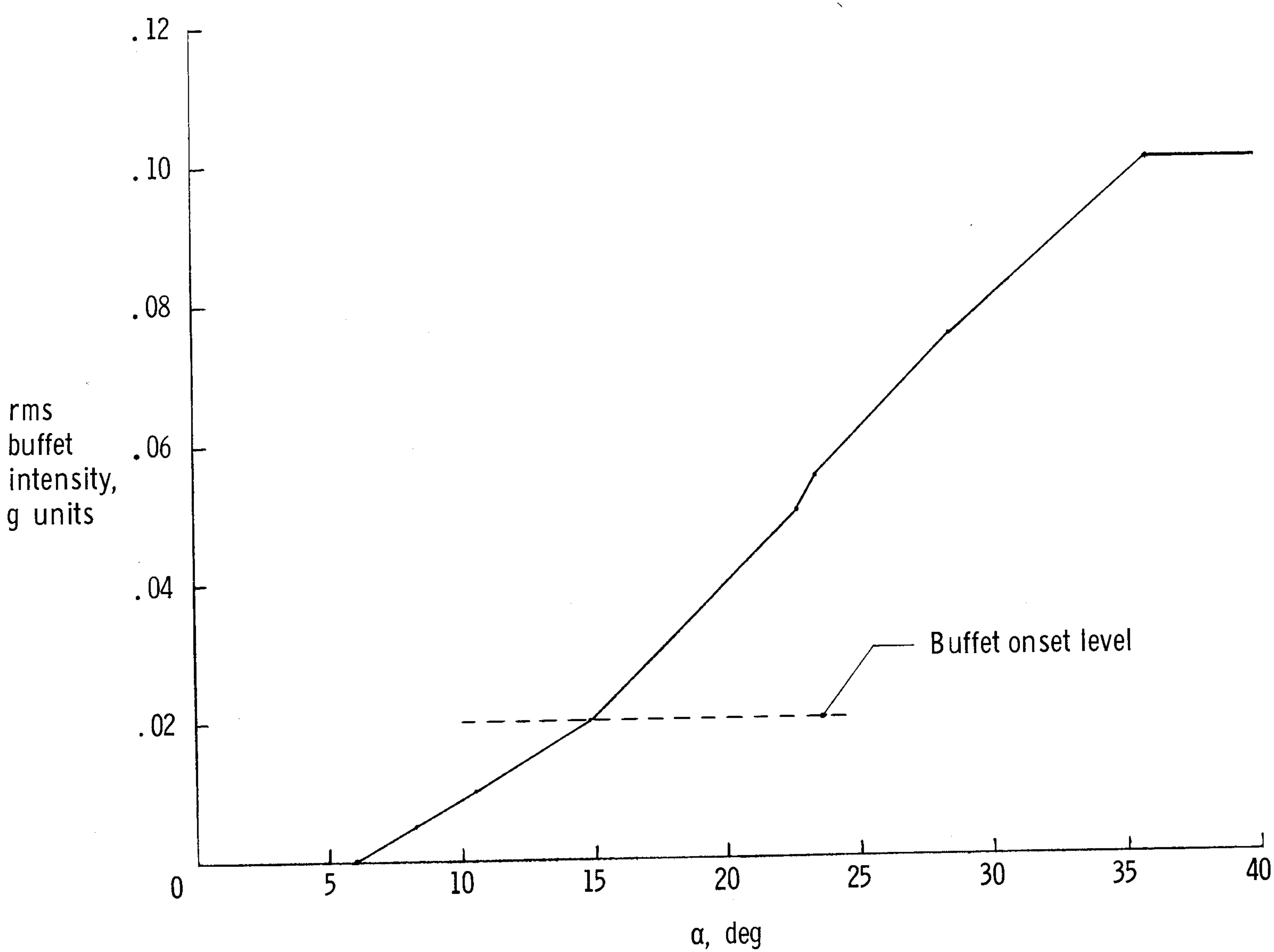

Figure 67.- Variation of buffet intensity with angle of attack.

1. Report No. NASA TP-1538	2. Government Accession No.	3. Recipient's Catalog No.
4. Title and Subtitle SIMULATOR STUDY OF STALL/POST-STALL CHARACTERISTICS OF A FIGHTER AIRPLANE WITH RELAXED LONGITUDINAL STATIC STABILITY		5. Report Date December 1979
		6. Performing Organization Code
7. Author(s) Luat T. Nguyen, Marilyn E. Ogburn, William P. Gilbert, Kemper S. Kibler, Phillip W. Brown, and Perry L. Deal		8. Performing Organization Report No. L-12854
		10. Work Unit No. 505-06-63-03
9. Performing Organization Name and Address NASA Langley Research Center Hampton, VA 23665		11. Contract or Grant No.
		13. Type of Report and Period Covered Technical Paper
12. Sponsoring Agency Name and Address National Aeronautics and Space Administration Washington, DC 20546		14. Sponsoring Agency Code
15. Supplementary Notes		

16. Abstract

A real-time piloted simulation has been conducted to evaluate the high-angle-of-attack characteristics of a fighter configuration based on wind-tunnel testing of the F-16, with particular emphasis on the effects of various levels of relaxed longitudinal static stability. The aerodynamic data used in the simulation were based on low-speed wind-tunnel tests of subscale models. The simulation was conducted on the Langley differential maneuvering simulator, and the evaluation involved representative low-speed combat maneuvering. Results of the investigation showed that the airplane with the basic control system was resistant to the classical yaw departure; however, it was susceptible to pitch departures induced by inertia coupling during rapid, large-amplitude rolls at low airspeed. The airplane also exhibited a deep-stall trim which could be flown into and from which it was difficult to recover. Control-system modifications were developed which greatly decreased the airplane susceptibility to the inertia-coupling departure and which provided a reliable means for recovering from the deep stall.

17. Key Words (Suggested by Author(s)) Relaxed longitudinal static stability High angle of attack Deep stall Departure prevention		18. Distribution Statement Unclassified - Unlimited Subject Category 08	
19. Security Classif. (of this report) Unclassified	20. Security Classif. (of this page) Unclassified	21. No. of Pages 223	22. Price* $9.25

* For sale by the National Technical Information Service, Springfield, Virginia 22161

NASA-Langley, 1979

National Aeronautics and
Space Administration

Washington, D.C.
20546

Official Business

Penalty for Private Use, $300

SPECIAL FOURTH CLASS MAIL
BOOK

Postage and Fees Paid
National Aeronautics and
Space Administration
NASA-451

U.S.MAIL

NASA

POSTMASTER: If Undeliverable (Section 158
Postal Manual) Do Not Return